Innovative & Sustainable Chemistry

December - 2023   E-ISSN - 2348-7143

Innovative & Sustainable Chemistry

Editorial Board

INDEX

Equilibrium Studies: Adsorption of Crystal Violet Dye on Rui Leaf Powder

Fakir Akhtar Sattar Shah[1], Mohd Mustaqeem Mohd Shareef[1], G. A. Usmani[2]

1. Department of Chemistry, H. J. Thim college of Arts and Science, Mehrun, Jalgaon, (425001), India.

2. Head, Department of Oil Technology, University Institute of Chemical Technology, Kavayitri Bahinabai Chaudhari North Maharashtra University, Jalgaon, (425001), India.

Abstract:

In current research the adsorption of crystal violet (CV) dye from its aqueous solution using Rui leaf powder (RULP) has been investigated. The effects of solution pH, adsorbent dose, CV concentration and particle size of adsorbent have been studied. The measurements were taken at 30 °C and optimum pH 11. It was found that the adsorption data fitted well to Freundlich adsorption isotherm. The maximum adsorption efficiency (q_{max}) was found to be 5.43 mg/g.

Key words: Adsorption, Langmuir isotherm, Freundlich isotherm Rui leaf powder, crystal violet.

1. Introduction:

In the environmental pollution and contamination of waste water dyes act as a major source (A. Shokrollahi et al., 2011). Dyes play vital role in pollution of effluents from various industries such as; leather, cosmetics, paper, textile dyeing etc industries. Hence the decolorization is needed before discharging of such dye contaminated water (M. Sarioglu and U.A. Atay, 2006). The enhanced polluted and colorful water have unbearable taste and it loses its aesthetic properties (A. Hashim, 2011).

The investigations show that the dyes have 7×10^5 metric tons/ annum overall the world synthesis (A. K. Asiagwu et al., 2012, M. Soni et al., 2012). It was accounted that around 40,000 tones dyes / year are discharged into water bodies (A. Achmad et al., 2012). CV is carcinogenic for animals, which belong to the triphenyl methane family.

Many methods have been tested in removal of dyes from waste water such as; bioremediation and biodegradation (M. Mariyappan et al., 2009), *physical methods* such as; nano-filtration, electrolysis, reverse osmosis and membrane-filtration (H. Patel and R. T. Vashi, 2010, O. S. Amodu et al., 2015). Previous studies have been illustrated that the adsorption is one cost effective technique and have low energy consumption in removal of colouring matter from effluents (C. Chen et al., 2012).

The present work aims to prepare the cheap, efficient, easily available and *eco-friendly* biosorbent in removal of dyes from wastewater. In adsorption of CV by RULP can be realized by equilibrium study and effects of various parameters.

2. Materials and methods

2. 1 Preparation of adsorbent and dye solution

The mature leaves of Rui plant (*Calatropis procera*) were collected from Nerinaka area of Jalgaon. Then the leaves were washed, cooked in hot water for 1 hour and then, sundried 2-3 days. Further the dried leaves were grounded and sieved to suitable sizes. The powder then poured in 2 N sulphuric acid to remove acid soluble matters and then, washed with 1 % sodium bicarbonate to remove excess of acid. Again the powder of RULP was dried and stored in plastic

containers. The stock solution of dyes was prepared by weighing 500 mg of CV (purchased from Loba Chemie, Mumbai, India) and dissolved to 1 litre volume of solution.
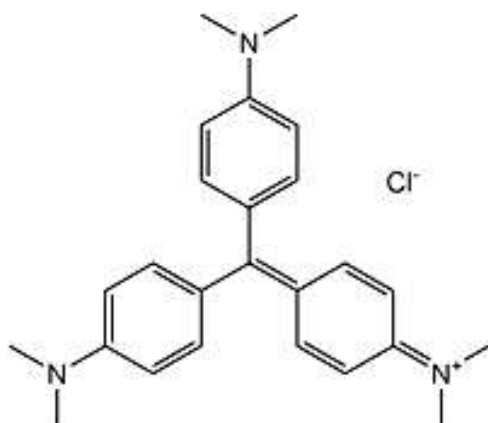
Crystal violet (CV)

2.2. Equilibrium Isotherm studies

Different Erlenmeyer's flasks of 100 ml capacity have been taken with different concentrations i.e. 5, 8, 10, 15 and 17 mg/L of CV dye solutions of 25 ml volume. Then, 100 mg biosorbent of particle sizes from 150 to 355 μ were added in each flask. The temperature of shaker incubator was maintained at three temperatures one by one; 30, 40 and 50 ºC, then these CV solutions with RULP containing flasks were shaken at optimum pH and 250 rpm agitation speed up to the equilibrium achieved. The supernant solutions were withdrawn, centrifuged and then the absorbance of the supernant solution was evaluated on Spectrophotometer (Systronics, Model 104) as a function of concentration of residual CV dye.

The linear Langmuir adsorption isotherm equation (1) is useful to evaluate maximum adsorption efficiency (q_{max}) at equilibrium.

$$\frac{C_e}{q_e} = \frac{C_e}{q_{max}} + \frac{1}{q_{max} . K_L} \qquad (1)$$

The Langmuir isotherm plot is C_e/q_e versus C_e, which have a constant said to be separation factor R_L given in equation (2) (J. Pal and M. K. Deb, 2014).

$$R_L = \frac{1}{(1 + K_L . C_o)} \qquad (2)$$

The Freundlich adsorption isotherm equation (3) is obtained by plotting $logq_e$ versus $logC_e$ having 1/n and K_F as constants.

$$logq_e = logK_F + \frac{1}{n} . logC_e \qquad (3)$$

3. Results and discussions

The pH is an important factor that controls the adsorption of CV on RULP. It was observed that as pH was raised then the adsorption efficiency was also increased. This is due to the dissociation of -COOH and -OH groups which are present on the surface of RULP, which bind CV cationic dye. The obtained maximum adsorption efficiency was 2.28 mg/g at P^H 11 as shown in figure 1.
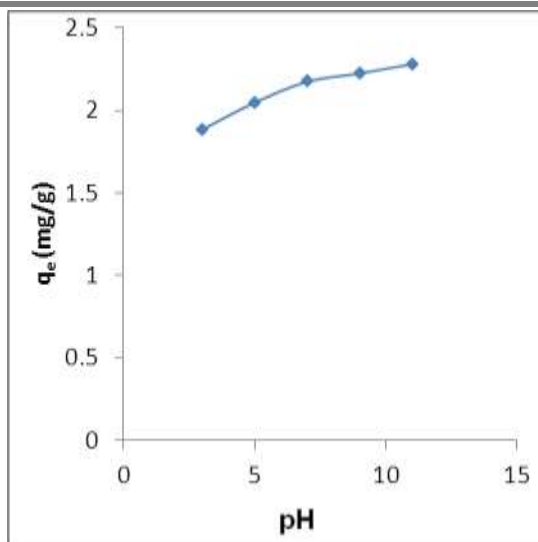
Fig 1: Effect of pH on adsorption efficiency of CV on RULP (T = 30 ^{o}C, agitation speed = 250 rpm, contact time = 50 min), C_o = 10 mg/L, particle size = 150 – 355 nm)

The effect of adsorbent dose on % removal of CV on RULP is illustrated in figure 2. The adsorbent dose provided more number of adsorption sites to bind CV molecules. It is observed from figure 2 that as adsorbent dose increased the percent removals are also increased. For 50 mg dose of the RULP the percent removal was 81.1 0%, while for 250 mg dose the percent removal of CV was 94.7 % as shown in Table 1.

Table 1 Effect of adsorbent dose on % removal of CV on RULP (T = 30 ^{o}C, V = 25 mL, agitation speed = 250 rpm, pH and contact time = optimum, C_o= 10 mg/L, particle size = 150 – 355 nm)

Dose (mg)	q_e (mg/g)	% Removal
50	4.06	81.1
100	2.08	91.1
150	1.47	92.0
200	1.14	93.8
250	0.93	94.7
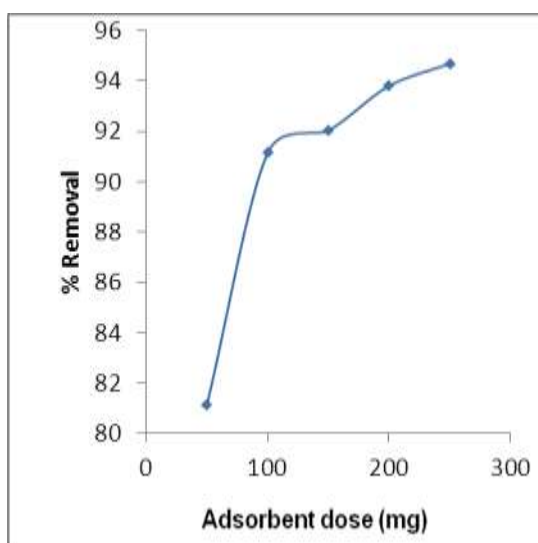
Fig 2: Effect of adsorbent dose on % removal of CV on RULP (T = 30 $^{\circ}$C, agitation speed = 250 rpm, contact time = 50 min), C_o = 10 mg/L, particle size = 150 – 355 □)

The table 2 illustrates that for smaller particle sizes of adsorbent, high will be the available surface area and high is the % removal of CV. It is observed that the % removal of CV decreases for any given concentration with increase in the range of particle sizes such as; 53 – 150 □, 150 – 355 □and 355 to 1180 □It was observed that as the concentration of CV dye increases the percentage removals were decreases as shown in figure 3.

Table 2: Effect of particle size of adsorbent on adsorption of CV on RULP (adsorbent dose = 100 mg/ 25 mL, pH = 11 and contact time = 50 min, agitation speed = 250 rpm, T = 30 $^{\circ}$C, a = 355 – 1180 nm, b = 150 – 355 nm and c = 53 – 150 nm)

C_o mgL^{-1}	Particle size (nm)					
	355 – 1180		150 – 355		53 – 150	
	q_e (mg/g)	% Remo.	q_e (mg/g)	% Remo.	q_e (mg/g)	% Remo.
5	1.06	85.4	1.18	95.0	1.20	96.1
8	1.68	83.9	1.86	93.0	1.88	94.4
10	2.03	81.1	2.28	91.1	2.31	92.4
15	2.99	79.9	3.34	89.1	3.39	90.5
17	3.32	78.1	3.72	87.5	3.81	89.6
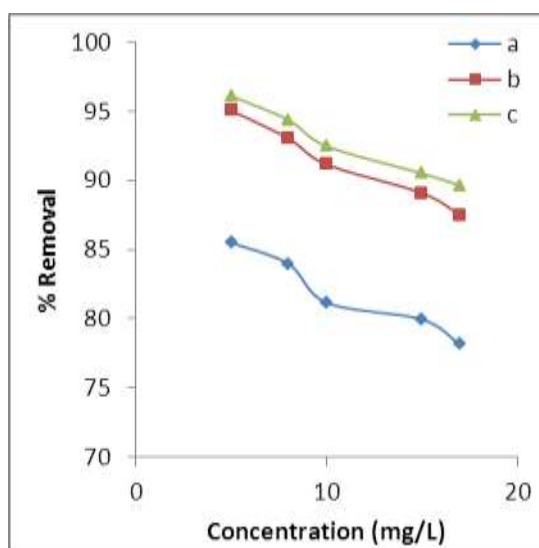
Fig 3: Effect of particle size of adsorbent on adsorption of CV on RULP (T = 30 $^{\circ}$C, adsorbent dose = 100 mg/25 mL solution, agitation speed = 250 rpm, pH = 11, C_o = 10 mg/L, particle size = 150 – 355 nm)

Figure 4a shows the Langmuir adsorption isotherms at 30, 40 and 50 $^{\circ}$C. Freundlich adsorption isotherms are shown in figure 4b. The plots are linear with good correlation coefficients which are close to unity.

The table 3 illustrates the obtained experimental parameters of Langmuir and Freundlich isotherms. The obtained q_{max} value is 5.43 mg/g at 30 $^{\circ}$C for adsorption of CV on RULP. If the value of n is greater than 1 then the adsorption will be physical as well as favorable in nature.

Table 3 illustrates that all values found in the range of 1.87 to 2.46. Hence the adsorption of CV on RULP was favorable. The K_F is roughly an adsorption capacity which has value 3.01 mg/g at 50 $^{\circ}$C. The high value of correlation coefficients (R^2) for the adsorption of CV on RULP show that the Freundlich isotherm fitted well. This demonstrates the presence of energetically favorable heterogenous sites of adsorption, which further responsible for multilayer adsorption of CV on RULP.

Table 3: Langmuir and Freundlich isotherm parameters for the adsorption of CV on RULP (adsorbent dose = 100 mg/ 25 mL, C_o = 5 – 17 mg/L, pH = 11, contact time = 50 min, agitation speed = 250 rpm, particle size = 150 – 355 nm)

T (°C)	Langmuir isotherm parameters			Freundlich isotherm parameters		
	q_{max} (mg/g)	K_L (L/mg)	R^2	K_F (mg/g)	n	R^2
30	5.43	0.96	0.974	2.50	1.87	0.998
40	5.32	1.17	0.959	2.69	1.96	0.996
50	4.97	1.68	0.960	3.01	2.46	0.967

a **b**
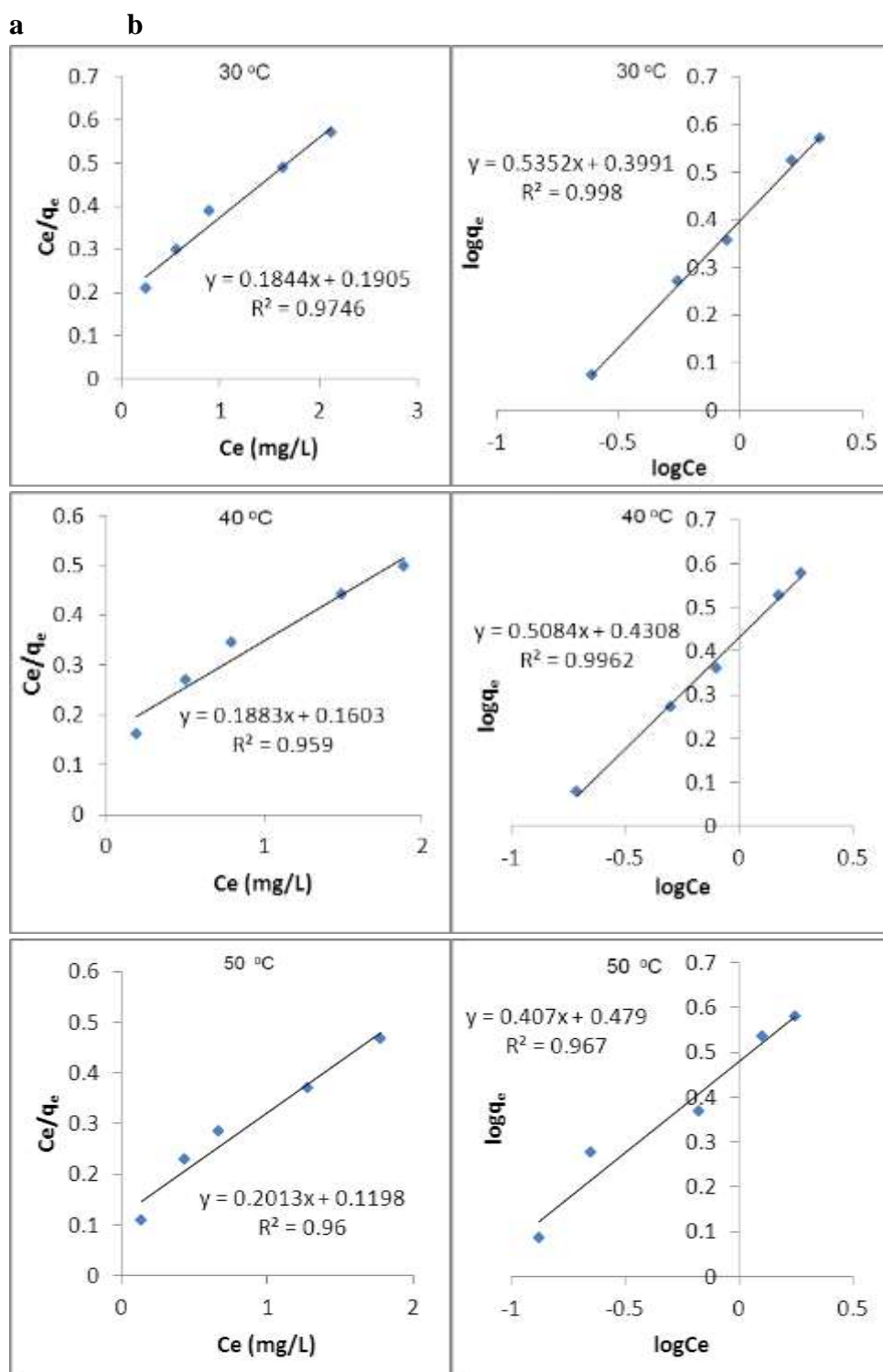
Fig.4: a Langmuir and **b** Freundlich isotherms for the adsorption of CV onto RULP at different

'RESEARCH JOURNEY' International E- Research Journal
Special Issue – 333 : Innovative & Sustainable Chemistry
Impact Factor 6.625 (SJIF)   Peer Reviewed Journal

E-ISSN : 2348-7143
December - 2023

temperatures (adsorbent dose = 100 mg/ 25 mL solution, agitation speed = 250 rpm, C_o = 5, 8, 10, 15, 17 mg/L, pH = 11, contact time = 50 minute, particle size = 150 – 355 □

The value of separation factor (R_L) decides the type of adsorption such as; if (R_L = 1) linear, (R_L = 0) irreversible, (R_L > 1) unfavorable while ($0 < R_L < 1$) favorable adsorptions. In this investigation of the adsorption of CV on RULP table 4 shows that all values of separation factor (R_L) are in the range of 0.03 to 0.17. Hence the adsorption process is favorable.

Table 5 shows the comparisons of maximum adsorption capacities of CV with some reported adsorbents in literatures and current work.

Table 4: Separation factor (R_L) for the adsorption of CV on RULP (adsorbent dose = 100 mg/ 25 mL, C_o = 5 – 17 mg/L, pH = 11, contact time = 50 min, agitation speed = 250 rpm, particle size = 150 – 355 nm)

T ºC	C_o (mg/L)				
	5	**8**	**10**	**15**	**17**
30	0.17	0.11	0.09	0.06	0.06
40	0.14	0.09	0.08	0.05	0.05
50	0.10	0.07	0.06	0.04	0.03

Table 5: Comparisons of maximum adsorption capacity (q_{max}) of CV with some reported adsorbents

Adsorbent	q_{max} (mg/g)	References
Gossypium hirsutum	66.6	N. Sivarajasekar et al., 2016
Neem saw dust	3.99	S. D. Khattri and M. K. S., 2000
Calotropis procera	4.10	H. Ali, S. K. Muhammad, 2008
Citrullus Lanatus	11.9	B. K. Suyamboo, R. S. P., 2012
Pea Peels	17.6	T. A. Khan et al., 2016
Rui leaf powder	5.43	Present work

4. Conclusion:

In this investigation the biosorbent was prepared by Rui leaf powder which is economically feasible and environmental friendly. The RULP is an alternative to costly and environment polluting conventional adsorbents. The RULP was capable of removing CV with maximum efficiency 5.43 mg/g at 30 ºC. The RULP can be useful in treatment of highly coloured dye effluents. The Freundlich isotherm was slightly better than Langmuir isotherm. The adsorption of CV was physical, favorable and multilayer on heterogenous surface of RULP.

References:
1. A. Achmad, K. Jain, T. K. Suan, R. C. Amat and L. S. Tan (2012), *Equilibrium, kinetic and thermodynamic studies on the adsorption of direct dye onto a novel green adsorbent developed from Uncaria gambir extract.*   J. Phy. Sci., 23(1): 1 – 13.
2. A. Hashim (2011), *A thermodynamic study of adsorption leshman's stain dye by germanium oxide and yttrium oxide.* Euro. J. Soc. Sci., 3(25): 364 – 371.
3. Shokrollahi, A. Alizadeh, Z. Malekhosseini and M. Ranjbar (2011), *Removal of bromocresol green from aqueous solution via adsorption on Ziziphus nummularia as a*

new, natural, and low cost adsorbent: Kinetic and thermodynamic study of removal process, J. Chem. Eng. Data 56: 3738 – 3746.

4. B. K. Suyamboo and R. S. Perumal (2012), *Equilibrium, thermodynamic and kinetic studies on adsorption of a basic dye by Citrullus lanatus rind,* Iranica J. Energy Environ., 3(1): 23 – 34.

5. Chen, M. Zhang, Q. Guan and W. Li (2012), *Kinetic and thermodynamic studies on the adsorption of xylenol orange onto MIL-101(Cr),* Chem. Eng. J. 183: 60 – 67.

6. H. Ali and S. K. Muhammad (2008), *Biosorption of crystal violet from water on leaf biomass of Calatropis procera.* J. Env. Sci. Tech. 1(3): 143 – 150.

7. H. Patel and R. T. Vashi (2010), *Adsorption of crystal violet dye on to tamarind seed powder,* Elec. J. Chem., 7(3): 975 – 984.

8. J. Pal and M. K. Deb (2014), *Efficient adsorption of congo red dye from aqueous solution using green synthesized coinage nanoparticles coated activated carbon beads*, Appl. Nanosci., 4: 967 – 978.

9. M. Mariyappan, N. Kannan and J. Rejinis (2009), *Removal of Azure A from aqueous solution by CAC and new activated carbon from orange peel and lemon peel,* Elec. J. Env. Agri. Food Chem., 8(8): 574 – 583.

10. M. Sarioglu and U.A. Atay (2006), *Removal of methylene blue by using biosolid,* Glob. Nes. J., 8(2): 113 – 120.

11. M. Soni, A. K. Sharma, J. K. Srivastava and J. S. Yadav (2012), *Adsorptive removal of methylene blue dye from an aqueous solution using water hyacinth root powder as a low* A. K. Asiagwu, H. I. Owamah and V. O. Illoh (2012), *Kinetic and thermodynamic models for the removal of aminophenol (dye) from aqueous solutions using groundnut (Arachis hypogea) shells as the biomass,* Adv. Appl. Sci. Res., 3(4): 2257 – 2265.

12. N. Sivarajasekar, R. Baskar, T. Ragu, K. Sarika, N. Preethi and T. Radhika (2016), *Biosorption studies on waste cotton seed for cationic dyes sequestration: Equilibrium and thermodynamics.* Appl. Water Sci., DOI 10.1007/s13201-016-0379-2.

13. O. S. Amodu, T. V. Ojumu, S. K. Ntwampe and O. S. Ayanda (2015), *Rapid adsorption of crystal violet onto magnetic zeolite synthesized from fly ash and magnetite nanoparticles.* J. Enc. Ads. Sci., 5: 191 – 203.

14. S. D. Khattri and M. K. Singh (2000), *Colour removal from synthetic dye waste water using a bioadsorbent.* Water Air Soil Poll., 120: 283 – 294.

15. T. A. Khan, R. Rahman and E. A. Khan (2016), *Decolorization of bismarck brown R and crystal violet in liquid phase using modified pea peels: Non-linear isotherm and kinetics modeling.* Mod. Ear. Sys. Env., 2: 141 – 149.

Recent Advances in Biogenic Synthesis of Metal Nanoparticles by Plant Extract

Mahadev B. Suwarnkar

Dept. of Chemistry, Baburaoji Adaskar Mahavidyalaya, Kaij,

Dist. Beed. (MS), India.

Email: msuwarnkar@gmail.com

Abstract:

    In the arena of material sciences, one of the burning topics for research has been biogenically synthesizing nanoparticles from plant derivatives and studying their applicability to be used as sustainable catalysts. A variety of chemical, physical, and biological methods have been working to synthesize nanomaterials. Various biological systems such as bacteria, fungi, actinomycetes, yeasts, viruses, and plants have been reported to produce various metal and metal oxide nanoparticles. Among these, biosynthesis of nanoparticles from plants seems to be a very efficient method in developing a nontoxic, clean, rapid, and eco-friendly technology. The use of plant biomass or extracts for the biosynthesis of novel metal nanoparticles (silver, gold, platinum, and palladium) would be more significant. Due to the rich biodiversity of plants, their potential use toward the synthesis of these nobel metal nanoparticles is yet to be explored. The aim of this article is to present the recent trends which are concerned in the phytosynthesis of nobel metal nanoparticles in the past decade.

Keywords : Nanoparticles, Phytosynthesis, Gold, Silver.

Introduction:

    Nanobiotechnology represents the intersection of nanotechnology and biotechnology, which is an emerging field dedicated to creation, improvement, and utility of nanoscale structures for advanced biotechnology [1]. Nanomaterials have better biological and physicochemical properties than their bulk phase counterparts. This made them worthy of attention among other materials. Nanomaterials have high surface reactivity due to larger surface to volume ratios. Their size varies from 1 to 100 nm [2]. In particular noble metal nanoparticles have wide applications in various fields such as medicine, electronics, energy and catalysis [3]. Generally metal nanoparticles have been prepared by physical and chemical methods [4]. However, due to their negative impact, there is an urgent need to replace the chemical method with clean, non toxic and environmentally acceptable biological method.

    Through the last two decades, the biosynthesis of nobel metal nanoparticles (silver, gold, platinum, and palladium) has received significant interest due to the increasing need to develop environmental friendly technologies in material synthesis [2]. The nanoparticles are of great attention due to their extremely small size and large surface to volume ratio, and they exhibited entirely novel characteristics compared to the large particles of bulk material [5]. Not only in pharmaceutical and medical-based products but also in the production of daily consumer products like soaps, toothpaste, detergents, cosmetic products, etc., noble metal nanoparticles (such as gold, silver, platinum, palladium, etc.) have found wide applications [6]. Gold nanoparticles have been commonly used in medicine [7], disease diagnostic and drug delivery systems [8]. Silver nanoparticles have been working in sensor technology [9], biological leveling, and various new biomedical applications [10]. Platinum nanoparticles are also widely used as catalysts and in many biomedical applications in combination with other nanoparticles in

alloy, core shell, and bimetallic nanostructures [11]. Similarly, palladium nanoparticles have an extensive application in catalysis and electrocatalysis, sensing, and plasmonic wave guiding [12].

A huge deal of effort has been constant toward the biosynthesis of metal nanoparticles using bacteria, fungi [13], actinomycetes, yeast [14], and viruses [15]. In adding to the above-mentioned synthesis methods, phytosynthesis that utilizes parts of whole plants as biological factories to synthesize metallic nanoparticles is under development and is an advantageous and profitable approach [16]. In comparison to microorganisms, the phytosynthesis technique is devoid of complex and multistep processes like microbial isolation, culturing, maintenance etc., and also is a very fast and cost-effective approach that can be easily scaled up for bulk production of nanoparticles [17]. Furthermore, it has been shown that the rate of nanoparticle synthesis is rapid using plants than microbes, and the produced nanoparticles are more stable. In addition, phytosynthesis is truly a "green" synthesis path in comparison to other known methods of nanoparticle synthesis. Plants are known to harbor a broad range of metabolites. Yet, their potential is yet to be fully utilized in full throttle for synthesizing metallic nanoparticles. The aim of this evaluation is to provide the recent trends involved in phytosynthesis of nobel metal nanoparticles.

Biosynthesis of Noble metals:

The use of plant systems has been considered a green route and a reliable method for the biosynthesis of nanoparticles owing to its environmental friendly nature [18]. It is clear from the previous reports that plants have been exploited effectively for rapid and extracellular biosynthesis of nobel metal nanoparticles [19]. Shankar et al. [20] reported that gold and silver nanoparticles can be produced using plant extracts at rates similar to those of chemical methods. In a separate study, this group reported the formation of gold nanotriangles when lemongrass leaf extract was allowed to react with aqueous $AuCl_4^-$ ions. In addition, leaf extracts of several plants, viz. lemongrass, neem, tamarind, geranium, and Aloe vera, have been reported to confirm their potential in reducing Au (III) ions into gold nanoparticles as well as converting silver ions into silver nanoparticles [21]. Also, synthesis of platinum and palladium nanoparticles have been reported using extracts of various parts of different plant species [22].

Silver Nanoparticles:

Along with biological processes, phytosynthesis of silver nanoparticles has been shown as an easier and faster method than the tedious and time-consuming microbial synthesis processes. For instance, parts of plants or their extracts have been explored for the reason of silver nanoparticle synthesis using silver ions as substrates. The synthesis of highly stable and crystalline silver nanoparticles (16−40 nm) by exposing the aqueous geranium leaf extract to silver nitrate solution. The synthesis rate of nanoparticles was found to be very high during the reaction (reaction time about 60 min). The use of plants instead of microorganisms for biosynthesis of metal nanoparticles is a more rapid and reproducible process. Li et al. [23] revealed the synthesis of silver nanoparticles from the leaf extracts of Aloe vera and Capsicum annum plants, respectively.

Leela et al. [24] performed an attractive experiment using the leaf extracts of plants, namely, Helianthus annus, Basella alba, Oryza sativa, Saccharumof f icinarum, Sorghum bicolar, and Zea mays, and concluded that among all the tested plant extracts, H. annus exhibited the strongest potential for rapid reduction of silver ions. Jain et al. [25] demonstrated the rapid synthesis of silver nanoparticles using the fruit extract of Carica papaya and found that the

synthesized nanoparticles were extremely toxic against diverse multidrug resistant human pathogens. Begum et al. [26] showed fast synthesis of stable silver nanoparticles of different shapes using black tea leaf extract. Extracellular synthesis of silver nanoparticles has been reported using leaf extract of Pine, Persimmon, Ginkgo, Magnolia, and Platanus plants. In addition, silver nanoparticles were effectively synthesized using the latex and seed extract of Jatropha curcas. Dubey et al. [27] revealed the use of methanolic extract of Eucalyptus hybrid leaves in the extracellular biosynthesis of silver nanoparticles. Likewise, rapid synthesis (reaction time <30 min) of silver nanoparticles by Acalypha indica leaf extract and their antibacterial activity against water borne pathogens has been reported by Krishnaraj et al. [28], Sathiskumar et al.[29] has studied the compatibility of the bark and powder extracts of Curcuma longa toward the formation of silver nanoparticles and reported that bark extract could produce a higher amount of silver nanoparticles compared to the powder extract. The resulting nanoparticles differ in shape and size but had strong antibacterial activity against the Escherichia coli.

Gold Nanoparticles:

Gold nanoparticles are relatively the most attractive member of nobel metal nanoparticles because of their potential applications in the fields ranging from catalysis, nonlinear optics, nanoelectronics, gene expression, and disease diagnosis [30]. Improved environmental concerns over chemical synthesis routs have drawn significant interest toward phytosynthesis of gold nanoparticles. The extracellular synthesis of gold nanoparticles using the leaf extract of Coriandrum sativum has been attempted by Narayanan and Sakthivel [31]. They establish that the synthesized nanoparticles were triangle, truncated, and decahedral in morphology with an average size of 7−57 nm. Very recently, Singh and Bhakatt [32] reported the synthesis of gold nanoparticles using leaves and bark of Ficus carica. In addition, synthesis of spherical gold nanoparticles have been reported on the reduction of $AuCl_4^-$ by the leaf extract of Sphearanthus amaranthoids [33] and Putranjiva roxburghii [34]. Synthesis of gold nanoparticles of different sizes in the range of 15−25 nm was obtained by controlling the synthetic parameters using leaf extract of fenugreek.

Platinum and Palladium Nanoparticles:

The development of palladium nanoparticles using the aqueous extract of Gardenia jasminoides was reported by Jia et al. [35] and confirmed the antioxidants, namely, geniposide, chlorogenic acid, crocins, and crocetin played an essential role in reducing and stabilizing the nanoparticles whereas the dispersity of these nanoparticles were temperature dependent.

Satishkumar et al. [36] generated palladium nanoparticles with uniform sizes (15−20 nm) using the bark extract of Cinnamon zeylanica m. Bankar et al. [37] obtained palladium nanoparticles of 50 nm average size using peeled extract of Musa paradisica. In addition, synthesis of platinum nanoparticles was achieved by S ong et al. [38] using the leaf extract of Diopyros kaki. They reported that more than 90% of the platinum ions were converted into nanoparticles using 10% leaf biomass concentration at 95 °C, and the average size of synthesized nanoparticles ranged from 2 to 12 nm. Furthermore, Yang et al. [39] reported one-pot biogenic production of palladium nanoparticles with leaf broth of Cinnamomum camphora. Phytosynthesis of platinum nanoparticles with controlled shapes and sizes has also been reported by using plant wood nanomaterials.

Mechanism Behind Phytosynthesis:

A variety of studies have been commenced on the screening and identification of plants for controlled synthesis of nobel metal nanoparticles, very small work has been performed to understand the actual mechanism behind the synthesis of nanoparticles [40]. Clarification of the actual mechanism and biochemical pathways, leading to the biosynthesis of metal nanoparticles, is an essential to expand a rational approach in this field. Research on the underlying molecular mechanism is therefore an essential to control the size, shape, and crystallinity of the metal nanoparticles. In recent years, several hypothesis have been proposed for nanoparticles synthesis [41]. In this section, the research works done during the past decade toward elucidating the mechanistic aspect behind the phytosynthesis of metal nanoparticles have been summarized.

Gardea-Torresdey et al. [42] published their first report on the development of gold nanoparticles inside living plants, but the actual mechanism was not elucidated in their report. After one year, this research group reported that alfalfa roots are capable of absorbing silver as Ag (0) from the agar medium and then transfer it to the shoot portion in the same oxidation state. The TEM/STEM analysis in this study recommended that silver atoms accumulated inside the alfalfa plant tissues undergo nucleation and subsequently form nanoparticles. While working with the dead tissues of oats (Avena sativa), it was recommended that the functional group such as carbonyl, amino, and sulfhydryl present in the cell wall may also add to the reduction of Au (III) to Au nanoparticles [43].

Conclusion:

This paper has summarized the recent research work in the field of phytosynthesis of nobel metal nanoparticles and notably discusses the various mechanisms planned behind it. Due to the rich biodiversity of plants, their potential for the synthesis of nobel metal nanoparticles is yet to be fully explored. Massive numbers of plant species are available in nature, and many of them can be excellent candidates for nanoparticle synthesis. Explanation of mechanism behind phytosynthesis of precious metal nanoparticles is necessary in order to develop a rational approach. A thorough understanding of biochemical mechanisms involved in the plant mediated nanoparticle synthesis is a prerequisite in order to make this approach economically competitive with the conventional methods.

References:

1. Goodsell, D. S. , John Wiley & Sons, Inc.: Hoboken, NJ, 2004.
2. Geonmonond, R. S.; Silva, A. G. M.; Camargo, P. H. C., An. Acad. Bras. Cienc. 2018, 90, 719-724.
3. T.J.I. Edison, M.G. Sethuraman, Sustainable Chem. Eng., 2013, (1), 1326–1332.
4. Mudassir, M. A.; et al. , ACS Appl. Mater. Interfaces 2017, 9, 24190.
5. M. Liu, M. Leng, C. Yu, X. Wang, C. Wang, Nano Res., 2010, (3), 843–851.
6. Kumar, Y.; Yogeshwar, P.; Bajpai, S.; Jaiswal, P.; Yadav, S.; Pathak, D. P.; Sonker, M.; Tiwary, S. K. , Mater. Adv. 2021, 2 (16), 5318−5343.
7. Pérez, J.; Bax, L., Escolano, C. , Willems & van den Wildenberg (W&W) Espana sl: Barcelona, Spain, 2005.
8. Bhumkar, D. R.; Joshi, H. M.; Sastry, M.; Pokharkar, V. B. , Pharm. Res. 2007, 24 (8), 1415−1426.
9. Gomez-Romero, P. , Adv. Mater. 2001, 13 (3), 163−174.

10. Asha Rani, P. V.; Mun, G. L. K.; Hande, M. P.; Valiyaveettil, S. ,ACS Nano 2009, 3 (2), 279−290.

11. Hrapovic, S.; Liu, Y.; Male, K. B.; Luong, J. H. T. , Anal. Chem. 2004, 76 (4), 1083−1088.

12. Chen, Z. H.; Jie, J. S.; Luo, L. B.; Wang, H.; Lee, C. S.; Lee, S. T. ,Nanotechnology 2007, 18, 345502.

13. Husseiny, M. I.; El-Aziz, M. A.; Badr, Y.; Mahmoud, M. A. , Spectrochim. Acta, Part A 2007, 67 (3−4), 1003−1006.

14. Kowshik, M.; Arhtaputre, S.; Kharrazi, S.; Vogel, W.; Urban, J.;   Kulkarni, S. K.; Paknikar, K. M. , Nanotechnology 2003, 14, 95−100.

15. Shenton, W.; Douglas, T.; Young, M.; Stubbs, G.; Mann, S., Adv. Mater. 1999, 11 (3), 253−256.

16. Iravani, S. , Green Chem 2011, 13 (10), 2638−2650.

17. Shankar, S. S.; Rai, A.; Ahmad, A.; Sastry, M., J. Colloid Interface Sci. 2004a, 275 (2), 496−502.

18. Bhattacharya, D.; Gupta, R. K. ,Crit. Rev. Biotechnol. 2005, 25 (4), 199−204.

19. Shankar, S. S.; Rai, A.; Ankamwar, B.; Singh, A.; Ahmad, A.; Sastry, M. , Nat. Mater. 2004b, 3 (7), 482−488.

20. Shankar, S. S.; Ahmad, A.; Sastry, M. , Biotechnol. Prog. 2003b, 19 (6), 1627−1631.

21. Ankamwar, B.; Damle, C.; Ahmad, A.; Satry, M. , J. Nanosci. Nanotechnol. 2005b, 5 (10), 1665−1671.

22. Nadagouda, M. N.; Varma, R. S. , Green Chem. 2008, 10 (8), 859−862.

23. Li, S.; Shen, Y.; Xie, A.; Yu, X.; Qiu, L.; Zhang, L.; Zhang, Q. , Green Chem. 2007, 9 (8), 852−858.

24. Leela, A.; Vivekanandan, M. , Afr. J. Biotechnol. 2008, 7 (17), 3162−3165.

25. Jain, D.; Daima, H. K.; Kachhwala, S.; Kothari, S. L. , Dig. J. Nanomater. Biostruct. 2009, 4 (3), 557−563.

26. Begum, N. A.; Mondal, S.; Basu, S.; Laskar, R. A.; Mandal, D. , Colloids Surf., B 2009, 71 (1), 113−118.

27. Dubey, M.; Bhadauria, S.; Kushwah, B. S. , Dig. J. Nanomater. Biostruct. 2009, 4 (3), 537−543.

28. Krishnaraj, C.; Jagan, E. G.; Rajasekar, S.; Selvakumar, P.; Kalaichelvan, P. T.; Mohan, N. , Colloids Surf., B 2010, 76 (1), 50−56.

29. Sathishkumar, M.; Krishnamurthy, S.; Yun, Y. S. , Biores. Technol. 2010, 101 (20), 7958−7965.

30. Aromal, S. A.; Philip, D. Spectrochim. Acta, Part A 2012, 97, 1−5.

31. Narayanan, K. B.; Sakthivel, N. , Mater. Lett. 2008, 62 (30), 4588−4590. Cinnamomum camphora leaf. Nanotechnology 2007, 18 (10), 105−106.

32. Singh, P. P.; Bhakat, C. , Int. J. Sci. Res. Pub. 2012, 2 (5), 1−4.

33. Nellore, J.; Pauline, P. C.; Amarnath, K. Dig. J. ,Nanomater. Biostruct. 2012, 7 (1), 123−133.

34. Badole, M. R.; Dighe, V. V. , Int. J. Drug Discovery Herbal Res. 2012, 2 (1), 275−278.

35. Jia, L.; Zhang, Q.; Li, Q.; Song, H. , Nanotechnology 2009, 20, 385601.

36. Sathishkumar, M.; Sneha, K.; Kwak, I. S.; Mao, J.; Tripathy, S. J.; Yun, Y. S. , J. Hazard. Mater. 2009, 171 (1−3), 404−404.

37. Bankar, A.; Joshi, B.; Kumar, A. R.; Zinjarde, S. , Mater. Lett. 2010, 64 (18), 1951−1953.
38. Song, J. Y.; Kwon, E. Y.; Kim, B. S. , Bioprocess Biosyst. Eng. 2010, 33 (1), 159−164.
39. Yang, X.; Li, Q.; Wang, H.; Huang, J.; Lin, L.; Wang, W.; Sun, D.; Su, Y.; Opiyo, J. B.; Hong, L.; Wang, Y.; He, N.; Jia, L. , J. Nanopart. Res. 2010, 12 (5), 1589−1598.
40. Lin, X.; Wu, M.; Wu, B.; Kuga, S.; Endo, T.; Huang, Y., Green Chem. 2011, 13 (2), 283−287.
41. Sathishkumar, M.; Krishnamurthy, S.; Yun, Y. S., Biores. Technol. 2010, 101 (20), 7958−7965.
42. Gardea-Torresdey, J. L.; Parsons, J. G.; Gomez, E.; Peralta- Videa, J. R.; Troiani, H. E.; Santiago, P.; Jose-Yacaman, M., Nano Lett. 2002, 2 (4), 397−401.
43. Armendariz, V.; Herrera, I.; Peralta-Videa, J. R.; Jose-Yacaman,.; Troiani, H.; Santiago, P.; Gardea-Torresdey, J. L., J. Nanopart. Res. 2004, 6 (4), 377−382.

Plant-Mediated Zno Nanoparticles for Antimicrobial Activity: A Short Review

Abhimanyu P. Pawar[a*], Arvind J. Mungole[b], Kishor S. Naktode[a], Darshana N. Urade[a]
Dalesh M. Parshuramkar[c],   Atul N. Yerpude[c]

[a]Department of Chemistry, NevjabaiHitkarini College, Bramhapuri, Maharashtra 441 206, India
[b]Department of Botany, NevjabaiHitkarini College, Bramhapuri, Maharashtra 441 206, India
[c]Department of Physics, NevjabaiHitkarini College, Bramhapuri, Maharashtra 441 206, India
*Corresponding author: - abhaypawar1988@gmail.com

Abstract:

Nanoparticles have found utility in virtually every branch of science, including the medical field, and continue to offer intriguing possibilities for extensive research, owing to their diminutive size. The synthesis of nanoparticles using plant extracts has demonstrated remarkable efficacy, particularly in the realm of antimicrobial activity against human pathogenic bacteria. Among the multitude of newly synthesized nanoparticles, Zinc Oxide nanoparticles have emerged as a subject of significant interest. Traditionally, Zinc Oxide nanoparticles have been synthesized using chemical agents as reducing agents, which poses a considerable risk due to their inherent toxicity. Consequently, there exists a pressing need to develop biological or green synthesis processes, utilizing plant-based resources. Such an approach not only mitigates environmental risks but also harnesses the controlled conversion of plant-based biomolecules into nanoparticle-compatible forms. In this paper, we present a comprehensive review of Zinc Oxide nanoparticles concerning their applications in antimicrobial activity. This research sheds light on the potential of green synthesis methods utilizing plant-based materials, emphasizing both their eco-friendliness and their controlled transformation of biomolecules into nanoparticles.

1. Introduction:

Nanotechnology, a rapidly advancing interdisciplinary field, centers on manipulating materials and structures at the nanoscale, typically below 100 nanometers. At this minute scale, materials exhibit unique properties and behaviors, differing from their macroscopic counterparts, providing a myriad of applications. Recent years have seen the emergence of nanomaterials with exceptional capabilities, driving efforts to address diverse practical challenges. These nanoscale structures hold enormous potential in fields such as pharmaceuticals, cosmetics, medicine, agriculture, catalysis, food preservation, environmental conservation, and electronics **(Kargozar et al., 2018, Ghotekar et al., 2020, Malik et al., 2023).**The versatility of nanotechnology offers tangible benefits to humanity, ranging from more effective medical interventions and sustainable agricultural practices to enhanced environmental stewardship and advanced consumer goods. As the field of nanotechnology matures, it promises further breakthroughs, all while considering the essential ethical and safety considerations that accompany these advancements. The extraordinary utility of nanomaterials can be attributed to their minute dimensions, varied structures, and a plethora of advantageous biochemical and physicochemical attributes. Among these, metallic and metal oxide nanoparticles stand out as particularly superior. Their prominence is largely due to their expansive surface area-to-volume ratio, exceptional biocompatibility, adjustable synthesis methods, and robust stability, as detailed by **Chandrakala et al., 2016, andAhmed et al., 2022.** These inherent qualities have sparked significant enthusiasm among researchers, fueling extensive efforts in the development and synthesis of nanoparticles. This

heightened interest in metallic and metal oxide nanoparticles stems from their potential to revolutionize numerous fields by virtue of their unique properties and versatile applications.In pursuit of green synthesis and sustainable development, alternative methods are crucial. Physical and chemical synthesis methods, due to their environmental pollution, health risks and energy consumption, often fall short of being optimal (**Gilbertson, et al., 2015**). To address these concerns, the twelve green chemistry principles guide researchers toward environmentally friendly synthesis methods (**Kurowska-Susdorf et al., 2017, Ivanković et al., 2017,and Abdussalam-Mohammed et al., 2020**). Green synthesis methods prioritize environmental friendliness, safety, and superior performance over physical or chemical approaches(**Nadaroglu et al., 2017**). This approach relies on locally available, cost-effective, and easily sourced raw materials, significantly reducing nanoparticle production costs through energy efficiency and simplified processes (**Parveen et al., 2016 and Ramya et al., 2012**). In the realm of biosynthesis, three primary pathways are utilized—microorganisms, biomolecules, and plants. In these biogenic processes, natural compounds within plant and microbial extracts serve as both reducing and stabilizing agents, allowing for the conversion of metal sources into nanoparticles, as demonstrated in the work of **Nguyen et al., 2022 and Malik et al., 2023.** Green synthesis not only offers economic benefits but also minimizes the environmental impact, making it a preferred choice in nanoparticle production.

2. Biological Synthesis of Nanoparticles

The plant extract-based synthesis of nanoparticles is an emerging and versatile area of research. It holds promise for a wide range of applications in environmental remediation, pharmaceuticals, food, and cosmetic industries. Biological synthesis, often referred to as green synthesis, offers a sustainable, reliable, and environmentally friendly approach for producing metal and metal oxide nanoparticles. This method is valuable in mitigating the adverse impacts linked to conventional laboratory and industrial nanoparticle synthesis techniques. Nanoparticles exhibit size-dependent properties, with characteristics like surface area-to-volume ratio varying with size. At the nanoscale, metal oxides can confine electron motion due to their small dimensions. This allows for the fine-tuning of their band gaps, granting control over their light absorption and emission wavelengths. This unique property is of significant importance for applications in various fields, as it enables the customization of nanoparticle properties to meet specific requirements.Numerous investigations have delved into the synthesis and application of metal nanoparticles derived from various plant extracts, including Malvaparviflora, Drypetessepiaria, Aloe vera, Withaniasomnifera, Tinosporacordifolia, Jatropha curcas, Mushroom, Bauhinia racemose, Clitoriaternatea, and Solanum nigrum. These studies have been conducted by **Zayed et al., 2012,Narasaiah et al. 2017, S. Maensiri et al., 2008, Nagati et al., 2012, Jayaseelan et al., 2011, Bar et al., 2009, Eskandari-Nojedehi et al.,2018, N. Krithiga et al. 2015, Chouke et al.,2020, and Zheng et al., 2013.**These nanoparticles exhibit remarkable catalytic properties, including antibacterial, antifungal, antioxidant, photocatalytic and anticancer activities.Notably, biologically synthesized nanoparticles demonstrate superior efficiency in biomedical applications when compared to their physicochemical counterparts.Nanoparticles synthesized from a variety of metals, including Gold, Silver, Copper, Zinc, Iron, Titanium, Nickel, Palladium, Platinum, Aluminum, Tin, Indium, Ruthenium, Molybdenum, Bismuth, Cerium, Zirconium, and Magnesium, find extensive applications across a diverse range of field (**Mungole et al., 2021**). These applications encompass environmental remediation, drug

delivery, molecular sensing, and catalysis (**Falcaroet al., 2016**). Furthermore, they play crucial roles in the textile, medical, food packaging, water treatment, and biomedical research sectors(**Makvandi, et al., 2021,Sheikh et al., 2022, and Mujahid, et al., 2022). They** contribute to the development of medicines for anti-cancer and antimicrobial purposes against bacteria and viruses, while also exhibiting antioxidant activity (**Zafar et al., 2016, Abhimanyu et al., 2023 and Alavi et al., 2020).**The versatility and unique properties of these metal-based nanoparticles make them indispensable in addressing a multitude of challenges and enhancing various industries and scientific research endeavors.

3. Antimicrobial Properties of Zinc Oxide Nanoparticles

In this article, our primary objective is to provide an overview of the antimicrobial activities exhibited by Zinc Oxide nanoparticles (ZnO NPs) synthesized through green or biological routes using various plant extracts. Biologically synthesized ZnO nanoparticles have demonstrated superior effectiveness in several crucial applications, including antibacterial, anti-cancer, antioxidant, antifungal, and biomedical applications. A series of studies have investigated the antimicrobial potential of Zinc Oxide nanoparticles (ZnO NPs) synthesized using diverse plant extracts. These studies have demonstrated the ability of these nanoparticles to combat a wide range of microorganisms, including bacteria and fungi. The use of plant extracts in the synthesis process appears to enhance the antimicrobial properties of ZnO NPs, as observed in studies such as those by **Upadhyaya et al., 2018 and Kumar et al., 2020.** Additionally, the work of**Rokhum et al., 2020 and Dobrucka et al. 2017** revealed strong antibacterial and antifungal activities, underscoring the potential of these nanoparticles in medical and pharmaceutical applications. These findings collectively suggest that ZnO NPs hold promise as effective antimicrobial agents with possible therapeutic and industrial applications.In the study by **Upadhyaya et al., 2018** and **Kumar et al., 2020,** plant extracts played a significant role in the synthesis of ZnO NPs, influencing the antimicrobial properties of these nanoparticles. Upadhyaya and colleagues found that the inclusion of mehendi (henna) extract during synthesis enhanced the antibacterial properties of the nanoparticles. This suggests that the choice of plant extract can play a crucial role in tailoring the antimicrobial characteristics of ZnO NPs. Similarly, **Kumar et al., 2020** synthesized ZnO NPs using Cotoneasteracuminatus leaf extract, which resulted in nanoparticles exhibiting antimicrobial properties. This research implies the potential use of these nanoparticles in the development of medicinal products.The study by **Rokhumet al., 2020**demonstrated the successful synthesis of ZnO NPs using Tecomastans leaf extract. These nanoparticles displayed potent antibacterial properties against several bacterial strains and exceptional antifungal activity against fungal strains. The high zones of inhibition observed against Achromobacterspanius and Penicilliumcitirinum for bacterial and fungal strains, respectively, underline the efficacy of these nanoparticles as antimicrobial agents. This study highlights the potential applications of ZnO NPs in addressing microbial infections and fungal diseases.**Dobruckaet al., 2017** examined the antimicrobial efficacy of ZnO nanoparticles synthesized with trifoliumpratense flower extract. Their research evaluated the antimicrobial activity of these nanoparticles against clinical and standard strains of S. aureus and P. aeruginosa, as well as a standard strain of E. coli. The findings suggest that these biologically synthesized ZnO nanoparticles could find applications in both medical and pharmaceutical fields.In a similar vein, **Rahman et al., 2022**reported the successful synthesis of ZnO nanoparticles using Cocos nucifera leaf extract. These nanoparticles exhibited antimicrobial

activity against T. harzianum and S. aureus, two significant microbial targets. The potential utility of these nanoparticles in antibiotic development and the pharmaceutical industry was implied, further underscoring their versatile nature in tackling microbial infections. **Sivasankarapillaiet al., 2022** conducted research on ZnO nanoparticles synthesized using scopariadulcis plant extract, evaluating their antibacterial and antifungal activities. The nanoparticles displayed excellent antimicrobial activity against E. coli, Staphylococcus aureus, Candida albicans, and Aspergillus niger. Additionally, the nanoparticles exhibited high antioxidant activity. These findings indicate that ZnO NPs can serve dual purposes, as both antimicrobial and antioxidant agents, thus widening their potential applications in the medical and health sectors.The study by **Jatranaet al., 2022**synthesized ZnO nanoparticles using Mesuaferrea plant extract. These nanoparticles exhibited notable antibacterial and antifungal activity against Pseudomonas aeruginosa and Aspergillus awamorii. The report suggests that the observed antimicrobial effects are a result of the synergistic action of the ZnO nanoparticles and the plant extract. Furthermore, it hints at the presence of inherent medicinal properties within the Mesuaferrea plant.In the study conducted by **Kahsayet al., 2021,**the antimicrobial potential of Zinc Oxide nanoparticles (ZnO NPs) synthesized from Becium grandiflorum leaf extract was comprehensively examined. Their investigation encompassed a range of bacteria, including both gram-positive (e.g., Staphylococcus epidermidis) and gram-negative (e.g., Escherichia coli) species. The study's findings underscore the efficacy of these ZnO NPs in inhibiting bacterial growth, with notable variations observed in inhibition zones. A key mechanistic insight is provided, emphasizing the crucial role of Zn^{2+} ion release, which disrupts bacterial cellular functions, leading to the generation of reactive oxygen species (ROS) and subsequent oxidative stress. This research significantly contributes to our understanding of potential antimicrobial strategies, offering valuable prospects for addressing bacterial infections effectively.**R. Nivethithaet al., 2021**explored biosynthesized Zinc Oxide nanoparticles from Abieswebbiana extract, revealing potent antimicrobial activity against oral pathogens. These nanoparticles show promise as novel treatments for pathogenic oral diseases. While effective, further purification is needed to isolate the active extract components for large-scale, targeted drug delivery against a broad range of oral infections, making them a valuable addition to dental care advancements.In the study by **Amrita Rajet al., 2018,**green-synthesized Zinc Oxide nanoparticles (ZnO NPs) using Rosa indica leaves extract exhibited potent antimicrobial activity against both gram-positive and gram-negative bacteria. Notably, gram-positive bacteria were more effectively inhibited compared to gram-negative strains.**Urgeet al., 2023**studied the antimicrobial potential of zinc oxide nanoparticles synthesized through an eco-friendly method using garlic bulb and ginger extracts. Results reveal that a combination of both extracts yields ZnO nanoparticles with the highest inhibition zones against gram-negative Pseudomonas putida and gram-positive Streptococcus pyogenes. These findings suggest the synergistic effects of garlic and ginger, promising new avenues in antibacterial research.

Antibacterial activity has been explored through the synthesis of ZnO nanoparticles mediated by various plant extracts. These nanoparticles have shown significant potential in combating a wide spectrum of bacterial strains. Among the strains tested, Anisochiluscarnosus, Atalantiamonophylla, Polygala tenuifolia, Aspalathuslinearis, Carissa edulis, Averrhoa carambola, Pandanus tectorius, Scopariadulcis, Plumeria, Punicagranatum, andSaponaria officinalis have been found to be susceptible to the antibacterial effects of these nanoparticles. The antibacterial potential of ZnO nanoparticles has been documented in studies conducted by

various researchers, including **Anbuvannan et al., 2015, Vijayakumar et al., 2018, Nagajyothi et al., 2015,Diallo et al., 2015,Fowsiya et al., 2016,Chakraborty et al., 2020, Florence et al., 2022,Sivasankarapillai et al., 2022**, **Halanayake et al., 2021**, **Sukri et al., 2019, and Tănase et al., 2021.** Two recent studies have demonstrated the remarkable properties of Zinc Oxide (ZnO) nanoparticles. In the study conducted by **Abdelghany et al., 2023,** ZnO nanoparticles were found to exhibit significant antioxidant, anticancer, and antimicrobial activities against pathogenic microorganisms.In a separate study, published very recently by **Omran et al., 2023,** Zinc Oxide nanoparticles were synthesized using a green approach, employing an extract derived from Cyperusrotundus rhizomes. These nanoparticles were found to possess a wide range of applications, including their remarkable potential as antioxidants, antibacterial agents, anticancer agents, and as efficient photocatalysts.The findings from these two studies highlight the versatile and beneficial attributes of ZnO nanoparticles in various domains, ranging from health and medicine to environmental applications.

Conclusion:

In conclusion, the green synthesis of Zinc Oxide nanoparticles using plant extracts has shown promising antimicrobial efficacy. These nanoparticles exhibit broad-spectrum activity against bacteria and fungi, with the choice of plant extract significantly impacting their antimicrobial potential. This eco-friendly approach holds great promise in medical and pharmaceutical applications. Ongoing research in this field offers sustainable solutions for combating microbial infections and emphasizes eco-consciousness. Green-synthesized Zinc Oxide nanoparticles emerge as versatile tools to address diverse challenges in healthcare and industry, reflecting their potential for innovative, environmentally responsible advancements.

References:

1. Kargozar, S., &Mozafari, M. (2018). Nanotechnology and Nanomedicine: Start small, think big. Materials Today: Proceedings, 5(7), 15492-15500.
2. Malik, S., Muhammad, K., &Waheed, Y. (2023). Nanotechnology: A revolution in modern industry. Molecules, 28(2), 661.
3. Ghotekar, S., Pagar, T., Pansambal, S., &Oza, R. (2020). A review on green synthesis of sulfur nanoparticles via plant extract, characterization and its applications. Advanced Journal of Chemistry-Section B, 2(3), 128-143.
4. Chandrakala, V., Aruna, V., &Angajala, G. (2022). Review on metal nanoparticles as nanocarriers: Current challenges and perspectives in drug delivery systems. Emergent Materials, 5(6), 1593-1615.
5. Ahmed, S. F., Mofijur, M., Rafa, N., Chowdhury, A. T., Chowdhury, S., Nahrin, M., ...& Ong, H. C. (2022). Green approaches in synthesising nanomaterials for environmental nanobioremediation: Technological advancements, applications, benefits and challenges. Environmental Research, 204, 111967.
6. Gilbertson, L. M., Zimmerman, J. B., Plata, D. L., Hutchison, J. E., &Anastas, P. T. (2015). Designing nanomaterials to maximize performance and minimize undesirable implications guided by the Principles of Green Chemistry. Chemical Society Reviews, 44(16), 5758-5777.
7. Kurowska-Susdorf, A., Zwierżdżyński, M., Bevanda, A. M., Talić, S., Ivanković, A., &Płotka-Wasylka, J. (2019). Green analytical chemistry: Social dimension and teaching. TrAC Trends in Analytical Chemistry, 111, 185-196.

8. Ivanković A (2017) Review of 12 Principles of green chemistry in practice. Int J Sustain Green Energy 6:39. https:// doi. org/ 10. 11648/j.ijrse. 20170 603. 12

9. Abdussalam-Mohammed, W., Ali, A. Q., &Errayes, A. O. (2020). Green chemistry: principles, applications, and disadvantages. Chem. Methodol, 4(4), 408-423.

10. Nadaroglu, H., GÜNGÖR, A. A., &Selvi, İ. N. C. E. (2017). Synthesis of nanoparticles by green synthesis method. International Journal of Innovative Research and Reviews, 1(1), 6-9.

11. Parveen, K., Banse, V., &Ledwani, L. (2016, April). Green synthesis of nanoparticles: Their advantages and disadvantages. In AIP conference proceedings (Vol. 1724, No. 1). AIP Publishing.

12. Ramya, M., &Subapriya, M. S. (2012). Green synthesis of silver nanoparticles. Int J Pharm Med BiolSci, 1(1), 54-61.

13. Nguyen, N. T. T., Nguyen, L. M., Nguyen, T. T. T., Nguyen, T. T., Nguyen, D. T. C., & Tran, T. V. (2022). Formation, antimicrobial activity, and biomedical performance of plant-based nanoparticles: a review. Environmental Chemistry Letters, 20(4), 2531-2571.

14. Malik, A. Q., Mir, T. U. G., Kumar, D., Mir, I. A., Rashid, A., Ayoub, M., & Shukla, S. (2023). A review on the green synthesis of nanoparticles, their biological applications, and photocatalytic efficiency against environmental toxins. Environmental Science and Pollution Research, 1-28.

15. Zayed, M. F., Eisa, W. H., &Shabaka, A. A. (2012). Malvaparviflora extract assisted green synthesis of silver nanoparticles. SpectrochimicaActa Part A: Molecular and Biomolecular Spectroscopy, 98, 423-428

16. Narasaiah, P., Mandal, B. K., &Sarada, N. (2017). Biosynthesis of copper oxide nanoparticles from drypetessepiaria leaf extract and their catalytic activity to dye degradation. Iop Conference Series Materials Science and Engineering, 263, 022012.

17. S. Maensiri, P. Laokul, J. Klinkaewnarong, S. Phokha, V. Promarak, S. Seraphin, Indium oxide (In2O3) nanoparticles using Aloe vera plant extract: synthesis and optical properties, J. Optoelectron. Adv. Mater. 10 (2008) 161–165

18. V.B. Nagati, J. Alwala, R. Koyyati, M.R. Donda, R. Banala, P.R.M. Padigya, Green synthesis of plant-mediated silver nanoparticles using Withaniasomnifera leaf extract and evaluation of their anti-microbial activity, Asian Pac. J. Trop. Biomed. 2 (2012) 1–5.

19. C. Jayaseelan, A.A. Rahuman, G. Rajakumar, A.V. Kirthi, T. Santhoshkumar, S. Marimuthu, Synthesis of pediculocidal and larvicidal silver nanoparticles by leaf extract from heart leaf moon seed plant Tinosporacordifolia, Miers. Parasitol. Res.109 (2011)185–194.

20. H. Bar, D.K. Bhui, G.P. Sahoo, P. Sarkar, S. Pyne, A. Misra, Green synthesis of silver nanoparticles using seed extract of Jatropha curcas, Colloids Surf. A 348(1) (2009) 212−216.

21. M. Eskandari-Nojedehi, H. Jafarizadeh-Malmiri, J. Rahbar-Shahrouzi, Hydrothermal green synthesis of gold nanoparticles using mushroom (Agaricusbisporus) extract: physicochemical characteristics and antifungal activity studies, Green Process Synth. 7(1) (2018) 38-47.

22. N. Krithiga, A. Rajalakshmi, A. Jayachitra, Green synthesis of silver nanoparticles using leaf extracts of Clitoriaternatea and Solanum nigrum study of its antibacterial effect against common nosocomial pathogens, J. Nanosci. 2015 (2015) 928204:1-8.

23. Chouke, P. B., Potbhare, A. K., Dadure, K. M., Mungole, A. J., Meshram, N. P., Chaudhary, R. R., ... & Chaudhary, R. G. (2020). An antibacterial activity of Bauhinia racemosa assisted ZnO nanoparticles during lunar eclipse and docking assay. Materials Today: Proceedings, 29, 815-821.

24. Zheng B, Kong T, Jing X, Odoom-Wubah T, Li X , 47 Sun D, Lu F, Zheng Y, Huang JJ. Colloid Interface Sci., 48 2013; 396:138-145.

25. Mungole, A. J., Pawar, A. P., Sheikh, S., Pandhurnekar, H. C., Pandhurnekar, C. P., &Kanfade, H. P. (2021). BIOLOGICAL SYNTHESIS OF SILVER NANOPARTICLES FOR ANTIMICROBIAL APPLICATIONS: A SHORT REVIEW. Journal of Advanced Scientific Research, 12.

26. Falcaro, P., Ricco, R., Yazdi, A., Imaz, I., Furukawa, S., Maspoch, D., ...&Doonan, C. J. (2016). Application of metal and metal oxide nanoparticles@ MOFs. Coordination Chemistry Reviews, 307, 237-254.

27. Makvandi, P., Iftekhar, S., Pizzetti, F., Zarepour, A., Zare, E. N., Ashrafizadeh, M., ...& Rossi, F. (2021). Functionalization of polymers and nanomaterials for water treatment, food packaging, textile and biomedical applications: A review. Environmental Chemistry Letters, 19, 583-611.

28. Sheikh, S., Mungole, A. J., &Krambe, S. (2022). A Review on Plant Extract Mediated Biological Synthesis of Zinc Oxide Nanoparticles and Its Antimicrobial Applications. Int. J. Res. Biosci. Agric. Technol, 2, 286-289.

29. Mujahid, M. H., Upadhyay, T. K., Khan, F., Pandey, P., Park, M. N., Sharangi, A. B., ...& Kim, B. (2022). Metallic and metal oxide-derived nanohybrid as a tool for biomedical applications. Biomedicine & Pharmacotherapy, 155, 113791

30. Zafar, N., Madni, A., Khalid, A., Khan, T., Kousar, R., Naz, S. S., & Wahid, F. (2020). Pharmaceutical and biomedical applications of green synthesized metal and metal oxide nanoparticles. Current Pharmaceutical Design, 26(45), 5844-5865.

31. Abhimanyu, P., Arvind, M., & Kishor, N. (2023). Biosynthesis of CuO Nanoparticles Using Plant Extract as a Precursor: Characterization, Antibacterial, and Antioxidant Activity. Nano Biomedicine and Engineering.

32. Alavi, M., Kamarasu, P., McClements, D. J., & Moore, M. D. (2022). Metal and metal oxide-based antiviral nanoparticles: Properties, mechanisms of action, and applications. Advances in Colloid and Interface Science, 102726.

33. Upadhyaya, H., Shome, S., Sarma, R., Tewari, S., Bhattacharya, M., & Panda, S. (2018). Green synthesis, characterization and antibacterial activity of zno nanoparticles. American Journal of plant Sciences, 09(06), 1279-1291.

34. Kumar, G., Badoni, P., Khajuria, A., Singh, M., Tyagi, S., & Singh, N. (2020). Cotoneaster acuminatus leaf extract mediated synthesis, characterization and in vitro evaluation of antimicrobial activity of zinc oxide nanoparticles. Oriental Journal of Chemistry, 36(6), 1043-1048.

35. Rokhum, S., Biswas, A., Changmai, B., Vanlalveni, C., Lalfakzuala, R., &Nath, S. (2020). Biosynthesis of triangular-shape zno nanoparticles using tecomastans and its antimicrobial activity.

36. Dobrucka, R., Długaszewska, J., &Kaczmarek, M. (2017). Cytotoxic and antimicrobial effects of biosynthesized zno nanoparticles using of chelidoniummajus extract. Biomedical Microdevices, 20(1).

37. Rahman, F., Patwary, M., Siddique, M., Bashar, M., Haque, M., Akter, B., …& Uddin, A. (2022). Green synthesis of zno nanoparticles usingcocosnuciferaleaf extract: characterization, antimicrobial, antioxidant, and photocatalytic activity.

38. Sivasankarapillai, V., Krishnamoorthy, N., Eldesoky, G., Wabaidur, S., Islam, A., Dhanusuraman, R., &Ponnusamy, V. (2022). one-pot green synthesis of zno nanoparticles using scopariadulcis plant extract for antimicrobial and antioxidant activities. Applied Nanoscience

39. Jatrana, A., Chauhan, S., Maan, S., &Kayasth, M. (2022). Green synthesis of zno nanoparticles using mesuaferrea leaves extract and its antimicrobial activity. Current Journal of Applied Science and Technology, 29-34.

40. Kahsay, M.H. Synthesis and characterization of ZnO nanoparticles using aqueous extract of Becium grandiflorum for antimicrobial activity and adsorption of methylene blue. Appl Water Sci 11, 45 (2021).

41. Nivethitha, R., Jeevitha, M., Rajeshkumar, S., &Jayaraman, S. (2021). antimicrobial activity of zinc oxide nanoparticles synthesized using leaves extract of abieswebbiana. Journal of Pharmaceutical Research International, 3702-3710.

42. Raj, A. and Lawerence, R. (2018). Green synthesis and charcterization of zno nanoparticles from leafs extracts of rosaindica and its antibacterial activity. Rasayan Journal of Chemistry, 11(3), 1339-1348.

43. Urge, S., Dibaba, S., &Gemta, A. (2023). Green synthesis method of zno nanoparticles using extracts of zingiberofficinale and garlic bulb (allium sativum) and their synergetic effect for antibacterial activities. Journal of Nanomaterials, 2023, 1-9.

44. Anbuvannan, M., Ramesh, M., Viruthagiri, G., Shanmugam, N., &Kannadasan, N. (2015). Anisochiluscarnosus leaf extract mediated synthesis of zinc oxide nanoparticles for antibacterial and photocatalytic activities. Materials Science in Semiconductor Processing, 39, 621-628.

45. Vijayakumar, S., Mahadevan, S., Arulmozhi, P., Sriram, S., &Praseetha, P. (2018). Green synthesis of zinc oxide nanoparticles using atalantiamonophylla leaf extracts: characterization and antimicrobial analysis. Materials Science in Semiconductor Processing, 82, 39-45.

46. Nagajyothi, P., Ju, S. G., Yang, I. J., Sreekanth, T., Kim, K. J., & Shin, H. M. (2015). Antioxidant and anti-inflammatory activities of zinc oxide nanoparticles synthesized using polygala tenuifolia root extract. Journal of Photochemistry and Photobiology B: Biology, 146, 10-17.

47. Diallo, A., Ngom, B., Park, E., &Mâaza, M. (2015). Green synthesis of zno nanoparticles by aspalathuslinearis: structural & optical properties. Journal of Alloys and Compounds, 646, 425-430.

48. Fowsiya, J., Madhumitha, G., Al-Dhabi, N. A., &Arasu, M. V. (2016). Photocatalytic degradation of congo red using carissa edulis extract capped zinc oxide nanoparticles. Journal of Photochemistry and Photobiology B: Biology, 162, 395-401.

49. Chakraborty, S., Farida, J. J., Simon, R., Kasthuri, S., & Mary, N. (2020). Averrhoecarrambola fruit extract assisted green synthesis of zno nanoparticles for the photodegradation of congo red dye. Surfaces and Interfaces, 19, 100488.

50. Florence, S., Manna, C., Prabha, K., Bakri, M., Hagazy, R., Sowjanya, M., …&Shariq, M. (2022). Antibacterial activity of biosynthesized znonanoflakes using pandanustectorius leaf extracts. Journal of Optoelectronic and Biomedical Materials, 14(2), 35-41.

51. Sivasankarapillai, V., Krishnamoorthy, N., Eldesoky, G., Wabaidur, S., Islam, A., Dhanusuraman, R.,&Ponnusamy, V. (2022). One-pot green synthesis of zno nanoparticles

using scopariadulcis plant extract for antimicrobial and antioxidant activities. Applied Nanoscience.

52. Halanayake, K., Kalutharage, N., &Hewage, J. (2021). Microencapsulation of biosynthesized zinc oxide nanoparticles (zno-nps) using plumeria leaf extract and kinetic studies in the release of zno-nps from microcapsules. Sn Applied Sciences, 3(1).

53. Sukri, S., Shameli, K., Wong, M., Teow, S., Chew, J., & Ismail, N. (2019). Cytotoxicity and antibacterial activities of plant-mediated synthesized zinc oxide (zno) nanoparticles using punicagranatum (pomegranate) fruit peels extract. Journal of Molecular Structure, 1189, 57-65.

54. Tănase, M., Marinescu, M., Oancea, P., Raducan, A., Mihaescu, C., Alexandrescu, E., …&Cinteza, L. (2021). Antibacterial and photocatalytic properties of zno nanoparticles obtained from chemical versus saponaria officinalis extract-mediated synthesis. Molecules, 26(7), 2072.

55. Abdelghany, T. M., Al-Rajhi, A. M., Yahya, R., Bakri, M. M., Al Abboud, M. A., Yahya, R., & Salem, S. S. (2023). Phytofabrication of zinc oxide nanoparticles with advanced characterization and its antioxidant, anticancer, and antimicrobial activity against pathogenic microorganisms. Biomass Conversion and Biorefinery, 13(1), 417-430.

56. Omran, A. M. (2023). Characterization of green route synthesized zinc oxide nanoparticles using Cyperusrotundus rhizome extract: Antioxidant, antibacterial, anticancer and photocatalytic potential. Journal of Drug Delivery Science and Technology, 79, 104000.

Benzimidazole Synthesis with Ionic Liquid Catalysts: A Greener Path to Derivative Formation

1Manoj P Palve, 2Jaysing M Dinore, 3Pritam A Mule

1,2,3Department of Chemistry, Indraraj Arts, Commerce and Science College, Sillod.Dist: ChhatrapatiSambhaji Nagar. Maharashtra. Pin: 431112.

Corresponding author E-mail Id:manojpalve999@gmail.com

Abstract:

In the present study we report ionic liquid (NMPyTs) which is efficient and environmentally begin catalyst for the synthesis of benzimidazoles and its derivatives. The products were obtained by the treatment of substituted orthophenylenediamines and aldehydes at room temperature. Green reaction conditions, high quantitative yields and the easy isolation of products, easy separation and recovery of the catalyst and short reaction times are some of the advantages of our procedure.

Keyword:- Aryl aldehyde, orthophenylenediamines, Ionic liquid, benzimidazoles.

1. Introduction:

Heteroaromatic rings are essential because they provide similarity with respect to the biologicallyactive compounds within our body for e.g. all the nucleic acids, hormones, neurotransmitters, which constitute one or the other heteroaromatic ring. Among many heteroaromatic rings present, fused and pendent benzimidazoles are also ubiquitous featureofmanypharmaceutical products. Heterocyclic compounds possessing two hetero atoms in a ring are of massive biological importance in clinical research field. Heterocyclic compounds possess acyclic structure with two or more differentkinds of atoms in the ring. These type ofcompounds are very widely distributed in nature and are essential to life, playing avital role in the metabolism of all living cells e.g. the pyrimidine and purine bases of the genetic material DNA, the essential amino acids proline, hisitidine, the vitamins and coenzymes etc. There are a vast number of pharmacologically active heterocyclic compounds, many of which are in regular clinical use. A wide range of synthetic and naturally occurring heterocyclic compounds find their use in medicine and also aspesticides, agrochemicals, polymers etc,paving the way for considerable amount ofresearch leading to new heterocyclic molecules having an array of biologicalactivities. Among such heterocycles of importance, benzimidazoles have occupied a distinct place in medicinal chemistry. The benzimidazole ring system is an important pharmacophore in medicinal chemistry and modern drug discovery [1].The interest in benzimidazole as chemotherapeutic agent was realized whenin 1950 it was found that 5, 6-dimethyl-1-(D-ribofuranosyl) benzimidazole was an integral part of the structure of Vitamin B12. Benzimidazole derivatives possesses broad spectrum of biological activities, rangingfrom widely used human and veterinary anthelmintic [2] to anticancer properties[3]. Several reviews appeared in literature which discusses anarray of biological properties of benzimidazole nucleus [4]. Along with this, benzimidazole derivatives with different pharmacological properties such as, anti-ulcer [8], cardiotonic [11],antihypertensive [12], antibacterial and antiviral [13] antitumor [14] antiallergetic [16]have already been reported. In literature, it was revealed that the substitution at 1, 2, and 5 positions ofbenzimidazole nucleus is crucial pointwhereby it can exhibit wide range ofpharmacological activities. Benzimidazole derivatives exhibit various effects, in both type and strength upon the central nervoussystem, including psychostimulant,

narcoleptic, antidepressant, tranquilizer (anxiolytic), anticonvulsant, and hypnotic action [21]. The benzimidazole is a bicyclicaromatic imidazole ring system, where a benzene ring is fused to the 4 and 5-position of the imidazole ring [22]. Benzimidazoleare also called by other names such as benziminazole and 1,3benzodiazole.They possess both acidic and basiccharacteristics. The NH group present inbenzimidazoles is relatively strongly acidic and also weakly basic.

2.Experimental
2.1 Material and Methods

All products are knowncompounds and their physical data; IR and 1H NMR spectra were essentiallyidentical with those of authenticsamples.Reagents and aldehydes used in the experiments were sourced from commercial suppliers without prior purification. Melting points were determined using an open capillary apparatus and were reported without correction. The reactions were tracked using thin-layer chromatography (TLC). Infrared (IR) spectra were obtained using a Perkin-Elmer FT spectrophotometer with KBr discs, while 1H NMR spectra were recorded on a Varian 300 MHz spectrophotometer with DMSO-d6 as the solvent and TMS as the internal standard.

2.2 Procedure for the preparation of ionic liquid N-methyl pyridiniumtosylate (NMPyTs)

The ionic liquid was synthesized in accordance with a previously documented procedure. In a 25 mL round-bottom flask, methyl-4-toluene sulfonate (1 mol) was combined with pyridine at room temperature, with pyridine being added drop by drop while vigorously stirring. Following the reaction's completion, the mixture was stirred for an additional 2 hours. The resulting ionic liquid, denoted as NMPyTs, was then filtered and subjected to ethyl acetate washing to eliminate any unreacted reagents. Subsequently, it was dried. The physical properties of the obtained ionic liquid closely matched those reported in the literature.

2.3 General Procedure for the Synthesis of Benzimidazoles

The aldehyde (1 mmol), asubstitutedortho-phenylenediamine (1.05 mmol) and methanol (5 ml) were added to a 25 ml round-bottom flask equipped with magnetic stirrer. To this solution, Ionic Liquid NMPyTs(0.05 mmol) was added and stirred for the appropriate time at room temperature. Then the reaction mixture was extracted with ethyl acetate. The organic phase was washed with water and dried Na_2SO_4. The solvent was removed in vacuum to give the crude product which was recrystallized from hot methanol.
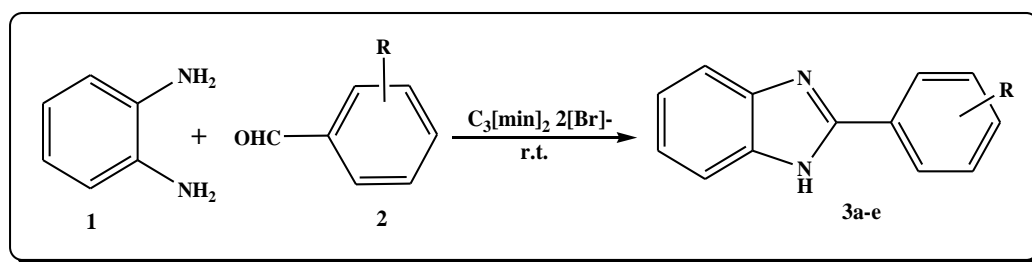
Fig.1 Synthesis of benzimidazole derivatives catalyzed by Ionic Liquid ($C_3[min]_2 2[Br]^-$).

3. Result and Discussion

This study introduces a novel synthetic pathway for the synthesis of benzimidazole derivatives, employing NMPyTs as a highly efficient and recyclable catalyst. Following the synthesis of the catalyst, a model reaction was designed to optimize various parameters, including the catalyst quantity, solvent, and reaction temperature. This model reaction involved

the condensation of orthophenylenediamine 1 (1mmol) and aromatic aldehyde 2 (1.05mmol) in 5 mL of methanol.

Table 1: Model reaction of o-phenylenediamine (1.0mmol) withbenzaldehyde (1.05mmol) by using different amounts of catalystNMPyTsat room temperature.

Entry	Amount of catalyst (%)	Reaction time (Minutes)	Yield (%)[a]
1	-	180	-
2	5	90	70
3	10	70	85
4	15	60	95
5	20	60	95

[a]Isolated yield.

The optimization of the reaction involved varying the catalyst quantity, with the model reaction chosen as the condensation between o-phenylenediamine 1 and benzaldehyde 2a. Initially, a control reaction was performed without any catalyst, and even after 180 minutes, no product was observed (Entry 1, Table 1). Subsequently, the model reaction was conducted again with different amounts of NMPyTs, specifically 5, 10, 15, and 20 mol%. The best outcome, yielding a 95% product (3a) was achieved using a 15% catalyst amount (Table 1, entry 4). Employing these optimized conditions, various benzimidazole derivatives 3a-e were efficiently synthesized in shorter reaction times and high yields using NMPYTs as the catalyst. It's noteworthy that a 20 mol% catalyst did not lead to a reduction in reaction time or an enhancement in yield. The use of ionic liquids as a reaction medium proved beneficial by improving reactant solubility and reducing by-product formation. Additionally, ionic liquids facilitated the separation and purification of the product.

Next we concentrate our attention over choice of best solvent for the synthesis of benzimadazol derivatives in presence of 1 mol % of NMPTs catalyst. The choice of solvent is a crucial factor in chemical reactions, as it can significantly impact reaction rates, yields, and the environmental sustainability of the process. The model reaction was repeated in several solvents, and the results were compared to determine the most suitable solvent for this transformation.The results of our study indicated that the methanol is the best choice of solvent for benzimidazole synthesis (95% yield) using NMPyTs as the catalyst.
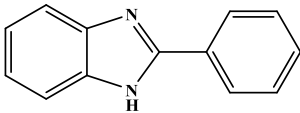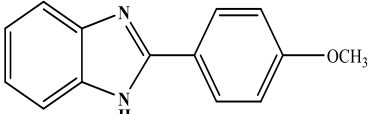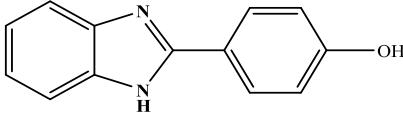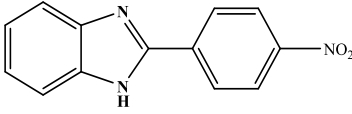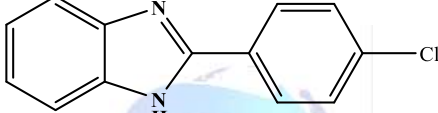
Table 2 : Effect of solvents on the reaction yield.

Entry	Solvent	Time (minutes)	Yield[b]%
1	H_2O	185	Trace
2	Ethanol	90	84
3	Acetonitrile	110	62
4	Methanol	60	95

[b]Isolated

A wide range of aromatic aldehydes weresubjected to prove the general applicability of our presentprocedure which is summarized in Table 3. It was observedthat the aromatic aldehyde bearing an electron-donatingsubstituent as well as electron-withdrawing substituent underwent the reaction smoothly to give high yields of the corresponding products. (Table 3). It indicates the method's robustness and versatility in accommodating a wide range of substrates.

Table 3.Preparation of benzimidazole derivatives using Ionic Liquid NMPyTs.

Entry	Aldehyde	Product	Melting Point (°C)	Yield (%)
1	C_6H_5-CHO	a	292-293	95
2	4-MeO-C_6H_4-CHO	b	220-222	92
3	4-HO-C_6H_4-CHO	c	241-243	90
4	4-NO_2-C_6H_4-CHO	d	311-315	96
5	4-Cl-C_6H_4-CHO	e	289-291	94

Spectral Data:

3 a. 2-Phenyl-1Hbenzo[d]imidazole:

M.P.294–295ºC. 1H NMR: (300 MHz, CDCl3): δ 7.23–7.26 (m, 2H),δ 13.06 (s, 1H,NH), 7.56 (dd, J = 21.2,13.6 Hz, 5H), 8.10 (d, J = 4.0 Hz, 2H), 10.92 (s, 1H); 13CNMR (100 MHz, DMSO-d6): δ 151.18, 143.78, 134.96,130.14, 129.79, 128.90, 126.40, 122.49, 121.62, 118.84,111.28; ESI-MS (m/z): 195.1 [M + H]+.

Conclusion:

Here we have used ionic liquid NMPyTs, as green catalyst for the synthesis of benzimidazoles. The easy work-up procedure, lack of chromatographic separation and very good yields make this method a validcontribution to the existing methodologies.Compared with other ways of synthesis of benzimidazoleit was found that ionic liquid worked well and the conversion found take place rapidly giving excellent yield.

References:

1. Ouattara M., Sissouma D., Kone M.W., Menan H.E., Toure S.A. and Ouattara L., Trop. J. Pharm. Res., 2011; 10: 767-775.
2. Brown, K. L. Chemical Review on Vit B12, Chem. Rev.2005,105, 2075.
3. Baliharova, V.; Skalova, L.; Mass, R. F. M.; De-Vrieze, G.; Bull, S.; Fink-GremmelsJ. Res. Vet. Sci.2003,75, 61.
4. Habib, N. S.; Soliman, R.; Ashour, F. A.; El-Taiebi, M.Pharmazie, 1997, 52, 746.

5. Sharma, S.; Abuzar, S.Prog. Drug Res.1983, 27, 85.

6. Li, X. C.; Widdop, R. E.Hypertension, 1995, 26, 989. (b) Wright, J. B.Chem. Rev.1951,48, 397.

7. Hubschwerlen, C.; Pflieger, P.; Specklin, J. L.J. Med. Chem.1992, 35, 1385.

8. Chen, A. Y.; Yu, C.; Bodley, A.Cancer Res.1993, 53, 1332.

9. Daugel-Dauge, N. O.; Dumev, A. D.; Kulakova, A. V.; Vestn. Ross.Akad.Med. Nauk1995,1, 29

10. Sala, M.; Braida, D.; Calcaterra, P.Eur. J. Pharmacol. 1992,217, 37.

11. Townsend, L. B.; Wise, D. S.Parasitology, Today, 1990,6 (4),107.

12. Elderfield, R. C. Ed.Heterocyclic Compounds; John Wiley and Sons, Inc.:New York,1975;Vol. 5.

Green Synthesis, Characterization and Biological Activity of Transition Metal Complexes of Novel Schiff Base Ligand

S S Sonune[1], S P Moharir[2*], M.G.Undegaonkar[3], S N Sinkar[4], A.S.Kirdant[5].

[1,2]Department of Chemistry, Siddharth Art's, Commerce and Science College Jafrabad Dist. Jalna[3]Department of Chemistry; ASC College Badnapur, Dist. Jalna (M.S) India.
[4]M.S.S. Art's, Commerce and Science CollegeAmbad Dist. Jalna
[5]Department of Chemistry, Vasant college kaij, Dist. Beed (M.S) India.
Corresponding author email: sharad9939moh@gmail.com.

Abstract-

Novel Schiff base ligand was synthesized by using Scientific Microwave oven. The Schiff base 2,6-dimethoxy-4-(1-(1-methyl-1H-benzo[d]imidazol-2-ylimino)ethyl)phenol was derived from 2-amino-1-methyl benzimidazole with 3,5-dimethoxy-4-hydroxy acetophenone followed by its metal complexes. The metal salts used are Ni(II) chloride and Mn(II), Fe(III), Cd(II), Cu(II), Zn(II), Co(II), Ag(I) nitrate. The metal complexes characterized by UV-Visible spectroscopy, IR spectroscopy, and thermo gravimetric analysis. The metal complexes exhibit coordination number 6, so metal complexes exhibit octahedral geometry. The complexes are colored and stable in air. The antimicrobial activity of synthesized metal complexes show a good activity against the gram -positive bacteria Staphylococcus aureus, Gram-negative bacteria Salmonella Typhi and fungi Aspergillus Niger . The antimicrobial results also indicate that the metal complexes are better antimicrobial agents as compared to the novel Schiff base ligand.

Keywords: Biological activity, Escherichia coli, Microwave method, Staphylococcus aureus, Salmonella Typhi.

Introduction-

Novel Schiff bases have been studied in the field of coordination Chemistry due to their superficial synthesis, easily availability, electronic properties and good solubility in common solvents[1].The co-ordination chemistry of nitrogen-oxygen donor ligands is an interesting area of research. Such ligands and their complexes due to a better understanding of metal protein binding have been of great interest for many years [2].

Microwave-assisted synthesis belongs to green chemistry due to so many factors like less reaction time, maximum yield etc. The application of microwave assisted synthesis on organic, organometallic and co-ordination chemistry continues to develop at an astonishing pace [3]. Microwave-assisted reaction under solvent free or less solvent condition offer reduced pollution, low cost and better yield and ease in processing and handling [4].In microwave assisted organic synthesis, accidents during boiling, toxic and poisonous solvents are frequently avoided [5-6]. The use of microwave irradiation for the synthesis of drugs and organic compounds has proved to be effective, safe and environmentally nonthreatening techniques with shorter reaction time [7]. The prominent features of microwave irradiation technique are shorter reaction times, simple reaction conditions and enhancements in yields [8]. Compounds containing azomethine group (-HC=N-) are known as Schiff base [9]. They are condensation products of ketones or aldehydes with primary amines and were first reported by Hugo Schiff in 1864[10]. Schiff bases are biological active compounds and shows a lot of biological activities such as anticancer[11], plant growth inhibitors[12], insecticidal[13], antidepressant[14],antibacterial[15],anti-inflammatory[16],anti-tuberculosis[17], antimicrobial[18] and anticonvulsant activity[19].

In the present paper, we have described the coordination behaviour of novel Schiff base towards some transition elements, which may help in more understanding of the mode of chelation of ligands toward metals.

1. Experimental Section

1.1 Material and Methods

Metal salts Mn(II)Chloride, Fe(III)Nitrate, Co(II)Nitrate, Ni(II)Nitrate, Cu(II)Nitrate, Zinc(II) Nitrate, Cd(II)Nitrate, Ag(I)Nitrate were purchased from Loba Chem & Merck. All the chemicals were used as received. The Schiff base 2,6-dimethoxy-4-(1-(1-methyl-1H-benzo[d]imidazol-2-ylimino)ethyl)phenol, synthesized by Sonune et al in scientific microwave oven.

2- amino-1- methyl benzimidazole

3,5-Dimethoxy-4-hydroxy acetophenone

2,6-dimethoxy-4-(1-(1-methyl-1*H*-benzo[*d*]imidazol-2-ylimino)ethyl)phenol
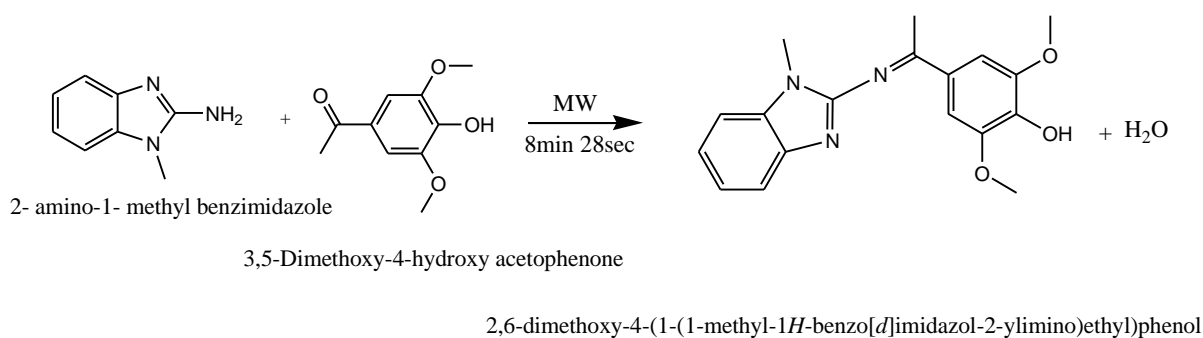
Fig. 1 S SSonune et al [20]

1.2 Technique:

Melting point of all metal Complexes were determined on melting point apparatus. FT-IRmeasurements were recorded on Shimadzu- 8300 spectrophotometer in range of (4000-400 cm^{-1}) as KBr disc. Electronic spectra were recorded using UV-Vis spectrophotometer type CECIL with quartz cell of (1cm) path length in range (200-1000)nm in ethanol at room temperature.For determing mass,The TGA were carried out in dynamic nitrogen atmosphere 30 ml/min with heating rate of 10°C/min using Perkin Elmer thermal analyser.

2.3Synthesis of Metal Complexes:

2mmol of novel ligand [L1]and 1 mmolof each metal salt are mixed together properly in mortarand pestle. The mixture was kept for some time. Then the mixture is kept in scientific microwave oven. The mixture was irradiated periodicallyon 750 Volt and the time required was in the range of 6 sec to 440 sec. The formation of compound was confirmed by TLC and melting point. The final products were washed with hot ethanol, filtered and dried at room temperature. The metal salts used are Ni(II), Mn(II), Fe(III),Cd(II), Cu(II), Zn(II), Co(II) &Ag(I).

2.4Study of Biological Activity

The antimicrobial Activity of metal complexes was determined by the agar well diffusion. The bacteria strains used are gram positive staphylococcus aureus, gram negative salmonella typhi and Aspergillus niger fungi were used. They were maintained on nutrient agar using ethanol as a solvent .The concentration of compounds in this method was 10-³ m by using disc sensitivity test. The plates were incubated aerobically at 37°Cto 24 hours and antimicrobial activity was checked by measuring the inhibition halo of microbial growth around the well. This method involves the exposure of the zone inhibition towords the diffusion of micro-organism agar plate.

3. Resultsand Discussion

The aim of present study is to synthesize, characterization and bioactivity study of N(II), Mn(II), Fe(III), Cd(II), Cu(II), Zn(II),Co(II), Ag(I) complexes. Electronic absorption and IR analysis are used for determing the structure. With this melting point also useful all the metal complexes are having melting point less than 350℃. By repeating the synthesis process the results were checked [21].All the metal complexes are soluble in DMSO.All the metal complexes and ligand shows biological activity.

3.1 Physical properties

Table 1

Sr.No.	Molecular Formula	Colour	M.P.	Time	Yield %
1	$[(C_{18}H_{19}N_3O_3)_2]$	Faint Orange	119^0C	8 min 25 Sec.	75.80
2	$[(C_{18}H_{19}N_3O_3)_2(H_20)_2]Ni$	Grenish Black	150^0C	2min 36 Sec.	60
3	$[(C_{18}H_{19}N_3O_3)_2(H_20)_2]Mn$	Brown	280^0C	3 min 20 Sec.	70
4	$[(C_{18}H_{19}N_3O_3)_2(H_20)_2]Fe$	Black	240^0C	7 min 20 Sec.	65
5	$[(C_{18}H_{19}N_3O_3)_2(H_20)_2]Cd$	Purple	140^0C	6 Sec.	75
6	$[(C_{18}H_{19}N_3O_3)_2(H_20)_2]Cu$	Bluish Black	260^0C	2min 40 Sec.	80
7	$[(C_{18}H_{19}N_3O_3)_2(H_20)_2]Zn$	Faint Brown	220^0C	20 Sec.	50
8	$[(C_{18}H_{19}N_3O_3)_2(H_20)_2]Co$	Rose red	210^0C	3min10 Sec.	65
9	$[(C_{18}H_{19}N_3O_3)_2(H_20)_2]Ag$	Faint Orange	139^0C	1min30 Sec.	50

3.2Infrared Spectral Analysis

Table 2

Sr.no.	Ligand/comlex	V(C=N)	V(M-N)	V(C=C)	V(C-H)	V(H20)
1	$(C_{18}H_{19}N_3O_3)_2$	1675	_____	1482	3058	
2	$[(C_{18}H_{19}N_3O_3)_2(H_20)_2]Co$	1607	490	1507	3005	3605
3	$[(C_{18}H_{19}N_3O_3)_2(H_20)_2]Ag$	1668	475	1503	2999	3630

For determine the nature of Functional group attached to functional group the IR spectra is useful. It gives valuable information about Functional group.

IR spectral study of Co complex: Co Complex shows azomethine stretching at1607cm^{-1}. This azomethine stretching vibration observed at1675 cm^{-1} in parent ligand. The (C=C) in aromatic ring stretching vibration of metal complex of Co observed at 1507 cm-1,this stretching vibration observed atb1482 cm^{-1} in parent ligand. The (C-H) stretching vibration present in aromatic ring observed at 3005 cm^{-1}while this stretching vibration observed at 3058 cm^{-1} in parent ligand.The metal nitrogen stretching vibration at 490 cm^{-1} observed for complex of Co ,this stretching vibration indicates bonding of metal with nitrogen.This (M-N) stretching vibration is not observed in parent ligand.This confirms the formation of metal complexe.

IR spectral study of Ag complex: The characteristic azomethine (C=N) stretching vibration for metal complex of Ag observed at 1668 cm^{-1} while this azomethine stretching vibration seen at 1675 cm^{-1}in parent ligand [22-24]%.The (C=C) stretching vibration of aromatic ring observed at 1482 cm^{-1} while this stretching vibration observed at 1503 cm^{-1} in parent ligand.The (C - H) stretching vibration of aromatic ring observed at 2999cm^{-1}while this stretching vibration observed at 3058 cm^{-1}.The characteristic (M-N) stretching vibration observed at 450 cm^{-1} in metal complex which is absent in parent ligand.This confirms the formation metal complex.

3.3 UV–VIS Studies of Metal Complexes

The electronic spectral of π-π* and n-π* transition of metal complexes were recorded in the region of 200 to 800 nm in DMSO [25].

Table 3

Sr.no.	Metal complexe	Wave length	Assignment	Geometry
1	$[(C_{18}H_{19}N_3O_3)_2(H_2O)_2]Co$	270 320	π-π* n-π*	Octahedral
2	$[(C_{18}H_{19}N_3O_3)_2(H_2O)_2]Ag$	270 320	π -π* n-π*	Octahedral

Thermogravimetric analysis

Table 4

TGA data for L1Co		TGA data for L1Ag	
Weight loss %	Temperature	Weight loss %	Temperature
0	30.59	0	32.90
10	200.00	10	225.00
20	211.25	20	275.00
30	225.00	30	330.00
40	331.99	40	370.27
50	338.00	50	410.00
60	355.01	60	445.70
70	371.00	70	460.90
80	488.00	80	478.90
82.45 (Total weight loss)	500	86.54 (Total weight loss)	500

Thermo gravimetricanalysis of the Complexes was carried out in the temperature range from room temperature up to 500^0C. The heating is carried out in the dynamic nitrogen atcnosphere. Heating rate was controlled at 10^0C/ min^{-1}

The ligand –Co complex thermogram clearly shows, Total weight loss of 79.50%. In First step water of Crystallization got removed in the range of 30.20^0C to 199^0C with 10% weight loss observed. After this weight loss of water of crystallization loss of organic moiety look place with total weight loss of 70 % up to 471^0C

A Stable curve indicates formation of stable metal oxide.

The ligand – Ag complex thermogram clearly shows, total weight loss of 80.10% in first step.Water of crystallization got removed in the range of 34.80^0C to 180^0C with 10% weight loss observed. After this weight loss of 80% up to 450.18^0C, A stable curve indicate formation of stable metal oxide

3.4 Biological Activity Study

Table 5Diameter -Zone of inhibition diameter is measured in mm

Sr.no.	Ligand/Complex	Salmonella typhi	Satyphlpcoccus Aureus	Aspergillus Niger
1	$(C_{18}H_{19}N_3O_3)_2$	9.1	11.7	15.4
2	$[(C_{18}H_{19}N_3O_3)_2(H_20)_2]Ni$	8.7	12.1	8.0
3	$[(C_{18}H_{19}N_3O_3)_2(H_20)_2]Mn$	NZ*	NZ*	NZ*

4	$[(C_{18}H_{19}N_3O_3)_2(H_20)_2]Fe$	8.9	8.1	NZ*
5	$[(C_{18}H_{19}N_3O_3)_2(H_20)_2]Cd$	25.1	20.6	25.3
6	$[(C_{18}H_{19}N_3O_3)_2(H_20)_2]Cu$	9.0	7.7	NZ*
7	$[(C_{18}H_{19}N_3O_3)_2(H_20)_2]Zn$	8.6	13.6	NZ*
8	$[(C_{18}H_{19}N_3O_3)_2(H_20)_2]Co$	11.1	16.5	NZ*
9	$[(C_{18}H_{19}N_3O_3)_2(H_20)_2]Ag$	14.3	11.3	NZ*

Bi dentate Schiff base ligand synthesized by the condensation of 2-amino–1-methyl benzimidazole with 3,5-dimethoxy-4-hydroxyacetophenone. And ist Ni(II), Mn(II), Fe(III), Cd(II), Cu(II), Zn(II), Co(II) & Ag(I) complexes showed biological activities against the gram positive bacteria staphylococcus aureus, gram negative bacteria salmonella typhi ad Aspergillus Niger fungi. The bacteria like staphylococcus aureus,salmonella typhi and Aspergillus Niger fungi which were grown Overnight at 37℃ [26-27].The all metal complexes with novel Schiff base ligand (L1) showed inhibition diameter against the gram positive bacteria staphylo coccus qureus. The all metal complexes and Ligand also shows inhibition diameter against the gram negative bacteria salmonella typhi. With Aspergillus niger Fungi the biological activity observed.The novel schiff base ligand L1 shows zone of inhibition 9.1,11.7,15.4 for salmonella typhi, staphylococcus aureus and aspergillus Niger fungi respectively.These values indicates that novel schiff base ligand L1 shows good antibacterial activity.Metal complex of Ni and Cd both shows very nice biological activity against staphylococcus aureus, salmonella typhi and aspergillus Niger fungi.The metal complexe of Cd shows largest zone of inhibition as compared to other metal complexes. This Cd complexe shows zone of inhibition 25.1,20.6 and 25.3 for salmonella typhi, staphylococcus aureus and aspergillus Niger fungi respectively.The metal complexes of Cu,Zn,Coand Ag shows good antibacterial activity but they did not showed the zone'of inhibitionfor aspergillus Niger fungi.In short all the metal complexes shows good antibacterial activity.

References:

1. M.Srasvanthi,et al Green route for efficient synthesis of biologicaly active Schiff base ligand derived from 2- hydroxy Acetophenone.Structural, spectroscopic,anti- microbial and molecular modelling studies.International research journal of pharmacy (2019)10(3):215-220.https://Dx.doi.org/10.78797/2330-8407.1003107

2. Vahabi.V and Hatamjafarif, microwave assisted convenient one pot synthesis of coumarin derivatives via pechmann condensation catalysed by FeF3 under solvent free condition and antimicrobial activites of the product molecule,(2014),19,13093-13103

3. V.Polshettiwar.Aqueous Microwave Assisted Chemistry: Synthesis and Catalysis, 2010, Royal Society of Chemistry,ISBN 978-1-84973-038-9, Cambridge,UK.

4. Sadashiv N Sinkar et al, solvent free synthesis, characterization and biological activity of transition metal complexs of Schiff base ligand derived from 2 aminobenzimidazole with 4',4'dibromobenzil.letters in applied nanobioscience platinum open Access Journal (ISSN:2284-6808). https://doi.org/19.33263/LIANB5113.38343842.

5. K Mahajan,N .Fahmi,R V. Singh, Indian J. Chem,A46(2007)1221

6. K Sharma,R.singh,N.Fahmi,R V Singh,Sectrochim,Acta,A 75(2010) 422

7. K Mahajan,B.S.Kumari,G.Rijulal,J Rare earth 26(2008)16

8. Y.Sun,.M.C.Machala.,FN.Castellano,Inorg.Chim,Acta 363(2010) 283

9. R.Garg.,M.K.Saini,N.Fahmi,RV.Singh, Transition met Chem 31 (2006)362

10. K Mahajan,M.Swami,R.V. Singh,Russ.J.Coord.Chem,35(2005) 170

11. Al zayd,KM (2009) microwave and ultrasound promoted synthesis of substituted New Aryl hydrazinopyridinone,Arebian Journal of chemistry,2,89-94.

12. Kapadnis,K,H,et al (2016) Four synthesis method of schiff base ligands and preparation of their metal complex with IR and antibacterial Investigation.

13. Patil.S.,JadhavS.D and PatilU.P.natural acid catalysed synthesis of schiff base under solvent-free condition.As a green approach.Archives of Applied Science research,2012,4,1074-1078.

14. Hasan A.Mohamed,NishadIsmealTaha.International journal of organic chemistry.2017,7,412-419

15. Mishra A.PurwarH,JainR,GuptaS.Microwave synthesis, spectal, Thermal and antimicrobial studies of some Co(II),Ni(II) and Cu(II) complex containing 2 aminothiazolemoiety.E - Journal of chemistry: 2912:9 (4) : 77-85

16. Bell SC.Conklin GL, Children SJ.TAM chemSoC 1963:18:2868:2869.

17. EnamulHassain,Chaluvaraju K C.Niranjan MS, Xaranappa,santosh C, International research journal of phrmacy (2013),4,(11)

18. Moshin Abbas Khan, samarAkhtar,khadijicaShahid, synthesis, characterization and In vitro biological assay of triphenyltin derivatives of phenylhydrazine s, International journal of pharmaceutical sciences and research 28,(1) sep Oct 2024: 147-151

19. Shaharyar M, Mazumdar A Salahuddin.GargR,PandeyRD Synthesis, characterization and pharmacological screening of novel benzimidazolederivatives.Arabian Journal of chemistry 1016,9,342-S347, https:// doi org./10.1016/j.poly.2017.04.031.

20. S SSonune, S P Moharir, M G Undegaonkar, A S Kirdant. Synthesis under solvent-free condition, characterization and bioactivity study of novel schiff base ligand derived from 2-amino-1-methyl benzimidazole and 3,5- dimethoxy-4-hydroxy acetophenone.Journal of the Oriental Institute M.S. University of Baroda,October - December: 2022, Vol. 71, Issue. 04, No. 11, 121-126.

21. Venugopal, P.;Krishnakuty, K. synthesis and characterization of Cobalt -nickel, Copper and zinc(II) complexes of morin. J Indian chem.society 1997, 74 ,562 -563.

22. Dharmara,j N.;Vishwathamurthi, P.; Natarajan, K Ruthenium(II) complexes containing bidentate schiff bases and their antifungal activity.J transition Met Chem.2001,26,105-109.

23. Omidi,S.;Kakanejadifard,A review on biological activites of schiff base ,hydrazone and oxime derivatives of curcumin RSC Advanced 2020,.10,30186-39202,https://doi.org/10.1039/FORA05720G.

24. Mishra ,A.P .;Rajendra ,K. Jain conventional and microwave synthesis ,spectral ,thermal and antibacterial studies of some transition metal complexes containing 2- amino-5-methylthiazolemoiety.Journal of Saudi chemical society 2014,18,814-824, https://doi org/10.1016/j.jscs.2011.09.013.

25. Pandey, M.K .; sandur, S .K.; Sung, B. ; Sethi, G.; Kunnumakkara, A.B.; Aggarwal,B B. Butein, a tetrahyhydroxychalcone,inhibits nuclear factor(NF).-B and NF-B regulated gene expression through direction inhibition of IB kinase on cysteine 179 residue.J.Biol.Chem.2007,282,17340-17350,https://doi.org/10.1074/jbc.M700890200

26. Sharma ,S T.; Mehta, M. K .;Shah. Synthesis and spectral studies of transition metal complexes supported by a NO-bidentate Schiff base ligand .Der.Chem. Sin.2013, 4, 141 -

146 , https:// www.imedpub.com/abstract/synthesis and spectral studies of transition metal complexes supported by monobidentate schiff base ligand -12465 html.

27. Banfi,E.; Scialino,G.; Monti- Bragadin, C. Dedevelopment of a microdilution method to evaluate mycobacterium tuberculosis drug susceptibility. Journal of antimicrobial chemotherapy 2003,52, 79 6-800, https://doi.org/10.1093/jac/dkg439.

28. Stalons,D R.; Thomsberry,V.borth dilution method for determining the antibiotic susceptibility of anaerobic bacteria and Antimicrob Agents chemother the 1975 ,7, 15-21., https:// dio.org/ 10.1128/AAC.7.1.15.

Synthesis of 2,4,5-Triaryl-1H-Imidazole Derivatives Using Heterogenous SnO₂ Catalyst

Pritam A. Mule[1*], Manoj P. Palve[2], Vinod A. Shelke[3] , Ajeet A. Yelwande[4]

[*1,2,3]Indraraj Arts, Commerce and Science College, Sillod, Aurangabad-431112

[*1]Corresponding Author Email: pritamrajmule1991@gmail.com.

Abstract

synthesis of 2,4,5-triaryl substituted imidazole by using a mixture of an aromatic aldehyde, a benzil or benzoin and an ammonium acetate in ethanol as solvent in the presence of SnO_2 catalyst. This method provides several advantages such as being environmentally benign, reusable, possessing high yields with increased variations of the substituents in the product and preparative simplicity. The cleaner reaction, and easy workup make this protocol practical and economically attractive.

Keywords: Sol-Gel Method; 2,4,5-triaryl substituted Imidazole; SnO_2; Three Component Reaction;

Introduction:

Catalysis is a process in which the rate of a chemical reaction changes due to the participation of a substance called a catalyst. Catalysts may be in gaseous, liquid, or solid state. In homogeneous catalysis, the catalyst is molecularly dispersed in the same phase (usually gaseous or liquid) as the reactants. In heterogeneous catalysis the reactants and the catalyst are in different phases, separated by a phase boundary. Most commonly used heterogeneous catalysts are solids and the reactants are gases or liquids [1]. This distinction is linked to the fact that the catalyst operates respectively in the same phase as the reaction occurs (homogeneous catalysts) or in the different phase (heterogeneous catalysts). In principle, there is no limitation on the phase to be considered; as a matter of fact, the first industrial catalyzed reaction (1750) was the oxidation of SO_2 to SO_3 using NO as a homogeneous catalyst. On the other hand, most of the processes using homogeneous catalysts occur in a liquid phase whereas for the heterogeneous catalysts, the catalyst is usually in solid form, and the reaction occurs either in the liquid or gaseous phase. The fact that the catalyst is in a distinct phase with respect to the reaction medium, accounts for the major advantage of the heterogeneous catalysts over the homogeneous as it makes the separation techniques of heterogeneous catalysts are simple and cheap compared to the homogeneous catalysts.

In chemistry, heterogeneous catalysis is catalysis where the phase of catalysts differs from that of the reactants or products[2]. The process contrasts with homogeneous catalysis where the reactants, products and catalyst exist in the same phase. Phase distinguishes between not only solid, liquid, and gas components, but also immiscible mixtures (e.g. oil and water), or anywhere an interface is present. Heterogeneous catalysis typically involves solid phase catalysts and gas phase reactants [3]. In this case, there is a cycle of molecular adsorption, reaction, and desorption occurring at the catalyst surface. Thermodynamics, mass transfer, and heat transfer influence the rate (kinetics) of reaction. Heterogeneous catalysis is very important because it enables faster, large-scale production and the selective product formation. The merit of heterogenous catalyst catalyst can be easily separate from reactant. Heterogenous catalyst such as SnO_2, Zeolite, metal oxide, mix metal oxide, SnO_2/SiO_2 etc. [4].

SnO_2 composite materials containing several applications such as high thermal stability, high surface area, small in size, non-toxic, catalyst can be reused in several time such type of materials used in various type of reactions such as aminolysis of styrene oxide with aniline for the Meerwein–Ponndorf–Verley reduction of 4-tert-butylcyclohexanone [5], hydroxylation of phenols [6] Baeyer–Villiger oxidations [7] Meerwein–Ponndorf–Verley reductions [8] sugar isomerization [9] epimerization [10] oxidative dehydrogenation of cyclohexane [11] and Cannizzaro-type reactions [12].

Imidazoles are common scaffolds in highly significant biomolecules, including biotin, the essential amino acidhistidine, histamine, the pilocarpine alkaloids [13], and other alkaloids, which have been shown to exhibit interesting biological activities, such as antimicrobial, anticryptococcal, cytotoxic activities and inhibition of nitric oxide synthase[14], Many of the substituted imidazoles are known as inhibitors of P38 MAP kinase [15], fungicides and herbicides [16], plant growth regulators[17] and therapeutic agents [18]. Owing to the wide range of pharmacological and biological activities, the development of synthetic methods enabling facile access to this heterocycle is still desirable.

Several methods have been reported for the synthesis of imidazoles. 2,4,5-Triaryl-1H-imidazoles are generally synthesized by three-component cyclocondensation of a 1,2-diketone, α-hydroxyketone or α-ketomonoxime with an aldehyde and ammonium acetate, which comprises the use of ionic liquids[19]europiumtriflate[20], oxalic acid[21], TBAB [22], CAN [23], refluxing in AcOH [24] and silica sulfuric acid [25]. On the other hand, the synthesis of 1,2,4,5-tetraaryl-1H-imidazoles are carried out by four-component condensation of a 1,2-diketone, α-hydroxyketone or α-ketomonoxime with an aldehyde, a primary amine and ammonium acetate using microwaves [26], heteropolyacid [27], silica gel/$NaHSO_4$[28] $InCl_3\cdot3H_2O$ [29] or $HClO_4$–SiO_2[30]. In addition, they can also be accessed by hetero-Cope rearrangements [31] and condensation of a 1,2-diketone with an aryl nitrile and primary amine under microwave irradiation[32,33].

Here we wish to report, SnO_2 catalyzed synthesis of 2,4,5-triaryl-1H-imidazole derivatives using cyclocondensation of aldehydes, Benzil, aniline, ammonium acetate in ethanol at refluxed (scheme 1). The noticeable advantage of the present work is to introduce simple and eco-friendly procedure for the synthesis of 2,4,5-triaryl-1H-imidazole.

Experimental:

All Chemicals were purchased either from Merck or Fluka and used without further purification. Melting points were taken in an open capillary and are uncorrected. Thin layer chromatography was performed on Merck pre-coated silica gel 60-F254 plates. ^{1}H NMR spectra were recorded on a 300 MHz FT-NMR spectrometer in $CDCl_3$ as a solvent and chemical shifts values are recorded δ (ppm) relative to tetramethylsilane (Me_4Si) as an internal standard.

Preparation of SnO_2 catalyst:

SnO_2 nanocomposite catalytic materials were synthesized by using sol-gel method. Generally, SnO_2 catalysts was synthesized by using 0.846 gm of Tin(IV) chloride dissolved in 20 mL double distilled water was added drop wise in an autoclave bottle. The resulting mixture was stirred and 1% solution of cetyltrimethylammonium bromide (CTAB) in 20 mL ethanol was added drop wise with constant stirring. The pH ~10 of the reaction mixture was maintained using aqueous ammonia. This mixture was then hydrothermally treated at 60°C for 12 h in an autoclavable bottle. After drying at 110°C for 7 h in an oven, the obtained powder was

pulverized using mortar and pestle and finally calcined at 400°C for 2 h. to obtained SnO_2 catalytic materials.

General procedure for the synthesis of 2,4,5-triaryl-1H-imidazoles

A mixture of benzil (1 mmol), aldehyde (1 mmol), ammonium acetate (5 mmol) and catalytic amount SnO_2 (0.1g) in ethanol (15 mL) was refluxed for the specified times mentioned in Table 3. The progress of the reaction was monitored by TLC (petroleum ether: ethyl acetate = 7:3 as eluent). After completion of the reaction, the mixture was washed with cold ethanol and the crude product was recrystallized by ethanol to obtain the pure 2,4,5-triaryl-1H-imidazole derivatives in 90-93% yields.

Scheme 1
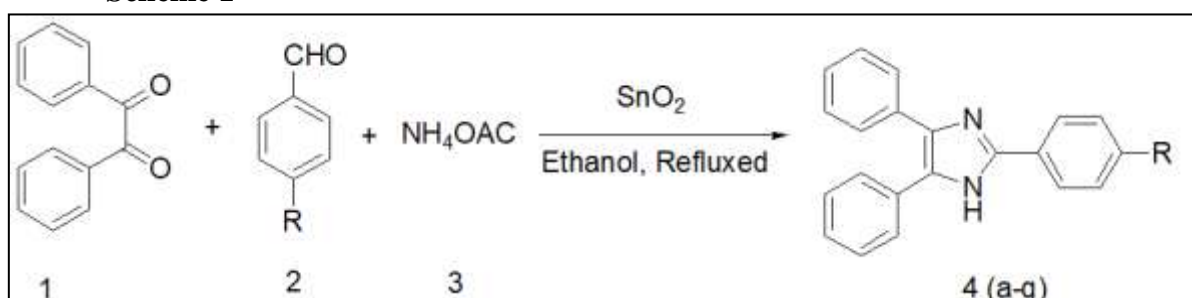
Spectral data of representative compounds

(4a) IR (KBr, cm^{-1}) n = 1217, 1639, 2471, 2991, 3433; 1 HNMR (CDCl$_3$, 200 MHz): d 7.44– 8.23 (m, 15H), 12.62 (bs, 1H); MS (ESI): m/z 296 (M +).

Result and Discussion

To examine the effect of catalytic activity of homogenous and heterogamous catalyst using summarized in (**Table 1**). When homogenous catalyst zirconium oxychloride, tin chloride gave good to well yield but catalyst cannot be reused in model reaction of benzil, benzaldehyde, ammonium acetate was refluxed in ethanol. Using heterogeneous catalyst natural silica exhibits poor catalytic activity in term of reaction time and product. With synthesized SnO2 composite materials gave good to excellent yields and catalyst can be reused at least three times.

Table 1 catalytic activity of homogenous and heterogonous catalyst[a]

Entry	Catalyst	Time (h)	Yield (%)[b]
1	$ZrOCl_2$	3	75
2	$SnCl_2$	3.1	80
3	Natural silica	4.5	45
4	SnO_2	2.5	94

[a]**Reaction condition:** benzil (1 mmol), benzaldehyde (1 mmol) ammonium acetate (5 mmol) catalyst (0.1g) and ethanol 15 ml; [b]Isolated yield.

After conformation of catalytic materials to optimized the effect of various solvents such as acetonitrile, di-chloro methane (DCM), methanol, acetone and ethanol with SnO_2 catalytic materials. When di-chloro methane (DCM) and acetonitrile gave moderate amount yield methanol and acetone gave less amount of yields (**Table 2**). The best result was found in ethanol as a solvent in term of reaction time and yield of the product hence we have chosen ethanol as a solvent for the synthesis of 2,4,5-triaryl-1H-imidazole derivatives.

Table 2 Solvent stability of catalyst[a]

'RESEARCH JOURNEY' *International E- Research Journal*
Special Issue – 333 : Innovative & Sustainable Chemistry
Impact Factor 6.625 (SJIF)   **Peer Reviewed Journal**

E-ISSN : 2348-7143
December - 2023

Entry	Solvent	Time (h)	Yield (%)[b]
1	Di-chloro methane (DCM)	4.5	60
2	Acetonitrile	4.5	55
3	Methanol	4	70
4	Acetone	4	75
5	Ethanol	2.5	94

[a]**Reaction condition:** benzil (1 mmol), benzaldehyde (1 mmol) ammonium acetate (5 mmol) catalyst (0.1g) and ethanol 15 ml; [b]Isolated yield.

Table 3 shows the generality of the present protocol for variety of different substituted aromatic aldehyde possessing electron rich and electron deficient groups gave good to excellent yields (89-94%) of the respective product and reaction were completed within 2.5-4 h was refluxed in ethanol.

One of the significant advantages of heterogeneous catalyst is the possible recovery and reusability of catalyst as this is important from an industrial and an economic point of view. After the completion of the reaction the catalyst was separated by filtration, washed with n-hexane and dried at 80°C for 1 h before next catalytic run. Reusability of the catalyst was investigated for three times and it was found to retain almost consistent activity (**Table 3 entry 4a**)

Table 3 Synthesis of 2,4,5-triaryl-1H-imidazole derivative[a]

Entry	Aldehydes	Time (h)	Yield (%)[b]	M.P. (°C)
4a	C_6H_5	2.5	94 (93,92,91)[c]	276-278
4b	$4\text{-Cl-}C_6H_4$	3	90	261-263
4c	$2\text{-Cl-}C_6H_4$	3.5	89	198-200
4d	$4\text{-NO}_2\text{-}C_6H_4$	3.5	90	235-237
4e	$4\text{-OH-}C_6H_4$	3.6	91	265-267
4f	2-furyl	4	90	233-235
4g	$2\text{-OH }C_6H_4$	3.5	91	204-206

[a]**Reaction condition:** benzil (1 mmol), benzaldehyde (1 mmol) ammonium acetate (5 mmol) catalyst (0.1g) and ethanol 15 ml; [b]Isolated yield.

Conclusion:

In conclusion, an efficient catalytic system has been developed for the synthesis of 2,4,5-triaryl-1H-imidazolederivatives from three component condensation of benzil, aromatic aldehyde, ammonium acetate in ethanol at refluxed in SnO_2. Present method offers remarkable advantages such as non-toxic, non-corrosive and an inexpensive reaction condition. Simply recovery and reusability of the catalyst makes the reaction successful under environmental benign conditions**.**

References:

1. Encyclopediabritannica online, **2004.**
2. Schlögl, Robert (9 March 2015). "Heterogeneous Catalysis". Angewandte Chemie International Edition. **54** (11): 3465–3520.
3. Rothenberg, Gadi (17 March 2008). Catalysis: concepts and green applications. Weinheim [Germany]: Wiley-VCH
4. Information., Lawrence Berkeley National Laboratory. United States. Department of Energy. Office of Scientific and Technical (2003).
5. D. Skoda, A. Styskalik, Z. Moravec, P. Bezdicka, J. Bursik, P.H. Mutine, J. Pinkas, RSC Adv. 6, 68739 (2016)

6. X. Wang, H. Xu, X. Fu, P. Liu, F. Lefebvre, J.M. Basset, J. Mol. Catal. A: Chem. 238, 185 (2005)

7. A. Corma, M.A.T. Navarro, M. Renz, J. Catal. 219, 242 (2003)

8. A. Corma, M.E. Domine, S. Valencia, J. Catal. 215, 294 (2003)

9. H.J. Cho, P. Dornath, W. Fan, ACS Catal. 4, 2029 (2014)

10. W.R. Gunther, Y. Wang, Y. Ji, V.K. Michaelis, S.T. Hunt, R.G. Griffin, Y. Rom´an-Leshkov, Nat. Commun. 3, 1109 (2012)

11. S. Samanta, N.K. Mal, A. Manna, A. Bhaumik, Appl. Catal. A 273, 157 (2004)

12. E. Taarning, S. Saravanamurugan, M. Spangsberg Holm, J. Xiong, R.M. West, C.H. Christensen, ChemSusChem, 2, 625 (2009)

13. M.R. Grimmett A.R. Katritsky, E.F.V. Scriven (Eds.), Comprehensive Heterocyclic Chemistry II, Vol. 3, Pergamon, Oxford (1996), pp. 77-220.

14. L. De Luca Curr. Med. Chem., 13 (2006), p. 1

15. J.C. Lee, J.T. Laydon, P.C. McDonnell, T.F. Gallagher, S. Kumar, D. Green, D. McNulty, M. Blumenthal, J.R. Heys, S.W. Landvatter, J.E. Strickler, M.M. McLaughlin, I.R. Siemens, S.M. Fisher, J.P. Livi, J.R. White, J.L. Adams, P.R. Young Nature, 372 (1994), p. 739

16. Maier, T.; Schmierer, R.; Bauer, K.; Bieringer, H.; Buerstell, H.; Sachse, B US Patent 4820335, 1989; Chem. Abstr. 1989, 111, 19494.

17. Schmierer, R.; Mildenberger, H. Buerstell, H. German Patent 361464, 1987; Chem. Abstr. 1988, 108, 37838.

18. J. Heeres, L.J.J. Backx, J.H. Mostmans, Van Custem J. Med. Chem., 22 (1979), p. 1003

19. (a) A.Y. Usyatinsky, Y.L. Khmelnitsky Tetrahedron Lett., 41 (2000), p. 5031 (b) H.A. Oskooie, Z. Alimohammadi, M.M. Heravi Heteroat. Chem., 17 (2006), p. 699

20. (a) S.A. Siddiqui, U.C. Narkhede, S.S. Palimkar, T. Daniel, R.J. Lahoti, K.V. Srinivasan Tetrahedron, 61 (2005), p. 3539 (b) H. Zang, Q. Yingming Mo, C. Su, Bo-Wen, S. Jun Ultrasonics Sonochem., 17 (2010), p. 749

21. C.M. Yu, M. Lei, W.K. Su, Y.Y. Xie Synth. Commun., 37 (2007), p. 3301

22. N.D. Kokare, J.N. Sangshetti, D.B. Shinde Synthesis, 18 (2007), p. 2829

23. M.V. Chary, N.C. Keerthysri, S.V.N. Vupallapati, N. Lingaiah, S. Kantevari Catal. Commun., 9 (2008), p. 2013

24. J. Sangshetty, N.D. Kokare, S.A. Kotharkara, D.B. Shinde J. Chem. Sci., 120 (2008), p. 463

25. J. Wang, R. Mason, D.V. Derveer, K. Feng, X.R. Bu J. Org. Chem., 68 (2003), p. 5415

26. A. Shaabani, A. Rahmati J. Mol. Catal. A: Chem., 249 (2006), p. 246

27. S. Balalaie, A. Arabanian Green Chem., 2 (2000), p. 274

28. (a) E. Rafiee, H. Mahdavi, M. Joshaghani Mol. Divers., 15 (2011), p. 125 (b) M.M. Heravi, F. Derikvand, F.F. Bamoharram J. Mol. Catal. A: Chem., 263 (2007), p. 112

29. A.R. Karimi, Z. Alimohammadi, J. Azizian, A.A. Mohammadi, M.R. Mohammadizadeh Catal. Commun., 7 (2006), p. 728

30. S.D. Sharma, P. Hazarika, D. Konwar Tetrahedron Lett., 49 (2008), p. 2216

31. S. Kantevari, S.V.N. Vuppalapati, D.O. Biradar, L.J. Nagarapu Catal. Mol. A: Chem., 266 (2007), p. 109

32. I. Lantos, W.Y. Zhang, X. Shui, D.S. Eggleston J. Org. Chem., 58 (1993), p. 7092
    S. Balalaie, M.M. Hashemi, M. Akhbari Tetrahedron Lett, 44 (2003), p. 1709

Innovations in Technology and Green Chemistry
for Sustainable Development

Ms. Mohini S.Nikam[a], Dr. Gokul P. Borse [b]

a.Head and Asst. Prof., Department of Chemistry, SSSVPM's ACS College Ravalgaon,
Tal. Malegaon, Dist. Nashik (M.S.) India.mrsmba2020@gmail.com
b.Head andAsst. Prof., Department of Chemistry, Rani Laxmibai Mahavidyalaya, Parola, Dist.
Jalgaon (M.S.) India.

Abstract :-

    Modern chemistry is the backbone of our society, but on the other side it is majorly contributing to the global environmental pollution and thus ongoing climate crisis. The transition towards the sustainable future requires the information of how chemistry is designed, developed and used.

    Green chemistry is one of the most explored topic in our current globalized world. Major research on green chemistry aims to maximize the desired product in an eco-friendly way and to minimize the production of harmful bi-products. Technology along with green chemistry is tool for innovation towards sustainable future. Hence scientists and chemists can significantly minimize the damage to environment and health of human beings with the help of valuable ideology of green chemistry with technology. There are various innovations in these such as cradle to cradle design, solvent reduction with more efficient synthesis and high efficiency formulation. This conceptual paper presents those innovations, proposed areas, objectives, challenges and factors affecting, future research needs to be taken by various industries to engulf technology and green chemistry for a sustainable development.

Key Words :- Green chemistry, sustainability, innovations, technology, chemists, development.

Introduction :-

    Green chemistry aims for safer products, less hazardous consequences to the environment, saving energy and water along with it includes broader issues which can promote in the end sustainable development.Now a days there is a rapid development of new chemical technologies and chemical products thus turning the attention towards remedial actions for monitoring environment pollution, reduction of pollutants etc. But the fact is that the most effective way to reduce this negative impacts is to design and innovate the manufacturing processes by considering atom economy, use and generation of secondary materials which are dangerous and finally the life cycle of the products and their practical recycling into new materials.In recent years Green chemistry has gained a strong foothold in the areas of research and development in both industry and academia, especially in the developed industrial countries. Several international conferences, scientific journals, numerous publications and new courses in universities testify to the increasing influence of Green Chemistry philosophy.The 12 principles of green chemistry are obviously very difficult to apply immediately for many chemical processes. After many years of Green Chemistry initiatives and industrial applications it is amazing to see many creative innovations at various scientific and industrial processes. The cooperation of chemists, engineers, scientists and technologists has achieved interesting results. The interdisciplinary approach has expanded the fields of green chemistry and produced some excellent non-toxic materials and feedstock savings in chemical industries.

Chemistry has long been described as a complex system. When all its aspects are considered together, its highly complex supply chains, business models, wide range of stakeholders, interactions of molecules with products, humans, and the environment, chemistry becomes an example of a complex dynamic interacting system. Finding chemical solutions with positive impacts toward sustainability depends on making chemical data more transparent and available for decision support tools that are suitable for addressing complex problems, including emerging tools from the field of artificial intelligence and digitalization.Systemic innovation in chemical research and development, assessment, management, and education is required to facilitate a transition toward a sustainable future. Such an innovation can benefit, to a large extent, from the increased uptake and systematic adoption of digitalization and digital tools to optimize the management of entire chemical life cycles, from chemical supply chains and chemical manufacturing to use and end-oflife. Digitalization in chemistry will enable development of more flexible data exchange models, more transparent international and cross-sector chemical information transfer, and chemistries that are both safe and sustainable by design. With that, digitalization is key to a radical transformation to more sustainable and collaborative business models in the growing chemical industry sector.

In a short term, green chemistry has been heavily focused on developing new and environment friendly chemical processes using many technologies. Globalization era will demand increasing emphasis on product but it is important that the manufacturing should be through green chemistry methods. Green chemists and engineers employ biological systems and life cycle to create chemicals that lead to foundation of our economy. There are numerous application of Green Chemistry in industry such as plastics, renewable energy technologies, pesticides, textile manufacturing, water purification, pharmaceuticals and basic chemical feedstock's. It is believed that, overtime Green Chemistry will change a chemistry as a whole towards an economy based on sustainable renewable energy, green jobs, bio-based productions.

Proposed Areas :-

Under the green chemistry principles the areas proposed for special focus were as following,

1. Use of alternative feedstock's.
2. Use of less hazardous reagents.
3. Use of natural processes, like bio catalytic techniques.
4. Use of alternative solvents.
5. Design of safer chemicals and products.
6. Developing alternative reaction conditions.
7. Minimizing energy consumption.

Objectives :-

To shift the chemistry innovation activities in technology and green chemistry towards sustainable chemistry 10 most favorable objectives are,

1. Decreasing chemical hazard
2. Avoiding undesirable substitutions and alternatives
3. Sustainable sourcing of resources and feedstock's
4. Production processes sustainability advancing
5. Advancing sustainability of products
6. Decreasing pollution and chemical releases
7. Permitting non-toxic circularity

8. Increasing social benefits
9. Shielding workers, consumers and unsafe populations
10. Developing solutions for sustainability challenges.

Cradle to Cradle Design :-

Under the "Cradle-to-cradle" approach the design of commercial products is a modern and innovative concept to make products through a continuous use and recycling of biological and technological materials, thus avoiding waste and using renewable materials. The "Cradle-to-cradle" design also known as C2C / cradle 2 cradle / regenerative design is a new philosophy of how to make green things without pollution and waste. Cradle-to-cradle for its innovators wants industry to protect and enrich ecosystems and nature's biological metabolism while also maintaining safe, productive technical metabolism for the high-quality use and circulation of organic and synthetic materials, in its idealistic way. It is a holistic economic, industrial and social framework that seeks to create systems that are not just efficient but essentially waste free. The cradle-to-cradle model is not limited only to industrial design and manufacturing; but it can be applied to many different aspects of human civilization.

The Cradle to Cradle Certified programme is a multi-attribute eco-label that assesses a product's safety to humans and the environment and design for future life cycles. The programme provides guidelines to help businesses implement the Cradle to Cradle framework, which focuses on using safe materials that can be disassembled and recycled as technical nutrients or composted as biological nutrients. The model has been implemented by a number of companies, organizations and governments around the world.

Solvent Reduction :-

In recent years, under the influence of green chemistry principles, some solvents have been replaced and methodologies changed to more favorable techniques. Some of these changes are listed belowbriefly.

a) Oxidations under Green Chemistry principles to reduce solvents

Many oxidation techniques in chemical processes have changed under green chemistry principles. Many oxidations now are performed in water, in supercritical CO_2 or with less toxic solvents and under room temperatures. The hydrogen peroxide (H_2O_2) is considered as a very good oxidative reagent that performs at normal temperatures. There are numerous research efforts to apply oxidations with high selectivity and as by-production only water. Homogeneous and heterogeneous reactions in combination with catalysts are used in many oxidations. Oxidations are very important in the pharmaceutical industry and in many petrochemical processes. Oxygen and nitrogen oxides (NOx) are oxidative agents with green chemistry credentials which are used in the oxidation of benzene, cyclopentanone and propylene.

b) Catalytic selectivity in synthesis to reduce solvents

Catalytic selectivity can be another research effort for the reduction in the use of solvents and with higher yields and lower amounts of waste. Many industrial processes are based in new catalysts, such as inorganic polyacids and heteropolyacids which act as green catalysts in oxidations, in the hydration of butane mixtures and in the polymerization of tetrahydrofuran (THF). The heterogeneous catalytic method showed cleaner products, minimum waste and easy separation of the products.

Current Challenges in Sustainability Development :-

- Data gaps
- Poor data quality
- Poor prediction models
- Limited spatiotemporal resolution
- Methodological gaps
- Lack of considering interdependency
- Difficult to characterize chemicals
- Missing link between chemical pressure on ecosystems and ecological capacities for chemical pollution.

Challenges and enabling factors of introducing digitalization into chemistry:-

- **Increasing transparency:** It is expected that digitalization of chemistry will facilitate wider access to data, providing the ingredients for disruptive innovation alternatives and unveiling bottle necks, similar to the introduction of open standards in computing and the development of digital collaboration tools for coding. Increasing transparency of the value chain will advance the knowledge of manufacturing processes of compounds that are currently restricted. A wider and more systemic adoption of digitalization may be required to trace those procuring materials for synthesis of restricted materials.

- **Reskilling/upskilling of professionals:** The digitalization of chemical and manufacturing requires a new set of skills. This can be obtained by reskilling/upskilling the current workforce or bringing new professionals to work within the chemical industry. Chemists and material scientists would benefit from being able to work with large datasets, assisted by AI and machine learning. Although digital transformation brings along operational benefits, large companies have enough resources to bring or develop new skills within its workforce. Nevertheless, the impact of change tends to be harder for small and medium enterprises, especially when competing for highly skilled workforce.

- **Providing additional high-performance infrastructure and new devices:** Digitalization of chemistry entails increasing the use of smart devices and sensors to collect more data and pushing computational performance to interpret increasingly larger amounts of data. The manufacturing of new electronic devices, especially on a large scale, will increase the over-exploitation of natural resources, such as metals required for processors and batteries. Toxic wastes generated from production, recycling, and end-of-life of electronics are a serious environmental concern. The path toward sustainable and non-polluting digitalization should consider these aspects and push for longer product lifetimes through circularity processes, such as repair, reuse, and remanufacture, and especially designing devices within a circular and life cycle-based approach. E-wastes should be appropriately included in related chemical and product life cycle performance assessments. Furthermore, efficiency of computing power should be paired with clean energy consumption. It is key that environmental benefits brought by digitalization are not cancelled by the infrastructural environmental costs.

Future Research Needs for Sustainable Development:-

- Depolymerization and defunctionalization methods for existing chemicals that can allow circularity, especially for plastics.

- Design of circular systems with consideration of human health and eco-toxicity, ideally via rational design of benign commodity chemicals.
- Systematic application of life-cycle analysis, or thinking, and process metrics in developing new manufacturing/ synthetic routes.
- Implementation of machine learning and other big-data methods to drive innovation toward new paradigms of circularity.

Conclusion :-

The goal of green chemistry is to create better, safer and efficient environment by reducing waste and eliminate the hazardous materials in chemicals. Our future challenges in society, environmental, economic and resources demand for efficient and environmental friendly chemical processes and products. Therefore, this paper presents proposed areas, objectives, challenges and factors affecting, future research needs to be taken by various industries for a sustainable development through technology and green chemistry.Digitalization of research partnering, access to open data and globally digital experiment facilities promise a revolution in the speed of chemistry and the possibility to pose research questions worthy of challenge of developing a sustainable global society.Finally, the success of green chemistry along with technology is on the scientists and chemists who will use the new perspective for transformative innovations for sustainability.

References :-

1. Mulvihill, M. J., Beach, E. S., Zimmerman, J. B., & Anastas, P. T. Green chemistry and green engineering: a framework for sustainable technology development. Annual review of environment and resources, 36, 271-293, 2011.
2. McDonough W, Braungart M., Cradle to Cradle. Remaking the Way, We Make Things. North Point Press, New York, 2002.
3. Sharma SK. Green Chemistry for Environmental Sustainability. Series: Advancing Sustainability Through Green Chemistry and Engineering. CRC Press, Boca Raton, FL, 2010.
4. Peter Fantke, Claudio Cinquemani, Polina Yaseneva, Jonathas De Mello, Henning Schwabe, Bjoern Ebeling and Alexei A. Lapkin, Transition to sustainable chemistry through digitalization, Chem 7, 2866–2882, November 11, 2021.
5. Sumathi Ganasen , V.Sharmilah Velaichamy, Innovations in green chemistry towards sustainable development, OIDA International Journal of Sustainable Development, 2016.

Facile Synthesis of TiO₂ and Ag@TiO₂nano particles and its Application as A Photoanode in Dye Sensitized Solar Cells

Rupali S. Patil[1], Nikita D. Sangtani[1], Kajal R. Patil[1], Rahul S. Salunke[2], Veena A. Uddhage[1]

School of Chemical Sciences[1] and School of Physical Sciences[2], Kavayitri Bahinabai Chaudhari North Maharashtra University, Jalgaon

Abstract-

In the present investigation, TiO₂ nanoparticle were synthesized by sol-gel &hydrothermal method together with synthesis of Ag@TiO₂. Which then used as a photoanode inhigh-performance dye-sensitized solar cells.The synthesis materials were characterized by X-Ray diffraction, SEM, UV- visible absorption. It revealed thesize of TiO₂ nanoparticles obtained by sol-gel method is 103.9 to 160.8 nm, 89.37 to 101.4 nm by hydrothermal method and 87.16 to 94.90 nm by Ag@TiO₂doping method. The incorporation of Ag on the TiO₂ surface significantly influenced the optical properties. Because of the surface plasmon resonance effect. The dye-sensitized solar cells(DSSCs) assembled with the Ag@TiO₂-modified photoanode demonstrated an enhanced solartoelectricalenergy conversionefficiency compared to that of bare TiO₂ due to theplasmonic effect of Ag.In addition, the Ag nanoparticles functioned as an electron sink, which retarded thechargerecombination.Theincreased solar energy conversionefficiency of the Ag@TiO₂ nanocomposite makes it a promising substitution to conventional photoanodebasedDSSCs.

Keywords: TiO₂, Ag@TiO₂, DSSC, Sol-gel Method, Hydrothermal Method.

1. Introduction-

Over the past two decades due to increase in population and lifestyle of human, demand for energy is also increases simultaneously. To fulfil the demand of energy use of non-renewable energy resourcesis not sufficient due to depletion as well as they are caucusing serious environmental and health hazard.This forced mankind to pay attention to clean energy resources. The search for cheap and clean energy progressed towards review the renewable sources. Geothermal, wind, hydro and solar energy are the presentative sources of renewable energy. Whereas wind power, geothermal and hydropower can be limited on geographical grounds, solar energy is the most available source on earth.Every year 3×10^{24} joules of energy strikes the Earth surface from the Sun[1-2].The tapping of this energy to a considerable amount will fulfil most of world's energy needs. Scientist have taken significant effort for developing the technology to harvest solar energy. Out of many techniquesthird generation Dye Sensitized Solar Cell (DSSC) is one of the most efficient, low cost, low toxicity to the environment and simple processes technique.The potential of DSSC was invented by work of Gratzel and O'Regan in 1991 for converting solar energy into electricity. Since then, scientific community is get attracted toward it. DSSC consist offour components as counter electrodes, an electrolyte, photo sensitizer(dyes), and photoanode materials.Efficiency of the DSSC is improved by introducing novelty in different component. Among the all component photoanode and dye play an important role in improving the efficiency of DSSC.To prepare photoanodesemiconducting metal–oxide with widebandgap (suchas,TiO₂, ZnO,Nb₂O₅, SnO₂, etc) are coated over transparent conducting glass substrates, with a monolayer of dye molecules adsorbed on it as a sensitizer. Upon illumination of sunlight, the dye becomes photo excited and injects electrons into the metal-oxide layer. The metal oxide then conducts the electrons from the dye to transparent to

anode.Among all titanium dioxide TiO₂ is most commonly used as a metal oxide layer due to itsvarying properties such as low cost, easy to synthesis, having wide band gap, non-toxic and high-power conversion efficiency[3-4].

However, when TiO₂ is used as photoanode it have some limitation that it transportelectron randomly.This will cause electron-hole recombination.Which will deteriorate the overall performance of the DSSC[5].In order to overcome this problem, photoanode is design with an well-organized charge transport pathway to enhance the DSSC performance. With this aim, DSSC is fabricated by surface modification of TiO₂ by doping of metal or non-metal, semiconductor coupling and hybridization with a carbon material have been attempted and show improved result[5].

The modification of surface area of TiO₂ is carried out by doping with nobel metal such as Silver(Ag)[6], Gold(Au)[7] andplatinum(Pt)[8] are reported in the literature to prevent the recombination of the photogenerated electron–hole pairs and improve the charge transfer efficiency.

In the present work, to improve the performance of DSSC, TiO₂ surface area is modified by doping with Ag nanoparticle. Because silver play an important role to improve the absorption coefficient of pigment, they act as an electron sink for photo induced charge carriers, interfacial charge transfer process is also get enhanced[5]. Silver doping on TiO₂ surface minimize the charge recombination by this mean increase in electron transfer process in DSSC and enhancing the overall performance of DSSC.

In the present work synthesize TiO₂ nanoparticles (As a semiconductor for photo anode) and to check the efficiency of DSSC, different methods used for synthesis of TiO₂ nanoparticles are sol gel, hydrothermal method and metal doping. Prepared Photoanodic material is characterised by analytical technique such as UV-Vis, XRD and SEManalysis.

The photovoltaic performance of DSSC is assessedby fabricating the device TiO₂based photoanode, betalaninsdye, electrolyte and Graphite or Au counter electrode under full simulated sunlight illumination.

2. Experimental Method

2.1. Chemicals and Reagents

TTIP was purchased from Avra Synthesis Private Limited.Silver nitrate (AgNO₃), HCl (35%) and Ethanol(absolute) were purchased from Merck.Acetic acid (extra pure grade) NH₄OH (25%) were used purchased from S.D. Fine Chemicals (India). DI water was prepared by tripal distillation. All chemicals were used as received without further purification.

2.2. Synthesis of TiO₂ by sol-gel method

Procedure:

The TiO₂ nanoparticle materials were prepared by sol-gel method. In a sol gel method, 3.7 ml of TTIP was added in 40 ml of distilled water and kept for stirring for 30 min on magnetic stirrer. Then 9 ml of glacial acetic acid was added to above solution. And kept with continuous stirring for 3hr maintain temperature between 70-80^{0}C. Then the milky solution was kept to aging for about 94 hrs. Further suspended particles were precipitated by changing pH of suspension from 2.61 to 11 by adding concentrated NaOH and then give washing of tripal D.W to decrease pH till 8.4. TiO₂ sludge thus obtained was dried in oven at 80^0 C for 13 hours. The white powder obtained was grinded in mortar and pastel to yield a fine TiO₂ powder. The powder further was calcinated at 450^0 C for 2 hours in muffle furnaceand stored under a dark condition.

2.3. Synthesis of TiO_2 by hydrothermal method

Procedure-

The TiO_2 nanoparticle materials were prepared by hydrothermal method.Initially,1.8 ml of HCl dilute it with 40 mL D.W. to make 0.5 M solution of HCl. 3 ml of TTIP solution was added drop by drop to the HCl solvent with constant stirring until it dissolves completely. The above solution was kept in hydrothermal reactor for 6 hours at 120^0 C to carry out hydrothermal reaction. The color of solution was turned from transparent to white during the reaction. After completion of reaction the solution was kept for centrifugation (in centrifuge tubes at 15000 r.p.m for 10 mins) and give it washing with double D.W. with the help of Sonicator and centrifugation. After the washing with D.W.reaction mixture againwash two time by ethanol. Then the solution was taken out in Petridiswas kept on hotplate for drying solution into powder at 27 to 31^0 C.Theprecipitate obtain was dried 50^0 C for 6 hours in convection drying oven and make fine powder with mortar and pastel and stored under a dark condition.

2.4. Synthesis of Ag@TiO_2

Procedure:

The Ag@TiO_2 nanoparticle materials were prepared using a sol-gel method. Firstly prepare TTIP- Methanol (20 wt% solution - 34.56g of TTIP and 160 ml methanol) and add 0.71 g of $AgNO_3$ was added with continuous stirring followed by dropwise addition of aqueous ammonia in solution under continuous stirring till pH of 9-10.The resulting gel obtained was milky and was stirred for 2 hours at room temperature.The gel was than filtered and washed with methanol several times to remove the nitrates.The gel was dried at room temperature for 2 hours and then at 80^0 Cfor 12 hours.The dried sample was calcined for 4 hrs. at 400^0 C to obtain Ag@TiO_2 samples.

2.5. Fabrication of DSSC:

2.5.1. Steps involved in Fabrication of Device

➢ Substrate Preparation: This step involves cleaning and preparing the substrate, which is typically made of glass or transparent conductive material like indium tin oxide (ITO).

➢ Preparation of Nanocrystalline Titanium Dioxide (TiO_2) Layer: Depositing a porous layer of nanocrystalline TiO_2 onto the TCO layer.

➢ Preparation of Dye from natural source and Adsorption of Dye molecule onto the surface of the TiO_2, allowing them to capture light energy.

➢ Preparation of electrolyte and injecting electrolyte between the electrodes.

➢ Assembly of the DSSC: A second conductive material, typically carbon (graphite), is deposited onto the dye adsorption layer. This material serves as the counter electrode.

➢ Testing and Characterization: The fabricated DSSC undergoes various tests and characterizations to evaluate its efficiency, current-voltage characteristics.

The main of this work is to develop TiO_2 nanoparticles using different methods (such as Sol-gel, hydrothermal, Ag doping) which are deposited on ITO to develop photoelectrodes. This photoelectrode is used for fabrication of DSSC along with dye which is also synthesized naturally from beetroot.

A] **Method of Extraction of Dyefrom natural source –**

Beetroot (Betalanins):

1. Peel out beets, then cut them into large chunks.
2. Place the beets into a blender pot and blend it with the help of mixer to get the paste.

3. Remove the paste in clean muslin cloth and pour paste on it.
4. Gently squeeze the cloth so that liquid is obtained from the paste.
5. Finally, we collected the pure 'betanin dye', solution of beet root red color which is ready for further process.

2.5.2. Dye as a Light Absorber:

- Dye act as light absorber, generates excited state electron that could be injected into MOS (metal oxide semiconductor) and initiates flow that produces current.
- Dye that has more than one functional group could be absorbed onto the surface of photo electrode and injects excited state electron with higher efficiency.
- More functional group generates more current.
- Shorter the distance between the excited state electron density, and functional group anchoring hydrogen atom, the more efficiently the electron could be injected into the MOs. Increase in the ISC is expected, as well as increment of efficiency.

Nanostructured Photoelectrode (TiO_2) preparation:

- In the old generations of photo electro chemical solar cells (PSC) photo electrodes were made from bulky semiconductor materials such as Si, Ga, As or CdS.
- However, these kinds of photo electrodes when exposed to light undergo photo corrosion that results in poor stability of the photo electrochemical cell.
- The use of sensitized wide bandgap semiconductors such as TiO_2, or ZnO resulted in high chemical stability of the cell due to their resistance to photo corrosion.

2.5.3 Preparation of TiO_2 Plate by using Doctor Blade Method:

1. Take 0.05 gm of TiO_2 powder.
2. Added 0.2-0.5 ml Acetic Acid in the TiO_2 powder to make fine paste.
3. Take a simple transparent glass plate.
4. Stick the cello tape on both side corners of the glass plate. (Note: to keep the cells in place, it is important to place a piece of tape on the left and right sides of the plate so that the plate will not be moving around as shown in figure).

Figure: 1. Coating of TiO2 nano particles using Doctor Blade Method.

5. The tape is overlapping on the top also allowing for uniform thickness of the TiO_2 film as the TiO_2 paste will only fill into the space below the tape, when the glass rod is rolled over.

6. Put the TiO_2 paste on the glass surface of the plate.Titanium Dioxide is applied to the conductive side of one plate by using a glass rod and rolling it on the plate until a neat coating is achieved.

7. A similar piece of glass should also be placed directly in contact (at the bottom) with the plate so that the titanium dioxide paste may have a neat coating to the edge.

2.5. 4. Preparation of Electrolyte solution:

The electrolyte solution consists of three different materials that we used in our research which is pure Iodine, potassium iodide and Ethylene glycol. We got about 0.1269 g of pure Iodine and 0.83 g of Potassium iodide and we put both in 10 ml of Ethylene glycol.

2.6. Construction of cell:

The solar cellswere created with two glass plates coated with Iodine Tin Oxide (ITO). This thin semiconducting layer allows charge to flow since glass is nonconductive. The plates are first tested to find the conductive side of the glass. This conductive side will be covered with other materials. Titanium dioxide is applied to the conductive side of one plate by using Doctor Blade method (using glass rod and rolling it on the plate until a neat coating is achieved). A similar piece of glass should also be placed directly in contact (at the bottom) with the plate so that the titanium dioxide paste may have a neat coating to the edge. This plate is then placed above a Bunsen burner for about 30 minutes so that the TiO_2 is bonded to the plate. This process is called sintering and allows a three-dimensional network to be achieved so that electron flow may occur. Following the sintering process, the plate is allowed to cool and is then placed in a bath of the dye's solution for 2-3 minutes. This is where the importance of the TiO_2 nanoparticles comes into play. The increased surface area allows for a greater amount of dye molecules to be absorbed, which will be of great importance during the test. The amounts of electrons allowed to flow through the system are dependent upon the number of dye molecules present in the cells themselves. The greater surface area translates to an increased flow of electricity. After absorbing the dye, the plates are placed to dry and bond. The bottom plate is placed in a hood (conductive side up) so that the counter electrode in the form of thin carbon soot or platinum paste may be applied. The cells are sprayed so that an even coating is achieved. This process is repeated until the total number of desired cells is obtained. The individual pieces of glass are now ready to be combined. The electrolyte solution is then placed on the dyed side of the plate,enough to saturate the surface. The two plates are sandwiched together (conductive sides touching) and secured with binder clips.
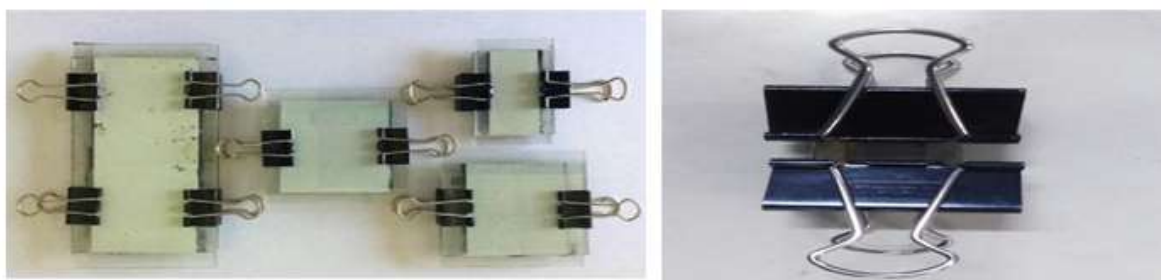
Figure: 2. Fabricated DSSC Solar Cell.
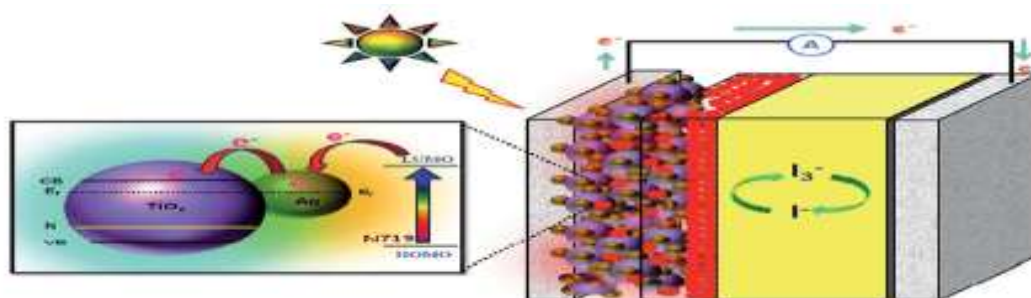
Figure: 3. General image of working of Dye-Sensitized Solar Cell[15]

3.Result and Discussion-

3.1: Characterization of TiO₂ nanoparticles –

The physical appearances of TiO_2 and $Ag@TiO_2$ with different method of synthesis is illustrated in figure 4. a, b, c. Figure 4.a presents the scanning electron microscopy (SEM) image of TiO_2 nanoparticles synthesized using the sol-gel method. The SEM image was obtained using an instrument with a specified range of detection and a magnification of 5000x. The sol-gel derived nanoparticles exhibited a randomly distributed and non-uniform cluster morphology. This suggests that the nanoparticles were not evenly dispersed and displayed a lack of uniformity in their spatial arrangement.

The average size of the sol-gel derived nanoparticles was determined through analysis of the SEM image. The measured sizes ranged from approximately 103.9 nm to 160.8 nm. This indicates that the nanoparticles in the sample exhibited a broad size distribution, with some particles being larger and others smaller within the observed range.

Moving on to Figure 4.b, which depicts the SEM image of nanoparticles prepared via the hydrothermal synthesis method. In this case, the image reveals a higher level of agglomeration among the nanoparticles. Agglomeration refers to the phenomenon where nanoparticles tend to cluster together, forming larger aggregates. The agglomeration observed in the image suggests that the nanoparticles did not disperse uniformly but rather formed non-ordered arrangements. The average size of the hydrothermal derived nanoparticles was determined based on the SEM image analysis, ranging from approximately 89.37 nm to 101.4 nm. This indicates that the nanoparticles in the hydrothermal sample were generally smaller than those prepared via the sol-gel method.

Moving on to Figure 4.c, it displays the SEM image of nanoparticles prepared through the sol-gel method with silver (Ag) doping. The image reveals the grain size of the Ag-doped nanoparticles, which ranged from approximately 87.16 to 94.90 nm. This indicates that the presence of Ag as a dopant affected the particle size and led to a different range compared to the undoped nanoparticles.

Furthermore, the SEM image of the sol-gel Ag-doped nanoparticles shows that the distribution of the dopant metal (Ag) on the surface of TiO_2 (titanium dioxide) is uniform. This uniform distribution suggests that the Ag dopant did evenly coat the TiO_2 surface.

Additionally, the SEM image reveals that the doped species (Ag-doped nanoparticles) exhibit irregularly shaped particles, which are aggregations of tiny crystals. This aggregation phenomenon indicates that the Ag-doped nanoparticles may have undergone crystallization or coalescence during the synthesis process, resulting in the formation of larger agglomerates or irregularly shaped particles.

In summary, the SEM images of the nanoparticles synthesized via sol-gel, hydrothermal, and sol-gel Ag-doped methods provide valuable insights into their morphological characteristics. These images demonstrate the differences in particle distribution, agglomeration levels, and the effects of doping on particle size and distribution. Such observations are essential for understanding the structural properties and potential applications of these synthesized nanoparticles. Particle size is greater in sol-gel method than hydrothermal which in turn is larger than Ag –doped TiO_2 particles. As nanoparticles become smaller, their surface area increases relative to their volume. This higher surface-to-volume ratio provides more active sites for chemical reactions or interactions with other substances.
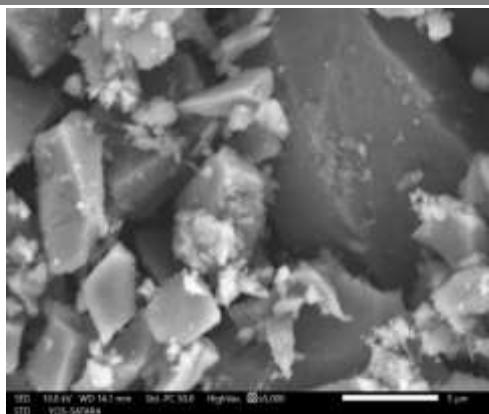
a) SEM micrographs of TiO$_2$ Nanoparticles synthesized via Sol-Gel method
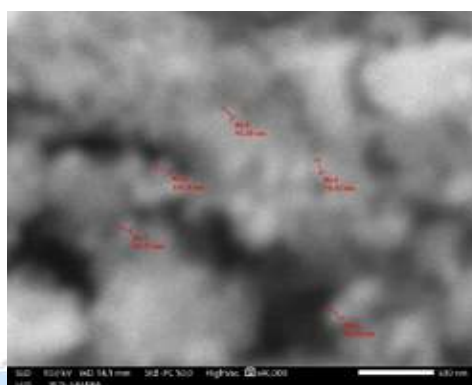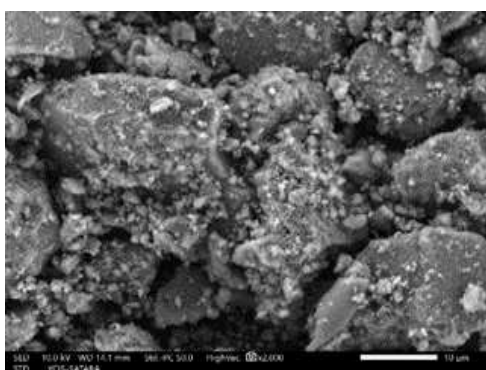
b) SEM micrographs of TiO$_2$ Nanoparticles synthesized via hydrothermal method
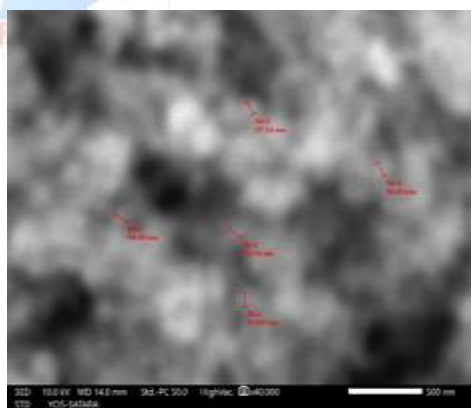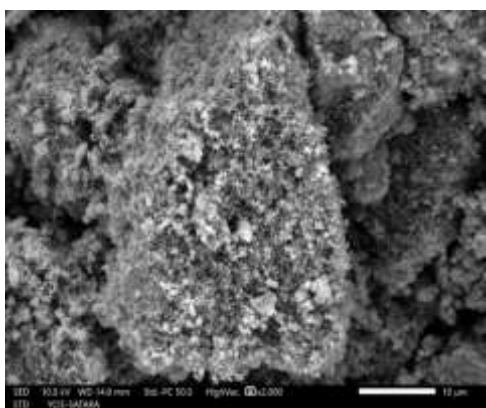
c) SEM micrographs of Ag@TiO$_2$ Nanoparticles synthesized via sol-gel method

Figure: 4.a), b), c) SEM micrographs of TiO$_2$ Nanoparticles synthesized via sol-gel and hydrothermal method and Ag-Doping by sol-gelmethod.

3.2: UV – Visible absorption spectra and Band gap -

In order to determine the nature of the band gap of TiO$_2$ nanophase, UV-absorption spectroscopy was performed, and the following relation was utilized:

$$(\alpha h\upsilon) = A(h\upsilon - Eg)^n$$

Here, α represents the absorption coefficient, hv is the photon energy, Eg is the photonic band gap, A is a photonic-energy independent constant, and n is a parameter dependent on the nature of the transition. In this case, n is determined to be ½, indicating a direct transition.

By plotting $(\alpha hv)^2$ against hv, one can extrapolate to determine the band gap energy. The intercept of the tangent to this plot provides an approximation of the band gap energy for the material under investigation.

For the sol-gel derived TiO_2 nanoparticles, the determined band gap was 3.79 eV. Similarly, the hydrothermal derived TiO_2 nanoparticles exhibited a band gap of 3.70 eV, while the Ag-doped TiO_2 nanoparticles had a band gap of 3.82 eV. These values are larger than the bulk TiO_2 band gap, which is typically around 3.2 eV.

This phenomenon can be explained by the size-dependent nature of the band gap in semiconductors. As the particle size decreases, the band gap of the material tends to increase. This is known as the quantum confinement effect. In nanoscale TiO_2 particles, quantum confinement leads to a modification of the electronic structure and an increase in the band gap. The absorption edge, which represents the onset of absorption, is also shifted to higher energies (blue shift) as the particle size decreases. This blue shift is observed in the UV-absorption spectra of the TiO_2 nanoparticles, indicating the influence of particle size on the electronic properties. Therefore, the larger band gaps observed in the sol-gel, hydrothermal, and Ag-doped TiO_2 nanoparticles compared to bulk TiO_2 can be attributed to the quantum confinement effect caused by the reduced particle size. This size-dependent band gap has important implications for the optical and electronic properties of TiO_2 nanophase materials and their potential applications in various fields, including photocatalysis, solar cells, and sensors.

The UV-vis absorption spectra of the TiO_2 and Ag@TiO_2 were recorded and are shown in Figure6. The TiO_2 synthesised by sol-gel method did not show any absorbance in the visible region because of the wideband gap. TiO_2 synthesised by hydrothermal method did not show any absobtion band in the visible region. The deposition of Ag on the TiO_2 surfacesignificantly influenced the absorption in the visible regions as compared to TiO_2ofwhich was due to the surface plasmon resonance(SPR) band of Ag nanoparticles[5].The presence of Ag nanoparticles significantly influenced the visible light absorption properties of TiO_2.

(A)

(B)

(C)   **(D)**   **(E)**   **(F)**
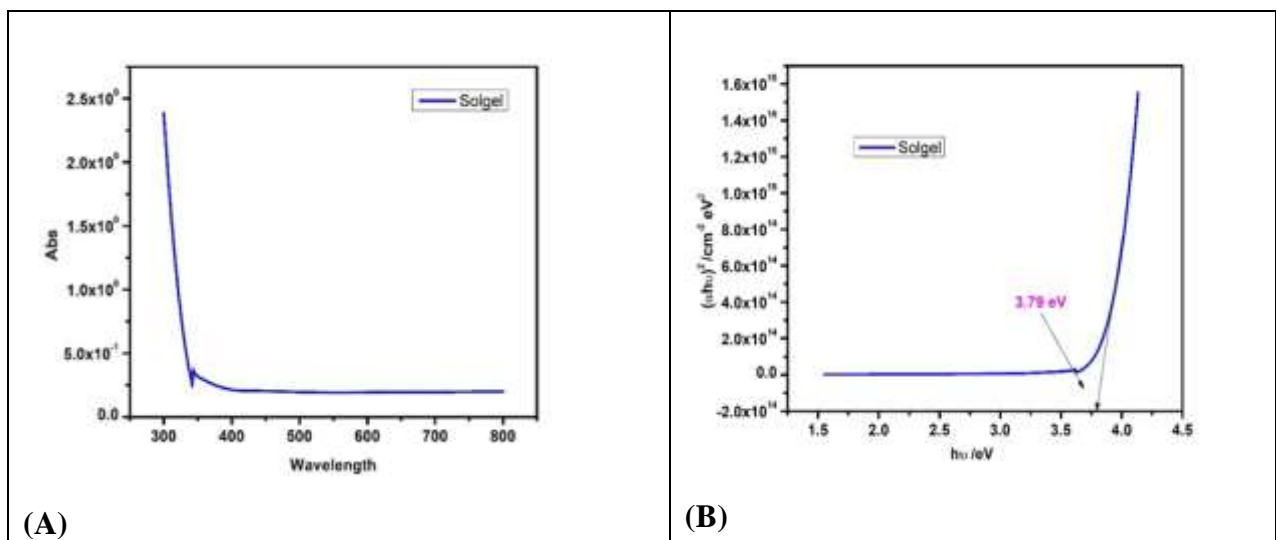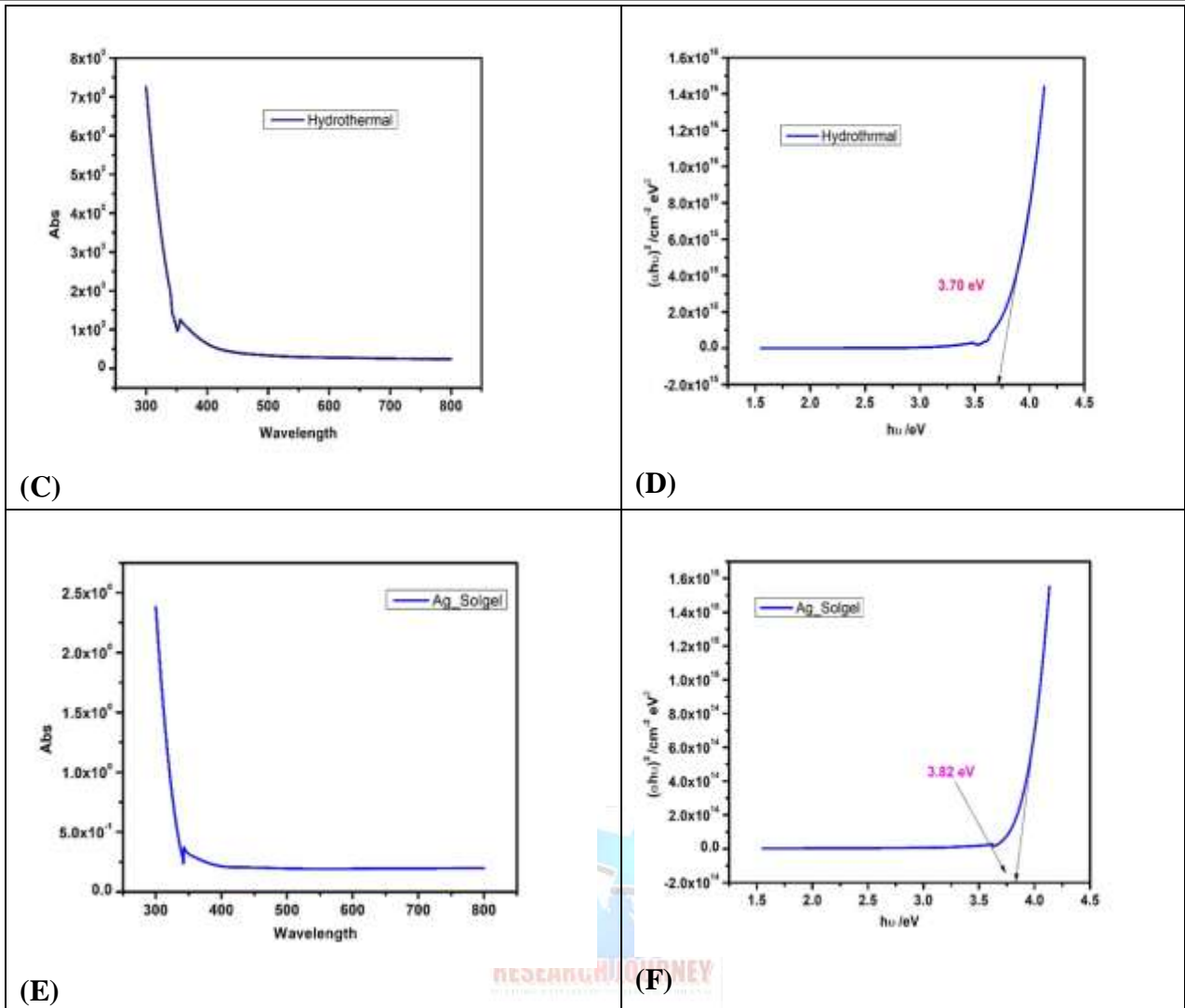
Figure: 5. The UV- vis absorption spectra and Band gap obtained by extrapolating the linear portion of the $(\alpha h\upsilon)^2$ versus $h\upsilon$ of TiO$_2$ nanoparticles prepared by (A) & (B) sol-gel, (C) & (D) Hydrothermal (E) & (F) Silver doping by sol-gel.
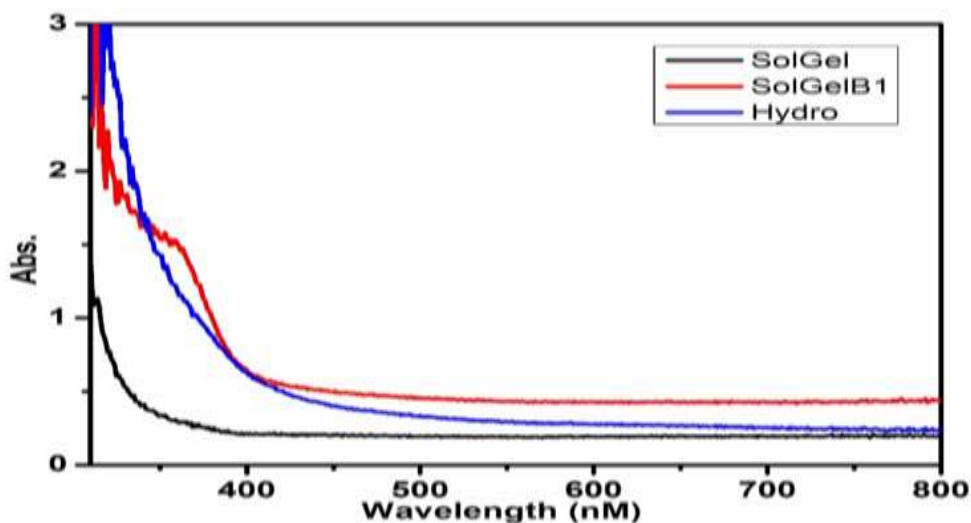
Figure: 6. PL spectra of TiO$_2$ nanoparticles prepared by sol-gel, hydrothermal and silver doping by sol-gel

3.3. The X-ray diffraction (XRD) -

The X-ray diffraction (XRD) pattern of the TiO_2 sample displays distinct peaks at various angles. These peaks provide valuable information about the crystal structure and phase composition of the material. Upon analysis, the following peaks were identified:At 24.8 degrees, there is a peak corresponding to the (101) plane of anatase TiO_2. This phase is characterized by a tetragonal crystal structure and is represented by the JCPDS card number 21-1272. Another peak is observed at 37.4 degrees, which also corresponds to the (004) plane of anatase TiO_2, supporting the presence of this phase in the sample. At 47.5 degrees, a peak is found corresponding to the (200) plane of rutile TiO_2. Rutile TiO_2 is another polymorph of titanium dioxide, characterized by a tetragonal crystal structure. The JCPDS card number for rutile TiO_2 is 21-1276. Moving forward, at 53.5 degrees, there is a peak related to the (105) plane of anatase TiO_2, further confirming the presence of this phase in the sample. Additionally, a peak is observed at 54.6 degrees, corresponding to the (211) plane of rutile TiO_2, reinforcing the presence of rutile phase in the material. At 62.4 degrees, a peak is found corresponding to the (204) plane of anatase TiO_2, providing additional evidence for the existence of anatase phase in the sample. Lastly, at 74.7 degrees, a peak is observed, which corresponds to the (220) plane of rutile TiO_2. This peak further supports the presence of the rutile phase in the material.

The presence of both anatase and rutile phases in the TiO_2 sample is revealed by the distinct peaks in the XRD pattern. The characterization and identification of these phases are essential as they can significantly influence the material's properties and applications. The X-ray diffraction (XRD) analysis of the Ag-TiO_2 sample did not show any peaks corresponding to silver (Ag) or Ag-containing phases. One possible explanation for this is that the concentration of Ag incorporated into the TiO_2 matrix was below the detection limit of the PXRD analysis. It is important to note that XRD analysis typically has a detection limit, and if the concentration of Ag is too low, it may not be observable in the XRD pattern.

Despite the absence of Ag-related peaks, the XRD pattern still exhibited characteristic peaks corresponding to the anatase and rutile phases of TiO_2, as described in the previous paragraph. These peaks confirmed the presence of the TiO_2 phases in the Ag-TiO_2 sample. It is worth considering that the Ag doping concentration, the synthesis conditions, and the interaction between Ag and TiO_2 at the atomic level can all influence the detection and observation of Ag-containing phases in the XRD analysis. Additional characterization techniques, such as electron microscopy or energy-dispersive X-ray spectroscopy (EDX), might be required to confirm the presence of Ag and provide a more comprehensive understanding of its distribution within the TiO_2 matrix.

To summarize, the XRD analysis of the Ag-TiO_2 sample did not reveal any Ag or Ag-containing phases, likely due to the low concentration of Ag incorporated, which fell below the detection limit of the PXRD analysis. However, the XRD pattern did confirm the presence of the anatase and rutile phases of TiO_2 in the sample. Further characterization techniques can be employed to investigate the presence and distribution of Ag at lower concentrations.Ref: Maury-Ramirez, A. (Ed.). (2015). Photocataytic Coatings for Air-Purifying, Self-Cleaning and Antimicrobial Properties. MDPI AG.
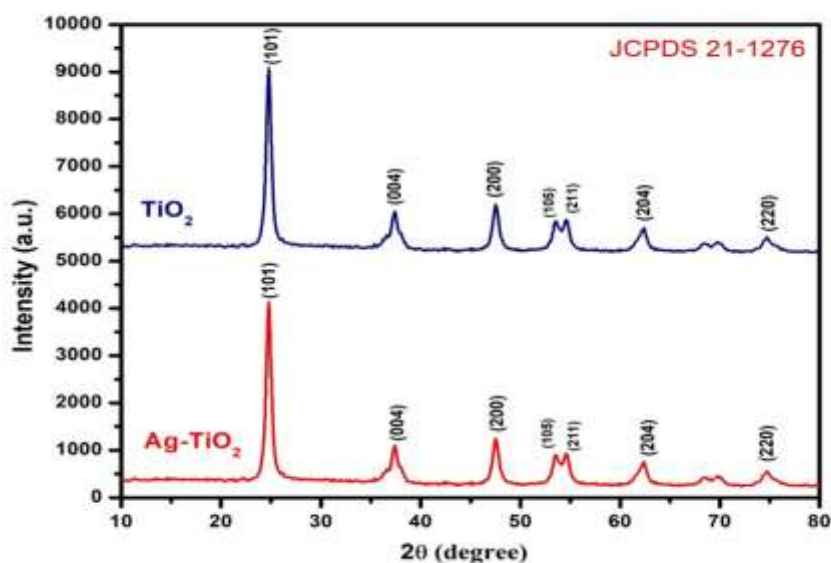
Figure: 7.XRD patterns of TiO₂ nanoparticles prepared by different methods: (a) sol-gel (b) hydrothermal (c) silver doping by sol-gel method.

Table: 1. Obtained values of XRD patterns of TiO2 nanoparticles.

Degree	Plane	Form
24.8	(101)	Anatase
37.4	(004)	Anatase
47.5	(200)	Rutile
53.5	(105)	Rutile
54.6	(211)	Rutile
62.4	(204)	Anatase
74.7	(220)	Rutile

4. Conclusion:

In summary, a facile approach was proposed towards the synthesis of TiO_2 nanospheresand deposition of Ag nanoparticles on the surface of TiO_2via sol-gel, Hydrothermal method to fabricate photoanodes for DSSCs. The prepared TiO_2 and Ag@TiO_2Nano particles materials were used as photoanode inthe dye-sensitized solar cells to investigate the solar to electricalenergy conversion ability.The incorporation of Ag on the TiO_2surface significantly influenced the size and properties. The TiO_2 nanoparticles prepared via sol-gel route were flex shape with size (103.9 nm) as compared to the one prepared by hydrothermal method (93.30 nm). Ag@TiO_2 prepared by sol-gel method having the size (84.89 nm). Due to Ag doping particle size is get reduced. The band gap of the synthesised nanoparticles was found to be size dependent. The band gap value of sol-gel synthesised TiO_2 is 3.79, TiO_2 synthesised by hydrothermal method is 3.70 and that of Ag- doped TiO_2 is 3.82 eV.

The improvementwas mainly approved to the Ag nanoparticles, which increasedthe visible light adsorption due to its light harvesting propertyin the visible range because of the surface plasmon resonanceeffect.UV-vis absorption spectra reveal that the addition of dopant suppresses the growth of TiO_2 grains, agglomerates them and shift the absorption band of TiO_2 from ultraviolet to visible. Photoluminescence investigation revealed that the incorporation of Ag

nanoparticles on the surface TiO$_2$ nanoparticles minimize the recombination between the electron in TiO$_2$ CB and electrolyte or dye there by improve the interfacial charge transfer process, which is more beneficial for the DSSC.

References-

1. Bhojanaa, K.B., M. Ramesh, and A. Pandikumar. "Complementary Properties of Silver Nanoparticles on the Photovoltaic Performance of Titania Nanospheres Based Photoanode in Dye-Sensitized Solar Cells." *Materials Research Bulletin* 122 (2020): 110672. https://doi.org/10.1016/j.materresbull.2019.110672.

2. Bera, S, D Sengupta, S Roy, and K Mukherjee. "Research into Dye-Sensitized Solar Cells: A Review Highlighting Progress in India." Journal of Physics: Energy 3, no. 3 (2021): 032013. https://doi.org/10.1088/2515-7655/abff6c.

3. Pandikumar, Alagarsamy, Su-Pei Lim, Subramaniam Jayabal, Nay Ming Huang, Hong Ngee Lim, and Ramasamy Ramaraj. "Titania@gold Plasmonic Nanoarchitectures: An Ideal Photoanode for Dye-Sensitized Solar Cells." Renewable and Sustainable Energy Reviews 60 (2016): 408–20. https://doi.org/10.1016/j.rser.2016.01.107.

4. Kishore Kumar, D., Jan Kříž, N. Bennett, Baixin Chen, H. Upadhayaya, Kakarla Raghava Reddy, and Veera Sadhu. "Functionalized Metal Oxide Nanoparticles for Efficient Dye-Sensitized Solar Cells (Dsscs): A Review." Materials Science for Energy Technologies 3 (2020): 472–81. https://doi.org/10.1016/j.mset.2020.03.003.

5. Lim, Su Pei, Alagarsamy Pandikumar, Nay Ming Huang, and Hong Ngee Lim. "Enhanced Photovoltaic Performance of Silver@titania Plasmonic Photoanode in Dye-Sensitized Solar Cells." RSC Adv. 4, no. 72 (2014): 38111–18. https://doi.org/10.1039/c4ra05689b.

6. Lim, Su Pei, Alagarsamy Pandikumar, Nay Ming Huang, and Hong Ngee Lim. "Facile Synthesis of Au@tio2 Nanocomposite and Its Application as a Photoanode in Dye-Sensitized Solar Cells." RSC Advances 5, no. 55 (2015): 44398–407. https://doi.org/10.1039/c5ra06220a.

7. Gao, Yuanpeng, Pengfei Fang, Feitai Chen, Yang Liu, Zhi Liu, Dahai Wang, and Yiqun Dai. "Enhancement of Stability of N-Doped Tio2 Photocatalysts with Ag Loading." Applied Surface Science 265 (2013): 796–801. https://doi.org/10.1016/j.apsusc.2012.11.114.

8. Huang, L.H., C. Sun, and Y.L. Liu. "PT/n-Codoped Tio2 Nanotubes and Its Photocatalytic Activity under Visible Light." Applied Surface Science 253, no. 17 (2007): 7029–35. https://doi.org/10.1016/j.apsusc.2007.02.048.

9. Umale, Sanjivani V., Sneha N. Tambat, Vediappan Sudhakar, Sharad M. Sontakke, and Kothandam Krishnamoorthy. "Fabrication, Characterization and Comparison of DSSC Using Anatase Tio 2 Synthesized by Various Methods." Advanced Powder Technology 28, no. 11 (2017): 2859–64. https://doi.org/10.1016/j.apt.2017.08.012.

10. Umale, Sanjivani V., Sneha N. Tambat, Vediappan Sudhakar, Sharad M. Sontakke, and Kothandam Krishnamoorthy. "Fabrication, Characterization and Comparison of DSSC Using Anatase Tio 2 Synthesized by Various Methods." Advanced Powder Technology 28, no. 11 (2017): 2859–64. https://doi.org/10.1016/j.apt.2017.08.012.

Antibacterial and Antifungal Study of Schiff Base Ligand and its Ln(III) Complexes Derived from 4-Nitrobenzaldehyde

Atish R Mehetre[1*], Ganesh B Andhale[2], Prabhakar Kute[3], Kailash R Borude[4], Sandeep R. Deshmukh[5]

[1*]Department of Chemistry, Shivaji Arts, Commerce and Science College Kannad, (MS) India

[2]Department of Chemistry JijamataMahavidyalayaBuldhana, (MS) India

[3]Department of Chemistry, PratishthanMahavidylayaPaithan, (MS) India

[4]Department of Chemistry, KKM College Manvat, (MS) India

[5]Department of Chemistry,R.M.G. Arts, Commerce and Science College Saoli, (MS)India

* Correspondence e-mail: mehetrear@shivajicollegekannad.org

Abstract:

Antimicrobial activity of Lanthanide Schiff base Complexes were studied in-vitro. 4-amino-3-hydroxy benzoic acid and 4-nitrobenzaldehyde were used to prepare Schiff base and nitrates of Neodymium, Gadolinium and Dysprosium were used as source of metal in complexes. Synthesized compounds were structurally characterized by UV, IR, NMR, HRMS, TGA, magnetic moment and molar conductance. Disc diffusion method and minimum inhibitory concentration (MIC) method were used to study antibacterial and antifungal activity of Schiff base ligand and its Ln(III) complexes. Antibacterial activity studied in-vitro against gram-positive bacteria Bacillus subtilis and with gram-negative bacteria Pseudomonas aeruginosa. Antifungal activity studied in-vitro against Saccharomyces cerevisiae.

Keywords: Antimicrobial activity, Complex, Lanthanide, Schiff base.

Introduction:

Lanthanide ions prevent the growth of bacteria, fungus, and soil nematodes [1]. Various Ce(III) salts (acetate, stearate, chloride, and nitrate) were shown to have antibacterial action in the 19th century and Ce(IV) sulfate was used as an antiseptic powder due to Ce(IV)'s oxidizing capabilities, Since then, Lanthanides have been used with varying degrees of effectiveness as anticoagulants, anti-atherosclerotic agents, and treatments for tuberculosis [2]. The success story for lanthanides as therapeutic metals is the acceptance of lanthanum carbonate, or Fosrenol, as a phosphate binder for the treatment of hyperphosphatemia in renal dialysis patients in USA and Europe [3]. Numerous studies have reported that the C=N linkage in azomethine derivatives is essential for biological activity and that these compounds exhibit significant anticancer, antifungal, and antibacterial properties [4,5,6].Due to a wide range of applications, such as anticancer and antibacterial properties, the synthesis of Schiff base complexes with lanthanide has grown in importance over the past few years [7,8].Lanthanide complexes have received attention for a long time due to their uses in diagnostic medicine, such as contrast agents for magnetic resonance imaging [9].To make the lanthanide ions more sensitive, neutral and carboxylic acid ligands with N- and O-atoms served as antenna.These kinds of rare earth complexes showed strong antibacterial activity [10].Keeping this in view, Schiff base and its Lanthanide complexes were prepared and screened for their antibacterial and antifungal activity.

Materials and Methods:

Chemicals used in the experiments were bought from S.D. Fine and Alfa aesar.In the antimicrobial activity microorganism used, its strain name and reference are as [Bacillus subtilis NCIM 2250], [Pseudomonas aeruginosa (NCIM 2036)] and [Fungi (yeast) Saccharomyces

cerevisiae (NCIM 3050)].[NCIM: National Collection of Industrial Microorganisms, National Chemical Laboratory (NCL), Pune 411008 (India)]

Experimental:

Synthesis of Schiff base and its Lanthanides Complexes:

Schiff base namely (E)-3-hydroxy-4-((4-nitrobenzylidene)amino)benzoic acid was prepared by using 4-amino-3-hydroxy benzoic and 4-nitrobenzaldehyde, as mention in reference[11].The complexes were prepared by using nitrate of Neodymium, Gadolinium and Dysprosium. Ethanolic solution of Schiff basecontaining NaOHmixed with lanthanide nitrateas mention in reference [11].

Characterization:

Schiff base ligand and its lanthanide complexes were characterized by different analytical sophisticated instrument techniques. UV, IR, NMR, HRMS, TGA, magnetic moment and molar conductance were used to characterize the compounds. All synthesizedLn(III) complexes were correspond to the formula$[LnL_2(H_2O)_2]2H_2O$. All the complexes were stable in air and non-hygroscopic in nature.

Formation of Schiff base ligand was confirmed by NMR, a singlet pick observed at 8.88 δ assigned to Schiff base proton [12]. HRMS for Schiff base calculated [M+H] is 287.0668 and in the spectra found at 287.0664 which confirms the proposed structure. A strong absorption band at 1626cm^{-1}, which may be attributed to the azomethine group [HC=N], carbonyl[C=O] of COOH group observed at 1692 cm^{-1} [13]. In the complexes carboxylate group shows bidentate coordination. Symmetric and Asymmetric stretching frequencies have Δ difference between 83 cm^{-1} to 108 cm^{-1} which confirms bidentate coordination [14]. Metal-oxygen band found at 447 cm^{-1} and 453 cm^{-1}[15]. UV–Vis spectra of complexes are different from that of the free Schiff base, which indicates formation of new complexes.Blue shift observed in the electronic spectra of ligand [16]. The thermo gram of Dy (III) complex showed the coordinated water molecules and lattice water molecules.The TGA results showed that the Schiff base and its lanthanide complexes are thermally stable at room temperature [17].The magnetic moments of the complexes remain unchanged upon coordination with Schiff base ligands, indicating thereby that 4f electrons do not participate in bond formation [18].Molar conductance studies suggest non-electrolytic nature of the complexes.

Antimicrobial studies:

The disc diffusion method was used to examine the antibacterial and antifungal properties of Schiff base and its Ln(III) complexes of Neodymium, Gadolinium, and Dysprosium. In the antibacterial activities, compounds were tested at 1000 ppm concentration against Pseudomonas aeruginosa and Bacillus subtilis using chloramphenicol as standard. The synthetic compounds were further tested for their antifungal efficacy against Saccharomyces cerevisiae at a concentration of 1000 ppm using Amphotericin B as standard [19,20].Disc diffusion was used to monitor the antibacterial and antifungal activity in vitro using disc size 6 mm. The nutrient agar medium was used for screening the antibacterial activity and the potato dextrose agar and MGYP medium was used for screening the antifungal activity.The plates were incubated at 37°C for 24 hours, and the diameter of the inhibition zones (zones where bacterial growth is inhibited) was measured [21,22].

Table 1.Antimicrobial activity of Schiff base and its Ln(III) complexes

Test Compound	Bacillus subtilis	Pseudomonas aeruginosa	Saccharomyces cerevisiae
Schiff base	10.02	10.09	27.12
Nd(III) complex	10.25	9.12	15.12
Gd(III)complex	00.00	00.00	15.12
Dy (III)complex	7.08	7.02	9.56
Chloramphenicol	26.12	24.53	NA
Amphotericin B	NA	NA	28.19

Zone of inhibition = Diameter in mm calculated by Vernier Caliper, NA = Not applicable

Minimum Inhibitory Concentration (MIC) Studies:

Minimum Inhibitory concentration (MIC) of Schiff base and its lanthanide complexes was tested in-vitro.The compounds were tested at the differentconcentration and prepared in DMF. Stock solution 10.24 mg per 5 ml[equivalents to 2048 microgram per ml] of each compound was prepared in DMF.Further dilutions were prepared in water. In this double dilution method variousconcentrations Viz.1024, 512, 256, 128, 64, 32, 16, 8, 4, 2, 1, 0.5, 0.25, 0.125microgram/mL were used. The incubation of tubes placed for 24 h at 37 °C and minimum inhibitory concentration (MIC) of each tube was measured. The results obtained werecompared with known standard drug. Obtained data is presented in table [21,22].

Table 2. Minimum inhibitory concentration (MIC) of Schiff base and its Ln(III) complexes.

Test Compound	Bacillus subtilis	Pseudomonas aeruginosa	Saccharomyces cerevisiae
Schiff base	512	512	8
Nd(III) complex	256	512	64
Gd(III)complex	>1024	>1024	>1024
Dy (III)complex	>1024	>1024	>1024
Chloramphenicol	0.125	4.0	NA
Amphotericin B	NA	NA	0.2

Minimum inhibitory concentration (MIC) microgram per ml (μg/ml)

Results and discussion:

Testing was carried out against Gram +ve microbe and Gram -ve microbe which includes Bacillus subtilis and Pseudomonas aeruginosa and antifungal activity against fungi Saccharomyces cerevisiae by disc diffusion method.The data from the inhibitory zone shows that several strains of bacteria and fungus were moderately inhibited by the Schiff base and its metal complexes.The impermeability of microbe cells or differences in ribosomes in microbial cells affect the toxicity of various complexes against various species [23-25].

The findings of the minimum inhibitory concentration (MIC) test show that the majority of the tested compounds need higher concentrations than the standard.In addition to being a requirement for antibacterial activity, chelation is also thought to be a result of steric hindrance, electronic, and pharmacokinetic variables working along with the mechanistic pathway.It has also been observed that solubility, conductivity, dipole moment, size of the metal ion, stability constants of the complexes, and their magnetic moments affect the activity of compounds against microbes [26-28]. The inhibitory zone data reveals that both Schiff base and its complexes showed good to moderate activity against strain Saccharomyces cerevisiae than the other compounds.

Conclusion:

The disc diffusion method and double dilution method were used to investigate the antibacterial activity of the Schiff base and its Ln(III) complexes against the gram positive strains Bacillus substilis as well as the gram negative strains Pseudomonas aeruginosa. According to the findings Schiff base and its complexes shows inhibition. Although the majority of the tested compounds were determined to be modestly active compared to the standard. In minimum inhibitory concentration (MIC) studies show that the majority of the tested compounds need higher concentrations than the standard. amongst all strains compounds good activity against strain Saccharomyces cerevisiae compared to others.

Reference:

1. Wakabayashi, T., Ymamoto, A., Kazaana, A., Nakano, Y., Nojiri, Y., &Kashiwazaki, M. (2016). Antibacterial, Antifungal and Nematicidal Activities of Rare Earth Ions. Biological Trace Element Research, 174(2), 464–470.

2. Cota, I., Marturano, V., &Tylkowski, B. (2019). Ln complexes as double faced agents: Study of antibacterial and antifungal activity. Coordination Chemistry Reviews, 396, 49–71.

3. Fricker, S. P. (2006). The therapeutic application of lanthanides. Chemical Society Reviews, 35(6), 524.

4. Yousif, E., Majeed, A., Al-Sammarrae, K., Salih, N., Salimon, J., & Abdullah, B. (2017). Metal complexes of Schiff base: Preparation, characterization and antibacterial activity. Arabian Journal of Chemistry, 10, S1639–S1644.

5. Kuchtanin, V., Kleščíková, L., Šoral, M., Fischer, R., Růžičková, Z., Rakovský, E., …Segľa, P. (2016). Nickel(II) Schiff base complexes: Synthesis, characterization and catalytic activity in Kumada–Corriu cross-coupling reactions. Polyhedron, 117, 90–96.

6. Abdel-Kader, N. S., El-Ansary, A. L., El-Tayeb, T. A., &Elnagdi, M. M. F. (2016). Synthesis and characterization of Schiff base complexes derived from cephradine: Fluorescence, photostability and photobiological applications. Journal of Photochemistry and Photobiology A: Chemistry, 321, 223–237.

7. Alghool, S., Abd El-Halim, H. F., Abd El-sadek, M. S., Yahia, I. S., &Wahab, L. A. (2012). Synthesis, thermal characterization, and antimicrobial activity of lanthanum, cerium, and thorium complexes of amino acid Schiff base ligand. Journal of Thermal Analysis and Calorimetry, 112(2), 671–681.

8. Łyszczek, R. (2011). Hydrothermal synthesis, thermal and luminescent investigations of lanthanide(III) coordination polymers based on the 4,4′-oxybis(benzoate) ligand. Journal of Thermal Analysis and Calorimetry, 108(3), 1101–1110. doi:10.1007/s10973-011-1987-6

9. Kapadia, M. A., Patel, M. M., & Joshi, J. D. (2009). Coordination polymers of Ln(III): Synthesis, characterization, catalytic and antimicrobial aspects. InorganicaChimicaActa, 362(9), 3292–3298.

10. Zhou, M.-X., Ren, N., Zhang, J.-J., & Wang, D.-Q. (2019). Synthesis, crystal structure, thermal, luminescent property and antibacterial activity of lanthanide ternary complexes with p-chlorobenzoic acid and 5,5′-dimethyl-2,2′-bipyridine. Journal of Molecular Structure, 127049.

11. Atish R Mehetre (2021). Synthesis Characterization and Application of Metal Complexes of Ligands Having N, S or O as Donor Atom. Thesis submitted to Dr. BabasahebAmbedkarMarathwada University Aurangabad.

12. Nihal O. Shaker; Fatma H. Abd El-Salam; Bahyiam. El-Sadek; Eman M. Kandeel and Sharbat A. Baker(2011). Anionic Schiff Base Amphiphiles:Synthesis, Surface, Biocidal And Antitumor Activities, Journal of American Science, 7(5), 427-436.

13. Jigna Parekh, Pranavinamdhar, RathishNair,Shiprabaluja And SumitraChanda (2005). Synthesis and Antibacterial Activity of Some Schiff Bases Derived From 4-Aminobenzoic Acid, J. Serb. Chem.Soc., 70(10), 1155–1161.

14. G.B. Deacon and R.J. Phillips, Relationships Between The Carbon-Oxygen Stretching Frequencies Of Carboxylato Complexes and The Type Of Carboxylate Coordination.Coordination Chemistry Reviews, 33 (1980) 227-250.

15. Basavaraj M. Kalshetty A, Shambuling S. KarabasannavarB,Ramesh S. Gani B, Mallikarjun B. Kalashetti C(2013). Synthesis, Characterization and anti-Microbial Study of Some Organometallic Complexes of Multi-Dentate Schiff Bases Derived From3-Aldehydosalicylic Acid At various Ph Ranges. Drug Invention Today 5,105-112.

16. Shi, S.-M., Chen, Z.-F., Liu, Y.-C., Mao, L., Liang, H., & Zhou, Z.-Y. (2008). Synthesis and crystal structures of lanthanide complexes with foliage growth regulator: phenoxyalkanoic acid. Journal of Coordination Chemistry, 61(17), 2725–2734.

17. Huang, W.-Y., Chen, Z.-L., Zou, H.-H., Liu, D.-C., & Liang, F.-P. (2013). Syntheses, structures, and fluorescence properties of cadmium(II) and zinc(II) complexes based on 1,1′-binaphthalenyl-2,2′-diamine-N,N,N′,N′-tetraacetic acid. Polyhedron, 50(1), 1–9. doi:10.1016/j.poly.2012.10.042 10.1016/j.poly.2012.10.042

18. Dhumwad, S. D., &Goudar, T. R. (1993). Synthesis and Characterization of Lanthanide(III) Complexes With 3,4-Methylenedioxybenzaldehyde Thiosemicarbazone., Polyhedron, 12(23), 2809–2813

19. Balouiri, M., Sadiki, M., and Ibnsouda, S. K. (2016). Methods for in vitro evaluating antimicrobial activity: A review. Journal of Pharmaceutical Analysis, 6(2), 71–79.

20. Razmavar, S., Abdulla, M. A., Ismail, S. B., &Hassandarvish, P. (2014). Antibacterial Activity of Leaf Extracts of Baeckeafrutescens against Methicillin-Resistant Staphylococcus aureus. BioMed Research International, 1–5.

21. Jorgensen J. H. and Turnidge (2007), Susceptibility Test methods : Dilution and Disk diffusion methods, In Manual of clinical Microbiology (Volume II), Ed. Murray P. R., Baron E. J., Jorgensen J. H., Landry M. L. Pfaller M. A. 1152-1173.

22. Espinel-Ingroff and Pfaller M. A. (2007) Susceptibility test methods: Yeasts and Filamentous Fungi, In Manual of clinical Microbiology (Volume II), Ed. Murray P. R., Baron E. J., Jorgensen J. H., Landry M. L. Pfaller M. A. 1972-1986

23. Siibak, T., Peil, L., Xiong, L., Mankin, A., Remme, J., &Tenson, T. (2008).Erythromycin- and Chloramphenicol-Induced Ribosomal Assembly Defects AreSecondary Effects of Protein Synthesis Inhibition. Antimicrobial Agents andChemotherapy, 53(2), 563–571.

24. Frei, A. (2020). Metal Complexes, an Untapped Source of Antibiotic Potential?Antibiotics, 9(2), 90.

25. Thangamani, S., Mohammad, H., Abushahba, M. F. N., Sobreira, T. J. P.,Hedrick, V. E., Paul, L. N., &Seleem, M. N. (2016). Antibacterial activity andmechanism of action of auranofin against multi-drug resistant bacterial pathogens.Scientific Reports, 6(1). 1-13.

26. Jadhav, S. M., Shelke, V. A., Munde, A. S., Shankarwar, S. G., Patharkar, V. R.,&Chondhekar, T. K. (2010). Synthesis, Characterization, Potentiometry, and Antimicrobial Studies of Transition Metal Complexes of A Tridentate Ligand. Journal of Coordination Chemistry, 63(23), 4153–4164.

27. Anacona, J. R., & Acosta, F. (2006). Synthesis and Antibacterial Activity of Cephradine Metal Complexes. Journal of Coordination Chemistry, 59(6), 621–627.

28. Singh, H. L., Varshney, S., &Varshney, A. K. (2000). Synthesis and Spectroscopic Studies of Organotin(IV) Complexes of Biologically Active Schiff Bases Derived From Sulpha Drugs. Applied Organometallic Chemistry, 14(4), 212–217.

Pharmacophore Modeling for N‑Phenylbenzamide Derivatives Targeting Wild Type of T. Brucei Parasites

Shrikant B. Bansod[1]*, Jayant R. Bansod[2], Sanjay P. Mote[3], Prashant S. Nawale[4]
1 Department of Chemistry ACS college Kiran nagar Amravati,
2 Department of Chemistry Vidya Bharati college Amravati,
3 B.B. Arts, N.B. Commerce & B.P. Science College, Digras Dist. Yavatmal
4 Department of Chemistry Vidya Bharati college Amravati
Email for Correspondence: shrikantbansod71@gmail.com

Abstract:

The current study employed a ligand-based drug design technique, namely consensus pharmacophoric analysis, to investigate the T. Brucei inhibitory activity of substituted N-phenylbenzamide derivatives. The aim was to identify significant aspects that may be optimized in the future. Structure drawing, optimization, file-based alignment, and pharmacophore model building are all part of the process. According to the study, aromatic rings and H-bond donor and acceptor groups are essential for the anti-T. Brucei activity. The results may prove beneficial in optimizing N-phenylbenzamide derivatives as treatments that prevent chagas disease.

Keywords: Anti-Chagas, T. Brucei, Pharmacophore modeling, N‑Phenylbenzamide derivatives

Introduction:

Trypanosoma cruzi, Trypanosoma brucei, and Leishmania are three kinetoplastid parasite-caused neglected tropical illnesses that inflict a tremendous deal of misery worldwide. Leishmaniasis and the American and African trypanosomiases pose a hazard to millions of individuals, primarily in the world's least developed nations [1-5].

The current treatments for these conditions are ineffective because they frequently have poor efficacy against drug-resistant parasite strains, target a specific stage of the illness or patient condition (such as late-stage rhodesiense sleeping sickness, chronic Chagas disease, and HIV/leishmaniasis coinfection), and frequently necessitate lengthy treatment regimens and high dosages with serious side effects[4-6]. Further limiting treatment possibilities include T. brucei rhodesiense, T. cruzi, and Leishmania spp., which are all zoonotic and cause disease in a variety of domestic animals. Therefore, to strengthen this far from perfect therapeutic armament, new antiprotozoal medications are required. Under the auspices of the Drugs for Neglected Diseases project (DNDi), a number of promising types of novel chemical entities (NCE) are presently undergoing clinical development.

In phase I trials for leishmaniasis and Chagas disease, for example, the polyadenylation specificity factor 3 (CPSF3) inhibitor acoziborole is a lead contender, while its derivative DNDI-6148 has advanced to phase IIb/III for the single-dose oral therapy of gambiense human African trypanosomiasis (HAT).

N-phenylbenzamide derivatives have recently been discovered by Jonathan Nué-Martinez et al. [5] to be effective anti-Chagas agents. Due to the wide range of substituents, the studied N-phenylbenzamide derivatives have a great degree of diversity in their anti-Chagas profile. In order to discover important scaffolds, extensive structure-activity relationships (SAR) were studied. However, this is the first attempt to explain the pharmacophoric characteristics or pattern associated with the anti-Chagas activity of derivatives of substituted N-phenylbenzamide.

Consequently, consensus pharmacophore modeling was done in the current investigation to identify the important structural characteristics that determine the anti-Chagas action of N-phenylbenzamide derivatives.

2. Materials And Methods

2.1. Dataset

Thirty-five N-phenylbenzamide derivatives containing a range of substituents, including heterocyclic rings, -CN, -OCH3, -Br, and other isomers, are included in the dataset. The chosen dataset thus spans a significant amount of chemical space. The anti-Chagas activity of the compounds was evaluated against wild type T. Brucei. The range of activity values denoted as EC50 is 0.12 to 85.6. Table 1 displays the tabulated dataset.

Cmpd	SMILES	T. brucei, WT EC50 (nM)
1a	O=C(NC1=CC=C(/N=C2NCCN\2)C=C1)C3=CC=C(/N=C4NCCN\4)C=C3.Cl.Cl	0.83
1c	O=C(NC1=NC=C(/N=C2NCCN\2)C=C1)C3=NC=C(/N=C4NCCN\4)C=C3.FC(F)(C(O)=O)F.FC(F)(C(O)=O)F	25.5 �7 3.2
1d	O=C(NC1=C(Cl)C=C(/N=C2NCCN\2)C=C1)C3=CC=C(/N=C4NCCN\4)C(Cl)=C3.FC(F)(C(O)=O)F.FC(F)(C(O)=O)F	nt
1e	O=C(NC1=CC=C(/N=C2NCCN\2)C(Cl)=C1)C3=CC=C(/N=C4NCCN\4)C(Cl)=C3.FC(F)(C(O)=O)F.FC(F)(C(O)=O)F	5.7 �7 0.7
1f	O=C(NC1=C(Cl)C=C(/N=C2NCCN\2)C=C1)C3=C(Cl)C=C(/N=C4NCCN\4)C=C3.FC(F)(C(O)=O)F.FC(F)(C(O)=O)F	10.4 �7 0.8
1g	O=C(NC1=CC=C(/N=C2NCCN\2)C(Cl)=C1)C3=C(Cl)C=C(/N=C4NCCN\4)C=C3.FC(F)(C(O)=O)F.FC(F)(C(O)=O)F	47.7 �7 13.2
1h	O=C(NC1=CC=C(/N=C2NCCN\2)C(OC(C)C)=C1)C3=C(OC(C)C)C=C(/N=C4NCCN\4)C=C3.FC(F)(C(O)=O)F.FC(F)(C(O)=O)F	17.6 �7 2.1
1i	O=C(NC1=C(F)C=C(/N=C2NCCN\2)C=C1)C3=CC=C(/N=C4NCCN\4)C(F)=C3.FC(F)(C(O)=O)F.FC(F)(C(O)=O)F	78.5 �7 6.1
2a	O=C(NC1=CC=C(/N=C2NC(C=CC=C3)=C3N\2)C=C1)C4=CC=C(/N=C5NC(C=CC=C6)=C6N\5)C=C4	85.6 �7 2.3
2c	O=C(NC1=NC=C(/N=C2NC(C=CC=C3)=C3N\2)C=C1)C4=NC=C(/N=C5NC(C=CC=C6)=C6N\5)C=C4	11.3 �7 0.2
2d	O=C(NC1=C(Cl)C=C(/N=C2NC(C=CC=C3)=C3N\2)C=C1)C4=CC=C(/N=C5NC(C=CC=C6)=C6N\5)C(Cl)=C4	1.96 �7 0.03
2e	O=C(NC1=CC=C(/N=C2NC(C=CC=C3)=C3N\2)C(Cl)=C1)C4=CC=C(/N=C5NC(C=CC=C6)=C6N\5)C(Cl)=C4	1.68 �7 0.06
2f	O=C(NC1=C(Cl)C=C(/N=C2NC(C=CC=C3)=C3N\2)C=C1)C4=C(Cl)C=C(/N=C5NC(C=CC=C6)=C6N\5)C=C4	5.56 �7 0.26
2g	ClC1=C(C(C(NC2=CC=C(/N=C3NC(C=CC=C4)=C4N\3)C(Cl)=C2)=O)C=CC(/N=C5NC(C=CC=C6)=C6N\5)=C1	2.64 �7 0.09
14	C1(/N=C2NC(C=CC=C3)=C3N\2)=CC=C(CCC4=CC=C(/N=C5NC(C=CC=C6)=C6N\5)C=C4)C=C1	2.3 �7 0.2
15	O=C(NC1=CC=C(/N=C2NC(C=CC=C3)=C3N/2)C=C1)NC4=CC=C(/N=C5NC(C=CC=C6)=C6N\5)C=C4	57.1 �7 1.4
16	C1(/N=C2NC(C=CC=C3)=C3N\2)=CC=C4C(CC5=C4C=CC(/N=C6NC(C=CC=C7)=C7N/6)=C5)=C1	2.44 �7 0.18
3a	O=C(NC1=CC=C(NC(C2=NC=CC=C2)=N)C=C1)C3=CC=C(NC(C4=CC=CC=N4)=N)C=C3	0.40 �7 0.02

'RESEARCH JOURNEY' *International E- Research Journal*
Special Issue – 333 : Innovative & Sustainable Chemistry
Impact Factor 6.625 (SJIF)   **Peer Reviewed Journal**

E-ISSN : 2348-7143
December - 2023

3b	O=C(NC1=NC=C(NC(C2=NC=CC=C2)=N)C=C1)C3=CC=C(NC(C4=CC=CC=N4)=N)C=C3.Cl.Cl	23.7 7 0.7
3b_b	O=C(NC1=NC=C(NC(C2=NC=CC=C2)=N)C=C1)C3=CC=C(N)C=C3.Cl	nt
3c	O=C(NC1=NC=C(NC(C2=NC=CC=C2)=N)C=C1)C3=NC=C(NC(C4=CC=CC=N4)=N)C=C3	0.12 7 0.01
3c_c	O=C(NC1=NC=C(NC(C2=NC=CC=C2)=N)C=C1)C3=NC=C(N)C=C3	nt
3d	O=C(NC1=C(Cl)C=C(NC(C2=NC=CC=C2)=N)C=C1)C3=CC=C(NC(C4=CC=CC=N4)=N)C(Cl)=C3.FC(F)(C(O)=O)F.FC(F)(C(O)=O)F	10.5 7 1.9
3e	O=C(NC1=CC=C(NC(C2=NC=CC=C2)=N)C(Cl)=C1)C3=CC=C(NC(C4=CC=CC=N4)=N)C(Cl)=C3.FC(F)(C(O)=O)F.FC(F)(C(O)=O)F	0.25 7 0.04
3f	N=C(C1=NC=CC=C1)NC2=CC(Cl)=C(C(NC3=C(Cl)C=C(NC(C4=NC=CC=C4)=N)C=C3)=O)C=C2.Cl.Cl	15.5 7 2.7
3g	O=C(NC1=CC=C(NC(C2=NC=CC=C2)=N)C(Cl)=C1)C3=C(Cl)C=C(NC(C4=CC=CC=N4)=N)C=C3.FC(F)(C(O)=O)F.FC(F)(C(O)=O)F	9.4 7 0.96
3h	N=C(C1=NC=CC=C1)NC2=CC(OC(C)C)=C(C(NC3=C(OC(C)C)C=C(NC(C4=NC=CC=C4)=N)C=C3)=O)C=C2.Cl.Cl	5.07 7 0.03
3i	N=C(C1=NC=CC=C1)NC2=CC=C(C(NC3=C(F)C=C(NC(C4=NC=CC=C4)=N)C=C3)=O)C=C2F	nt
3j	N=C(C1=NC=CC=C1)NC2=CC=C(C(NC3=CC=C(NC(C4=NC=CC=C4)=N)C(F)=C3)=O)C=C2F	nt
3k	N=C(C1=NC=CC=C1)NC2=CC(F)=C(C(NC3=C(F)C=C(NC(C4=NC=CC=C4)=N)C=C3)=O)C=C2	nt
3l	N=C(C1=NC=CC=C1)NC2=CC(F)=C(C(NC3=CC=C(NC(C4=NC=CC=C4)=N)C(F)=C3)=O)C=C2	nt

Note: nt:- not determined

2.2 Drawing, optimizing, and aligning structures

Thirty-five structures were drawn using the free ChemSketch 12 software, and all of the structures were optimized using the MMFF94 force field from TINKER, (3) The following stage involved running the Open3dAlign program to align all the optimal (4) Using the LIQUID plugin, consensus pharmacophore modeling was performed, using the default parameters and installed on PyMOl 2.2 [6-8].

3. Results And Discussion:
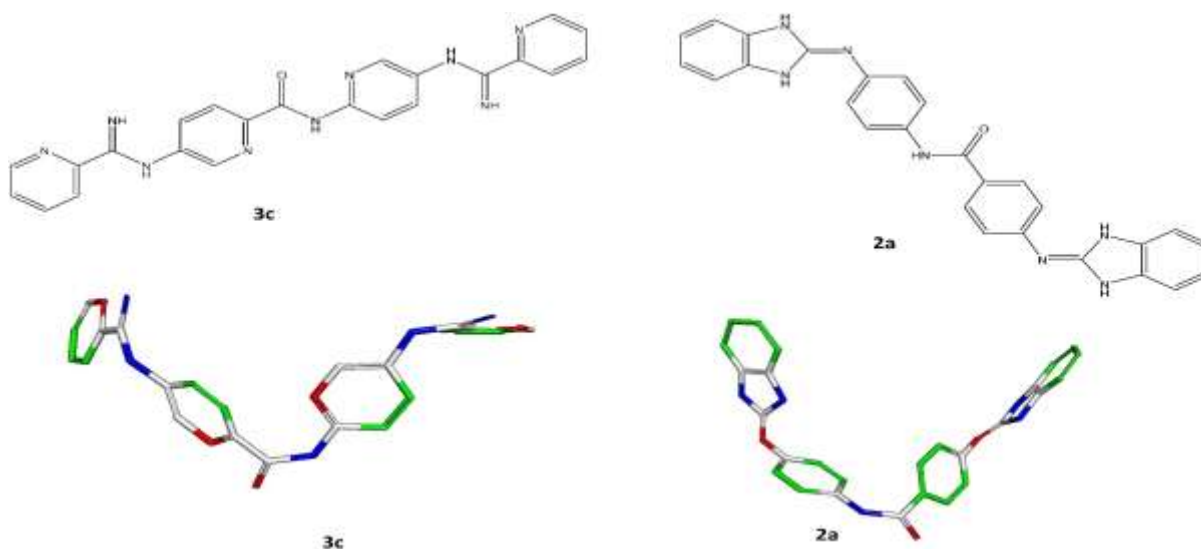
Figure 1: 2D and 3D- structure of most active molecule 3c and least active molecule 2a.

As per 2D structure the 3c molecules shows five pyridine rings while 2a molecule have N-phenylbenzamide ring bonded with 2 Aminobenzimidazole rings and According to 3D Structure the 3c molecule have U-Shape, while 2a molecules necklace shape.

3c   2a
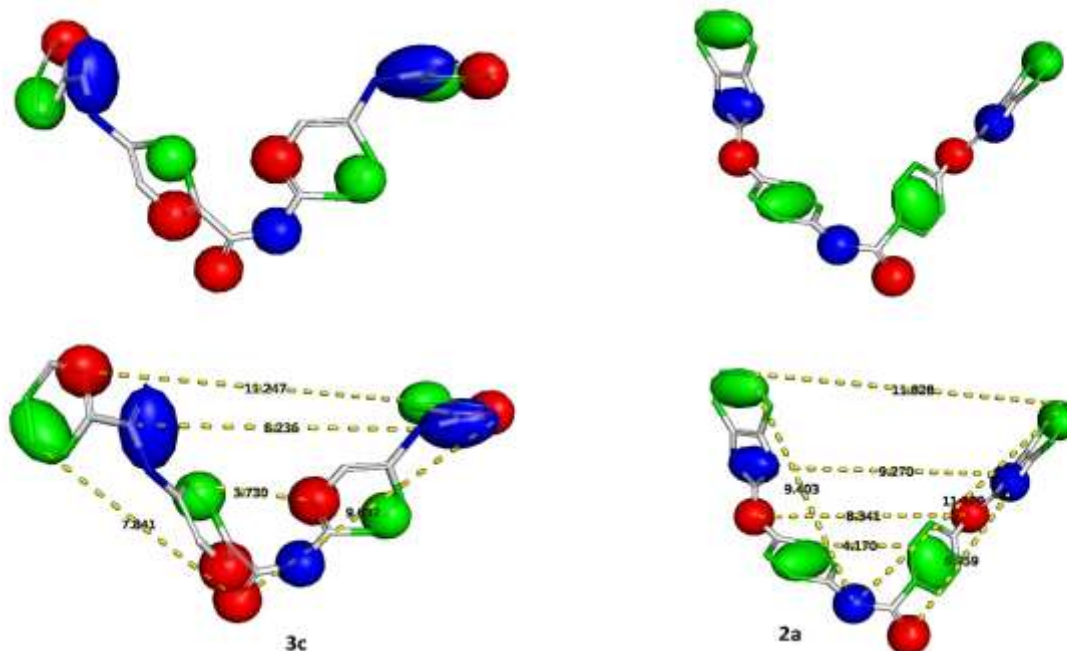
Figure 2. 3D- structures with pharmacophore model of most active molecule 3c and least active molecule 2a.

In 3c molecule largest distance Accepter (Red) to liphophile (Blue) is 11.247 A^0, Maximum distance between donor to Accepter is 9.832 A^0 , In 2a molecule maximum distance between liphophile to liphophile is 11.828 A^0 and donor to donor is 9.270 A^0, while lowest liphophileto liphophile is 4.170 A^0

3c   2a
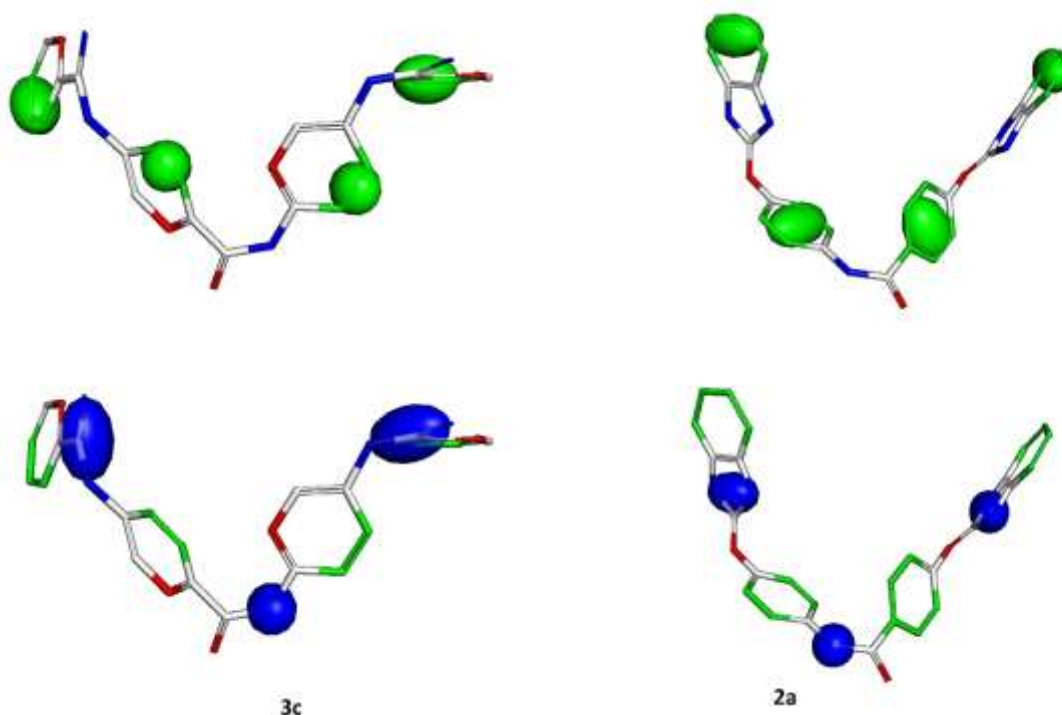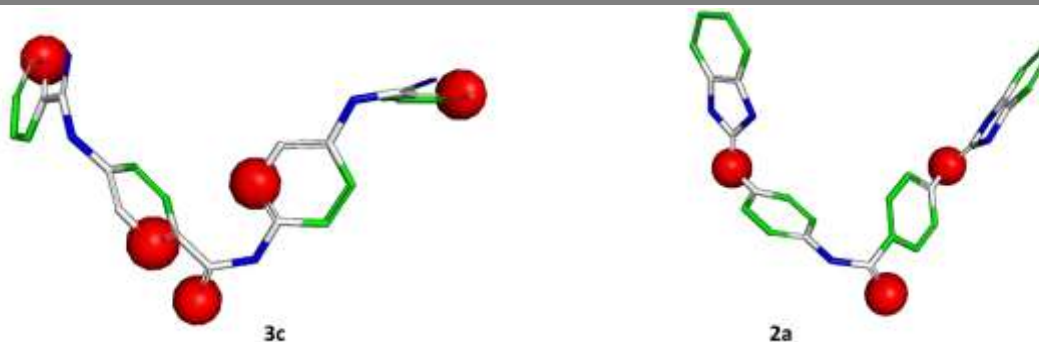
Figure 3: Lipophilic (green), H-bond donor (blue) and H-bond acceptor (red) contours for most active molecule 3c and least active molecule 2a.

In the above figure both molecule have same number of H-bond donor while 3c have five number of H-Bond accepter and 2a have only 3 H-Bond accepter.

Conclusions:

The present study indicates that the difference in the activity is due to H-bond acceptor regions. The second possible reason is difference in the shape of the molecule. In most active molecule 3c, the pharmacophore regions are separated by smaller distance than in least active molecule 2a. Thus, in future optimizations, H-bond acceptors should be give high preference.

References:

1. J. Jonathan Nué-Martinez, David Cisneros, María del Valle Moreno-Blázquez, Cristina Fonseca-Berzal, José Ignacio Manzano, Damien Kraeutler, Marzuq A. Ungogo, Maha A. Aloraini, Hamza A. A. Elati, Alexandra Ibáñez-Escribano, Laura Lagartera, Tomás Herraiz, Francisco Gamarro, Harry P. de Koning, Alicia Gómez-Barrio,* and Christophe Dardonville* Synthesis and Biophysical and Biological Studies of N-Phenylbenzamide Derivatives Targeting Kinetoplastid Parasites. Cite This: J. Med. Chem. 2023, 66, 13452−13480

2. Burza, S.; Croft, S. L.; Boelaert, M. Leishmaniasis. Lancet 2018, 392 (10151), 951−970. (2) Pinheiro, A. C.; de Souza, M. V. N. Current leishmaniasis drug discovery. RSC Med. Chem. 2022, 13 (9), 1029−1043.

3. Hina Shamshad1 · Rowaida Bakri2 · Agha Zeeshan Mirza3 Dihydrofolate reductase, thymidylate synthase, and serine hydroxy methyltransferase: successful targets against some infectious diseases. Received: 21 August 2021 / Accepted: 15 February 2022 / Published online: 7 March 2022 © The Author(s), under exclusive licence to Springer Nature B.V. 2022

4. Büscher, P.; Cecchi, G.; Jamonneau, V.; Priotto, G. Human African trypanosomiasis. Lancet 2017, 390 (10110), 2397−2409. (acccessed 2019/09/30)

5. Vijay H. Masand, Nahed N. E. El-Sayed, Vesna Rastija, Mithilesh M. Rathore & Maja Karnaš Identification of prodigious and underprivileged structural features for RG7834 analogs as Hepatitis B virus expression inhibitor Medicinal Chemistry Research ISSN 1054-2523 Volume 28 Number 12 Med Chem Res (2019) 28:2270-2278 DOI 10.1007/s00044-019-02455-w

6. Pérez-Molina, J. A.; Molina, I. Chagas disease. Lancet 2018, 391 (10115), 82−94. (acccessed 2023/01/17)

7. De Koning, H. P. The Drugs of Sleeping Sickness: Their Mechanisms of Action and Resistance, and a Brief History. Trop. Med. Infect. Dis. 2020, 5 (1), 14.

8. Croft, S. L.; Olliaro, P. Leishmaniasis chemotherapy�challenges and opportunities. Clin. Microbiol. Infect. 2011, 17 (10), 1478−1483.

9. Giordani, F.; Morrison, L. J.; Rowan, T. G.; De Koning, H. P.; Barrett, M. P. The animal trypanosomiases and their chemotherapy: a review. Parasitology 2016, 143 (14), 1862−1889.

10. Dantas-Torres, F.; Miró, G.; Baneth, G.; Bourdeau, P.; Breitschwerdt, E.; Capelli, G.; Cardoso, L.; Day, M.; Dobler, G.; Ferrer, L.; et al. Canine Leishmaniasis Control in the Context of One Health. Emerg. Infect. Dis. 2019, 25 (12), 1−4.

11. Desquesnes, M. 13 - Veterinary aspects. In American Trypanosomiasis Chagas Disease; Telleria, J., Tibayrenc, M., Eds., 2nd ed.; Elsevier, 2017, pp 283−298.

12. DNDi. DNDi Research & Development Portfolio. 2023. https:// dndi.org/research-development/portfolio/ (accessed 05-06-2023).

13. Betu Kumeso, V. K.; Kalonji, W. M.; Rembry, S.; Valverde Mordt, O.; Ngolo Tete, D.; Pretre,ˆ A.; Delhomme, S.; Ilunga Wa Kyhi, M.; Camara, M.; Catusse, J.; et al. Efficacy and safety of acoziborole in patients with human African trypanosomiasis caused by Trypanosoma brucei gambiense: a multicentre, open-label, single-arm, phase 2/3 trial. Lancet Infect. Dis. 2023, 23, 463−470. (acccessed 2022/12/15) (12) Mowbray, C. E.; Braillard, S.; Glossop, P. A.; Whitlock, G. A.; Jacobs, R. T.; Speake, J.; Pandi, B.; Nare, B.; Maes, L.; Yardley, V.; et al. DNDI-6148: A Novel Benzoxaborole Preclinical Candidate for the Treatment of Visceral Leishmaniasis. J. Med. Chem. 2021, 64 (21), 16159−16176

14. Mowbray, C. E.; Braillard, S.; Glossop, P. A.; Whitlock, G. A.; Jacobs, R. T.; Speake, J.; Pandi, B.; Nare, B.; Maes, L.; Yardley, V.; et al. DNDI-6148: A Novel Benzoxaborole Preclinical Candidate for the Treatment of Visceral Leishmaniasis. J. Med. Chem. 2021, 64 (21), 16159−16176.

Synthesis and Characterization of Azonapthaldehyde, Relevant Schiff Bases and Their Beta Lactam Derivatives

Anil H. Shinde and C. J. Patil* Rushi Nannavare

*Organic Research Laboratory (PG), Department of Chemistry, Smt. G. G. Khadse College, Muktainagar-425 306, Dist.: Jalgaon, MS, India

(anilhshinde1669@gmail.com; *drcjpatil@yahoo.com)

Abstract:

Azonapthaldehyde, (3) was prepared by reaction of 2-Hydrxy Napthaldehyde with diazonium salt of Aniline by diazotization method. Thus, synthesized Azonapthaldehyde, (3) was treated with variable 2-Amino-benzothiazoles (4a to 4f) to synthesize the Schiff bases (5a to 5f). The Beta lactam derivatives (6a to 6f) were also synthesized. All the newly synthesized compounds were characterized by color, physical constant, TLC, UV-Vis and FT-IR Spectral methods. The Beta lactam derivatives were also analyzed by 1H NMR and HR-MS spectral measurement. Future scope of this study is discussed.

Key words: Azonapthaldehyde, Schiff base, 2-Amino-benzothiozole and Beta lactam.

Introduction:

Schiff bases and their Beta lactam derivatives have variety of application in clinical, biological, analytical and pharmacological area. The organic compounds were studied by spectral [1-5] method. The schiff bases (-CH=N-) playes an important function as an organic synthone for newer molecules. In addition to spectral method literature shows reports on the antimicrobial activity of aldimines [6]. Study on the ionization constant of the ketimines [7] with reference to the influence of temperature for some acids and basic imines in 10 % ethanol, as reported in the literature. These imines are in a forms of syn or anti-oxime and phenolic or amino Schiff bases as reported in the literature. The azo compounds have different applications [8]. The synthesis of different types of compounds containing the chlro or an azo moiety [9] presence is known to lead them to exhibit herbicidal activity. The azo group in addition to the other groups in the same compounds have important biological activities antibacterial [10] and antioxidant [11].

Schiff base can be modified with the azo function. Azo linked schiff bases exhibited diverse applications in chemical as well as pharmacological activities. Literature shows some reports on the Azo Schiff bases. They have different properties and applications. Both these groups are having excellent coordinating properties [12-13]. The beta lactams are also very important moiety and are synthesized from varied Schiff bases [14].

Herein, an attempt is made in continuation of our previous reported study [15], to study synthesis of azo aldehydes and their relevant Schiff bases. This study is a. In view of these facts, this study is aimed at evaluating the structural characteristics of azo Schiff bases of Azonapthaldehyde and the varied Beta lactams synthesised from them. Recently we have published synthesis of variable Schiff bases, and their relevant Beta lactams of azo salicylaldehyde and characterised by UV-Vis, FT-IR, UV-Vis, FT-IR, ^{1}H NMR and HR-MS spectroscopy. (13)

'RESEARCH JOURNEY' *International E- Research Journal*
Special Issue – 333 : Innovative & Sustainable Chemistry
Impact Factor 6.625 (SJIF)   **Peer Reviewed Journal**

E-ISSN : 2348-7143
December - 2023

Main reaction:

Scheme-I: Synthesis of Azonapthaldehyde (3)
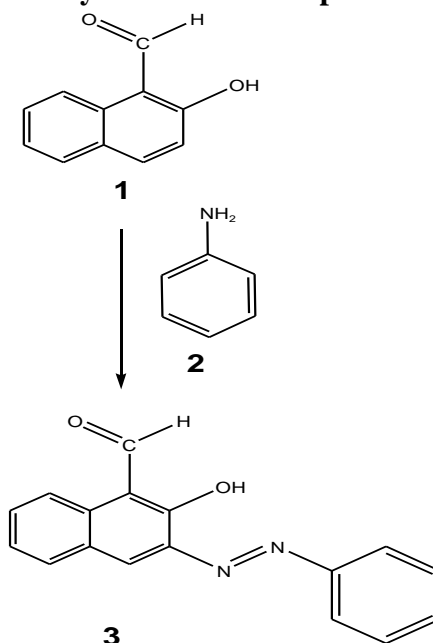
SCHEME-I

Scheme-II: Synthesis of Schiff bases (5a to 5f)

R_2

4a = -H
4b = 6-Cl-4-NO$_2$-
4c = 6-F-
4d = 4,6-F$_2$-
4e = 4-CH$_3$-6-NO$_2$-
4f = 6-NO$_2$-

4a-4f

5a - 5f
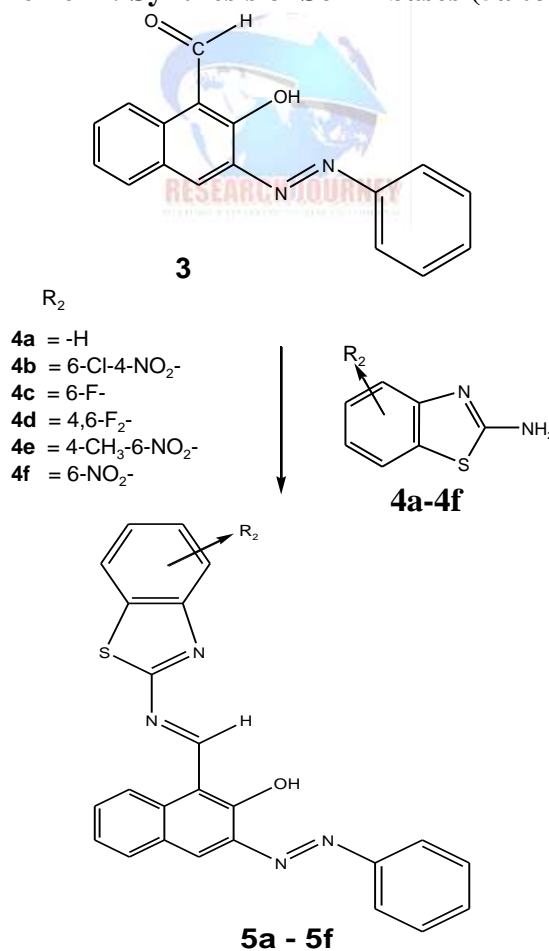
SCHEME-II

Scheme-III: Synthesis of Beta lactam derivatives (6a to 6f)
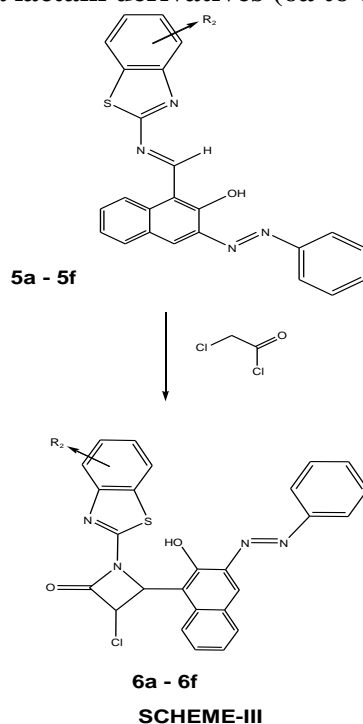
SCHEME-III

General method for synthesis of Azonapthaldehyde. : (3) (Scheme-I)

In 100 ml beaker charged 3.462 g. (0.0372 mole) Aniline. Then added to it 25 ml conc. HCl and 20 ml distilled water. Cooled the solution upto 0 ^{0}C by keeping it in ice bath (Solution-A).

In another 100 ml capacity beaker charged 3.105 g (0.045 mole) Sodium nitrite and dissolved it in about 15 ml water and cooled the solution up to 0 ^{0}C by keeping it in ice bath (Solution-B).

When both the solutions attain 0 ^{0}C temperature solution -B added dropwise in solution-A with constant stirring. During addition temperature was maintained up to 10 ^{0}C. The diazotized solution tested by starch iodied paper which gives blue colour. Pinch of solid Urea was added to decompose the excess of Nitrous acid. Filtered the solution and used in next step.

Then in 100 ml capacity beaker dissolved 6.39 g. (0.0372 mole) 2-Hydroxy napthaldehyde in 35 ml 10 % NaOH solution and stirred to get clear solution and cooled the solution up to 0 ^{0}C by keeping it in ice bath. Then above filtrate added to this content with constant stirring. During addition temperature maintained up to 10 ^{0}C. After complete addition allowed the charge to stand for 10 minutes in ice bath. Then filtered the brown coloured dye, washed with cold water, dried, recrystallized the crude product, weighed and stored in suitable container. This was recorded as (**3**) with Yield 66.55 % and m.p. 139-141 ^{0}C.

General method for synthesis of Scheme-II Azo Schiff bases (5a to 5f)

Equimolar proportion of relevant Benzothiazole and Azo aldehyde charged in 250 ml RBF. To this charge few drops of glacial Acetic acid and 70 ml Toluene was added. Attach and set Dean and Stark apparatus and refluxed upto 4 hrs. The product was checked by TLC. After clear TLC the solvent was removed under reduced pressure.

Recrystalized the crude product by Ethanol. Dried and preserved the pure product in tight container.

General method for synthesis of Scheme-III Beta lactam derivatives (6a to 6f).

In 100 ml capacity RBF flask with reflux condenser and thermometer pocket 0.00125 mole of Schiff base (**5a** to **5f)** and 0.15 ml TEA was dissolved in 20 ml 1, 4-Dioxane and kept it in ice bath and stirried for half an hour. To this cold solution 0.15 ml (0.00186 moles) Chloroacetyl chloride (CAC) was added slowely at $0\,^0$C to $5\,^0$C.

Then refluxed the content for 12-15 hrs. TLC checked after 9/11/13 hours. After clear TLC 1, 4-Dioxane was distilled off. The resultant content after removal of 1, 4-Dioxane was viscous liquid. It was washed with 10% NaHCO$_3$ to remove any unreacted Chloroacetyl chloride. Resulting product was washed with cold water and recrystallized by Methanol. Finally recorded the colour, physical constant and weight of product and labelled as (**6a** to **6f**) and packed in tight container. The physical and analytical data is depicted in **Table 8**.

The characterization of Schiff bases and Beta-lactam derivatives was done by usual methods viz.**UV-Vis, FT-IR**, **^{1}H NMR** and **HR-MS** spectroscopy.

Result and discussion:

C, H, and N data of synthesized Azonapthaldehyde (**3)** is depicted in **Table 1.** The values are in close agreement with the calculated one from the expected molecular formula of compound (**3**) and are in 5 % in statistics**.** Purity of compound (3) was checked by melting point determination by open capillary method and by TLC on aluminium plates coated with silica gel make Merck. Physical and analytical data of (**3**) is depicted in **Table 2.**The UV spectra ware recorded by UV-1800 of Shimadzu make from the stock solution (0.01) by serial dilution of solutions (0.001M) in Ethanol as solvent. While the **FT-IR** spectra were recorded by using SHIMADZU-FTIR-8400 or by Bruker alpha, in the frequency range of 4000-400 cm^{-1}.

The **UV-Vis** and **FT-IR** spectral data for (**3**) is depicted in **Table 3** respectively

Table 1: C, H and N data for Azonapthaldehyde (3) (Scheme-I).

Calc. =

Code	M.F.	% C		% H		% N	
		Calc.	Obs.	Calc.	Obs.	Calc.	Obs.
3	C$_{17}$H$_{12}$N$_2$O$_2$	73.91	72.15	4.35	3.95	10.14	9.89

Calculated and Obs. = Observed

Table 2: Physical and analytical data for Azonapthaldehyde (3)(Scheme-I).

Code	M.F.	Mol. wt. (g/mole)	Colour	m.p.range ^{0}C	RF value	% yield
3	C$_{17}$H$_{12}$N$_2$O$_2$	276	Orange	139-141	0.57	66.55
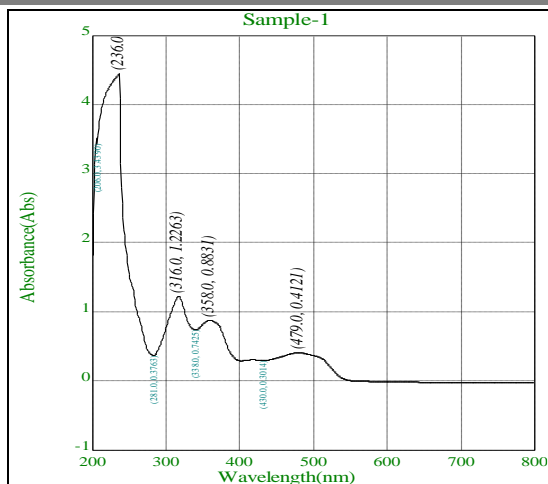
| **Fig. 1A:** UV-Vis spectra of Azo napthaldehyde (**3**) | **Fig. 1B:** FT-IR spectra of Azo napthaldehyde (**3**) |
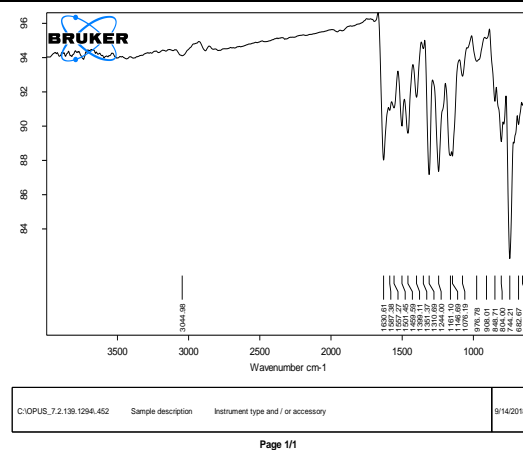
Table 3: The UV-Vis and FT-IR spectral data for Azonapthaldehyde (3) (Scheme-I).

Code	UV-Vis, λ_{max}, (nm)	FT-IR data (cm^{-1})
3	236 361 479	ν $_{–OH}$ 3480 ν $_{>C=O}$ 1630 ν $_{-C-H\ ar}$ 3044 ν $_{–CH=O\ ald.}$ 2830 ν $_{>C=C<}$ ar.1501-1551 ν $_{N=N}$ 1587

The UV spectrum in ethanol of (**3**) is shown in **Fig. 1A** indicates three bands at 479 nm, 361 nm and 236 nm. The excitation at 479 nm and 361 nm shows n→π* transition while the excitation at 236 nm arise due to π→π* transition.

Characteristic stretching frequencies of variable bonds in (**3**) are obtained from the **FT-IR** spectrum as shown in **Fig. 1B**. IR band at 3480 cm^{-1} indicates the stretching vibration of –OH group. A band at 3044 cm^{-1} is due to aromatic –C-H bond stretching vibration.IR band at 1630 cm^{-1} is due to >C=O Stretching, 1501 cm^{-1} to 1557 cm$^-$ is due to >C=C< in aromatic ring and 1587 cm^{-1} band is due to -N=N- moiety. While the **UV-Vis** and **FT-IR** spectral data for (**3**) is given in **Table 3** respectively.

The C, H and N data for (**5a** to **5f**) is depicted in **Table 4.** The values are in close agreement with the calculated one from the expected molecular formula of synthesized compound (**5a** to **5f**) and are in 5 % in statistics**.** Purity of compound (**5a** to **5f**) was checked by melting point determination by open capillary method and by TLC on aluminium plates coated with silica gel make Merck. Physical and analytical data of (**5a** to **5f**) is depicted in **Table 5**.The UV spectra ware recorded by UV-1800 of Shimadzu make from the stock solution (0.01) by serial dilution of solutions (0.001M) in Ethanol as solvent. While the **FT-IR** spectra were recorded by using SHIMADZU-FTIR-8400 or by Bruker alpha, in the frequency range of 4000-400 cm^{-1}. The **UV-Vis** and **FT-IR** spectral data for (**5a** to **5f**) is depicted in **Table 6**.

Table 4: C, H and N data for Azo Schiff bases (5a to 5f) (Scheme-II).

Code	-R	M.F.	% C		% H		% N	
			Calc.	Obs.	Calc.	Obs	Calc.	Obs.
5a	-H	$C_{24}H_{16}N_4OS$	70.59	69.75	3.92	3.34	13.72	13.12
5b	6-Cl,4-NO$_2$	$C_{24}H_{14}ClN_5O_3S$	59.08	58.64	2.87	2.34	14.36	13.95
5c	6-F	$C_{24}H_{15}FN_4OS$	67.61	66.13	3.52	3.12	13.14	12.95
5d	4,6-F$_2$	$C_{24}H_{14}F_2N_4OS$	64.86	64.01	3.15	3.02	12.61	12.13
5e	4-CH$_3$,6-NO$_2$	$C_{25}H_{17}N_5O_3S$	64.24	63.35	3.64	3.15	14.99	14.26
5f	6-NO$_2$	$C_{24}H_{15}N_5O_3S$	63.58	63.12	3.31	3.10	15.45	15.12

Calc. = Calculated and Obs. = Observed

Table 5: Physical and analytical data for Azo Schiff bases (5a to 5f) (Scheme-II).

Code	-R	M.F.	Mol. wt. (g/mole)	Colour	m.p.range ^{0}C	RF Value	% Yield
5a	-H	$C_{24}H_{16}N_4OS$	408	Dark Brown	167-169	0.40	79.3
5b	6-Cl,4-NO$_2$	$C_{24}H_{14}ClN_5O_3S$	487.5	Raddish Brown	109-111	0.44	90.81
5c	6-F	$C_{24}H_{15}FN_4OS$	426	Raddish Brown	199-201	0.44	87.80
5d	4,6-F$_2$	$C_{24}H_{14}F_2N_4OS$	444	Orange	197-199	0.49	81.43
5e	4-CH$_3$,6-NO$_2$	$C_{25}H_{17}N_5O_3S$	467	Dark Brown	175-177	0.50	74.73
5f	6-NO$_2$	$C_{24}H_{15}N_5O_3S$	453	Raddish Brown	241-243	0.48	82.63

5a

5b
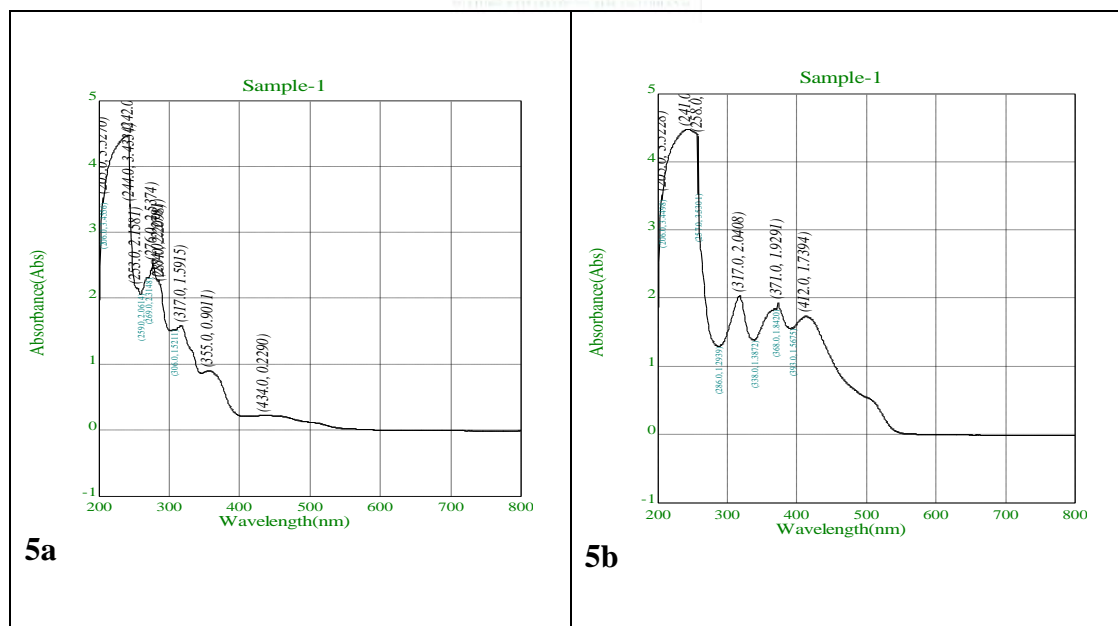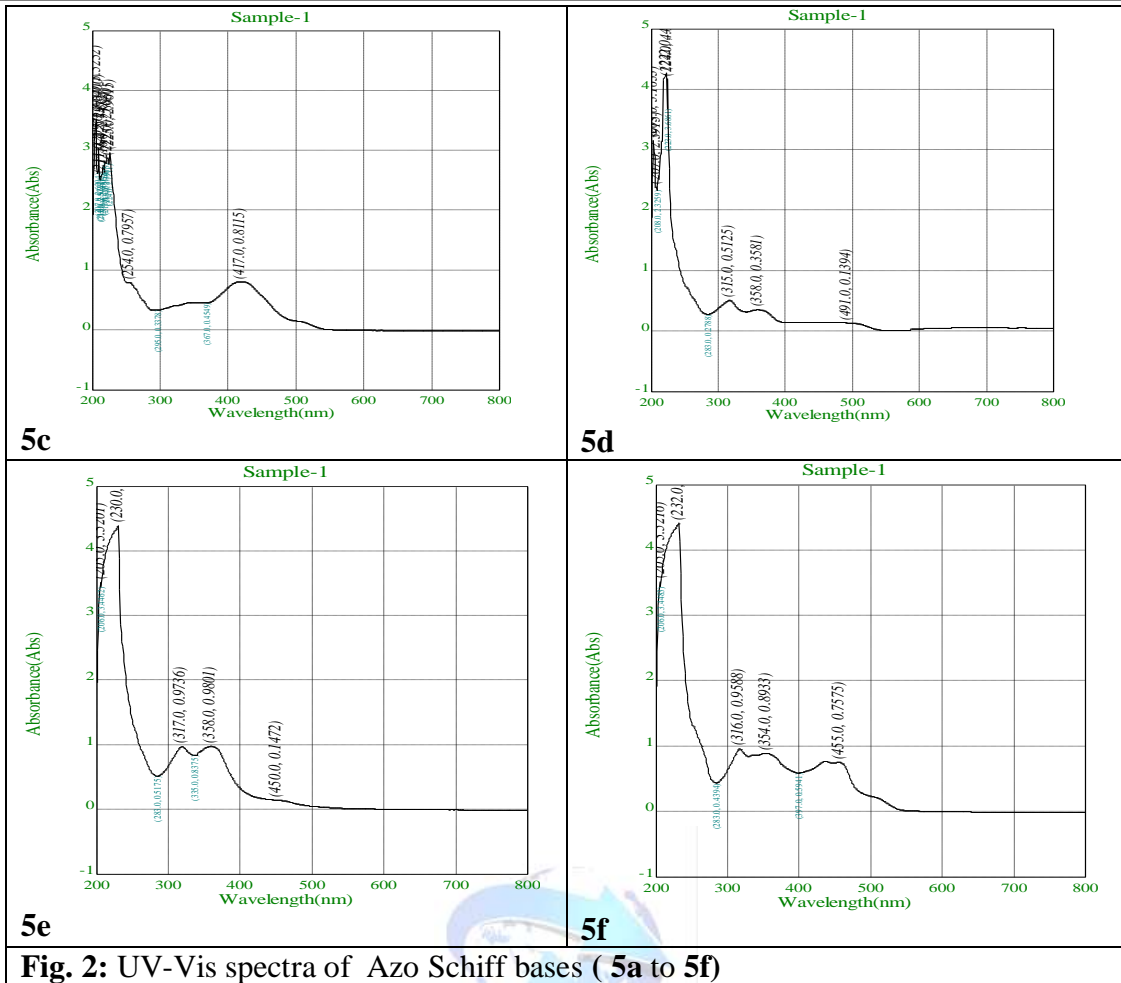
Fig. 2: UV-Vis spectra of Azo Schiff bases (**5a** to **5f)**
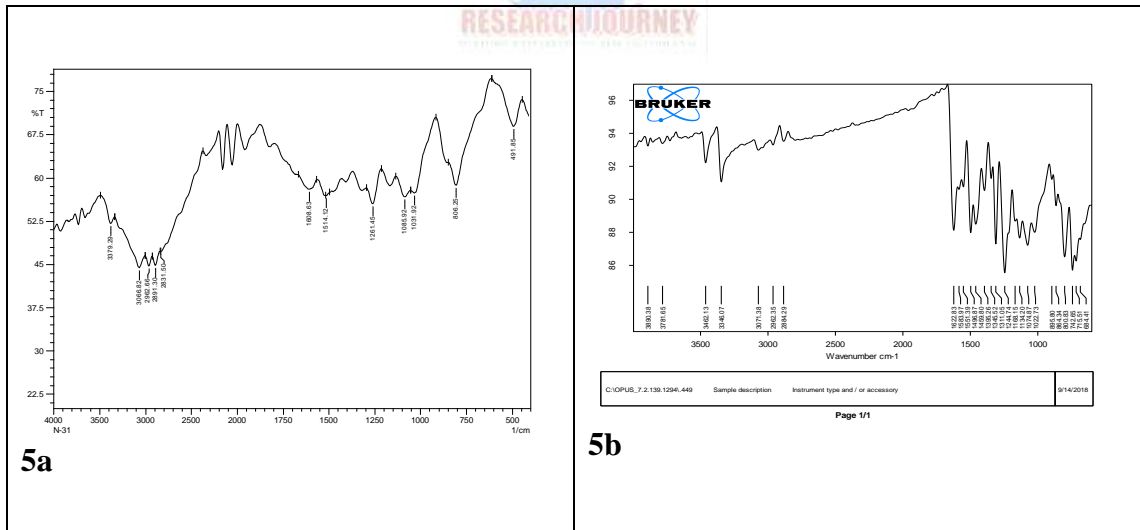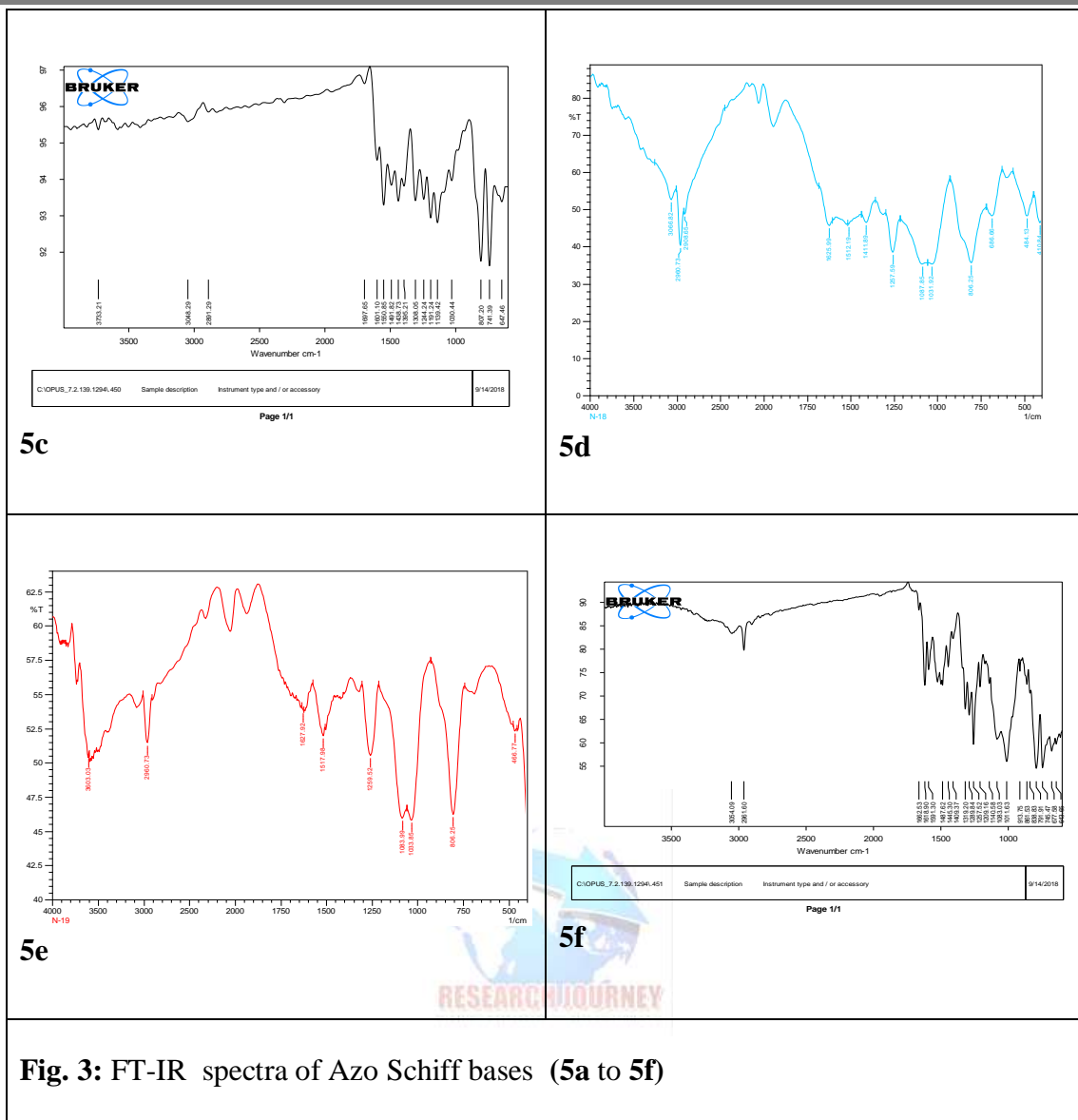
Fig. 3: FT-IR spectra of Azo Schiff bases **(5a** to **5f)**

Table 6: The UV-Vis and FT-IR spectral data of Azo Schiff bases (5a to **5f) (Scheme-II).**

Code	UV-Vis, λ_{max}, (nm)	FT-IR data (cm^{-1})
5a	244 355 253 434	ν_{-OH} 3379 $\nu_{-C-H\ ar}$ 3066 $\nu_{N=N}$ 1514 $\nu_{>C-O\ alc}$ 1085 $\nu_{>C=C<\ ar.}$ 1500 $\nu_{-C=N}$ 1608 ν_{-C-S} 806
5b	241 371 317 412	ν_{-OH} 3462 $\nu_{-C-H\ ar.}$ 3071 $\nu_{N=N}$ 1622 $\nu_{>C-O\ alc}$ 1134 ν_{-NO2} 1311 $\nu_{-C=N}$ 1583 ν_{-C-S} 684 ν_{C-Cl} 800 ν_{-NO2} 1459

'RESEARCH JOURNEY' *International E- Research Journal*
Special Issue – 333 : Innovative & Sustainable Chemistry
Impact Factor 6.625 (SJIF)   Peer Reviewed Journal

E-ISSN : 2348-7143
December - 2023

5c					
	254 417	ν_{-OH} 3470 $\nu_{-C=N}$ 1438	$\nu_{-C-H\ ar}$ 3048 ν_{-C-S} 647	$\nu_{N=N}$ 1601 $\nu_{>C=C<\ ar.}$ 1550	$\nu_{>C-O\ alc.}$ 1139 ν_{-C-F} 1355
5d					
	315 358 491	ν_{-OH} 3066 $\nu_{>C-O}$ 1087	$\nu_{N=N}$ 1512 ν_{-C-S} 806	$\nu_{-C=N}$ 1625	ν_{-C-F} 1411
5e					
	230 358 317 450	$\nu_{-C-H\ alk}$ 2960 $\nu_{>C-O}$ 1083	ν_{-NO2} 1517 ν_{-C-S} 806	$\nu_{N=N}$ 1512 ν_{-NO2} 1320	$\nu_{-C=N}$ 1627
5f					
	232 354 316 455	ν_{-OH} 3200 $\nu_{>C-O\ alc}$ 1011	ν_{-C-S} 643 ν_{-NO2} 1319	$\nu_{-C-H\ ar.}$ 3054 $\nu_{>C=C<\ ar.}$ 1409	$\nu_{N=N}$ 1618 $\nu_{-C=N}$ 1591

The UV spectrum in Ethanol of (**5a**) is shown in **Fig. 2** indicates four bands at 434 nm, 355 nm, 253 nm and 244 nm. The excitation at 434 nm and 355 nm shows n→π* transition while the excitation at 253 nm and 244 nm arise due to π→π* transition.

The FTIR characteristic stretching frequencies of various bonds present in (**5a**) are obtained from the **FT-IR** spectrum as shown in **Fig. 3**. IR band at 3379 cm^{-1} indicates the stretching vibration of –OH group. A band at 3066 cm^{-1} is due to aromatic –C-H bond stretching vibration. IR band at 1608 cm^{-1} is due to >C=N Stretching, 1500 cm^{-1} is due to >C=C< in aromatic ring and 1514 cm^{-1} band is due to -N=N- moiety. The IR band at 806 cm^{-1} is due to stretching vibration of C-S group. Whiie the **UV-Vis** and **FT-IR** spectral data for (**5a** to **5f**) **is** given in **Table 6 respectively**.

The C, H and N data for (**6a** to **6f**) is given in **Table 7.** The C, H and N data for (**6a** to **6f**) is depicted in **Table 7.** The values are in close agreement with the calculated one from the expected molecular formula of synthesized compound (**6a** to **6f**) and are in 5 % in statistics**.** Purity of compound (**6a** to **6f**) was checked by melting point determination by open capillary method and by TLC on aluminium plates coated with silica gel make Merck. Physical and analytical data of (**6a** to **6f**) is depicted in **Table 8**.The UV spectra ware recorded by UV-1800 of Shimadzu make from the stock solution (0.01) by serial dilution of solutions (0.001M) in Ethanol as solvent. While the **FT-IR** spectra were recorded by using SHIMADZU-FTIR-8400 or by Bruker alpha, in the frequency range of 4000-400 cm^{-1}. The **UV-Vis** and **FT-IR** spectral data for (**6a** to **6f**) is depicted in **Table 9**.

The representative compounds were screened by **^{1}H NMR** and **HR-MS** spectroscopy. **^{1}H NMR** spectra were recorded on Bruker Advance III, 400 MHz spectrometer in Chloroform solvents and the chemical shifts are shown in δ ppm scales. Multiplicities of NMR signals are designated as s (singlet), d (doublet), etc.

The **UV-Vis** and **FT-IR** spectral data for (**6a** to **6f**) **is** given in **Table 9** respectively.

Table 7: C, H and N data for Beta-lactams (6a to 6f) (Scheme-III).

Code	-R	M.F.	% C		% H		% N	
			Calc.	Obs.	Calc.	Obs.	Calc.	Obs.
6a	-H	$C_{26}H_{17}ClN_4O_2S$	64.39	63.85	3.53	3.40	11.55	11.42
6b	6-Cl,4-NO$_2$	$C_{26}H_{15}Cl_2N_5O_4S$	55.53	54.95	2.68	2.53	12.41	12.34
6c	6-F	$C_{26}H_{16}ClFN_4O_2S$	62.09	61.85	3.21	3.11	11.14	11.10
6d	4,6-F$_2$	$C_{26}H_{15}ClF_2N_4O_2S$	59.95	58.69	2.90	2.82	10.75	09.95
6e	4-CH$_3$,6-NO$_2$	$C_{27}H_{18}ClN_5O_4S$	59.61	58.95	3.34	2.93	12.87	12.24
6f	6-NO$_2$	$C_{26}H_{16}ClN_5O_4S$	58.93	58.35	3.04	2.82	13.22	13.04

Calc. = Calculated and Obs. = Observed

Table 8: Physical and analytical data for Beta lactams (6a1 to 6a6) (Scheme-III).

Code	-R	M.F.	Mol. wt. (g/mole)	Colour	m.p.range °C	RF Value	% Yield
6a	-H	$C_{26}H_{17}ClN_4O_2S$	484.5	Dark Brown	108-110	0.54	86.73
6b	6-Cl,4-NO$_2$	$C_{26}H_{15}Cl_2N_5O_4S$	564	Dark Brown	94-96	0.53	78.99
6c	6-F	$C_{26}H_{16}ClFN_4O_2S$	502.5	Light Brown	124-126	0.57	80.21
6d	4,6-F$_2$	$C_{26}H_{15}ClF_2N_4O_2S$	520.5	Dark Brown	135-137	0.55	82.93
6e	4-CH$_3$,6-NO$_2$	$C_{27}H_{18}ClN_5O_4S$	543.5	Dark Brown	128-130	0.53	81.57
6f	6-NO$_2$	$C_{26}H_{16}ClN_5O_4S$	529.5	Light Brown	164-166	0.49	74.65

6a

6b

6c

6d

6e

6f

Fig. 4: UV-Vis spectra of Beta lactams (**6a** to **6f**)

6a

6b

6c

6d

6e	6f

Fig. 5: FT-IR spectra of Beta lactams (**6a** to **6f**)
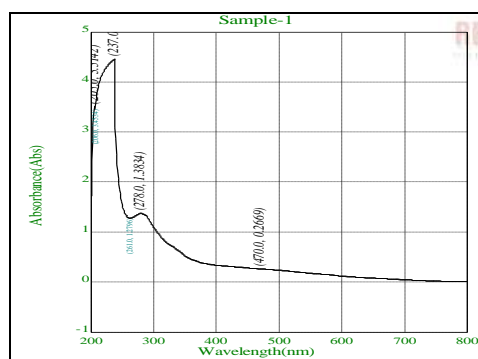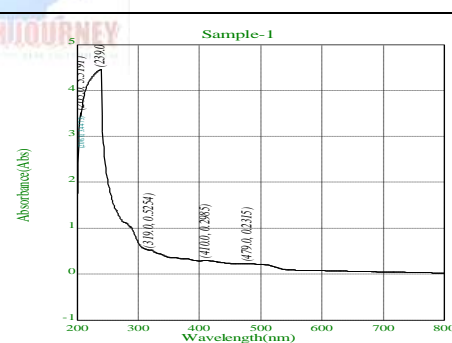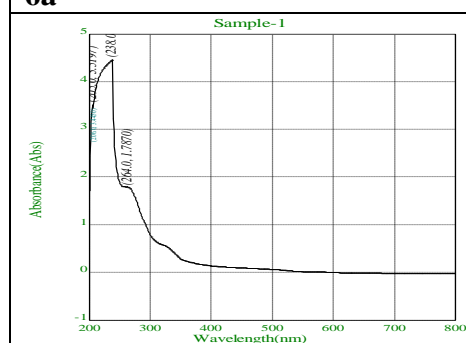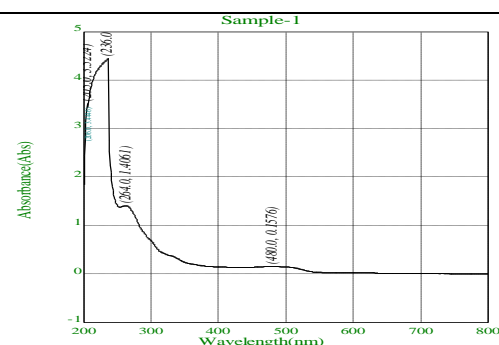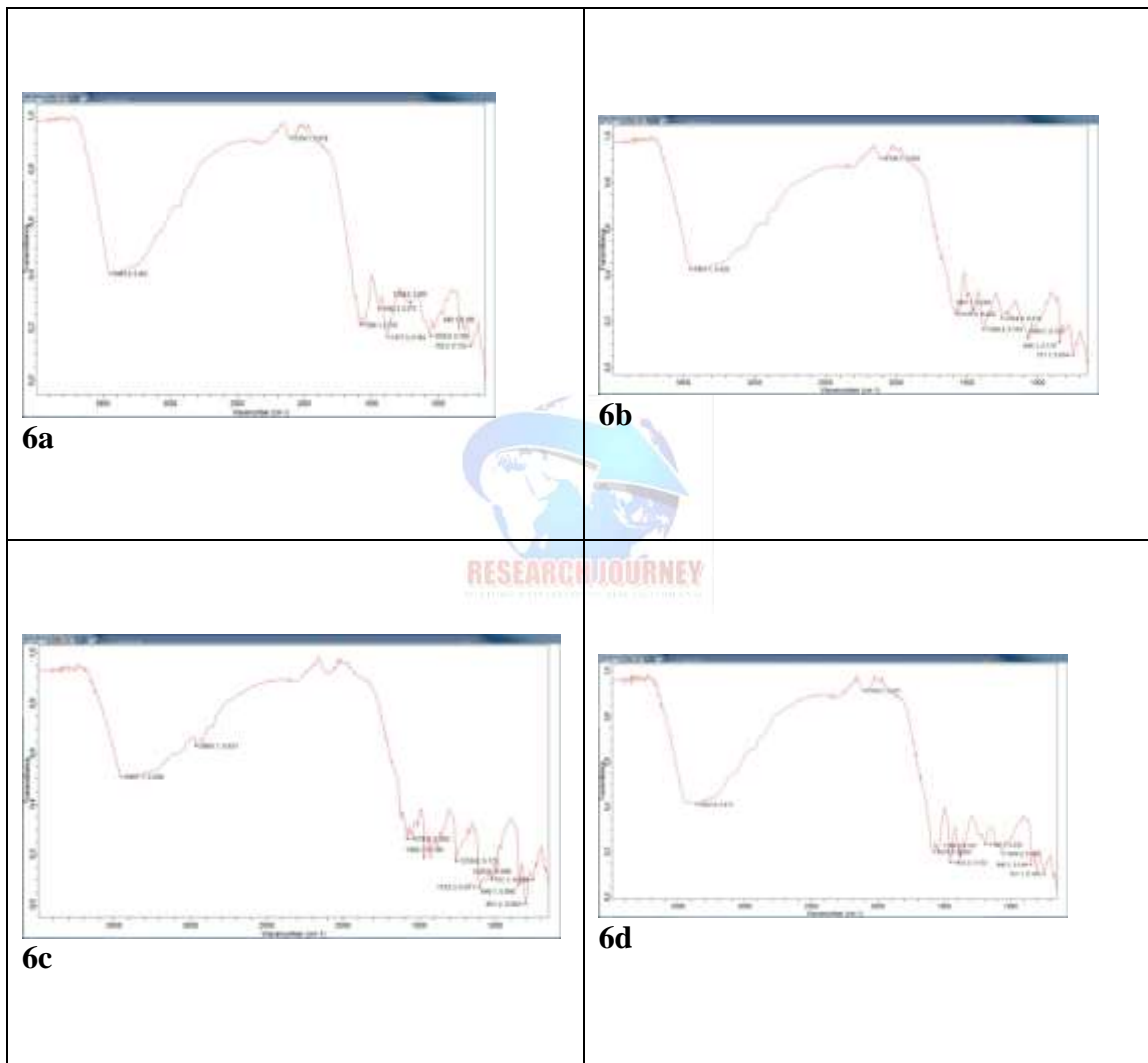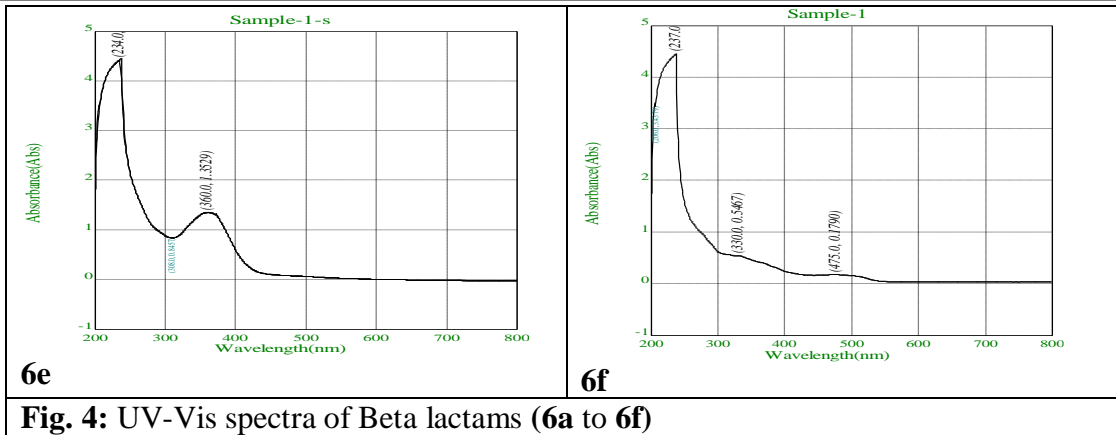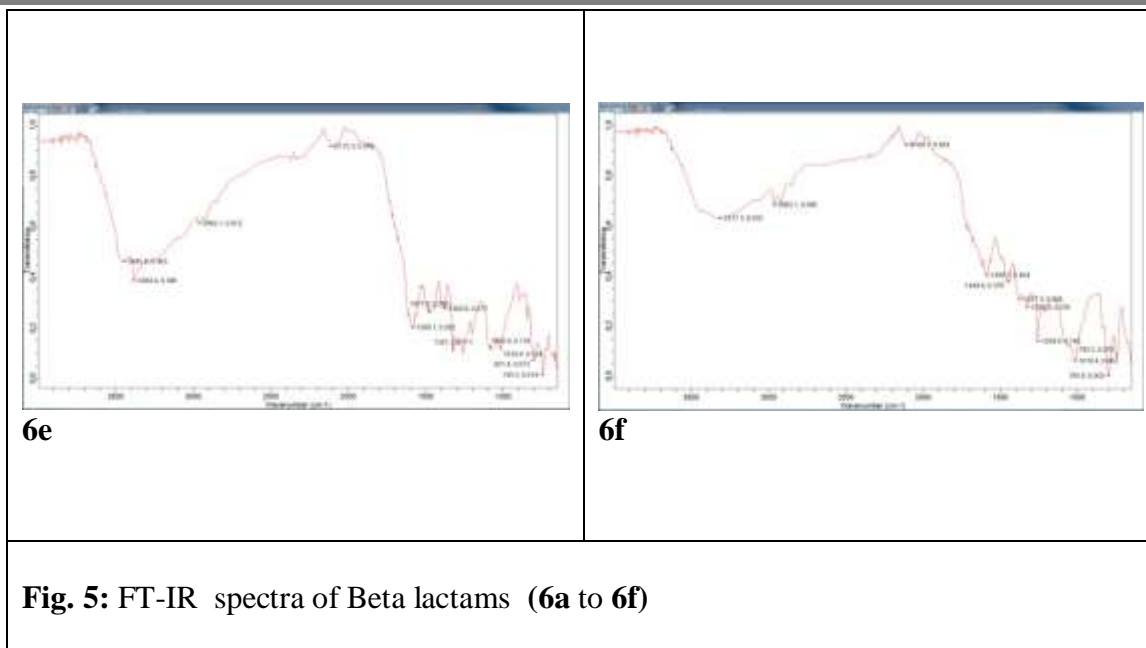
Table 9: The UV-Vis and FT-IR spectral data for Beta lactams (6a to 6f) (Scheme-III).

Code	UV-Vis, λ_{max}, (nm)	FT-IR data (cm^{-1})		
6a	205 237 278 470	$\nu_{-C–OH}$ 3445 $\nu_{-N=N-}$ 1584 $\nu_{–C-S}$ 846	ν_{-C-O}1058 $\nu_{>C=N-}$1444	$\nu_{-N-C=O}$2104 $\nu_{–C-Cl}$ 762
6b	410 239 479 319	$\nu_{-C–OH}$ 3457 $\nu_{-N-C=O}$ 2109 $\nu_{–C-Cl}$ 751	ν_{-C-O}1069 $\nu_{-N=N-}$1578 $\nu_{–C-S}$ 846	$\nu_{–NO2}$1254 $\nu_{>C=N-}$ 1461 $\nu_{–NO2}$ 1388
6c	205 238 264	$\nu_{-C–OH}$ 3457 $\nu_{-N-C=O}$ 2165 $\nu_{–C-Cl}$ 751	ν_{-C-O}1103 $\nu_{-N=N-}$ 1578 $\nu_{–C-S}$ 846	$\nu_{–C-F}$1025 $\nu_{>C=N-}$ 1466 $\nu_{–C-F}$ 1410
6d	205 236 264 480	$\nu_{-C–OH}$ 3367 $\nu_{-N-C=O}$2109 $\nu_{–C-Cl}$751	ν_{-C-O}1192 $\nu_{-N=N-}$1578 $\nu_{–C-S}$ 846	$\nu_{–C-F}$ 1064 $\nu_{>C=N-}$ 1455 $\nu_{–C-F}$ 1435

6e	234 308 360	ν_{-C-OH}3445 $\nu_{-N-C=O}$ 2115 ν_{-C-Cl} 745	ν_{-C-O}1080 $\nu_{-N=N-}$ 1589 ν_{-C-S} 801	$\nu_{-C-H\,alk}$2965 $\nu_{>C=N-}$ 1477 ν_{-NO2}1321
6f	237 330 475	ν_{-C-OH} 3317 $\nu_{-N-C=O}$ 2109 ν_{-C-Cl} 745 ν_{-NO2}1377	ν_{-C-O} 1019 $\nu_{-N=N-}$1589 ν_{-C-S} 795	$\nu_{-C-H\,alk}$2965 $\nu_{>C=N-}$ 1449 ν_{-NO2} 1320

The UV spectrum in Ethanol of (**6a**) is shown in **Fig. 4** indicates four bands at 470 nm, 278 nm 237 nm and 205 nm. The excitation at 470nm and 278 nm shows n→π* transition while the excitation at 237 nm and 205 nm arise due to π→π* transition.

The FT-IR characteristic stretching frequencies of various bonds present in (**6a**) are obtained from the **FT-IR** spectrum as shown in **Fig. 5**. IR band at 3445 cm⁻¹ indicates the stretching vibration of –OH group. A band at 2104 cm⁻¹ is due to aromatic O=C-N bond stretching vibration.IR band at 1584 cm⁻¹ is due to -N=N- Stretching, 1444 cm⁻¹ is due to >C=N group and 1377 cm⁻¹ band is due to –OH bending vibration. The IR band at 762 cm⁻¹ is due to stretching vibration of C-Cl group. The IR band at 846 cm⁻¹ is due to stretching vibration of C-S group. While the **UV-Vis** and **FT-IR** spectral data for (**6a** to **6f**) is given in **Table 9** respectively.
¹H NMR spectral study for Beta Lactams (6a to 6f):

6a

6b

'RESEARCH JOURNEY' *International E- Research Journal*
Special Issue – 333 : Innovative & Sustainable Chemistry
Impact Factor 6.625 (SJIF)   Peer Reviewed Journal

E-ISSN : 2348-7143
December - 2023

6c

6d

6e

6f
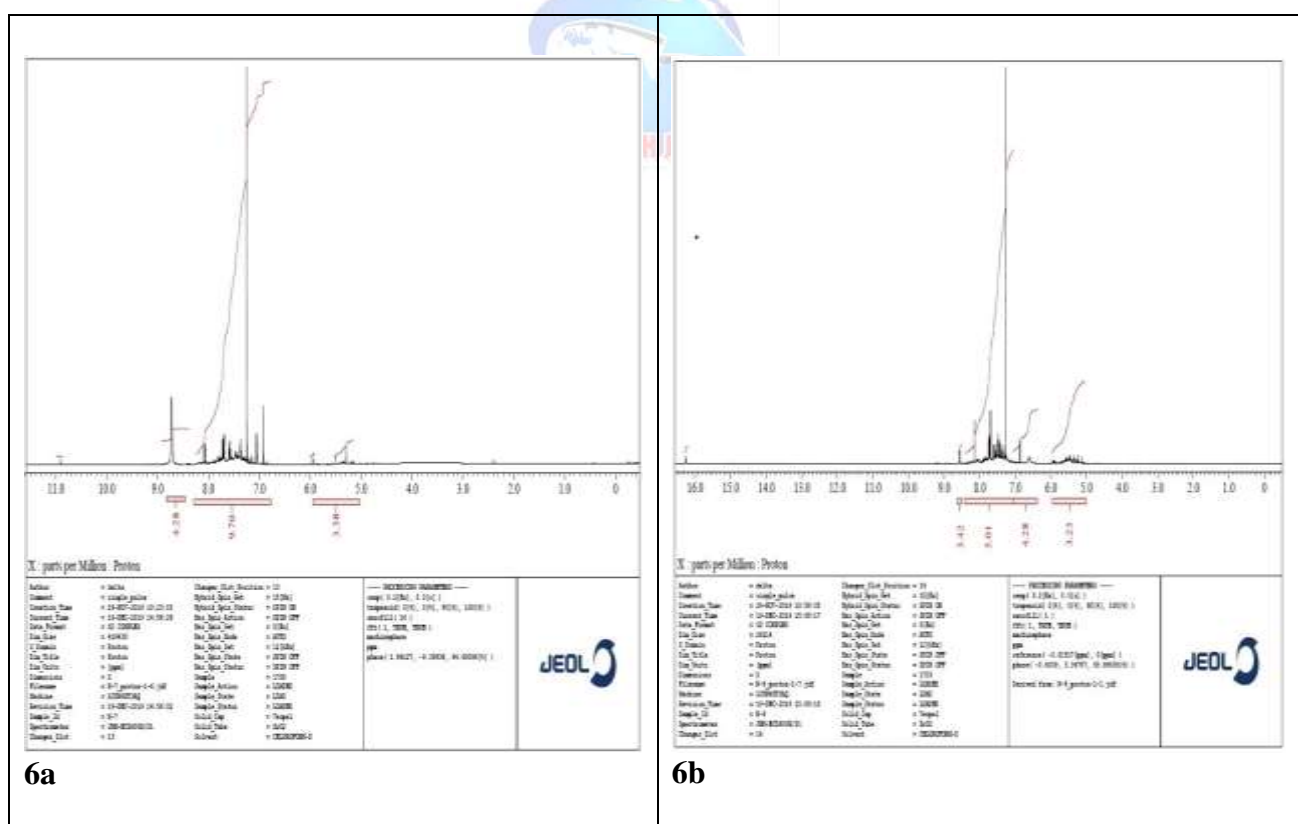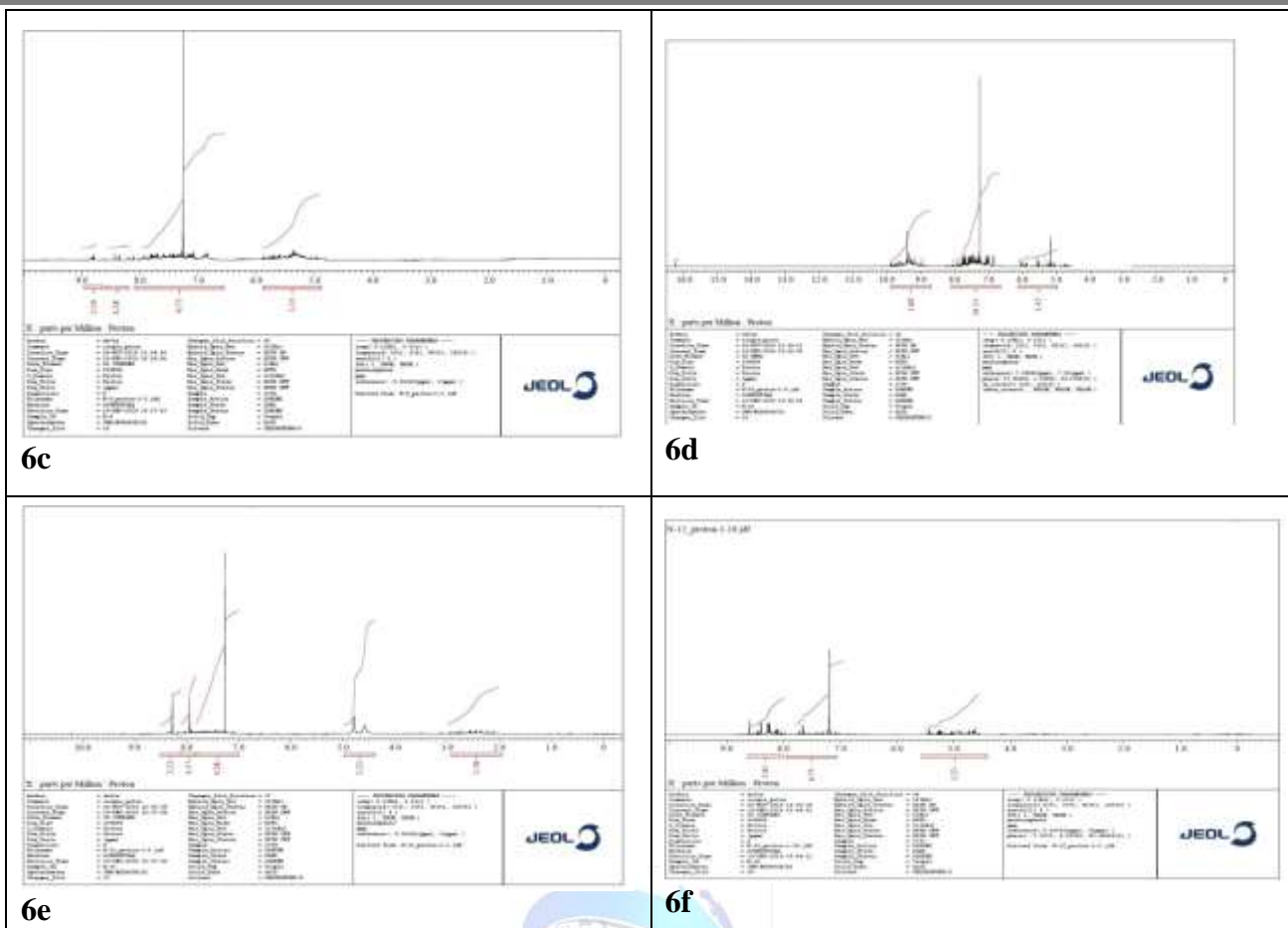
Fig. 6: ^{1}H NMR spectrum of Beta lactams (6a to 6f)

Table 10: ^{1}H-NMR spectral data for Beta lactams. (6a to 6f)

(Chemical shifts) (δ Values in ppm)

ID	-CH Aromatic	-CH Benzothiazole	-CH Propiolactam	-OH Aromatic
6a	6.90-8.20 (s, 10H)	8.85 (s, 2H), 8.70 (s, 2H)	5.45 (d, 1H), 5.0 (d, 1H)	5.00 (s, 1H)
6b	7.00-8.30 (s, 5H), 6.70-7.20 (s, 4H), 8.50 (s,1H)	8.70 (s, 2H), 8.60 (s, 1H)	5.50 (d, 1H), 5.25 (d, 1H).	5.25 (s, 1H)
6c	8.39 (s, 1H), 6.70-8.00 (s, 7H), 8.70-8.90 (s,2H)	8.85 (s, 1H), 8.25 (s, 1H), 8.00 (s, 1H)	5.30 (d, 1H), 5.45 (d, 1H).	5.30 (s, 1H)
6d	6.90-8.10 (s, 10H)	9.10 (s, 2H)	5.30 (d, 1H), 5.50 (d, 1H).	5.30 (s, 1H)
6e	: 8.15 (s, 1H), 7.80-8.10 (s, 5H), 7.00-7.80 (s,4H)	8.60 (s, 1H), 8.45 (s, 1H), 2.45 (s, 3H),	5.50 (d, 1H), 5.25 (d, 1H)	5.25 (s, 1H).
6f	7.10-7.90 (s, 7H), 8.30 (s, 1H), 8.15 (s, 1H), 8.10 (s, 1H)	8.70 (s, 1H), 8.65 (s, 1H), 8.60 (s, 1H)	5.35 (d, 1H), 5.00 (d, 1H)	5.00 (s, 1H).

S = singlet, d = doublet

'RESEARCH JOURNEY' *International E- Research Journal*
Special Issue – 333 : Innovative & Sustainable Chemistry
Impact Factor 6.625 (SJIF)   Peer Reviewed Journal

E-ISSN :
2348-7143
December - 2023

The ^{1}H-NMR spectra of Beta lactams (**6a** to **6f**) are as depicted in **Fig. 6** and the spectrum was measured in CDCl$_3$ solvent with TMS as an internal reference. In general the **^{1}H NMR** showed the two peak at ~ 5 ppm is attributed to Propiolactam and one peak at ~ 4.5 is attributed to –OH of aromatic ring, peaks in the range 6.9 - 9.2 for the aromatic protons. The detailed 1H NMR data of Beta Lactam derivatives, (**6a** to **6f**) are depicted as in **Table 10.**

HR-MS spectral study Representative of Beta lactam derivative:
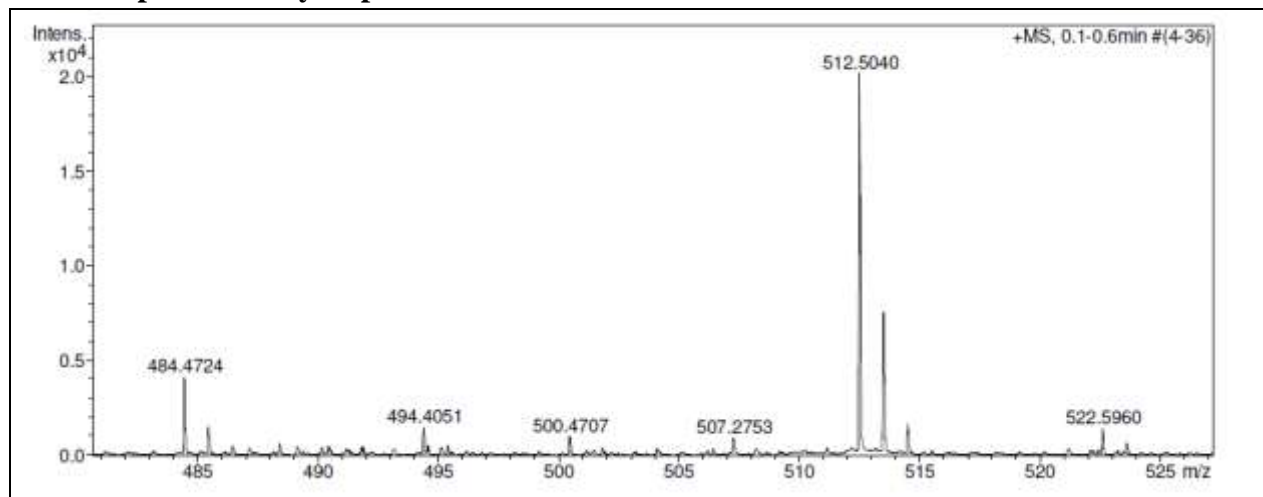
Fig. 7: Representative HR-MS spectra of Beta lactam derivative, 6a

HR-MS of **6a:** C$_{26}$H$_{17}$ClN$_4$O$_2$S (M+H) 484.5 (calculated), 484.4724 (observed). The HR-MS (intensity vs m/z) for **6a**, C$_{26}$H$_{17}$ClN$_4$O$_2$S (M+H) 484.5 (calculated), 484.4724 (observed) indicates the correct value for its mass number. Thus, it strongly reveals the predicted molecular formula of **6a**.

Conclusion:

A modified Azonapthaldehyde by azo group is synthesized and its relevant schiff bases and Beta lactam derivatives were synthesized and were characterized by analytical and spectral methods. These synthesized Azonapthaldehyde and the Azo Schiff base will be useful as building block for future target molecules by young budding researchers. Looking to the skeleton of the product it look like these products may have good potential in medicine and chemistry. In future we may synthesis the further derivatives of these schiff bases and find out the possibilities for the applications of these products in various fields in pharmacological industry such as anti-convulsion, anti-inflammatory, analgesic, anti-microbial and antioxidant activity, electrochemical properties, sensor applications, dying properties and corrosion etc.

Scope: Further, relevant Schiff bases and Beta lactams will be tested for pharmacological activities.

recording ^{1}H NMR spectral analysis in time. We are thankful to Dr.Ruchi of IISER Bhopal for providing HR-MS analysis in time.

References:

1. R. M. Silverstein, G. C. Bassler and T. C. Morrill, Spectrometric Identification of Organic Compounds, 5th Edn., Wiley, New York, 1991, pp. 430.

2. R. M. Silverstein, F. X. Webster and D. J. Kieml, Infrared Spectroscopy in Spectrometric Identification of Organic Compounds, 2005, New York.

3. L. D. Field, S. Sternhell and J. R. Kalman, Infrared Spectroscopy in Organic Structures from spectra, 4th Ed; Wiley, 2007, New York.

4. A. Rahman and M. Choudhary, The Basic of Modern NMR Spectroscopy In Solving problems with NMR Spectroscopy, 1991.

5. J. G. Smith, Infrared Spectroscopy in Organic Chemistry, 2nd Ed., 2008, New York.

6. R. U. Ambhure, S. R. Mirgane, D. U. Thombal S. U. Shisodia, S. S. Pandule, L. Kotai and R. P. Pawar, Eur. Chem. Bull., 2016, 5(10) 428-430, Synthesis and antimicrobial activity of Imines and their metal complexes.

7. A. S. P. Azzouz and R. D. Sulaiman, Asian J. Chem., 2013, 25(10) 5303-5306, DOI: 10.14233/ajchem/.2013.14063, Influence of Temperatures and Thermodynamic parameters on pKa Values for some Acids and Basic Imines derived 3-Acetyl and 4-Acetyl pyridines.

8. C. J. Patil and Sujay V. Rajput, Int. J. Rec. Sci. Res., 2019, 10 (4-G), 32144-156,10.24327/ijrsr.2019.1004.3105, Coupling Reactions involving Aryldiazonium Salt: Part-lX. Review on synthesis of Azo phenolic derivatives, their Applications and Biological activities.

9. S. Samadhiya, A. K. Halve, Synthetic utility of Schiff bases as potential herbicidal agents, Orient. J. Chem., 2001, 17, 199-122.

10. M. A. Abdelgawad, J. Appl. Pharm. Sci., 2019, 9(S1) 9-16, DOI: 10.7324/JAPS.2019.S102, Synthesis and antibacterial evaluation of new azo-pyrimidine derivatives.

11. S. Murtaza and J. Ashraf, Asian J. Chem., 2015, 27(10) 3551-3554, DOI: 10.14233/ajchem/.2015.18816, Synthesis, antioxidant and antimicrobial activity of 4-Aminophenol and 2-Aminobenzoic acid based novel Azo compounds.

12. G. Valarmathy, R. Subbalakshmi, R. Renganathan and R. Kokila, Asian J. Chem., 2018, 30(3) 645-650 (2018), DOI: 10.14233/ajchem.2018.21085, Synthesis of Schiff Base (E)-2-(((3-Hydroxyphenyl)imino)methyl)-6-methoxyphenol containing N and O Donors and its Metal complexes: Spectral, Thermal, Redox behaviour, Fluorescence Quenching, Antimicrobial and Anticancer studies.

13. D. N. Bhanvesh and K. R. Desai, Synthesis, characterization and biological activity of some novel azetidinones. Asian J. Chem., 2004, 16,1749.

14. a) C. J. Patil, Manisha C. Patil, Mrunmayee C. Patil and Sanjivani N. Patil, J. Chem, Biol. Phy. Sci., 2015, 6 (1), 220-227, Azomethines and Biological Screening: Part-2. Evaluation of Biological Properties of Schiff Bases from 2-Aminobenzothiazoles and 4-Chlorobenzaldehyde; b) C. J. Patil, Manisha C. Patil, Mrunmayee C. Patil and Sanjivani Patil, J. Chem. Biol. Phy. Sci., 2016, 6(4) 1437-1450, Synthesis of Thiazolidinones from Schiff Bases: Part-I. Synthesis of Schiff Bases, Azetidine-2-ones and Thiazolidin-4-ones involving 2-Amino-benzothiazoles.

Kinetics of Oxidative Deamination and Decarboxylation of L-Lysine by Tributylammonium Chlorochromate in Acid Medium

Prabhakar Kute[1], Aashish Dhokte[2*]Mahananda Raut[3], Ganesh Andhale[4], Amol Kute[6], Nandkishor Chaudhari[7], Atish Mehetre[8]

[1,2*,3] Department of Chemistry, PratishthanMahavidyalayaPaithan, Aurangabad (M.S)

[4]Department of Chemistry,JijamataMahavidyalaya, Buldana.(M.S)

5Department of Chemistry,Shankarrao Patil Mahavidyalaya, Bhoom (M.S)

[6]Department of Physics, PratishthanMahavidyalayaPaithan, Aurangabad (M.S).

[7]Department of Chemistry, Shivaji Arts, Commerce and Science college Kannad, (MS,India)

E-mail: kuteprabhakar@gmail.com, ashu.chem4@gmail.com

Abstract:

Kinetics of oxidation of L-Lysine by tributylammonium chlorochromate has been investigated Spectrophotometrically at 445 nm in acetic acid medium. Analysis of the kinetic results revealed that the rate of oxidation was first-order with respective Oxidant, L-lysine and fractional order to [H⁺].The reaction failed to induce polymerization of acrylonitrile. Changing monovalent and bivalent salts had no significant effect on the reaction rate. The reaction was studied at different temperatures and the activation parameters were calculated. The main products were identified as the corresponding carbonyl compound by spot test. A suitable mechanism has been proposed.

Key words: Kinetics, L-Lysine, Tributylammonium Chlorochromate, Oxidation, Mechanism.

Introduction:

L-lysine is an essential basic α-amino acid. It is a vital constituent of proteins that help bodily tissue grow and heal after injury. Also help the body to absorb calcium, iron, zinc and promote collagen growth, according to some researcher, supplementary L-Lysine may be able to assist in the prevention of herpes infections, including cold sores and genital herpes [1],normalize blood pressure [2].L-lysine is crucial for the body's ability to absorb calcium, maintain a healthy nitrogen balance, and preserve lean body mass [3]. Animal proteins like meat and poultry are the best source of L-Lysine, although it can also be found in dairy products, eggs, legumes, beans, nuts and soybeans. The studies related to oxidative decarboxylation and deamination of lysine are important to understand more complicated enzyme catalysed reactions and their mechanism. Using various oxidising agents, several researchers examined the oxidative decarboxylation, deamination, and mechanistic studies of lysine [4-11]. However, a review of the literature reveals that no studies have ever used TriBACC to oxidise lysine. Since this is the case, we have chosen to investigate the kinetic, mechanistic, and oxidative deamination and decarboxylation of Lysine by TriBACC.

Materials and Methods:

All reagents used were of AR grade and doubled distilled water was used throughout the kinetic study. Acetic acid was purified by distillation over CrO_3 followed by fractionation in the presence of acetic anhydride. Pure acetic acid fraction was collected over 118 ^{0}C. A solution of L-lysine (Merk) was prepared by dissolving an appropriate amount of recrystallized sample in doubled distilled water and acetic acid 1:1. The purity of L-lysine was checked by comparing its melting point 224-225^{0}C with literature data [MP-224^{0}C] and TLC. The required molar concentration of L-lysine was obtained from its stock solution. Tributyl Ammonium

Chlorochromate was prepared by reported method [12-13]. The stock solution of TriBACC was prepared in acetic acid and distilled water 3:1and stored in brown bottle to prevent its photochemical degradation. All other reagents were of AR grade. The reaction progress was carried out by UV-vis Spectrophotometer with 1 cm quartz cell at 445 nm in the temperature range 303-323 K.

Kinetic measurements:

The kinetic measurements were performed on UV-vis Spectrophotometer. The kinetics were followed under pseudo-first order condition, where L-lysine >>TriBACC at 303 K. unless specified. The reaction was initiated by mixing TriBACC with the L-lysine solution, which also contained the required concentration of sulphuric acid as a catalyst. The progress of the reaction was followed spectrophotometrically at 445 nm by monitoring the decrease in absorbance due to of TriBACC. It was observed that there is no interference from other species present in the reaction mixture at this wavelength. The reaction was followed to more than 80 % completion. Plots of log (TriBACC) versus time lead to the pseudo-first order rate constant was evaluated from the linear (r-0.990-0.999) regression coefficient. Duplicate kinetic runs showed that the rate constants were reproducible to within $\pm$ 3 %.

Results and discussion:

Stoichiometry and product analysis: -

Different sets of reaction mixtures containing varying ratios of TriBACC to L-lysine in the presence of constant amount of sulphuric acid and acetic acid medium were kept for 6 h in a closed vessel under nitrogen atmosphere. The remaining (TriBACC) was then analysed spectrophotometrically at 445 nm the result indicated that 1 mole of L-lysine react with 1 mole of oxidant.

Product analysis was carried under kinetic conditions. In a typical experiment, a mixture of L-lysine (0.1 mol dm^{-3}) and TriBACC (0.01 mol dm^{-3}) was made up to 50 ml with acetic acid in presence of HCl (0.8 mol dm^{-3}). The mixture was kept in the dark for twelve hours until completion of oxidation. It was then treated overnight with an excess (125 ml) of a freshly filtered saturated solution of 2, 4-dinitrophenylhydrazine in 2M HCl. The precipitated 2, 4-dinitrophenylhydrazone (DNP) was collected by filtration, dried, recrystallized from ethanol and weighed. The product was found identical m.p and mixed m.p with an authentic sample of DNP of 5-aminovaleraldehyde. The yield was 82%. Ammonia was identified by Nessler's reagent [14]. The presence of corresponding aldehyde and ammonium ions were also confirmed by the spot tests [15], with chromotropic acid and p-nitrobenzene diazonium chloride respectively.

Results:

Tables 1-6 show the outcomes ofTriBACC's oxidation of L-lysine.

Effect of changing the concentration of Lysine on the rate of reaction:

When L-lysine is oxidised with TriBACC in the presence of sulphuric acid in acetic acid to produce 5-aminovaleraldehyde acid, the concentrations of TriBACC and H_2SO_4 remain constant, but the concentration of L-lysine enhances the pace of reaction (Table 1). The first order dependency of rate on L-lysine is seen by the plot of the log of[L-lysine] vslog $k_{obs}$for the various beginning concentrations of L-lysine (Fig. 1).

Table:- 1 shows the impact of changing [L-lysine] on the rate of TriBACC oxidation

(TriBACC = 1 x10^{-3} mol dm^{-3}; [H_2SO_4] = 1mol dm^{-3}, temperature = 303K).

'RESEARCH JOURNEY' *International E- Research Journal*
Special Issue – 333 : Innovative & Sustainable Chemistry
Impact Factor 6.625 (SJIF)   **Peer Reviewed Journal**

E-ISSN : 2348-7143
December - 2023

Lys (mol dm^{-3})	kobs10^{-4}S^{-1}
0.01	12.3
0.02	13.4
0.03	14.6
0.04	15.4
0.05	16.6
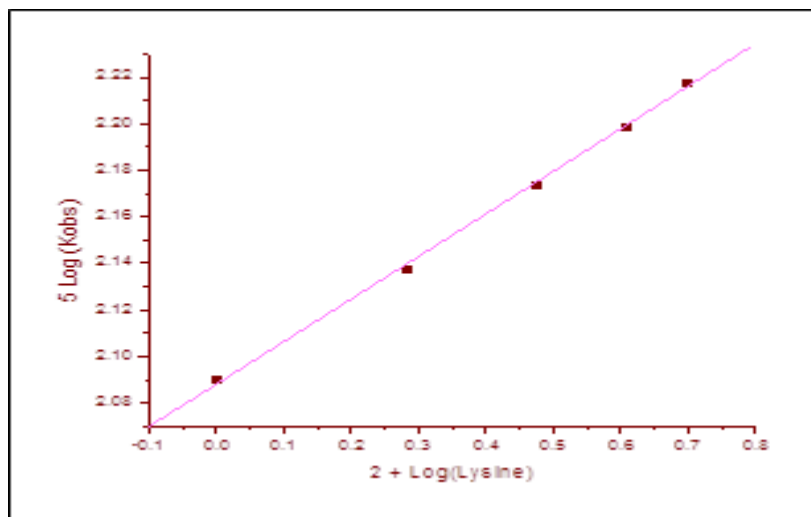
Fig.1:- 2 + log (Lysine) Vs 5 + log (Kobs)

Effect of changing [TriBACC] on the rate of lysine oxidation:

By changing the concentration of [TriBACC] from 2 x 10^{-3} to 6 x 10^{-3} mol dm^{-3} at constant [Lysine] and [H$_2$SO$_4$], the rate of reaction is increased. Table-2. The first order dependency of rate on TriBACC is shown in the plot of log [TriBACC] verses log kobs for various initial concentrations of TriBACC (Fig. 2).

Table: 2 shows the impact of changing [TriBACC] on the rate of Lysine oxidation.

TriBACC (mol dm^{-3})	kobs 10^{-4}S^{-1}
0.01	12.3
0.02	13.4
0.03	14.6
0.04	15.4
0.05	16.6
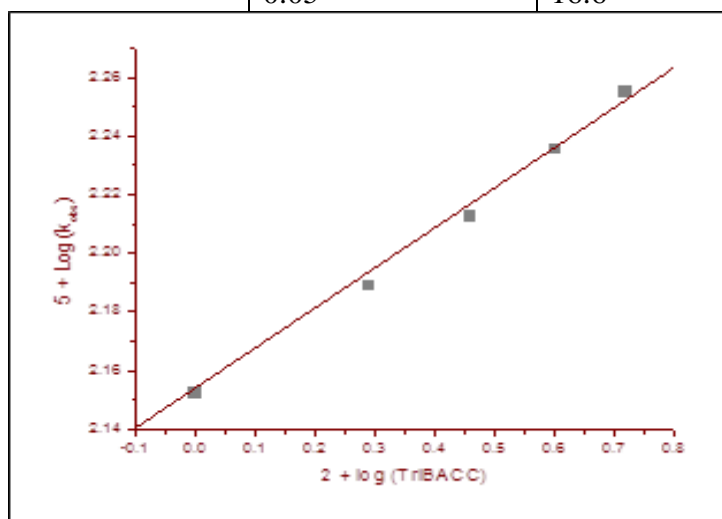
Fig.2: 2+log [TriBACC] Vs 5 + log (Kobs)

Effect of changing [H₂SO₄] on reaction rate:

The rate of reaction was studied by varying sulphuric acid concentration. The rate of reaction was increases with increasing the concentration of sulphuric acid and a plot of log [H_2SO_4] VS log (k_{obs}) was linear with a less than unit slope indicates the fractional order dependence of rate on [H^+] Table-3, (Fig. 3).

Table 3: The impact of changing [H₂SO₄] on the rate of Lysine oxidation

[Lysine] = 1 x10^{-2} mol dm^{-3}, [TriBACC] = 1 x10^{-3} mol dm^{-3}, Temperature. = 303K.

[H^+] mol dm^{-3}	kobs $10^{-4}S^{-1}$
2	13.1
3	15.2
4	16.9
5	18.9
6	20.8
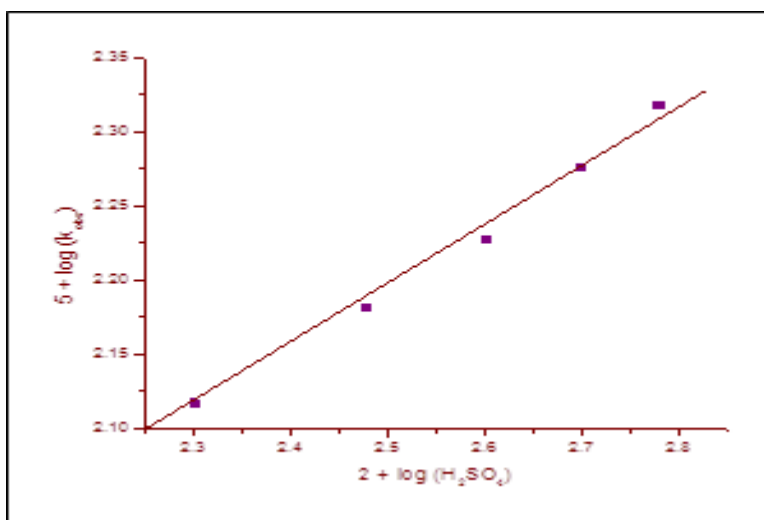
Fig.3: 2 + log [H₂SO₄] VS 5 + log (Kobs)

Effect of Salts:

By incorporating 0.001 mol dm^{-3} of the salts while maintaining constant concentrations of Lysine, H_2SO_4, and TriBACC, the impact of the additional salts on the reaction rate was investigated. It was shown that adding salts does not change the rate of oxidation. Table-4.

Table 4: The impact of salt variation on reaction rate.

Lysine 1x10^{-2} mol dm^{-3}; [TriBACC] = 1 x10^{-3} mol dm^{-3}; [H_2SO_4] = 1 mol dm^{-3}, Temp. = 303K

Salts 10^{-3} mol dm^{-3}	kobs $10^{-4}S^{-1}$
KCl	15.1
NaCl	15.2
CaCl$_2$	14.9
MgSO$_4$	15.2
Ag(NO$_3$)$_2$	15

Effect of Temperature:

By maintaining a constant concentration of Lysine, TriBACC, and H_2SO_4 at 303-323K, the impact of temperature on the rate of Lysine oxidation by TriBACC has been studied. Table-5 lists the rate constants. It was found that the 1/T vslog k Arrhenius graphs were linear (Fig. 4). The slope of the plots was used to compute the activation energy (Ea). The thermodynamic parameters $\Delta H^\#$, $\Delta S^\#$, and $\Delta G^\#$ were calculated based on this value (Table-6).

Table 5 shows the impact of temperature change on reaction rate.

Lysine 1×10^{-2} mol dm^{-3}; [TriBACC] = 1×10^{-3} mol dm^{-3}; [H_2SO_4] = 1mol dm^{-3}.

Temperature	kobs $10^{-4}S^{-1}$
303 K	21
308 K	23.1
313 K	25.2
318 K	27.1
323 K	29.2
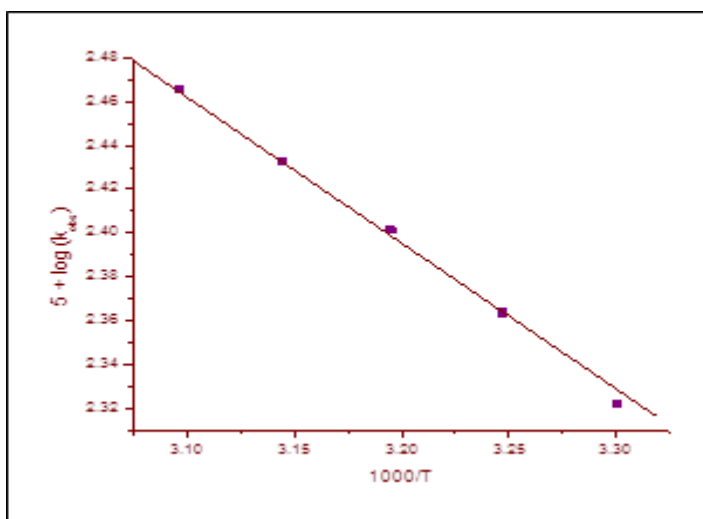
Fig. 4 1000/T Vs 5 + log (kobs)

Table-6: Activation Parameters

Lysine 1×10^{-2} mol dm^{-3}; [TriBACC] = 1×10^{-3} mol dm^{-3}; [H_2SO_4] = 1 mol dm^{-3}, Temp. = 303K

Activation Parameters	
Ea KJ mol^{-1}	12.38
$\Delta H^\#$ KJ mol^{-1}	9.701
$\Delta S^\# JK^{-1}$ mol^{-1}	-265.37
$\Delta G^\#$ KJ mol^{-1}	95.415

Effect of acrylonitrile as free radical detector

It was demonstrated that there were no free radicals present in the reaction mechanism when acrylonitrile was added to the reaction mixture at 35 and 45^0C as there was no change in the reaction rate, no polymerization, and no viscosity change was observed.

'RESEARCH JOURNEY' *International E- Research Journal*

Special Issue – 333 : Innovative & Sustainable Chemistry

Impact Factor 6.625 (SJIF)   **Peer Reviewed Journal**

**E-ISSN :
2348-7143
December - 2023**

Conclusion:

In an acid medium at 303 K, the oxidation of Lysine by Tributylammonium Chlorochromate was investigated. It demonstrates first-order rate dependence on TriBACC, Lysine, and fractional order on sulphuric acid. Lysine underwent oxidation to produce the appropriate carbonyl molecule. Both the addition of salt and the addition of acrylonitrile did not change the rate of the reaction. The parameters of thermodynamics have been assessed. The main product of the reaction is 5-aminovaleradehyde, and an appropriate kinetic mechanism has been given (Scheme-1).

Mechanism of oxidation of Lysine by TriBACC:

Scheme-1

Where R = NH_2-CH_2-CH_2-CH_2-CH_2- For Lysine
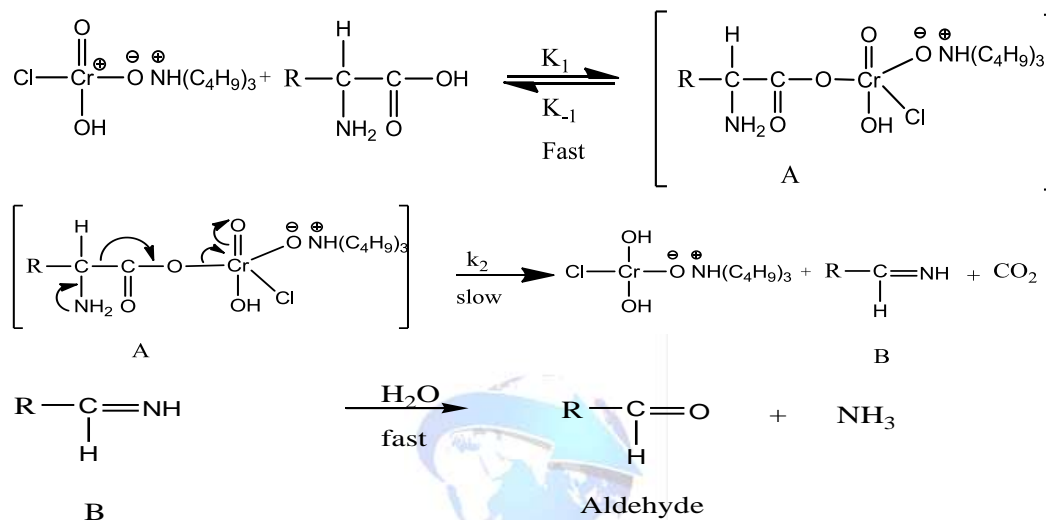
Refrences:

1. Flodin, N. W. (1997). The metabolic roles, pharmacology, and toxicology of lysine. *Journal of the American College of Nutrition*, *16*(1), 7-21.

2. Vuvor, F., Mohammed, H., Ndanu, T., & Harrison, O. (2017). Effect of lysine supplementation on hypertensive men and women in selected peri-urban community in Ghana. *BMC nutrition*, *3*(1), 1-7.

3. Civitelli, R., Villareal, D. T., Agnusdei, D., Nardi, P., Avioli, L. V., &Gennari, C. (1992). Dietary L-lysine and calcium metabolism in humans. *Nutrition (Burbank, Los Angeles County, Calif.)*, *8*(6), 400-405.

4. Kumar, P. S., Rani, S. K., &Easwaramoorthy, D. (2015). Copper (II) Catalysed Oxidative Deamination of Lysine by Peroxomonosulphate. In *National conference on Nanomaterials for Environmental [NCNER-2015]* (Vol. 8, No. 5, pp. 126-137).

5. Mohanty, B., Behera, J., Acharya, S., Mohanty, P., &Pantaik, A. (2013). Metal ion catalyzed oxidation of L-lysine by alkaline permanganate Ion-A kinetic and mechanistic approach. *Chem Sci Trans*, *2*, 51-60.

6. Hosamani, R. R., &Nandibewoor, S. T. (2009). Mechanistic study of ruthenium (III) catalysed oxidation of L-lysine by diperiodatoargentate (III) in aqueous alkaline medium. *Journal of chemical sciences*, *121*, 275-281.

7. Goel, A., & Sharma, R. (2012). A kinetic and mechanistic study on the oxidation of arginine and lysine by hexacyanoferrate (III) catalysed by iridium (III) in aqueous alkaline medium. *Journal of Chemical Engineering and Materials Science*, *3*(1), 1-6.

8. Rangappa, K. S., Chandraju, S., & Made Gowda, N. M. (1998). Manganese (III) oxidation of L-Lysine and L-Histidine in pyrophosphate solution: a kinetic and mechanistic study. *Synthesis and Reactivity in Inorganic and Matel-Organic Chemistry*, *28*(2), 275-294.

9. Basavaraj, T., Chimatadar, S. A., &Nandibewoor, S. T. (2020). A kinetic and mechanistic study of oxidation of L-lysine by diperiodatonickelate (IV) in aqueous alkaline medium. *indian Journal of Chemistry*. 59A, 1470-1475.

10. Sundar, M., Easwaramoorthy, D., Kutti Rani, S., &Palanichamy, M. (2007). Mechanistic investigation of the oxidation of lysine by oxone. *Journal of solution chemistry*, *36*(9), 1129-1137.

11. Choubey, O. N., &Mudaliar, U. (2004). Kinetics of oxidative decarboxylation of L-lysine by potassium permanganate. *Asian Journal of Chemistry*, *16*(3), 1315.

12. Ghammamy, S. (2007). An efficient and mild oxidation of thiols to disulfides with tributylammonium chlorochromate. *Asian Journal of Chemistry*, *19*(2), 917-920.

13. Kute, P., & Chaudhari, N. (2019). Kinetics and Mechanism of Oxidation of L-isoleucine by Tributylammonium Chlorochromate in acetic acid medium. *Journal of Current Pharma Research*, *10*(1), 3543-3551.

14. A.I. Vogel,A Text book of Practical Organic Chemistry including Qualitative Organic Analysis, 3rd Edition, ELBS Longman, London,1973, 332.

15. F.Feigl, Spot Test, Elsevier, Amsterdam New York, 1954, 349.

Studies of Ultrasonic Velocity, Viscosity and Density of Binary System of T-Butyl Alcohol, N-Butyl Alcohol and Iso-Pentyl Alcohol with O-Nitro Toluene At 298.15 And 308.15 K

R.D. Pawar[1] S.R. Patil[2] G.P. Waghulde[3].

1- Arts, Science and Commerce. College, Yawal , (Jalgaon), M.S. India.

2- Arts, Science and Commerce. College, Chopda , (Jalgaon), M.S. India.

3- D.D.N. Bhole College Bhusawal (M.S)

srpatil_001@rediffmail.com, rdpawar69@gmail.com

Abstract :-

The Ultrasonic velocity, Viscosity and Density of binary system of t-butyl alcohol, n-butyl alcohol and iso-pentyl alcohol with O-nitrotulune have been measured at 298.15 and 308.15 K. The measured data reported over entire range of mole fraction. The analysis of obtained calculated data gave information about parameter such as viscosity deviation (Δ_η) , excess molar volume (V^E), deviation in isentropic compressibility (ΔK_S) ,Excess free length (L_f^E), Internal pressure (π^E) ,available volume (V_a^E) and Gibbs free energy(G^{*E}) of binary system from these data attribute the intermolecular interaction between alcohols and O-nitrotolune solvent. The observed parameters and their changes well correlate to each other

Key word :– Ultrasonic velocity, Viscosity ,Density, Excess molar volume (V^E), Viscosity deviation (Δ_n) ,Excess free length (L_f^E), Internal pressure (π^E)

Introduction :–

Liquid binary mixtures are used in product formulation and processing system in many industrial applications rather than single liquid component system. There is different method to identify and strength of intermolecular interaction is one of such reliable and commonly used study.

The intermolecular free length decreases with decreases of temperature hence the close packing of molecules decreases. The sound velocity (1,2). The compressibility deceases with increase of velocity that gave structure making and structure breaking of component in binary mixtures (3,4,5,6).

To study the departure of real liquid mixture from ideabilility, thermodynamic and transport properties of liquid have been used (7,8).

In present binary system we report experimental values of ultrasonic velocity, viscosity and density at temperature 298.15 and 308.15 K. These data have been used to calculate various parameters.

Experimental –

The chemicals used of A.R. grade with minimum assay of 99.9% obtained from Sigma Aldrich or s. d. fine chemicals India. Bi-capillary pycnometer (10ml) was used to measured densities. An airtight stopper bottles were used to prepare and store the binary liquid mixtures of different known concentrations. The shimatzu electronic digital balance (± 0.1mg.) was used to measured weights of the samples. The Ubbelohde viscometer (20ml) was used to measure the viscosity. The efflux time was determined using a digital clock to within ±0.015sec. The ultrasonic velocities (U) in liquid mixtures were measured using an ultrasonic interferometer (Mittal, F-81, 2 MHz, ±0.1 ms^{-1}).

Theory and Calculation

The molar excess volume of the binary mixture have been calculated from the value of density and mole fractions –

$$V^E = \frac{M_1 X_1 + M_2 X_2}{\rho_{12}} - \frac{M_1 X_1}{\rho_1} - \frac{M_2 X_2}{\rho_2} \tag{1}$$

The viscosity of binary mixture can be determine by –

$$\ln\eta_m = X_1 \ln\eta_1 + X_2 \ln\eta_2 \tag{2}$$

The measured values of viscosities of binary mixture have been evaluated the viscosity deviation –

$$\Delta\eta_m = \eta_{12} - X_1\eta_1 - X_1\eta_2 \tag{3}$$

Deviation in isentropic compressibility have been calculated by following way –

$$\Delta k_S = k_S - \Phi_1 k_{S1} - \Phi_2 k_{S2} \tag{4}$$

Where k_{S1}, k_{S2} and K_S are isentropic compressibility of liquid mixtures and Φ is volume fraction of pure i^{th} component in the mixture and is defined as

Summary :-

From experimental data ultrasonic velocity (U), density (ρ) and viscosity (η) have been measured for binary system at 298.15 and 308.15 K. The data have been used to compute the parameters viscosity deviation (Δ_η) , excess molar volume (V^E), deviation in isentropic compressibility (ΔK_S),. It is a well justified that at higher temperature most of values showing negative values due to presence of bulky groups on aromatic ring which increases salvation effect in solution so it posses interaction between solvent and solute.

Table.1. Values of densities viscosities, ultrasonic velocity, Excess molar volumes and Deviation in viscosity and deviation in isentropic compressibility for binary system of 2-butanol and O-nitro toluene at 298.15 and 308.15 K.

Temp K	X_1	ρ (gm /cm³)	$\eta 10^3$ (Nsm⁻²)	U (M S⁻¹)	V^Ex10⁶(m³/ mole)	Δ ηx10³(Kg m⁻¹s⁻¹)	Δksx10¹¹ (m²N⁻¹)
298.15	0.0000	0.80210	2.95470	1451.0	0.0000	0.000	0.000
	0.1056	0.83140	2.37190	1483.9	-0.9900	-52.487	-19.64
	0.2119	0.85680	2.08440	1500.7	-1.4098	-74.839	-30.00
	0.3188	0.89150	1.97480	1517.3	-2.7197	-78.736	-41.94
	0.4265	0.92200	1.83930	1565.2	-3.4087	-84.392	-55.60
	0.5051	0.93510	1.55420	1599.0	-4.0673	-104.054	-47.41
	0.6148	0.98870	1.63930	1666.5	-4.9552	-85.641	-43.14
	0.7057	1.01290	1.60790	1700.7	-4.5311	-77.514	-33.51
	0.8184	1.04240	1.51270	1714.3	-5.4814	-74.106	-24.54
	0.9229	1.05410	1.43650	1730.5	-3.2514	-66.830	-17.03

| Temp K	X₁	ρ	η 10³	U	V^E×10⁶	Δη×10³	Δks×10¹¹
	1.0000	1.06920	1.92950	1932.0	0.0000	0.000	0.000
308.15	0.0000	0.79380	2.09760	1401.4	0.0000	0.000	0.000
	0.1056	0.82260	1.75580	1448.9	-0.9627	-31.418	-17.67
	0.2119	0.84780	1.57690	1456.0	-1.3778	-46.250	-34.30
	0.3188	0.88260	1.50860	1500.5	-2.7343	-49.704	-40.03
	0.4265	0.91280	1.43760	1520.8	-3.4114	-53.031	-51.50
	0.5051	0.92660	1.35960	1549.9	-4.1281	-56.602	-54.12
	0.6148	0.97890	1.32270	1558.5	-4.9346	-55.559	-40.40
	0.7057	1.00320	1.30330	1665.4	-4.5158	-52.114	-37.12
	0.8184	1.04280	1.24830	1669.2	-4.0030	-51.435	-35.65
	0.9229	1.05430	1.14580	1672.3	-3.3319	-48.565	-21.75
	1.0000	1.06030	1.60760	1719.2	0.0000	0.000	0.000

Table.2. Values of densities, viscosities, ultrasonic velocity, Excess molar volumes and Deviation in viscosity and deviation in isentropic compressibility for binary system of 3- methyl 1-butanol and O-nitro toluene at 298.15 and 308.15 K.

Temp K	X₁	ρ (gm /cm³)	η 10³ (Nsm⁻²)	U (M S⁻¹)	V^E×10⁶(m³/mole)	Δ η×10³(Kg m⁻¹s⁻¹)	Δks×10¹¹ (m²N⁻¹)
298.15	0.0000	0.80660	3.74590	1488.6	0.0000	0.000	0.000
	0.1066	0.83550	3.36850	1499.7	-1.1321	-25.644	-13.44
	0.2138	0.86450	2.82450	1525.5	-2.1086	-67.057	-23.52
	0.3212	0.88920	2.60070	1545.6	-2.3422	-75.269	-33.18
	0.4301	0.95330	1.95640	1601.2	-3.0904	-104.459	-46.97
	0.5091	0.96100	2.32250	1610.0	-5.0368	-91.284	-35.24
	0.6149	0.99590	2.13420	1630.7	-5.9413	-72.022	-27.94
	0.7159	1.08460	2.08160	1642.0	-6.3053	-57.520	-24.64
	0.8203	1.10090	1.96870	1687.8	-5.8342	-46.922	-20.59
	0.9128	1.11900	1.92200	1694.5	-4.3612	-27.525	-11.98
	1.0000	1.06920	1.92950	1932.0	0.0000	0.000	0.000
308.15	0.0000	0.79940	2.79410	1449.2	0.0000	0.000	
	0.1066	0.82790	2.59620	1450.2	-1.1181	-11.892	-10.08
	0.2138	0.85640	2.16230	1516.7	-2.0672	-46.799	-14.29
	0.3212	0.88090	2.03580	1538.3	-2.3002	-85.194	-28.36
	0.4301	0.94430	1.49470	1597.0	-4.0742	-94.349	-37.92
	0.5091	0.95230	1.79070	1600.2	-5.0371	-73.928	-46.73
	0.6149	0.98660	1.64660	1619.2	-5.9090	-56.521	-52.31
	0.7159	1.07570	1.70020	1633.0	-12.4484	-38.252	-40.82
	0.8203	1.09120	1.67040	1667.9	-10.8883	-26.934	-38.54
	0.9128	1.10940	1.61370	1678.3	-9.4195	-16.883	-24.62
	1.0000	1.06030	1.60760	1719.2	0.0000	0.000	0.000
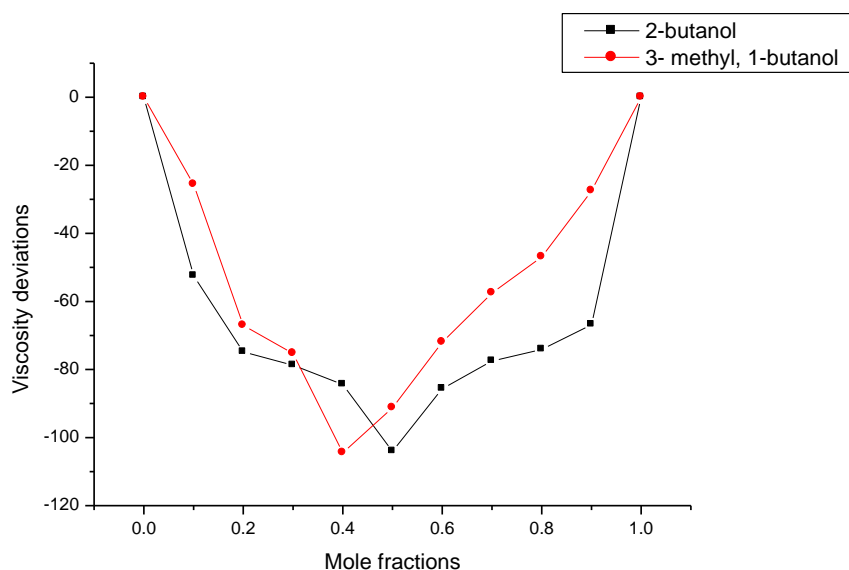
(a)
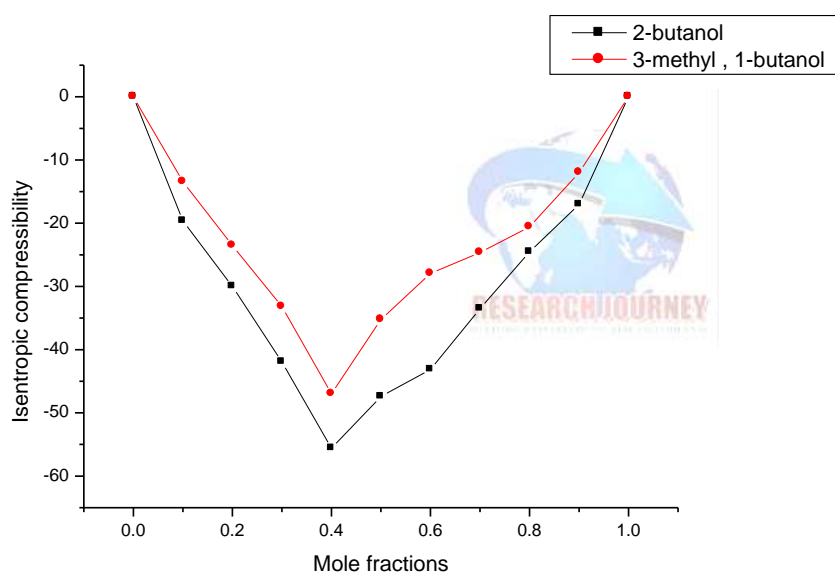
(b)

(a) $\Delta\eta$ against mole fraction for 2-butanol and 3-methyl, 1-butanol at 298.15 K.

(b) ΔK_S against mole fraction for 2-butanol and 3-methyl, 1-butanol at 298.15 K.

Result and Discussion :–

The measures values such as density (ρ), viscosity (η), ultrasonic velocity (U), viscosity deviation (Δ_η), excess molar volume (V^E), deviation in isentropic compressibility (ΔK_S), are given in Table-1 and Table-2 respectively. Figure :- a and ,b, Viscosity deviation (Δ_η) and Deviation in isentropic compressibility (ΔK_S) against mole fraction for binary system of 2-butanol and 3- methyl 1-butanol with O-nitro toluene at 298.15 K respectively.   From observed and reported value it shows that negative values around 0.4 to 0.5 mole fractions of alkanols.

References :-

1. Subramanyam Naidu., Ravindra Prasad., J. *Pure Applied Ultrason*. 27 (2005) 15.
2. Narendra K., Srinivasu Ch., Fackruddin Sk., Narayanamurthy P., *J. Chem. Thermodyn*. 43 (2011) 1604.
3. Arnett E. M., Michel E. J., Murthy T. S. S. R., *J. American Chem. Soc*. 96 (1974) 3875.
4. N. Santhi., P. L. Sabarthinam., J. Madhumitha., G. Alamelumangai., M. Emayavaramban., *Internatinal Letter Of Chemistry, Physics and Astronomy* 2 (2013) 18-35.
5. M. Durga Bhavani., A. Ratnakar., Ch. Kavith., *Internatinal Letter Of Chemistry, Physics and Astronomy* 5 (2013) 1-6.
6. Y. Sreedevi., Ch. Srinivasu., Sk. Fakruddin., K. Narendra., B.R. Venkateswara Rao., Y. Niramal Rajeev., *Internatinal Letter Of Chemistry, Physics and Astronomy* 7 (2) (2013) 120-124.
7. Oswel S. L., Oswel P., Phalak R.P., *J. Sol. Chem*. 27 (1998) 507.
8. Rajashekhar J., Naidu P*., J. Chem. Eng. Data* 41 (1996) 373.
9. D.S. Wankhede., M.K. Lande., B.R. Arbad., *J. Chem. Eng. Data* 50 (2005) 261-263.

Mechanistic and Spectral Investigation of Oxidation Ofp-Nitrochalcone (PNC)By Tripropylammonium Chlorochromates

Surendra N. Takale

Department of Chemistry,Sir Sayyed College, Aurangabad-431001(M.S.) India.

Abstract:

The Kinetics of oxidation of p-nitrochalcone by Tripropylammonium Chlorochromates [TriPACC] has been Studied Spectrophotometrically in aqueous acetic acid medium in the temperature range 292-318K.The reaction is first order with respect to both p-nitrochalcone and TriPACC. There is no kinetic or spectral evidence for the formation of complex between TriPACC and p-nitrochalcone. The activation parameters for the slow step were computed and calculated. Effect of ionic strength and dielectric constant of medium has been reported. A suitable mechanism has been proposed.

Key words:p-nitrochalcone, Tripropylammonium Chlorochromates, Oxidation, Kinetics.

Introduction:-

An extensive literature survey reveals that the kinetics and mechanism of oxidation of p-nitrochalcone have been carried out using various oxidants like trichloroisocyanuric acid (1), pyridinium chlorochromate (2), acid bromate (3), N-chloronicotinamide (4), hexacyanoferrate (III) (5), N-chlorosuccinimide (6), chloramine-T (7), morpholinium chlorochromate(8), peroxydisulphate(9) and periodate(10).p-nitrochalcone undergo a variety of chemical reactions and are found useful in the synthesis of variety of heterocyclic compounds. p-nitrochalcone have been used as intermediate for the preparations of compounds having therapeutic value. Literature review reveals that p-nitrochalcone derivatives exhibit diverse pharmacological activities such as potential cytotoxic agents, antimicrobial agents, antiviral, anti-inflammatory, anesthetics etc. Hence the study becomes important from the biological point of view. The results of kinetics of oxidation of p-nitrochalcone with TriPACC in aqueous acetic acid medium has taken for study.

Experimental Section:-

All the chemicals and reagents were of analytical grade. All the solutions used in the study were prepared by using distilled acetic acid and doubly distilled water. Tripropylammonium Chlorochromates was prepared by the following method: chromium (VI) oxide (15.0g, o.150 mol) was dissolved in water in a polyethylene beaker and 40% hydrochloric acid (11.3 ml, 0.225 mol) was added with stirring at 0°C. To the resultant orange solution, tripropylammine (28.3 ml, 0.150 mol) was added drop wise with stirring to this solution over a period of 30 minutes and stirring was continued for 30 minutes at 0°C. The orange colored precipitate was filtered, washed with petroleum ether and dried in vacuum for 2 hours at room temperature [11]. Yield was 26 g (96%); MP was 144°C.

The Tripropylammonium Chlorochromates was stored in polyethylene bottle for long period of time. TriPACC was soluble in water, DMF, acetonitrile, acetone and DCM and was sparingly soluble in benzene, chloroform and hexane.

Determination of Stoichiometry and Product Analysis:-

The Stoichiometry of the reaction was determined by carrying out several sets of experiment with varying amount of (TriPACC) largely in excess over p-nitrochalcone in 20% acetic acid by using 0.1N H_2SO_4. The remaining (TriPACC) was then analyzed

Spectrophotometrically. The result indicated that 1 mole of p-nitrochalcone react with 1 mole (TriPACC).

$$C_6H_5-CH=CH-COC_6H_5 + [C_3H_7]_3N^+H(CrO_3Cl) \xrightarrow{H^+} C_6H_5-COOH + C_6H_5-CH_2-CHO + [C_3H_7]_3NH(CrO_3H_2Cl)$$
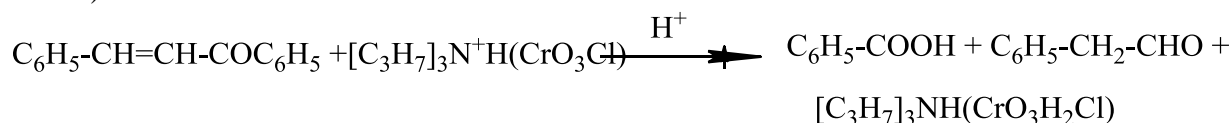
The product analysis was carried out under kinetic conditions. In a typical experiment, p-nitrochalcone (0.05 mol) and TriPACC (0.01) were made up to 50 ml in 20% acetic acid and kept in dark for about 24 hours to ensure the completion of the reaction. The solution was then treated with an excess (200 ml) of a saturated solution of 2, 4-dinitrophenylhydrazine in 2 mol dm^{-3} HCl and kept overnight in a refrigerator. The precipitated 2, 4-dinitrophenylhydrazone (DNP) was filtered off, dried, weighed, recrystallized from ethanol and weighed again. The yield of DNP before and after recrystallization was 2.0 g (90%) and 1.7 g (75%) respectively. The DNP was found identical with the DNP of acetone by meting point. The products were also characterized by TLC, IR, and NMR spectra.

Kinetic Measurements:-

The reactions were followed under pseudo-first-order conditions by keeping large excess (x 10 or greater) of the p-nitrochalcone over TriPACC. The temperature was kept constant to +/- 0.1 K. The solvent was acetic acid. The reactions were followed by monitoring the decrease in the concentration of TriPACC spectrophotometrically at 350 nm for 80% completion of the reaction. The pseudo-first-order rate constants K_{obs}, were evaluated from the linear (r=0.990-0.999) plots of log [TriPACC] against time. Duplicate kinetic runs showed that the rate constants were reproducible to within +/- 3%.

Result And Discussion:-

The results of oxidation of Chalconeby TriPACC are represented as follows.

Effect of variation of concentration of p-nitrochalcone:-

The oxidation of p-nitrochalcone withTriPACC in 20% of acetic acid in presence of sulphuric acid yields acetone. By keeping constant [TriPACC] and [H$_2$SO$_4$], the increase in (MCC) increases the rate of reaction (Table-1). The plot of log of k_{obs} versus log (MCC) for different initial concentration of p-nitrochalcone is linear with unit slope demonstrate the first order dependence of rate on p-nitrochalcone

Table 1: Effect of variation of p-nitrochalcone on reaction rate

[TriPACC]= 0.001 M, [H$_2$SO$_4$] = 0.1 N, Temperature =303 k, AA = 20% (v/v)

(PNC)	01M	02M	03M	04M	05M	06M	07M	08M
k x 10^{3}sec^{-1}	07	35	64	96	22	50	78	08

Effect of variation of concentration of TriPACC:-

At constant p-nitrochalcone and [H$_2$SO$_4$], the increase in [TriPACC] increases the rate of reaction (Table-2). The plot of log k_{obs} verses log [TriPACC] for different initial concentration of TriPACC is linear with unit slope present the first-order dependence of rate on TriPACC.

Table 2: Effect of variation of [TriPACC] on reaction rate

[MCC]= 0.01 M, [H$_2$SO$_4$] = 0.1 N, Temp =303 k, AA = 20% (v/v)

[T$_{ri}$PACC] Mole	001	0015	002	0025	003	0035	004	0045
k x 10^{3}sec^{-1}	07	33	58	84	09	31	55	79

Effect of variation of concentration of H⁺:-

In order to study the effect the H^+ ion concentration on the rate of oxidation reaction of m-chlorochalcone (MCC), the dependence of reaction rate has been investigated at different initial concentration of H_2SO_4. The rate of reaction increases with increase in [H_2SO_4] (Table-3). The plot of log K_{obs} verses log [H+] are also straight line with slope less than unity, Indicating a fractional order dependence on [H+].

Table 3: Effect of variation of [H₂SO₄] on reaction rate

[TriPACC]= 0.001 M,   (PNC) = 0.01 M, Temp. =303 k,   AA = 20% (v/v)

[H_2SO_4]	1M	2M	3M	4M	5M	6M	7M	8M
k x 10^3sec^{-1}	06	26	44	60	75	91	06	24

Effect of ionic strength:-

In the present investigation effect of salt on the rate of reaction is carried out. The salts selected are KCl, KBr, and KI. These will give effect of anion particularly halides on the rate of reaction. The divalent and trivalent cationic salt were also used such as $CaCl_2$, $Ca(NO_3)_2$, $Al(NO_3)_3$ and K_2SO_4. The experiments were carried out under pseudo- first- order condition. These results were used to determine first order rate constant. The rate constants for the oxidation of p-nitrochalconein presence of different salt are shown in [Table 4]. From table it is clear that, the rate increases with increase in cationic charge and decreases with increase in anionic charge. In case of KCl the rate of reaction decreases with the addition of KCl, this is due to the formation of less reactive species [19] by interaction between Cl^- ion and protonated TriPACC.

Table 4: Effect of variation of [salts] on reaction rate

[TP]= 0.001 M, (PNC) = 0.01 M, [H₂SO₄] = 0.1 N, Temp. =303 k,   AA = 20% (v/v)

alts 0.1M	Cl	Br	I	aCl₂	a(NO₃)₃	l(NO)₃	₂SO₄
x 10^3sec^{-1}	08	38	40	47	76	98	34

Effect of solvent composition:-

At fixed [PNC], [TriPACC] and [H⁺], the rate of oxidation of p-nitrochalcone with TriPACC increases with decrease in polarity of solvent (Table 5). This is due to polar character of transition state as compared to the reactant. The plot of log k_{obs} verses 1/D is linear with positive slope indicating ion- dipole type of reaction [20].

Table5: Effect of variation of Acetic Acid % on reaction rate

[TriPACC]= 0.001 M,   [H₂SO₄] = 0.1 N, [PNC] =0.01M, Temp=303 k

cetic acid	) %	) %	) %	) %	) %	) %	) %	) %
x 10^3sec^{-1}	98	07	22	34	46	58	72	86

Effect of temperature:-

The study of effect of temperature on rate of oxidation of m-chlorochalconesby TriPACC has been subjected to different temperature range 293K to 313K by keeping the concentration of p-nitrochalcone and reagent constant. Rate constants are given in [Table 6]. The plots of log of K_{obs} verses 1/T are linear.

Table 6: Effect of variation of Temperatures on reaction rate

[TriPACC]= 0.001 M, [PNC] = 0.01 M, [H$_2$SO$_4$] = 0.1 N, AA = 20% (v/v)

Temperatures (K)	293	298	303	308	313	318
k x 10^{3}sec^{-1}	1.27	1.69	2.06	2.45	2.87	3.27

Table 7: Activation Parameters

[TriPACC]= 0.001 M, [PNC] = 0.01 M.   [H$_2$SO$_4$] = 0.1 N, Temp. =303 k,   AA = 20 % (v/v)

Activation parameters	ΔE$_a$ KJ mole^{-1}	ΔH$^{\#}$KJmol^{-1}	ΔS$^{\#}$JK^{-1}mole^{-1}	ΔG# KJ mole^{-1}
	25.69	23.22	-226.06	90.84

Activation parameters are presented in [Table 7]. The negative values of entropy of activation reflect that the transition state is more rigid than initial state. The nearly constant ΔG value indicates that similar mechanism is operative for the oxidation of p-nitrochalcone

These above observations suggest that the rate law can be written as shown

$$- \frac{d[T_{ri}PACC]}{dt} = k_3C_1$$

$$= \frac{k_3k_2[OxH^+][S]}{1+ K_2[S]}$$

$$= \frac{k_3K_1K_2[Ox][H+][S]}{1+ K_2[S]}$$

Conclusion:-

The rate constants of the slow step involved in the mechanism were evaluated. Activation parameters were also computed. The negative value of **ΔS$^{\#}$** providessupport to the formation of rigid transition state. The overall mechanism described here is consistent with product and kinetic studies.

Acknowledgement:-

References:-

1. Annapoorna S. R., Prasad Rao M. and Sethuram B., Study of interactive linear free energy relationships on oxidation of phenyl styryl ketone and its substituted analogues by pyridinium chlorochromate in acid medium: A kinetic study, Indian J. Chem., 2001, 40A, 283-287

2. Anil Kumar J. and Sondu S., Kinetics and mechanism of oxidion of chalcones by (TCICA) in HOAc – HClO4 medium, Indian J. Chem., 46A (2007) 1792-1795.

3. Narasimha Char P., and others, Kinetics of Ru (III) –catalysed oxidation of chalcones by acid bromated in H2SO4 – HOAc medium, Indian J. Chem., 1989, 28A, 36-39.

4. Parimala Vaijayanthi S. and Mathiyalagan N., Oxidation of chalcone by N-chloronicotinamide in aqueous acetic acid medium: A kinetic and mechanistic study, Der Chem. Sin., 2011, 2(3), 41.

5. Mohapatra R. C. and Khandual N. C., Kinetics and mechanism of Os(VIII) - catalysed oxidation of chalcone by alkaline hexacyanoferrate (III), Indian J. Chem., 1982, 21A, 167-169.

6. Parimala Vaijayanthi S. and others, A mechanistic investigation of the oxidation of chalcone by N-chlorosuccinimide in aq. acetic acid medium, Int. J. Res. Pharm. Chem., 2012, 2(3), 722-727.

7. Parimala Vaijayanthi S. and Mathiyalagan N., Oxidative kinetics of p-nitrochalcone by chloramine-T, J. Chem. Bio. Phy. Sci., 2012, 2(3), 1281-1286.

8. Rajalakshmi K. and others, Oxidation of chalcone by morpholinium chlorochromate with oxalic acid as catalyst: Kinetic and mechanistic study, J. Chem., 2013, Article ID 1-5.

9. Pranati Mishra and Khandual N. C., Kinetics of oxidation of chalcone by peroxydisulphate catalysed by silver (I) ions, Indian J. Chem., 1989, 28A, 526-527. 386-388.

10. Murugesan. v., Pandugangan. A.React Kinet. Catal. Lett.1995, 54, 173.

11. Banerji.K.K, J. Chem. Society, Parkin Trans, 1998, 2, 547.

12. S.G. Patil, S.B. Joshi, Asian J. Chem., 2002, 14,130.

13. S.Kavita, A. Pandurangan, I. Alphonse. Indian J. Chem., 2005, 44A, 715.

14. Banerji.K.K, Bull Chem. Society, Japan. 1978, 51, 2732.

15. V. kumbhat, Sharma. P.K,Banerji.K.K. Indian J. Chem., 2000, 39A, 1169.

16. R.Gurumurty, M.Gopalkrishnan, B. Kathikeyan. Asian J. Chem., 1998, 10, 476.

17. I. Dave, V. Sharma, K.K. Banerji, J. Indian Chem. Society, 2002, 79, 347.

18. S.A. Chimatadar, M.S.Salunke, S.T.Nandibewoor, Indian J. Chem., 2006, 45A, 388.

19. D.S. Bhuvaneshwari, K.P. Elengo, Int. J.chem. Kinetics. 2005, 37, 166.

20. Mansoor. S.S, Asian J.Chem. 2010, 22(10), 7591.

21. Kassaee.M.Z, Sayyed-Alangi. S.Z, and Sajjadi-Ghotbabadi.H, Molecule, 2004, 9,825.

22. Mansoor S.S, and Shafi S.S, Reac. Kinet. Mech. Cat., 2010, 21,100(1).

23. Mansoor S.S,and Shafi S.S, E-Journal chem.,2009, 6,522.

24. Vibhute A. Y, Patwari S. B, Khansole and Vibhute Y.B, chin. Chem. Lett., 2009, 20, 256.

25. Weissberger A and prabankar S, Oganic Solvents physical properties and methods of Purification. 2nd. Interscience Publishers, Londan, 1995, 390.

26. Ghammamamy S and Hashemzadeh A, Bull Korean chem. Soc., 2004, 25, 1277.

Ionic Liquid Mediated an Effective Synthesis of 2-Arylbenzothiazol

Kiran F. Shelke

ᵃDepartment of Applied Chemistry, Sardar Patel College of Engineering, Andheri (W), Mumbai-400058 (MS) INDIA

*Corresponding author- E-mail: kiranshelke82@gmail.com

Abstract:

An effective synthesis of arylbenzothiazole from the cyclocondensation of *o*-aminothiophenol with aldehydes by using 1-benzyl-3-methylimidazolium dihydrogen phosphate ([bnmim]H_2PO_4) acidic ionic liquid at 70°C. This methodology gives eminent benefits like simple procedure, fast reactions, good yield and the ionic liquid was effectively reused for four cycles without critical loss of activity.

Keywords: Arylbenzothiazole, ionic liquid, aldehydes

Introduction:

Benzothiazole is a privileged bicyclic ring system. It contains a benzene ring fused to a thiazole ring. The small and simple benzothiazole nucleus is present in compounds involved in research aimed at evaluating new products that possess interesting biological activities like anticancer,[1] antimicrobial,[2] anticonvulsant,[3] antiviral,[4] antihelmintic,[5] analgesic,[6] antinflammatory,[7] antidiabetic.[8] In addition, the benzothiazole ring is present in various marine or terrestrial natural compounds, which have useful biological activities and also importance as photo sensitizers.[9] Due to their importance in pharmaceutical utilities, the synthesis of various benzothiazole derivatives is of considerable interests

There are several methods reported in the literature for the synthesis of arylbenzothiazole such as TMP[10], TBAF[11], Et_4NBrO_3[12], L-Proline[13], CAN[14]. Nonetheless, in over a few reported methods suffer from at least one disadvantages like prolonged reaction times, utilization of ecologically negative solvents, extreme reaction conditions and low yields. Consequently, the advancement of a productive and new methodology for the synthesis of arylbenzothiazole derivatives would be exceptionally attractive.

The utilization of ionic fluids in organic synthesis certainly stand out enough to be noticed because of their unique properties like great solvating capacity, extensive liquid range, non-inflammability, negligible vapor pressure, simple of reusing and high thermal stability[15-16]. They have been mentioned as designer solvents as their physical and chemical properties could be changed by a cautious decision of cation and anion. These days, ionic liquid-catalyzed organic processes have received a lot of interest[17-20].

FIGURE 1.

1-benzyl-3-methylimidazolium dihydrogen phosphate ([bnmim]H_2PO_4)

1   2(a-k)   3(a-k)
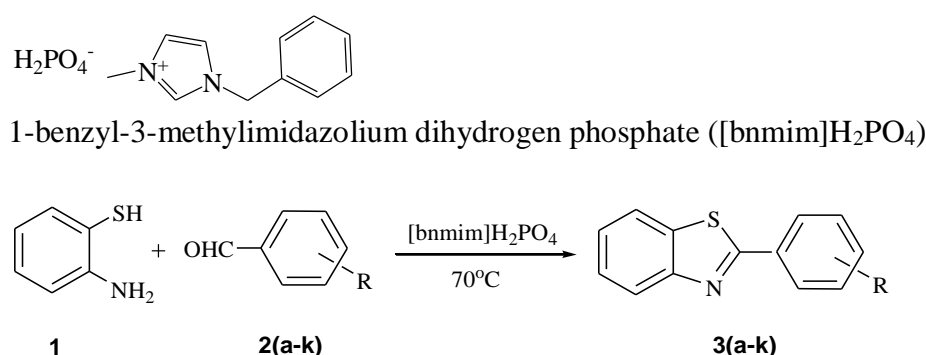
SCHEME 1

Experimental:

Materials and methods:

Without further purification, all chemicals were utilised directly after being obtained from the Merck, Aldrich, and Rankem chemical companies. The progress of the reactions was monitored by Thin Layer Chromatography. On a Perkin-Elmer FT spectrophotometer, IR spectra of a KBr disc were captured. ^{1}H NMR spectra were recorded on an 400 MHz FT-NMR spectrometer in $CDCl_3$ as a solvent and chemical shift values are recorded in units δ (ppm) relative to tetramethylsilane as an internal standard.

Typical experimental procedure:

A mixture of *o*-aminothiophenol (1 mmol), aldehyde 2a-k (1 mmol) and [bnmim]H_2PO_4 (5 mol%) were taken in single neck round bottom flask. The reaction mixture was stirred at 70°C in an oil bath for the appropriate time given in TABLE 2. Thin layer chromatography was used to keep track of the reaction's development. After the reaction was finished, the mixture was cooled to room temperature, and the product was extracted from diethyl ether (2×20 mL), with the insoluble [bnmim]H2PO4 being able to be reused right away in additional runs. The organic layer was removed using a rotary evaporator under reduced pressure after being washed with brine (2×10 mL) and dried over sodium sulphate, The solid obtained 3 (a-k) was recrystallized by ethanol to get pure product.

Spectral data of principal compounds:

2-Phenylbenzothiazole (3a)

^{1}H NMR (400 MHz, $CDCl_3$): δ ppm 8.03-8.14 (m, 3H), 7.90 (d, J = 8 Hz, 1H), 7.46-7.60 (m, 4H), 7.35-7.44 (m, 1H); ESI-MS (MeOH): m/z: 212 [M+H]+

2-(2-Chlorophenyl)-benzothiazole (3b)

^{1}H NMR (400 MHz, $CDCl_3$): δ ppm 8.18-8.28 (m, 1H), 8.14 (d, J = 8.16 Hz, 1H), 7.96 (d, J = 7.91 Hz, 1H), 7.49-7.57 (m, 2H), 7.36-7.48 (m, 3H); ESI-MS (MeOH): m/z: 246 [M+H]+, 248 [M+2+H]+

2-(3-Bromophenyl)-benzothiazole (3d)

^{1}H NMR (400 MHz, $CDCl_3$): δ ppm 8.28 (s, 1H), 8.07 (d, J = 8.16 Hz, 1H), 7.95 (d, J = 7.78 Hz, 1H), 7.90 (d, J = 8.03 Hz, 1H), 7.62 (d, J = 8.03 Hz, 1H), 7.51 (t, J = 7.72 Hz, 1H), 7.30-7.44 (m, 2H); ESI-MS (MeOH): m/z: 290 [M+H]+, 292 [M+2+H]+

2-Furan-2-yl-benzothiazole (3k)

^{1}H NMR (400 MHz, $CDCl_3$): δ ppm 8.05 (d, J = 8.14 Hz, 1H), 7.89 (d, J = 7.91 Hz, 1H), 7.61 (s, 1H), 7.48 (d, J = 7.42 Hz, 1H), 7.39 (d, J = 7.65 Hz, 1H), 7.20 (d, J = 3.39 Hz, 1H), 6.54-6.64 (m, 1H); ESI-MS (MeOH): m/z: 202 [M+H]+

Result and Discussion:

In this article, we would like to report a quick, efficient, and easy way to make 2-arylbenzothiazole by using [bnmim] H_2PO_4 as a catalyst at 70°C.

To improve the reaction conditions, the reaction of *o*-aminothiophenol **1** and benzaldehyde **2a** at 70°C was chosen as the model reaction. We screened several acidic ionic liquids such as 1-hexyl-2,3-dimethylimidazolium dihydrogen phosphate ([hdmim]H_2PO_4), 1-butyl-3-methylimidazolium dihydrogen phosphate ([bmim]H_2PO_4) and 1-benzyl-3-methylimidazolium dihydrogen phosphate ([bnmim]H_2PO_4) for the model reaction. All the results are listed in

TABLE 1. In ionic liquids such as [bmim]H_2PO_4 and [bnmim]H_2PO_4, the desired product was obtained in satisfactory yields. Bearing in mind the reaction time and yield of product, [bnmim]H_2PO_4 (**FIGURE 1**) was selected as the optimum ionic liquid to promote the synthesis of arylbenzothiazole (**TABLE 1**, entry 3).

TABLE 1. Effect of different acidic ionic liquid for the synthesis of 2-phenyl-1,3-benzothiazole **3a**[a].
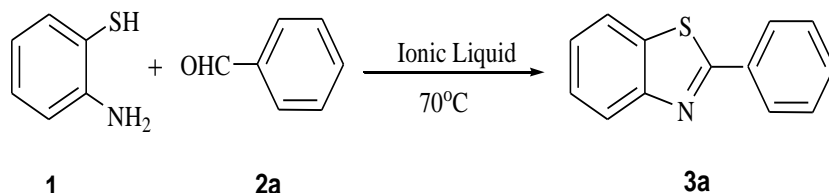
Entry	Ionic liquid	Time (min)	Yield (%)[b]
1	[hdmim]H_2PO_4	60	87
2	[bmim]H_2PO_4	60	91
3	[bnmim]H_2PO_4	30	94

[a]Reaction condition: **1** (1 mmol), **2a** (1 mmol) at 70°C. [b]Isolated yield.

Recovery and reuse of the ionic liquid is strongly preferred in light of cost-effective and environmentally friendly approaches. As indicated in **TABLE 2** (compound **3a**), After four consecutive runs, regenerated ionic liquid showed no degradation in yield or reaction time. To demonstrate the advantages of the current method in contrast to other previously described methods for similar reactions, we have tabulated some of the results in **TABLE 3**. As it is evidence from the results, present method found to be effective for the synthesis of 2-phenyl-1,3-benzothiazole.

We have established a newer path for the condensation of various aldehydes with o-benzothiazole catalyzed by [bnmim]H_2PO_4 at 70°C. The liberated water during the reaction was adsorbed by the ionic liquid and hence the reactions proceed well. In this methodology, condensation reactions were completed in shorter reaction times (30-90 min) and with excellent yields (85-94%).

TABLE 2. Synthesis of 2-arylbenzothiazole using [bnmim] H_2PO_4 at 70°C.

Compound	R	Time (min)	Yield (%)[a]	Mp (°C)[11]
3a	H	30	94 (90,88, 87, 87)[b]	112-114
3b	2-Cl	60	90	80-82
3c	4-F	60	92	100-102
3d	3-Br	60	86	90-92
3e	4-OCH$_3$	90	85	120-121
3f	2-CH$_3$	90	87	58-60
3g	2-OH	90	85	130-132
3h	4-OH	90	91	230-232
3i	3-NO$_2$	90	94	198-200
3j	4-NO$_2$	90	92	230-232
3k	2-Furyl	90	85	110-112

[a] Isolated yields based upon starting aldehyde. [b]The same ionic liquid was used for each of the runs.

TABLE 3. Comparison data with present method[a].

Entry	Reagent	Reaction condition	Time	Yield (%)	References
1	TBAF	H_2O/80°C	1-3 h	79-94	11
2	Et_4NBrO_3	MeOH aq	5-110 min	68-86	12
3	[bnmim] H_2PO_4	70°C	30-90 min	85-94	Present

[a]Synthesis of 2-arylbenzothiazole.

This approach doesn't employ solvents or harsh acids, and all that's needed to speed up the reaction is a catalytic amount of ionic liquid. The reactions were compatible with various substituents such as nitro, methyl, chloro, hydroxyl, methoxy etc. No any significant substituents effect was observed in regarding the reaction time and yield of product (**TABLE 2**). The identities of compounds **3**(**a-k**) were established by comparison of their physical and spectroscopic properties with those earlier reported[10-14].

Conclusion:

Finally, we created a straightforward, efficient, and environmentally friendly process for the synthesis of arylbenzothiazole derivatives by cyclocondensation of various aldehydes with *o*-aminothiophenol using [bnmim]H_2PO_4 at 70°C. The current method's salient advantages include short reaction times, and excellent yield of products. Additionally, the [bnmim]H_2PO_4 was successfully utilised four times with little to no activity loss. It is thus a rapid, convenient and environmentally benign method for the synthesis of compounds of type **3** (**a-k**).

References:

1. S. T. Huang and I. J. Hsei, Chen, Bioorg. Med. Chem. **14**, 6106- (2006).
2. M. Singh, S. K. Singh, M. Gangwar, G. Nath and S. K. Singh, RSC Adv., **4**, 19013- (2014).
3. N. Siddiqui, S. N. Pandey, S. A. Khau, J. Stables, A. Rana, M. Alam, F. Md. Arshad and M. A. Bhat, Bioorg. Med. Chem., **17**, 255- (2007).
4. T. Akhtar, S. Hameed, N. Al-Masoudi, R. Loddo and P. Colla, Acta Pharm., **58**, 135- (2008).
5. C. H. Suresh, J. V. Rao, K. N. Jayaveera and S. K. Subudhi Int, J. Pharma., **2**, 257- (2013).
6. N. Siddiqui, M. Alam and A. A. Siddiqui, Asian J. Chem., **16**, 1005- (2004).
7. B. M. Gurupadayya, M. Gopal, B. Padmashali and V. P. Vaidya, Indian J. Heterocycl. Chem., **15**, 169- (2005).
8. S. R. Pattan, C. Suresh, V. D. Pujar, V. V. K. Reddy, V. P. Rasal and B. C. Koti, Indian J. Chem., **44B**, 2404- (2005).
9. T. D. Bradshaw and A. D. West well, Curr Med Chem., **11**, 1009- (2004).
10. D. Chandrashekarachar, Chaitramallu and D. Kesagudu, Der Pharma Chemica, **7(10),** 490-492 (2015).
11. V. U. Mane, B. R. Choudhari and D. V. Mane, Chem Bio Inter, **7,** 48-56 (2017).
12. P. J. Das and S. Sarkar, Ind J Chem **52B**, 1214-1217 (2013).
13. S. Lee, C. H. Chung, Y. T. Chang and P. Lung Chen J. Applied Sci Engineering, **15**, 311-315 (2012).
14. F. A. Qalaf, R. A. Mekheimer and K. U. Sadek Molecules 13, 2908-2914 (2008).
15. Thomas W, Chem. Rev. **99**, 2071- (1999).
16. Zhao D, Wu M, Kou Y and Min K, Catal. Today **1**, 2654 (2002).
17. J. Peng and Y. Deng, Tetrahedron Lett. **42**, 403- (2001).
18. D. G. Gu, S. J. Ji, Z. Q. Jiang, M. F. Zhou and T. P. Loh, Synlett, **6**, 959- (2005).
19. H. Hagiwara, M. Seklfuji, T. Hoshi, K. Qiao and C. Yokoyma, Synlett, **8**, 1320- (2007).
20. K. Gong, Z. W. He, Y. Xu, D. Fang and Z. L. Liu, Monatsh. Chem., **139**, 913- (2008).

Recent Advances Ingreen Synthesis of Nanoparticles Using Plant Extracts and Their Biologicalactivity

D.T. Sakhare

U.G, P.G. & Research Centre, Department of Chemistry, Shivaji, Art's, Comm. & Science College Kannad.Dist. Aurangabad.431103, (M.S.) India.

E-mail- sakharedhondiram@yahoo.com

Abstract:

Nanoparticles (NPs) are elements derived from a cluster of atoms with one or moredimensions in the nanometer scale in the range of 1–100 nm. The bio nanofabrication of metallicNPs is now an important dynamic area of research, with major significance in applied research.Biogenic synthesis of NPs is more desirable than physical and chemical synthesis due to its ecofriendliness, non-toxicity, lower energy consumption, and multifunctional nature. Plants outperformmicroorganisms as reducing agents as they contain large secondary biomolecules that acceleratethe reduction and stability of the NPs. The produced NPs can then be studied spectroscopically(UV-Visible, XRD, Raman, IR, etc.) and microscopically (SEM, TEM, AFM, etc.). The biologicalreduction of a metallic ion or its oxide to a nanoparticle is quick, simple, and may be scaled upat room temperature and pressure. The rise in multi-drug resistant (MDR) microbes due to theimmoderate use of antibiotics in non-infected patients is a major cause of morbidity and mortality inhumans. The contemporary development of a new class of antibiotics with different mechanismsof action to kill microbes is crucial. Metals and their oxides are extremely toxic to microbes atunprecedentedly low concentrations. In addition, prevailing infections in plants and animals areraising significant concerns across the globe. NPs' wide range of bioactivity makes them idealantimicrobial agents in agricultural and medical fields. The present review outlines the synthesis ofmetallic NPs from botanicals, which enables the metals to be in a stabilized form even after ionization.It also presents a valuable database on the biofunctionalization of synthesized NPs for further drugdevelopment.

Keywords: Plant-mediatedGreen synthesis, Metallic Nanoparticles, Bio-functional, Antimicrobial activity.

1. Introduction:

Nanotechnology is a fast-expanding and multidisciplinary field with many applications in science and technology [1]. This field combines key concepts from a variety of disciplines, including chemistry, engineering, physics, and biology, in order to provide novel methods for controlling and generating nanoparticles (NPs). These NPs are particles with at least one dimension ranging from 1–100 nm. Nanotechnology deals with the synthesis, characterization, and applications of a variety of NPs. Noble metals, such as gold, silver, or platinum, are commonly used to synthesize NPs by a variety of chemical and physical techniques; however, these processes are not ecologically friendly [2].There is a pressing need to develop a non-toxic, environmentally friendly NPs production technology. Several safe, easy, cost-effective, reproducible, and scalable green synthesis approaches for NPs have been developed in recent years, inspired by the safety-by-design concept. As a result, several biological systems, such as yeast, fungus, bacteria, and plant extracts, are currently extensively employed in green synthesis approaches for the generation of NPs [3]. Plant-based NP green synthesis is now regarded as a gold standard among these green biological techniques owing to its ease of use and the diversity

of plants.This work serves both as editorial for the present Special Issue, composed of two reviews and sixteen research articles, as well as a brief overview of current trends in green synthesis, characterization, and applications of a range of plant-derived NPs.

Green nanotechnology is the perfect solution to decrease the negative effects of the production and application of nanomaterials, lowering the nanotechnology riskiness [1]. Figure 1 shows the key merits of green synthesis.
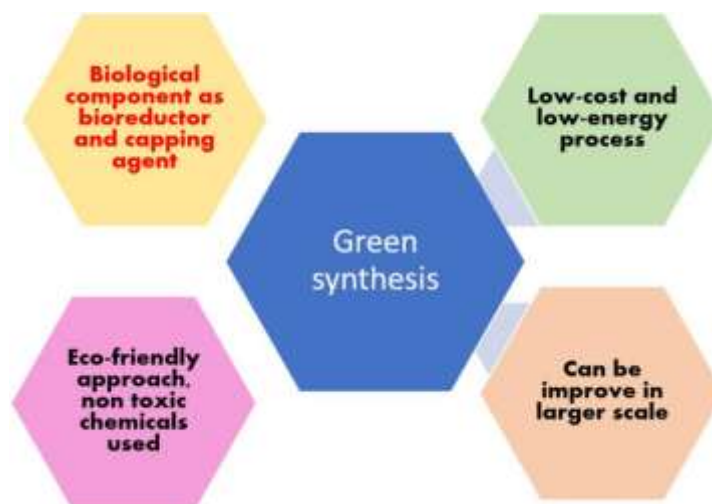

Figure 1: Key merits of green synthesis

The generation of engineered nanomaterials represents an essential breakthrough in nanotechnology and materials science. The real world should be created by moving these products beyond the laboratory. More than thousands of such products are available in the market, of which a large majority are integrated in everyday personal care products, cosmetics, and clothing. Development of the modern products that consumers need are expected to affect positively almost every industrial and production sectors, involving medicine and drug delivery. The continuous growth of the nanomaterials marketing and nano-assisted device is very obvious [4. The commercialization of successful disruptive technologies is fundamental for numerous implementations to humans and global development, but critical interest is necessary for potential, health assessment and environmental effects of these materials [5]. It is a clear reality that the health hazards due to nanoparticles exposure are slowly comprehended and need to be addressed rapidly and their manufacture and utilization are practically uncontrolled, particularly in the universe development. This is predominately discouraging when the new nano-based entities are being generated and incorporated into consumer products at an alarmingly quick rate, thus oversight mechanisms is an urgent need since the final existence of the majority of the nanotechnology innovations resulted from the research groups which considered simple startup work must based on instructions and recommendation from regulatory bodies and should not be oppositely affected by the boosted cost loads connected with such increased oversight [6]. Health and safety regulations will have to carefully negotiate regulatory testing cost load, which will in turn have an essential role in giving priority to hazards associated with nanomaterials [7]. The essential aspect of the green chemistry emerging sector is the utilization of a group of basics lowers or removes the hazardous substances utilization or generation concerning design or production and chemical products' application while designing new chemical processes visualizes small risk as the execution criteria.

Green chemistry basics implementation in the new materials expansion and enforcements is all the more considerable in opinion of the principle that the technology is an early expansion phase and is foreseeable to be widely utilized and doled out around the world. The strong relation between chemical structure and function groups that connects specifically to nanomaterials and boosting understanding "key" information for life cycle evaluation of such methods could lead to new "design principles" for the production of high rendering nanoscale materials that are benign and environmentally friendly [8].

The molecules, cells, and organs of the aforementioned plants have been bioengineered to provide new nanomaterials with demanding sustainable advantages. Green nanotechnology gives us the chance to prevent the negative effects. Green nanotechnology has an enterprising effect on the nanomaterials or the products design by removing or lowering pollution, which means that it remediates the existing environmental problems, as indicated in Figure 2.
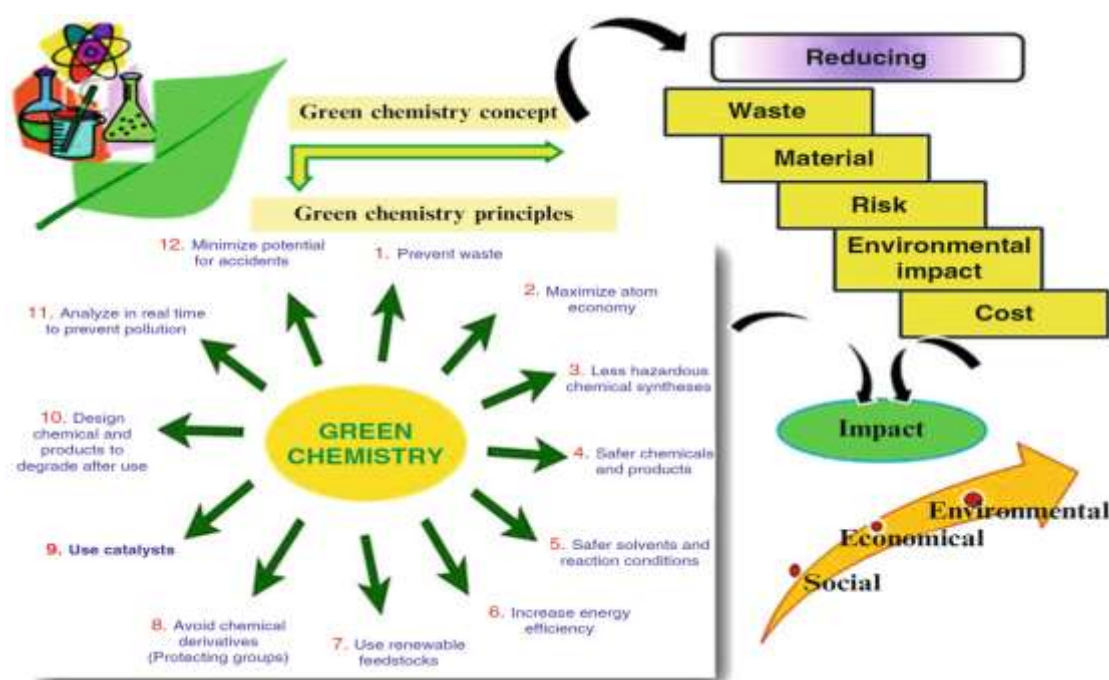
Figure 2: Schematic exemplifification of green chemistry combination in metal nanomaterials cloning

The environmental friendly methods such as catalytic potential, electrical conductivity, optical sensitivity, magnetic behavior or biological reactivity are used to characterize the chemical, physical, and biological properties of nanomaterials in addition to many factors such as size, shape, surface charge, chemical structure, surface area, and coagulation properties of nanoscale distinct materials. The organic solvents and chemical reagents are not used in the preparation of metal nanoparticles (MNPs). MNPs have unique properties with their nanostructures [9]. The atoms ordered to the nano-scale differ from the bulk metallic materials and the unique properties of MNPs and metal oxide nanoparticles (MONPs) are engendered from them. MNPs and MONPs have many applications such as catalysts drug delivery systems boosting contrast agent active food packaging materials components pointing to nano-biosensor construction gene transfer system antibiotics, antiseptics, and disinfectants to control pathogens and pests and nanoelectronic components [10].

2. Synthesis of Nanoparticle:

2.1. Perspectives of Nanoparticle Synthesis:

The methodology for making ultrafine NPs from ancient times is generally by the breakdown (top-down), and the build-up (bottom-up) approaches, as illustrated in Figure 3. The breakdown approach of NP synthesis is usually employed during NPs' physical and chemical synthesis. The size reduction of bulk material is used as a precursor ultimately to the nanosize by applying physical forces such as grinding, pulverization, etc., in the break down method which is also sometimes called the mechanochemical method [11]. It is challenging to obtain NPs by applying physical forces; usually, microparticles are easily obtained of 3 µm size, which is not significant. The second approach for obtaining NPs is by the build-up process; where major preparation methods for the synthesis of NPs can be achieved in two states of matter, liquid phase and solid phase, without any hazardous chemicals in biogenic synthesis, and remarkable increased use of chemicals in chemicalsynthesis are used. Biogenic synthesis of NPs falls under the bottom-up approach, where the uses of the biological system or its parts can be seen in the synthesis. To select the best organisms or extracts, one must evaluate their specific properties such as biochemical pathways, phytochemical contents, enzyme activities, cell growth circumstances, and ideal reaction [12]
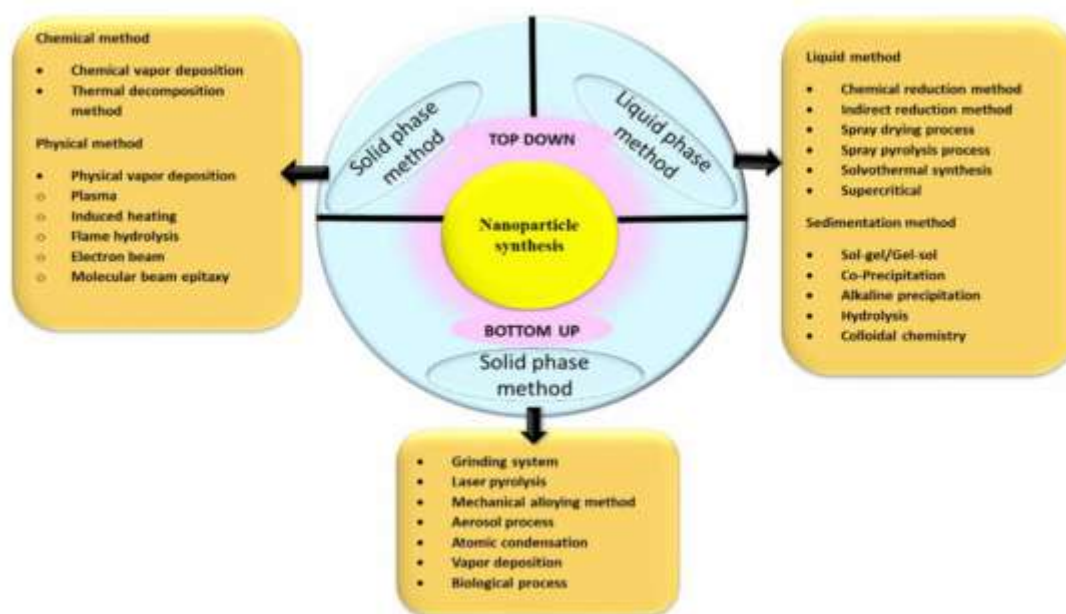
Figure 3. Various approaches for the synthesis of NPs

2.2. Secondary Biomolecules for Capping and Stabilization:

Plant extract not only acts as a reductant but also functions as a capping and stabilizing agent, as depicted in Figure 4.Prediction of biomolecules acting as capping and stabilizing agents was realistic when IR spectrum of tea extract showed the involvement of polyphenols, carboxylic acid, polysaccharide, amino acid, and proteins when coordinated with FTIR analysis. Zinc oxide NPs [ZnO NPs] showed peaks in 682–457 cm^{-1}, indicating the presence of a higher percentage of phenolics. The stability studies of silver NPs (Ag NPs) synthesized from Ziziphora tenuior extract at room temperature revealed that bionanofabrication of Ag NPs was due to some metabolite functional groups such as amines, alcohols, ketones, aldehydes, and carboxylic acid. A peak graph of FTIR between the treated and untreated sample showed significant changes and predicted amide group form of proteins possibly be the covering layer of metal NPs [13]. The

FTIR peak stretches in the OH, CH, C=C ring, and CH2 wagging of ascorbic acid indicated that Hibiscus cannabis extract comprises ascorbic acid responsible for reducing Ag NPs. The ferric chloride test of coconut shell extract revealed the presence of phenolic compounds; most importantly, benzoquinone yielded the formation of Au NPs. Calotropis gigantea, a large shrub, consists of phytoconstituents such as cardiac glycosides, β-sitosterol, saponins, alkaloids, tannins, trisaccharides, and flavanols FTIR spectra denote the interactions of the biomolecules with Ag NPs [14].

Figure 4. Biological reduction of NPs.

3. Green Synthesis and Characterization of Plant-Derived NPs:

During the last decade, the concept of "Green Chemistry" for "Sustainable Development" has been widely investigated. Sustainable development is described as development that meets the current demands while also b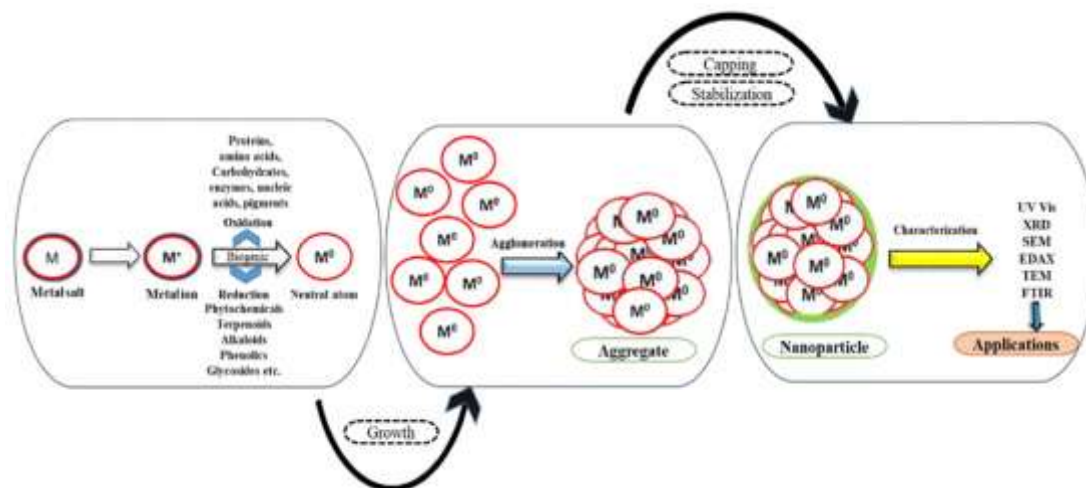alancing the ability of future generations to satisfy their needs. Due to its concern with the evidence of pollution and the indiscriminate use of natural resources, sustainable development is especially important for various chemistry-based sectors. The selection of a green or environmentally friendly solvent (the most widely used are water, ethanol, and their mixtures), a suitable non-toxic reducing agent, and a safe substance for stabilization are the three most important requirements for the green synthesis of NPs. Indeed, extensive synthetic pathways have been used to produce nanoparticles, with physical, chemical, and biosynthetic routes being the most popular. Chemical procedures are generally excessively costly and involve the use of toxic and hazardous chemicals that entail a variety of environmental risks [15]. In contrast, green synthesis is a safe, biocompatible, and environmentally friendly green method of synthesizing NPs for various applications, including biomedical uses. Fungi, algae, bacteria, and plants have been used to carry out this green synthesis. However, plant components, including leaves, fruits, roots, stems, and seeds, have been widely utilized to synthesize different NPs. Indeed, plant extracts have the ability to produce NPs with defined size, shape, and composition. Furthermore, the presence of a wide array of phytochemicals in their extract may function as natural stabilizing and/or reducing agents for NPs production. It is accepted that plant-derived NPs are also less likely to cause harmful side effects in humans when compared to chemically synthesized NPs, and exhibit a high biological potential with applications in agriculture, food science and technology, bioengineering, cosmetic or nanomedicine, and human health protection. It is essential that these NPs be precisely and thoroughly characterized in order to ensure reproducibility in their production, biological activity, and safety. For this purpose, a wide range

of physicochemical methods are used to very precisely characterized the synthesized NPs including ultraviolet-visible spectroscopy, Fourier transform infrared spectroscopy (FTIR), attenuated total reflection (ATR), Raman spectroscopy, photoluminescence analysis (PL), dynamic light scattering (DLS), UV-visible diffuse reflectance spectroscopy (UV-DRS), transmission electron microscopy (TEM), scanning electron microscopy (SEM), atomic force microscopy (AFM), field emission scanning electron microscopy (FE-SEM), X-ray diffractometer (XRD), X-ray photoelectron microscopy (XPS), energy dispersion analysis of X-ray (EDAX), thermal gravimetric differential thermal analysis (TG-DTA), or nuclear magnetic resonance (NMR) [16].

Table 1. Bio-reduction of platinum group NPs and their bioactivity.

Sr. No.	Botanical Names of Plants	Part Used	Size Range (nm) (SEM/TEM)	Characterization Tools	Bio-Functionalization
Platinum NPs					
1.	*Diospyros kaki*	Leaves	2–12	UV-Vis, XRS, FT-IR, HRTEM	• NR
2.	*Lantana camara* (L.)	Leaves	35	UV-Vis, RS, PSD, DLS, EDAX, XRD, FT-IR, SEM	• NR
Palladium NPs					
1.	*Sapium sebiferum*	Leaves	2–12	UV-Vis	• Antibacterial
2.	*Moringa oleifera*	Leaves	35	UV-Vis, RS, PSD, DLS, EDAX, XRD, FT-IR, SEM	• Antibacterial • Antioxidant • Anticancer

Note: NR = Not reported.

4. An Overview of the Different Types of Plant-Derived NPs:

Different types of plant-derived NPs are presented, and their synthesis, characterization, and applications are discussed and published in this Special Issue.Plant-based silver nanoparticles (AgNPs) are among the easiest to prepare.For the green synthesis of silver nanoparticles, a silver metal ion solution and a reducing biological agent are required. The easiest and least expensive method for producing AgNPs is to reduce and stabilize Ag ions using a mixture of biomolecules, such as polysaccharides, vitamins, amino acids, proteins, phenolics, saponins, alkaloids, and/or terpenes [17].

Almost all plants have the potential to be exploited to prepare AgNPs. Gold nanoparticles (AuNPs) have received tremendous attention because of their facile synthesis, easy surface functionalization, and unique characteristics, such as their high potential for use in medicine , low toxicity and highly biocompatible nature. Various chemical moieties in biogenic complexes operate as reducing agents in the production of gold nanoparticles, resulting in the reduction of gold metal ions and the formation of nanoparticles. Some studies have revealed that biomolecules, such as flavonoids, phenols, protein, and others, have an important role in the reduction of metal ions and the topping of gold nanoparticles in plant extracts [18].

Zinc oxide nanoparticles (ZnONPs) have received considerable attention over the last years because of their wide array of potential applications in biomedicine, cosmetic, optics, and electronics. Thus far, several investigations on the synthesis and utilization of ZnONPs by plants, microorganisms, and other species have been reported. Many studies have raised interest in their

low-cost, safe, and simple synthesis. ZnONPs may be made from a variety of plant components, including flowers, roots, seeds, and leaves. Remarkably, these nanoparticles exhibit a high exciton binding energy of 60 meV and a huge bandgap of 3.37 eV, giving them a wide range of semiconducting properties [19].

Copper (Cu) is a comparatively low-cost metal that is more cost-effective than Au and Ag, and CuNPs have been synthesized by the reduction of aqueous Cu ions by different plant extracts. The existence of a 578-nm peak on a UV-visible spectrometer, in particular, confirms their formation. However, numerous questions about their biosafety persist. Other metals, such as nickel (Ni) or manganese (Mn), are also presented. Note that some additional metals, such as titanium (Ti), palladium (Pd), cerium (Ce), or platinum (Pt), have lately been employed to prepare plant-based NPs with various biomedical or industrial applications [20].

5. Biological Activity of Nanoparticles:

5.1. Anti-Cancer Activity:

Nanomedicine is the use of nanotechnology in the treatment, screening, and diagnosis of a variety of diseases, including cancer. It adds complete procedures and effective approaches against cancer through cancer prediction and diagnostics, prevention and medication, as well as possible individualized therapy. Many plant-derived NPs have shown some potential against cancer cells. ZnONPs produced from a Cassia auriculata leaf extract, in particular, has shown tumoricidal activity against MCF-7 breast cancer cells while having no detrimental effect on normal MCF-12A human breast cells [21]. Similarly, green AuNPs produced from a Trachyspermum ammi seed extract inhibited cellular growth in HepG2 cancer cell lines in a concentration-dependent manner, which was linked to a reactive oxygen species (ROS)-driven apoptosis. This mechanism has recently been reported to be potentially connected to mitochondrial action via ROS-induced Caspase-3 gene expression and enzyme activity following mitochondrial membrane potential disruption caused by plant-based NPs [22].

However, in addition to a deeper understanding of the molecular mechanism of action of NPs against cancer cells, there is also a need to properly understand the fate of NPs.

These questions include how long NPs stay in the body, what conditions influence the duration of NP degradation, how to make NPs stay for longer or shorter periods, what are the long-term and short-term effects of NPs, how the body behaves towards these outsider entities on a micro and macro level, and how we can standardize NPs to ensure experiment reproducibility. These should be solved before introducing nanotechnologies into the healthcare industry. Aside from this, there are several questions that require further research and testing. In order to avoid any unanticipated consequences, we must also determine the possible risks linked with these nanomaterials. Furthermore, in order to obtain the safest and most successful therapy regimen, the numerous nanomedicines and nanoformulations targeting specific cancer cells must be thoroughly constructed. We conclude with the hope that nanotechnology will propel the development of more viable medicines to treat cancer, as well as offer researchers with powerful tools to overcome several bottlenecks in this health sector.

5.2. Anti-Leishmanial Activity:

Leishmaniasis is a protozoan vector-borne illness that affects almost 350 million people worldwide. Chemotherapeutic medicines were initially used to treat leishmaniasis, but they had adverse side effects. Due to their unique properties, such as bioavailability, reduced toxicity, targeted drug delivery, and biodegradability, a variety of nanotechnology-based techniques and

products have emerged as anti-leishmanial drugs, including liposomes, lipid nano-capsules, metal and metallic oxide nanoparticles, polymeric nanoparticles, nanotubes, and nanovaccines. AgNPs containing xylan (also known as nanoxylan) synthesized in a green synthesis route with corncob xylan as a reducing and stabilizing agent demonstrated effective inhibitory activity against Leishmania amazonensis promastigote viability, whereas xylan alone had no effect. This work nicely illustrates the potential of the nanoxylan as a promising new type of antiparasitic agent [23].

5.3. Antimicrobial Activity:

Antibiotic resistance is one of the most pressing issues of recent years, and it is only going to become worse. Bacteria have developed resistance to antimicrobial agents as a result of the rapid evolution of the bacterial genome. Thus, in the search for a new therapy, biogenic NPs have shown encouraging results in the treatment of multidrug-resistant bacteria and might be a potential choice in the fight against such resistant pathogenesis [24]. To improve the antimicrobial response, NPs and other conjugates have been combined with different organic and inorganic compounds. Ag has long been known for its antibacterial properties against a variety of bacterial strains. In particular, green AgNPs prepared from a Carissa carandas leaf extract demonstrated antibacterial efficacy against a variety of human pathogenic bacteria, with Gram-negative bacteria, particularly Shigella flexineri responsible for shigellosis, being more likely to be inhibited [25]. Similarly, bimetallic nanostructures coated with reduced graphene oxide generated from a stevia leaf extract, such as Pd-Ag nanostructures, can limit the development of Gram-negative bacteria Escherichia coli. AgNPs obtained from the Saudi Arabian desert plant Sisymbrium irio showed potent inhibition potential against multidrug-resistant Pseudomonas aeruginosa and Acinetobacter baumanii that are responsible for ventilator-associated pneumonia. Furthermore, antifungal activity of nanoxylan derived from corncob xylan against Candida albicans, Candida parapsilosis, and Cryptococcus neoformans has been described, whereas AgNPs obtained from the leaf extract of Clerodendrum inerme showed a dual antibacterial and antifungal actions against a wide range of human pathogenic strains [26].Interestingly, AuNPs produced from the same C. inerme extract also showed very similar inhibition capacity. The authors concluded that these NPs may have improved antimicrobial activity due to the synergistic effect of biologically active absorbed phytochemicals from this plant [26]. Antibiofilm action of AuNPs produced from a T. amni seed extract was also observed against Listeria monocytogenes and Serratia marcescens, most likely as a result of intracellular ROS production. ZnONPs also showed potential antimicrobial activity as evidenced by the action of ZnONPs derived from a Cinnamomum verum bark extract against E. coli and Staphylococcus aureus. Similarly, ZnONPs derived from a C. auriculata leaf extract exhibited antibacterial activity due to direct cell contact, which disrupted bacterial cell integrity [27].

Other metallic NPs, such as CuONPs derived from Cymbopogon citratus, can exhibit significant antimicrobial activity, including antibiofilm properties. Interestingly, these authors noted a variation in antibiofilm activity, which they suspect is due to differences in the cell wall compositions of the examined bacterial strains. MnONPs derived from an Abutilon indicum leaf extract demonstrated potent antibacterial activity against both Gram-negative and Gram-positive bacteria, whereas NiONPs deriving from stevia leaf extract were more effective against Gram-negative bacteria [28]. This shows that antimicrobial activity is influenced by the type of NPs produced, but also the composition of the coated phytochemicals on their surfaces, which is

affected by the plant extract used for NPs synthesis. Cell wall disruption, cell membrane disintegration, massive free radical production, specific (targeted) and/or specific actions against proteins, DNA fragmentation, vital enzyme inhibition, loss of cellular fluids, and disruption in electron transport have all been proposed as possible mechanisms for NPs antibacterial activity. Bio-mediated NPs might also have an antifungal effect by causing excessive ROS generation. However, few studies have focused only on fungus as of yet [20]. Despite advances in understanding of the antimicrobial efficacy of plant-based NPs, much remains unclear regarding their specific mechanism of action, toxicity, and possible environmental issues.

5.4. Antioxidant Activity:

Excessive oxidative stress generated by the action of mitochondria and other internal or external sources may result in oxidative damages to various cell macromolecules (membrane lipids, proteins, and DNA), leading to functional declines, degenerative diseases, and aging. Antioxidants may be able to reverse this detrimental process and may be used to treat aging and age-related diseases. Some green plant-derived NPs have been described for their antioxidant potential as shown for AgNPs produced from a C. carandas leaf extract, AuNPs and AgNPs deriving from a C. inerme leaf extract or NiONPs prepared from a stevia leaf extract [29]. The phytochemicals coated on the NPs surface have certainly a prominent influence in the observed antioxidant action. Commonly, just one in vitro assay, such as the DPPH (2,2-diphenyl-1-picrylhydrazyl) assay, is performed. However, due to the complex nature of phytochemicals, and in particular, because the determination of antioxidant activity is significantly reliant on the reaction mechanism involved, antioxidant activity of should not be measured using a single approach [30]. Therefore, the validity of the results from in vitro cell-free antioxidant tests must be restricted to the interpretation in terms of chemical reactivity, but in vivo (cellular) validation is strongly required.

5.5 Anti-inflflammatory Activity:

Nanoparticles have been developed as anti-inflammatory mediators in recent years. NPs have a large surface-area-to-volume ratio and are used for obstructing substances accompanying inflammation such as cytokines and inflammation-supporting enzymes, associated with other complements. Numerous metal-based NPs have been reported with excellent anti-inflammatory properties, such as those based on silver, gold, copper, and iron oxide. In this review, we demonstrate the mechanism for constructing anti- inflammatory properties in NPs. Figure 5 depicts the mechanism of nanoparticles in anti-inflammatory systems. Swelling is the body's instant response to interior damage, contagion, hormone inequity, and failure in the interior structures or external features, such as in an attack by pathogenic microorganisms or an external element. This leads to overweight, food allergies, or interactions with ecological contagions. Distinctive resistant cells possess antigen receptors capable of sensing biochemical signs. Swelling is caused by cellular and tissue injury resulting from an imbalance in the signals controlling the inflammation [31]. Upon injury or infection, muscles invoke an inflammatory response that leads to the deployment of macrophages and killer cells,
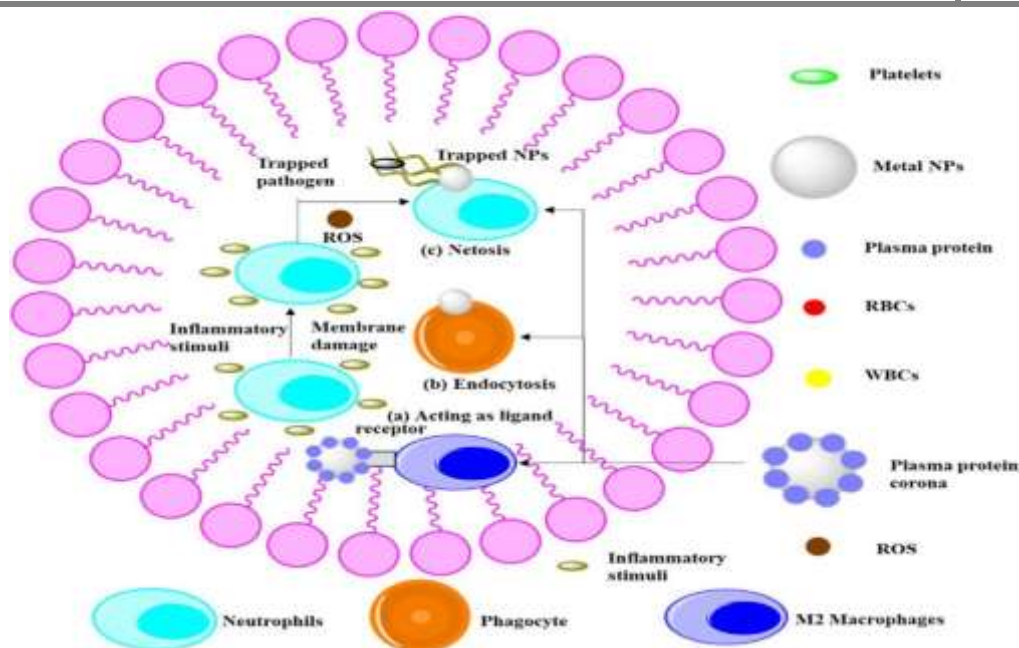
Figure 5. Anti-inflflammatory mechanism adopted by various nanoparticles.

6. Applications of Nanoparticles:

NPs possess tremendous advantages for use in many areas of day-to-day activities.Therefore, it is important to explore NPs in depth. Figure 6 shows a schematic representation of nanoparticle synthesis methods and the applications of NPs discussed in this review. NPs for use in the human body include biosynthesized noble metal NPs, which have many important applications. They make use of the molecular engine to address medicinal difficulties, and molecular information is used to support and advance human fitness at the molecular scale. This leads to the protection and development of human health. Fernández-Llamosas biosynthesized selenium NPs, which have many benefits for human health, using *Azoarcus sp. CIB*, [32]. The classification of different nanoparticle synthesis methods and their applications is depicted in Figure 6.

Figure 6. Applications of Nanoparticles

6.1. Agricultural Applications:

When agricultural pathogens are targeted, the antimicrobial activity outlined in the previous Section may be effective for crop protection. In particular, ZnONPs have demonstrated their wide agricultural interest showing an anti-phytopathogenic action against both bacteria as evidenced by ZnONPs derived from lemon fruit against soft rot bacteria pathogen Dickeya dadantii and fungi as illustrated by the fungicidal activity of ZnONPs produced using a Eucalyptus globules extract against major pathogens of apple orchards. It is noteworthy that TiO2NPs produced from lemon fruit showed antibacterial activity comparable to ZnONPs against D. dadantii [33]. Through modifying abscisic acid concentration, ion homeostasis, and defense mechanisms comprising both enzymatic and non-enzymatic antioxidants, AgNPs synthesized from a wheat extract significantly contributed to alleviate the negative effects of salinity stress in wheat. Interestingly, ZnONPs exhibited low toxicity and the capacity to stimulate the antioxidant response of flax seedlings as well [34].

6.2. An Overview of the Potential Applications of Plant-Derived NPs:

NPs are currently in high demand commercially due to their wide range of applications in industries, electronics, environment, energy, and more particularly in biomedical fields. NPs, such as the most commonly known Ag and Au NPs, have been widely explored in this sector and are of tremendous interest for biological applications. In general, plant-derived green NPs are also less likely to cause severe side effects in humans when compared to chemically synthesized NPs, and have a great application potential with applications in a variety of areas, including but not limited to:

- Nanomedicine and human health protection (antimicrobial, antiparasitic, antiproliferative, pro-apoptotic, pro- or anti-oxidative depending on the context, anti-inflammatory activities, etc.) [35];

- Agriculture (precision farming with controlled release of agrochemicals, target-specific delivery of biomolecules, more efficient nutrients absorption, detection and control of plant diseases, etc.) [36];

- Food science and technology (processing, storage, and packaging processes), in bioengineering (biocatalysts, photocatalysts, biosensors, etc.) [37];

- Cosmetics (sunscreen, anti-aging, hair growth, bioactive compounds delivery, nanoemulsion, etc.) [38].

With two review papers dealing with algae-based NPs synthesis and CuNPs, the current Special Issue sheds light on two less investigated tools and methodologies of green plant-based nanotechnology [39].

Algae are definitely ideal candidates for the green synthesis of NPs because they are rich in secondary metabolites that act as reducing and capping agents. Many potential

applications have been already described including antimicrobial or anticancer actions,

but also as antifouling, bioremediation or biosensing agents. However, unlike terrestrial medicinal and aromatic plants, algae were underutilized in the beginning of studies on the green synthesis of NPs using plant extracts. As this sector is still in its onset, scaling up for commercial applications is still challenging [39]. Cu is a relatively low-cost metal that is for example more cost-effective than Au and Ag. CuNPs have been produced via the reduction of aqueous Cu ions by various plant extracts.

The review by Letchumanan et al. [40] provides a very comprehensive overview and current update of plant-mediated Cu/CuO (Cu oxide) NPs, covering their synthesis, therapeutic uses, and mechanisms. Although Cu/CuO NPs have a variety of therapeutic benefits, their toxicity to normal cells and important organs in humans might have significant adverse effects. As a result, prior to the use of these NPs in medicine, this potential toxic issue should be extensively examined. The toxicity of these NPs, as well as their effectiveness in comparison to commercial NPs in both in vitro and in vivo research, are reviewed and discussed [40]. This review also sheds light on the future prospects for producing plantbased Cu/CuO NPs as a therapeutic agent for a variety of diseases (including microbial infection, cancer, wounding, or inflammation) [40].

6.3. Other Applications:

Other potential applications, such as (photo)catalytic and/or absorption potential applications, are also described. AgNPs produced by Matricaria chamomilla showed effective catalytic activity against Rhodamine B under UV light, which could make it a promising material for wastewater treatment. MnONPs produced from an Abutilon indicum leaf extract has shown efficient absorption activity against the heavy metal CrVI as well as strong photocatalytic activity, indicating the potential to remediate various organic and inorganic contaminants. Finally, the photocatalytic H2 production, mediated by Pd-Ag bimetallic nanostructures coated with reduced graphene oxide produced from a stevia leaf extract, can be noted [41].

7. Conclusions and Future Directions:

The growing demand for green chemistry and nanotechnology has pushed for the development of green synthetic methods for the production of nanomaterials using plants, microbes, and other natural resources. Researchers have been focusing on the green synthesis of NPs, using an environmentally favorable technique. Due to their cost-effectiveness, nontoxic approach, simple availability, and ecofriendly nature, considerable research has been conducted on plant extract-mediated NPs production and their prospective uses in numerous industries. Plants have a variety of unique compounds that help in the synthesis process and accelerate the synthesis kinetic. The use of plants for green nanoparticle synthesis is an interesting and emerging aspect of nanotechnology that has a significant impact on the environment and contributes to nanoscience's long-term sustainability and progress. Catalysis, medicine, cosmetic, agriculture, food packaging, water treatment, dye degradation, textile engineering, bioengineering sciences, sensors, imaging, biotechnology, electronics, optics, and other biological sectors are just some of the potential applications of these green plant-based NPs. These NPs might be the future impetus for the biomedical field in the drug delivery system. These green NPs might be also employed in a variety of ways, including phytopathogen treatment in agriculture or water disinfection for environmental cleanup. This green approach of NPs synthesis is becoming more popular and is expected to develop exponentially in the future; nevertheless, long-term impacts on animals and humans, as well as the accumulation of these NPs in the environment and their influence, must be addressed in the future. This Special Issue gathered cutting-edge research and review articles on the plant-based green synthesis of NPs, their production, characterization, and applications, with the goal of providing the most comprehensive overview of all these features and future challenges.

References:

1. D. T. Sakhare, Green Synthesis of Nanoparticles from Plant Extracts With Antiviral, Antioxidant and Antimicrobial Activity, Journal of Xi'an University of Architecture & Technology, 14(3),2022, 169-192.

2. D. T. Sakhare, Green Synthesis of Silver Nanoparticles from Sarcopharyngia ventricosa , Journal of Cardiovascular Disease Research , 2023, 14(8),2023, 2315-2329.

3. C.G. Sayes Reátegui, H. H. Nora And H. Emily, Synthesis of Silver Nanoparticles From Extract And Ethanolic And Aqueous Fractions of Leaves And Petals of Hibiscus Rosa-Sinensis L., J. Chil. Chem. Soc., 67, N3, 2022, 5595-5601.

4. D.T. Sakhare, Green Synthesis, Characterization and Biomedical Applications of Zn and ZnO Nanoparticles, Elixir Appl. Chem., 145(2020) 54666-54675.

5. A.Krishnasamy, M.Sundaresan, P.Velan, Rapid phytosynthesis of nano-sized titanium using leaf extract of Azadirachta indica. Int. J. Chem Tech Res. 8,2015, 2047–2052.

6. Monica JC, Heintz ME, Lewis PT. The perils of pre-emptive regulation. Nat Nanotechnol. 2007;2:68–70.

7. Owen R, Handy R. Viewpoint: formulating the problems for environmental risk assessment of nanomaterials. Env Sci Technol. 2007;41:5582–8.

8. Rajender SV. Greener approach to nanomaterials and their sustainable applications. Curr Op Chem Eng. 2012;1(2):123–8.

9. Raveendran P, Fu J, Wallen SL. Completely "Green" synthesis and stabilization of metal nanoparticles. J Am Chem Soc.2003;125(46):13940–1.

10. Wiederrecht GP, Wurtz GA, Hranisavljevic J. Coherent coupling of molecular excitons to electronic polarizations of noble metal nanoparticles. Nano Lett. 2004;4(11):2121–5.

11. Jamkhande, P.G.; Ghule, N.W.; Bamer, A.H.; Kalaskar, M.G. Metal nanoparticles synthesis: An overview on methods of preparation, advantages and disadvantages, and applications. J. Drug Deliv. Sci. Technol. 2019, 53, 101174.

12. Jayaseelan, C.; Ramkumar, R.; Rahuman, A.A.; Perumal, P. Green synthesis of gold nanoparticles using seed aqueous extract of Abelmoschus esculentus and its antifungal activity. Ind. Crops Prod. 2013, 45, 423–429.

13. D.T. Sakhare, Green Approach To Synthesis, Characterization of Silver Nanoparticles By Using Tridax Procumbens Leaf Extract And Their Antibacterial Activity, InternationalJournal of Food And Nutrition Science, 2022, 11(11),2022,126-133.

14. Mathew, S.; Victorio, C.P.; Sidhi, J.; Thanzeela, B.H.B. Biosynthesis of silver nanoparticle using flowers of Calotropis gigantea (L.) WT Aiton and activity against pathogenic bacteria. Arab. J. Chem. 2020, 13, 9139–9144.

15. Nath, D.; Banerjee, P. Green nanotechnology—A new hope for medical biology. Environ. Toxicol. Pharmacol. 2013, 36, 997–1014.

16. D.T. Sakhare, Green Synthesis ofNanoparticles from Plant Extracts With Antiviral, Antioxidant and Antimicrobial Activity.Journal of Xi'an University of Architecture & Technology, 2022,14(3),2022, 169-192.

17. Tolaymat, T.M.; El Badawy, A.M.; Genaidy, A.; Scheckel, K.G.; Luxton, T.P.; Suidan, M. An evidence-based environmental perspective of manufactured silver nanoparticle in syntheses and applications: A systematic review peed critical appraisal of peer-reviewed scientific papers. Sci. Total Environ. 2010, 408, 999–1006.

18. Jeong, S.; Choi, S.Y.; Lee, S.Y. Low-toxicity chitosan gold nanoparticles for small hairpin RNA delivery in human lung adenocarcinoma cells. J. Mater. Chem. 2011, 21, 13853–13859.

19. Ansari, M.A.; Murali,; Singh, S.B.; Asiri, S.M.M.; Ashwini, B.S.; et al. Cinnamomum verum Bark Extract Mediated Green Synthesis of ZnO Nanoparticles and Their Antibacterial Potentiality. Biomolecules 2020, 10, 336.

20. D.T. Sakhare, Green Synthesis, Characterization, Antimicrobial Activity and Applications of Cu, and CuO Nanoparticles, International Journal of Scientific & Engineering Research, 2020,Volume 11, Issue 6PP.1471-1499

21. Prasad, K.S.; Prasad, S.K.; Ansari, M.A.; Ankegowda, V.M.; Shivamallu, C. Tumoricidal and Bactericidal Properties of ZnONPs Synthesized Using Cassia auriculata Leaf Extract. Biomolecules 2020, 10, 982.

22. Anjum, S.; Khan, A.K.; Qamar, A.; Fatima, N.; Hano, C. Light Tailoring:Impact of UV-C Irradiation on Biosynthesis, Physiognomies, and Clinical Activities of Morus macroura-Mediated Monometallic (Ag and ZnO) and Bimetallic (Ag–ZnO) Nanoparticles. Int. J. Mol. Sci. 2021, 22, 11294.

23. D,T, Sakhare, Green Chemistry and Sustainable Development, International Journal for Innovative Research Multidisciplinary field , 2020, Special Issue 21 PP. 196-202.

24. Nadeem, M.; Ahmad, W.; Zahir, A. The current trends in the green syntheses of titanium oxide nanoparticles and their applications. Green Chem. Lett. Rev. 2018, 11, 492–502.

25. Singh, R.; Hano, C.; Sharma, B. Green Biosynthesis of Silver Nanoparticles Using Leaf Extract of Carissa carandas L. and Their Antioxidant and Antimicrobial Activity against Human Pathogenic Bacteria. Biomolecules 2021, 11, 299.

26. Khan, S.A.; Lee, C.-S. Green Synthesis of Gold and Silver Nanoparticles Using Leaf Extract of Clerodendrum inerme;Characterization, Antimicrobial, and Antioxidant Activities. Biomolecules 2020, 10, 835.

27. D.T. Sakhare, Green Synthesis of Transition metal & Transitions metal oxides of Nanoparticles and their Antimicrobial Activity, Journal of Xi'an Shiyou University, Natural Science Edition, 2020, Volume 16 Issue 7, PP. 207-237

28. Srihasam, S.; Lebaka, V.R.; Mallem, S.P.R. Phytogenic Generation of NiO Nanoparticles Using Stevia Leaf Extract and Evaluation of Their In-Vitro Antioxidant and Antimicrobial Properties. Biomolecules 2020, 10, 89.

29. Razavi, M.; Tayebi, L. Green chemical and biological synthesis of nanoparticles and their biomedical applications. In Green Processes for Nanotechnology; Springer: Berlin/Heidelberg, Germany, 2015; pp. 207–235.

30. Tungmunnithum, D.; Drouet, S.; Kabra, A.; Hano, C. Enrichment in Antioxidant Flavonoids of Stamen Extracts from Nymphaea lotus L. Using Ultrasonic-Assisted Extraction and Macroporous Resin Adsorption. Antioxidants 2020, 9, 576.

31. Brenner, P.S.; Krakauer, T. Regulation of Inflammation: A Review of Recent Advances in Anti-Inflammatory Strategies. Curr. Med. Chem. Anti-Allergy Agents 2003, 2, 274–283.

32. Fernández-Llamosas, H.; Castro, L.; Blázquez, M.L.; Díaz, E.; Carmona, M. Biosynthesis of selenium nanoparticles by Azoarcus sp. CIB. Microb. Cell Factories 2016, 15, 109.

33. Hossain, A.; Abdallah, Y.; Wang, Y.; An, Q. Lemon-Fruit-Based Green Synthesis of Zinc Oxide Nanoparticles and Titanium Dioxide Nanoparticles against Soft Rot Bacterial Pathogen Dickeya dadantii. Biomolecules 2019, 9, 863.

34. D.T. Sakhare, Synthesis of Silver Nanoparticles from Medicinal Plants and its Biological Activities, Juni Khyat , 2020 Vol-10 Issue-7 No.4PP. 154-168.

35. Saleem, K.; Khursheed, Z.; Hano, C.; Anjum, I.; Anjum, S. Applications of Nanomaterials in Leishmaniasis: A Focus on Recent Advances and Challenges. Nanomaterials 2019, 9, 1749.

36. D.T. Sakhare, Green Synthesis, Characterization and Biomedical Applications of Zn and ZnO Nanoparticles,Elixir International Journal, 2020, Volume 145 PP. 54666-54675

37. Shafiq, M.; Anjum, S.; Hano, C.; Abbasi, B.H. An Overview of the Applications of Nanomaterials and Nanodevices in the Food Industry. Foods 2020, 9, 148.

38. Abbasi, B.H.; Fazal, H.; Ahmad, N.; Ali, M.; Giglioli-Guivarch, N.; Hano, C. Nanomaterials for Cosmeceuticals: Nanomaterials-Induced Advancement in Cosmetics, Challenges, and Opportunities; Elsevier: Amsterdam, The Netherlands, 2020; ISBN 9780128222867.

39. Chaudhary, R.; Nawaz, K.; Khan, A.K.; Hano, C.; Anjum, S. An Overview of the Algae-Mediated Biosynthesis of Nanoparticles and Their Biomedical Applications. Biomolecules 2020, 10, 1498.

40. D.T. Sakhare, Green synthesis, characterization and application of nanoparticles, International Journal of Creative Research Thoughts, 2020,Volume 8, Issue 6 PP. 2817-2829.

41. Mallikarjuna, K.; Nasif, O.; Ali Alharbi, S.; Chinni, S.V.; Sreeramanan, S. Phytogenic Synthesis of Pd-Ag/rGO Nanostructures Using Stevia Leaf Extract for Photocatalytic H2 Production and Antibacterial Studies. Biomolecules 2021, 11, 190.

Study of Acoustical Properties of Substitutedschiff Bases At different Concentrations in 75% (DCM–Water) Mixture At 303K. By Ultrasonic Technique

Ganesh Andhale1*, Prabhakar Kute2, Chandrashekhar Devkate3, Atish Mehetre4

1P. G. Department of Chemistry Jijamata Mahavidyalaya, Buldhana, Dist. Buldhana (M.S.)

2Department of Chemistry, PratishthanMahavidylaya, Paithan, Dist. Sambhaji Nagar (M.S.) 431107

3Indraraj Arts, commerce & Science College Sillod, Aurangabad 431112

4Department of Chemistry Shri Shivaji Arts, Commerce & Science College, Kannad, India.

ganeshandhale005@gmail.com

Abstract:

The study of interaction between solute-solute and solute-solvent interaction of substituted Schiff bases in 75% (DCM+water) mixture by measuring ultrasonic velocity and density in different concentration of solutein the range ($1x10^{-2}$ M to $6x10^{-4}$ M) in 75% of solvent has performed. In the present investigation, different acoustical parameters, such as ultrasonic velocity (U), adiabatic compressibility (βs), partial molal volume (φv), intermolecular free length (Lf), apparent molal compressibility (φκ), specific acoustic impedance (Z), relative association (RA), solvation number (Sn) of substituted Schiff bases in 75% of DCM+water mixture at 303K have been studied. From the experimental results, the effect of concentrationof solute on different acoustical parameters in DCM-water mixtures at a constant temperature has been studied.

Key words: Ultrasonic velocity, Density, acoustical parameters, substituted Schiff base.

Introduction:

The sound wave having frequency greater than human audible range (20 Hz to 20 KHz) is known as ultrasonic wave. When the ultrasonic waves travels through a medium, the molecule in the medium vibrate over very short distance in the direction parallel to the stationary wave. During this vibration, momentum is transferred among the molecules. This produces the wave to pass through the medium. In the recent years, the ultrasonic wave has many important practical applications for the study of properties and structure of matter in applied science.

In the field of medical science, the sound waves are being used for the diagnosis of joint pains[1], for elimination of kidney and bladder stones, for detection of bone fractures, cancer tumors, physiotherapy, bloodless surgery, cardiology[2-3], gynecology etc. Ultrasonic waves are also used for proper extraction of broken teeth, to restore the contracted fingers, for reliving neuralgic and rheumatic pains etc.

At present, the ultrasonic and absorption studies especially in case of electrolyte solutions have led to new insight into the process of ion-association and complex-formation[4-5]. Many researchers such as M.S. Chouhan[6], S. Sasikumar[7], Shashi Kant [8], T. Sumathi[9], Chandami A. S.[10] and Azhagiri S.[11]have made ultrasonic study of electrolytic solutions and discussed about the variation of ultrasonic velocity with ion concentration. It has already been observed that extent of a lowering of compressibility and an increase in ultrasonic velocity with reference to that of water are proportionate to the number of ions existing in that medium. Most of the ultrasonic work in non-aqueous systems possesses an interpretation of solute-solvent interactions[12].

Solvation numbers have been obtained from the study of non-aqueous solutions by K.Kannagi et.al.[13], Harish Kumar[14].

In the present investigation, study of the interaction between solute-solute and solute-solvent of substituted Schiffbases in 75%, (DCM+water) solvents by measuring ultrasonic velocity and density in different concentration of solute in different percentage of solvent has been done.Therefore keeping the importance of these parameters in mind, the present attempt is made to study adiabatic compressibility's, properties of substituted chalconeimine in different percentage of (DCM+water) mixture at different concentrations of ligand.
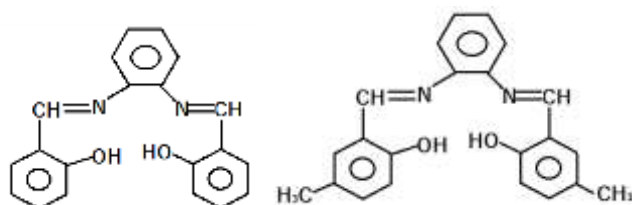
Ligand LALigand LB

Material and Method:

All the chemicals used were of AR grade. The density measurements were made with the precalibratedbicapillarypyknometer. All the weighing were made on one pan digital balance (petit balance AD-50B) with an accuracy of $\pm$ 0.001 gm.

The speed of sound waves was obtained by using variable path crystal interferrometer (Mittal Enterprises, Model F-81) with accuracy of $\pm$ 0.03% and frequency 2MHz.

Calculation:

The distance traveled by micrometer screw get one maximum in ammeter (D), from the value of D, wavelength of ultrasonic wave is calculated using relation.

$2D = \lambda$ ………….. (1)

Where λ is wave length and D is distance in mm. The ultrasonic velocity is calculated by using relation.

Ultrasonic velocity (U) = λ x Frequency x 10^3 ……….(2)

Using the measured data some acoustical parameters have been calculated using the standard relations.

The adiabatic compressibility of solvent and solution are calculated by using equations

Adiabatic compressibility (βs) = 1/ U_s^2x d_s …………….. (3)

Adiabatic compressibility (β_0) = 1/ U_0^2x d_0 ………………. (4)

Acoustic impedance (Z) = U_s x d_s ………………………. (5)

Where U_0, U_s are ultrasonic velocity in solvent and solution respectively. d_0 and d_s are density of solvent and solution respectively

The apparent molal volume (ϕ_v) and apparent molal adiabatic compressibilities ($\phi_{k(s)}$) of substituted Schiff bases in solutions are determined respectively, from density (d_s) and adiabatic compressibility(β_s) of solution using the equations

$\phi_v = (M/d_s) + [(d_o-d_s) \, 10^3] / md_sd_o$ …………….. (6) and

$\phi_{k(s)}=[1000(\beta_sd_o-\beta_od_s) / md_sd_o] + (\beta_s M / d_s)$ …………….. (7)

where, d_o and d_s are the densities of the pure solvent and solution, respectively. m is the molality and M is the molecular weight of solute. β_o and $\beta_s$are the adiabatic compressibilities of pure solvent and solution respectively.

Intermolecular free length (Lf) = $K\sqrt{\beta s}$ …………… (8)

Relative association (RA) = (d_s /d_0) x $(U_0 /U_s)^{1/3}$ ···················(9)

Solvation number (Sn) = $\varphi^\kappa / \beta_0 x (M/ d_0)$ ………….. (10)

The value of Jacobson's constant is calculated by using relation

$$K=(93.875+0.375 \times T)\times10^{-8} ……………..(11)$$

Where T is temperature at which experiment is carried out. The present investigation is carried out at temperature (T = 303K)

Table – 1

Ultrasonic Velocity of 75% (DCM+water) mixture.

Temp = (303 ± 0.1) K

Sr. No.	No. of Rotations of Screw	Micro meter Reading (mm)	Deflection between Reading (mm)	Distance traveled by Screw in One Rotation (mm)	Ultrasonic Velocity (U)x10³ m/sec	Average Velocity (U) m/sec
1	5	7.02				
2	10	10.85	4.88	0.868	3156	
3	15	14.75	4.94	0.881	3220	3138.4 x 10³
4	20	18.53	4.81	0.854	3108	
5	25	22.23	4.75	0.844	3068	
6	30	27.00	4.85	0.861	3140	

Table 2: Ultrasonic velocity, density, adiabatic compressibility (βS), Specific acoustic impedance (Z) Intermolecular free length (Lf) in 75% DCM solvent at 303K.

Conc. (m) Moles lit⁻¹	Density (ds) Kg m⁻³	Ultrasonic Velocity(Us) m s⁻¹	Adiabatic Compressibility (βs) x10⁻⁹ m²N⁻¹	Inter molecular free length (Lf) x10⁻¹¹ m	Specific acoustic impedance (Z) x10⁵ kg m⁻²s⁻¹
Ligand LA in 75% (DCM +water) solvent					
0.01	1324.1	3530.4	7.1983	6.1660	5.44397
0.008	1323.9	3429.6	7.5622	6.3155	5.31741
0.006	1322.3	3333.6	7.9394	6.4661	5.19689
0.004	1321.8	3242.4	8.3287	6.6173	5.08241
0.002	1316.0	3173.6	8.6739	6.7399	4.98070
Ligand LB in 75% (DCM +water) solvent					
0.01	1220.5	3504.0	6.6732	5.3602	4.27663
0.008	1219.6	3438.4	6.9354	5.4645	4.19347
0.006	1219.6	3401.6	7.0862	5.5236	4.14859
0.004	1218.7	3337.6	7.3660	5.6316	4.06753
0.002	1217.8	3188.8	8.0755	5.8966	3.88332

Table-3: Concentration (m), relative association (R$_A$), apparent molal compressibility factor (φκ), apparent molal volume (φv), solvation number (Sn) at 75% (DCM+ water) solvent at 303K.

Conc (m) Moles/lit	Apparent molal volume (φv) m3mole-1	Apparent molal compressibility (φk)x10−10 m2N-1	Relative association (RA)	Solvation number (Sn)
Ligand LA in 75% (DCM +water) solvent				
0.01	2.14784249	2.162954594	0.949525	0.693480
0.008	2.42572500	2.290963957	0.957775	0.734522
0.006	2.88784077	2.423652613	0.965908	0.777064
0.004	3.81053480	2.560563346	0.973897	0.820960
0.002	5.41019130	2.682010292	0.979147	0.859898
Ligand LB in 75% (DCM +water) solvent				
0.01	1.32129503	2.341042447	0.957982	0.747062
0.008	1.38822667	2.433675282	0.963326	0.776623
0.006	1.85096889	2.487001757	0.966787	0.793640
0.004	2.24810880	2.585890583	0.972209	0.825200
0.002	3.43639759	2.836632903	0.986373	0.905213

Results and Discussion:

In the present investigation, different acoustical parameters, such as ultrasonic velocity (U), adiabatic compressibility (βs), partial molal volume (φv), intermolecular free length (Lf), apparent molal compressibility (φκ), specific acoustic impedance (Z), relative association (RA), solvation number (Sn) of substituted Schiff bases in different percentage of DCM+water mixture at 303K have been studied.

From table 1 to 2, it is found that ultrasonic velocity decreases with decrease in concentration for all systems. This indicates that, there is significant interaction between ion and solvent molecules suggesting a structure promoting behavior of the added electrolyte. Variation of ultrasonic velocity in solution depends upon the increase or decrease of molecular free length after mixing the component, based on a model for sound propagation proposed by Eyring and Kincaid[15].This was happened because of significant interaction between ions and solvent molecules suggesting a structure promoting behavior of the added electrolyte. This may also indicates decrease in number of free ions showing the occurrence of ionic association due to weak ion-ion interaction. The value of specific acoustic impedance (Z) decreases with decrease in concentration for all substituted Schiffs bases in different percent solutions of (DCM+water) mixture. When concentration of electrolyte is decreased, the thickness of oppositely charged ionic atmosphere may increase due to decrease in ionic strength. This is suggested by decrease in acoustic impedance with decrease in concentration for all system investigated. The increase of

adiabatic compressibility with decrease of concentration of solution may be due to dispersion of solvent molecule around ions, supporting weak ion-solvent interaction.

From table 3, it is observed that apparent molal volume increases with decrease in concentration in all systems indicating the existence of strong ion-solvent interaction[16-17]The apparent molal volume increases due to decreasing dielectric constant of medium with decrease in concentration.

Thus substituted Schiffs bases are less electro strickted in sheath of non-polar solvent. The positive values of apparent molal volume indicate that it does not restrict molecular motion within the solution. The value of apparent molal compressibility increases with decrease in concentration of all systems in different percent of (DCM+water) mixture. It shows weak electrostatic attractive force in the vicinity of ions causing electrostatic salvation of ions.

References:

1. Horinaka H, Iwade T, Kanetaka Y, Ogushi F, *J.Appl.Phys*., 42, (**2003**), 3287.
2. Topchyan A, Tatarinov A, Sarvazyan N, *Ultrasonic*, 44 (3), (**2006**), 259.
3. Real N, Moal F, Wang J, Vuillemin E, *J.Appl.Phys*., 91, (**2001**), 1274.
4. HorinakaH ,Iwade T, Kanetaka Y, *J.Appl.Phys*., 42, (**2003**), 3287.
5. Topchyan A, Tatarinov A, Sarvazyan N, *Ultrasonic*., 44(3), (**2006**), 259.
6. M.S. Chouhan, K. Modi , B.D. Shrivastava, S.Patil, I. J..Sci. Res. Chem. Sci., 4.(4), (**2017**), 1-4.
7. S. Sasikumar, G. Meenakshi, I., J., Res. in Eng. and Tech., 04, (02), (**2015**), 263-268.
8. Shashi Kant, Parul, Kamini Sharma, I., J., Chem. Tech. Research, 5, (4), (**2013**), 1948-1958.
9. T. Sumathi and M. Varalakshmi, Rasayan J. Chem..3,(3), (**2010**), 550-555.
10. Chandami A. S., Hedaoo D. S. and Wadekar M. P., J. Chem. Pharm. Res., 8, (3), (**2016**), 646-651.
11. Azhagiri S., Jayakumar S., Padmanaban R., Gunasekaran S., Srinivasan S., J., Sol. Chem., 38(4), (**2009**),441-448.
12. M.Thirunavukkarasu, N.Kanagathara, Int., J.,Chem.Tech. Research.4, 1, (**2012**), 459-463.
13. K. Kannagi, E. Jasmine, Vasantha Rani, J. Elixier Ultrasonic, 49, (2012), 10018-10023.
14. Kumar H, Deepika, *Int.J.Res.Phys.Chem.,* 2(3), (**2012**), 20.
15. Eyring H, Kincaud J F*, J.Chem.Phys., 6, (1938), 620.*
16. AjayaBhattarai, S.K. Chatterjee, T.K. Deo, T.P. Niraula, J. Chem. Eng. Data, 56(8), 2011, 3406-3410.
17. S.D. Devsarkar, R.T. Sawale, T.M. Kalyankar, J. App. Pharm. Sci., 5(5), 2015, 13-17.

Alum (Kal(SO$_4$)$_2$.12H$_2$O) Catalysedsynthesis Of 1, 5-Benzothiazepines

Chandrashekhar G. Devkate[*1], Ajay M. Patil[2],Satish Kola[3], Ganesh B. Andhale[4]

[*1] Indraraj Arts, Commerce and Science College, Sillod, Aurangabad-431112

[2]Pratishthan Arts, Comm. & Science College, Paithan., Aurangabad-431107

[3]M.G. Arts, Science and Late N.P Commerce College, Armori, Maharashtra, India 441208

[4]Jijamatha Mahavidhyalaya Buldhana-443001

[*1]Corresponding Author Email: cgdevkate@gmail.com

Abstract:

Alum (KAl(SO$_4$)$_2$.12H$_2$O) catalysed synthesis of 1,5-benzothiazepines by the condensation of chalcone and o-aminothiophenol in aqueous media inultrasonic bath and was irradiated at 80- 100°C. The method is cost effective and eco-friendly. And use of water as a solvent makes the method greener and more efficient. The method has simple workup procedure and the products are obtained in good to moderate yields.

Key Words:1,5-benzothiazepines, chalcone, o-aminothiophenol, Alum (KAl(SO$_4$)$_2$.12H$_2$O).

Introduction:

The 1,5-benzothiazepines are very versatile and are present in number of famous drugs.1,5-benzothiazepines are being used as antidepressants, calcium antagonists and coronary Vasodilators. The 1,5-benzothiazepine is a honoured class of pharmacophore, as compounds having this structural component possess a large range of biological activities like squalene synthetase inhibitor [1], anticonvulsant, anti-anginal [2,3], anti HIV [4],V2 arginine [5], Ca+2 channel antagonist vasopressin receptor antagonist [6], HIV-1 reverse transcriptase inhibitor [7,9] etc. Thus there is need to develop novel methodologies for the synthesis of 1,5 benzothiazepines.

Recently many organic reactions are been carried out in water which is readily available, non-toxic, inexpensive and eco-friendly solvent. Here we are interested to use alum (KAl(SO$_4$)$_2$.12H$_2$O) which is also non-toxic, easy handling, eco-friendly and inexpensive catalyst which is previously been reported as effective catalyst for the synthesis of 5-arylidene-2,4-thiazolidinedione [10], coumarins [11], anthraquinone [12], dihydropyrimidine [13] and trisubstituted imidazoles [14].

Experimental Section

Table 1. Screening of solvents for the synthesis of 1,5-benzothiazepines

Entry	Solvents	Catalyst (20 mol %)	Time (min)	Yield (%)[b]
1	THF	Alum	140	40
2	DMSO	Alum	120	45
3	CH$_2$Cl$_2$	Alum	120	30
4	DMF	Alum	120	40
5	CH$_3$CN	Alum	90	35
6	Dioxane	Alum	90	48
7	Toluene	Alum	90	50
8	MeOH	Alum	70	62
9	EtOH	Alum	70	65
10	H$_2$O	Alum	60	93

[a]Reaction conditions: chalcone**1d** (1.0 mmol) and o-aminothiophenol **2d** (1.2 mmol) at room temperature.

[b]Isolated yield.
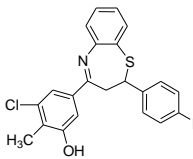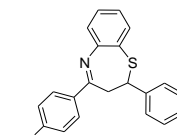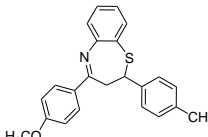
Procedure for the synthesis 1,5-benzothiazepines (3a-h).

A mixture of chalcone **1d** (1.0 mmol) and o-aminothiophenol **2d** (1.2 mmol) to that alum 20 mol% was added and the reaction mixture was kept in the ultrasonic bath and was irradiated at 8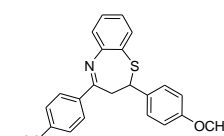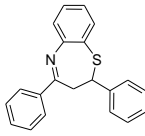0- 100ºC for about 20-30 min. (the progress of reaction was monitored by TLC) separately as indicated in (**Table 2**). After the reaction was completed the reaction mass was poured on crushed ice. The obtained solid was filtered, washed with water and dried. The crude compound was crystallized using DMF-Ethanol.

1a-h　　　　　**2**　　　　　**3a-h**
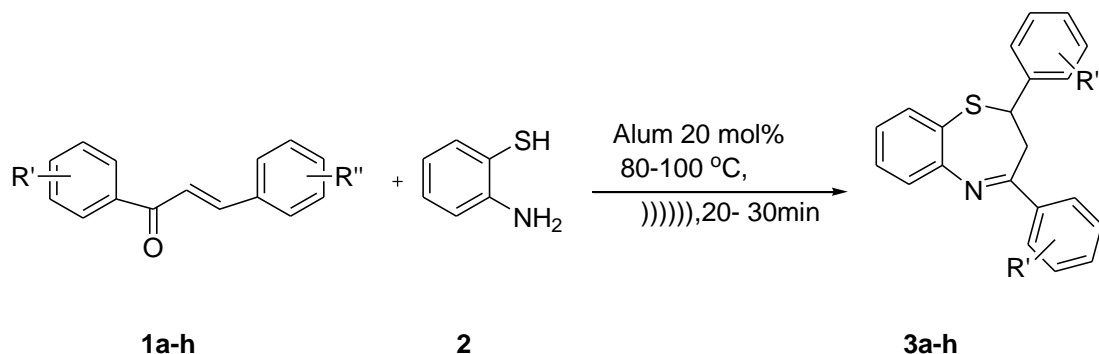
Scheme . Synthesis of 1,5-benzothiazepines from chalcones and o-aminothiophenol.

Table 2. One pot Synthesis of 1,5-benzothiazepines (**3a-h**) using alum 20 mol%.

Comp.	Product	m.pºC	Ultrasound Method	
			Time (min)	Yield (%)
3a		107 - 109	25	92
3b		112 - 116	25	93
3c		173 - 176	30	90
3d		116 - 118	30	92
3e		110 - 112	35	88

'RESEARCH JOURNEY' *International E- Research Journal*
Special Issue – 333 : Innovative & Sustainable Chemistry
Impact Factor 6.625 (SJIF)   **Peer Reviewed Journal**

E-ISSN :
2348-7143
December - 2023
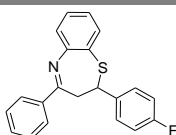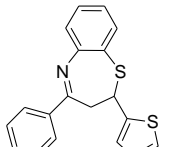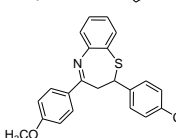
3f		101 - 103	35	92
3g		124-127	30	86
3h		133 - 135	30	88

Table 3. Effect of concentrations of alum for the synthesis of 1,5-benzothiazepines (**3c**)[a]

Entry	Alum (mol %)	Time (min)	Yield (%)[b]
1	5	80	65
2	10	80	73
3	15	50	80
3	**20**	**60**	**93**
4	25	60	93

Result and Discussion:

One pot cyclocondensationof chalcone**1d** (1.0 mmol) and o-aminothiophenol **2d** (1.2 mmol) that alum 20 mol% was added it was carried out under ultrasound irradiation which result into the subsequent 1,5-benzothiazepines (**3a-h**) as given in (**Table 2**). We have screened various percentageAlum (KAl(SO$_4$)$_2$.12H$_2$O)and optimization using different mol percentage for the reaction which was carried out under ultrasound irradiation. The results obtained are summarized in **Table 1**.

Here good yields was obtained for Alum (KAl(SO$_4$)$_2$.12H$_2$O)(entry 10) with water as solvent at 80 - 100 ºC for 30 min. And thus, the reaction was optimized and the method was used for further synthesis derivatives and the results obtained are given in **Table 2**. All the reaction (**3a-h**) is repeated with recovery of catalyst for three to four times the loss of catalyst was 2-3 % with good yield which is appreciable **Table 3**.

Conclusion:

In conclusion, we have developed a simple and highly efficient method were 1,5-benzothiazepines and their derivatives are synthesized using Alum (KAl(SO$_4$)$_2$.12H$_2$O) as heterogeneous catalyst which is reusable and cost-effective. The reaction is performed in water as solvent under ultrasound irradiation. Thus, the method is clean and efficient method. Further studies on the biological activities of the products and application of this methodology to other interesting benzothiazepines derivatives are underway in our laboratory.

References:

1. Grandolini, G.; Perioli, L.; Ambrogi, V. Eur. J. Med. Chem. **1999**, 34, 701.
2. Shinichi, Y.; Yoshikazu, M.; Katsuji, M.; Yoshinori, I.; Yasuhiko, O.; Ryuzo, Y.; Tadashi, N.; Hiroyasu, S. J. Org. Chem. 1996, 61, 8586.
3. Kurokawa, J.; Adachi Akahane, S.; Nagao, T. Eur. J. Pharmacol. **1997**, 325, 229.

4. Miyata, O.; Tetsuro, S.; Ichiya, N.; Takeaki, N. Tetrahedron. **1997**, 53, 2421.
5. Yang, X.; Buzon, L.; Hamanaka, E.; Liu, K. K.-C. Tetrahedron: Asymmetry. **2000**, 11, 4447.
6. Sarro, G. D.; Chimirri, A.; Sarro, A. D.; Gitto, R.; Grasso, S.; Zappala, M. Eur. J. Med. Chem. **1995**, 30, 925.
7. Urbanski, M. J.; Chen, R. H.; Demarest, K. T.; Gunnet, J.; Look, R.; Ericson, E.; Murray, W. V.; Rybczynski, P. J.; Zhang, X. Bioorg. Med. Chem. Lett. **2003**, 13, 4031.
8. Di Santo, R.; Costi, R. Farmaco. **2005**, 60, 385.
9. J. M. Harris, Poly(ethylene glycol) Chemistry,Biotechnological and Biomedical Applications, Plenum Press, New York, **1992**, p. 3.
10. Kiran, F. Shelke.; Suryakant, B. Sapkal.; Gopal, K. Kakade.; Sandip, A. Sadaphal.; Bapurao, B. Shingate.; Murlidhar, S. Shingare.Green Chemistry Letters and Reviews. **2010**, 3, 1, 17-21.
11. Minoo, Dabiri.; Mostafa, Baghbanzadeh.; Shadi, Kiani.; Yasamin, Vakilzadeh. Monatshefte fur Chemie. **2007**, 138, 997–999.
12. Balaji, R. Madje.; Kiran, F. Shelke.; Suryakant, B. Sapkal.; Gopal, K. Kakade.; Murlidhar, S. Shingare. Green Chemistry Letters and Reviews. **2010**, 3, 4, 269-273.
13. Azizian, J.; Mohammadi, A.A.; Karimi, A.R.; Mohammadizadeh, M.R. Appl. Catal. **2006**, 300, 85-88.
14. Mohammadi, A.A.; Mivechi, M.; Kefayati, H. Monatsh. Chem. **2008**, 139, 935_937.

Thermal Studies of Bidentate Organic Ligand and Their Some First Transition Series Metal Complexes

B. H. Jawale

Department of chemistry, B.S.S.Arts Science & Commerce College, Makani.Tq. Lohara Dist. Osmanabad Pin. 413604

Abstract:

Some First transition series metal complexes containing bidentateorganic ligand, 3-[3-(3-ethoxy-4-hydroxyphenyl)acryloyl]-4-hydroxy-6-methyl-2H-pyran-2-one derived from 3-acetyl-6-methyl-pyran-2,4(3H)-dione (dehydroacetic acid) and 3-ethoxy-4-hydroxy benzaldehyde, have been prepared and characterized by new modern spectroscopic techniques. Analytical & Spectral data, the complexes was found to be 1:2 (metal: ligand).High decomposition points of the complexes it indicate excellent thermal stability at normal temperature. In TG/DTA studies also supportive for the presence of coordinated two water molecule and Lattice water molecules in corresponding complexes. The X-ray diffractograms results shows that Co(II), Mn(II), Cu(II) and Ni(II) complexes are monoclinic system with lattice type-P.

Keywords :- Transition metal, Dehydroacetic acid, complex, chalcone, thermal,

Introduction:

Chalcones and their metal complexes play a prominent role in modern coordination chemistry. These compounds possessing novel structural features, interesting spectral and magnetic properties, have been the subject of intensive research due to their importance in medical, agriculture, analytical, biological and industrial fields, In recent years a number of β-dicarbonyl compounds in which the carbonyl function(s) bonded to olefinic linkage(s) have gained considerable importance[1-3]mainly because of the fact that such compounds are structurally related to the active chemical constituents of several traditional me dicinal plants. For instant, curcuminoids, the active chemical component present in Indian medicinal plant turmeric (curcuma longa, linn, zingiberacea family) contain three β-dicarbonyl compounds in which the diketo function is directly linked to olefinic group[3]. Such unsaturated β-dicarbonyl compounds and their metal complexes possess interesting biochemical properties such as antitumour, antioxidant, antifungal and antimicrobial activities[1-14].Therefore one of the oxygen hetrocyclic compounds 3-acetyl-6-methyl-2H-pyran-2,4(3H)-dione (DHA) was reported to be an excellent chelating agent & to possess promising fungicidal, bactericidal, herbicidal & insecticidal activities[15-18].It is also a versatile starting material for the synthesis of a wide variety of hetrocyclic ring systems[19]. A search of the literature revealed that no work has been done on transition metal complexes of the chalcones derived from 3-ethoxy-4-hydroxy benzaldehyde&Dehydroacetic acid.

Experimental:

Dehydroacetic acid (purity ≥ 99%) for synthesis was obtained from Merck, Germany & used as supplied. 3-ethoxy-4-hydroxy benzaldehydeof A.R. grade obtained from AVRA chemicals were used for the synthesis of the ligands. A.R. grade hydrated metal chlorides from Thomas Baker were used for the preparation of the complexes. The carbon, hydrogen & nitrogen content in each sample were measured on a Perkin Elmer(2400) CHNS analyzer. The

IR spectra (KBr), in the range of 4000-450 cm^{-1} were recorded on a Perkin Elmer (C-75430) IR spectrometer. The 1H-NMR spectrum of the ligand was measured in CDCL$_3$ on Bruker instrument. The mass spectrum of the ligand was measured in Qc-01 DAD Mass-spectrometer,thermogravimetric analysis differential thermal analysis (TGA-DTA) were realised on a METTLER-TOLEDO–DB V13.00 instruments. The UV-VIS spectra of the complexes were recorded on a Shimadzu UV-2202 Spectrophotometer. Magnetic susceptibility measurements of the complexes were performed using a Gouy balance at room temperature using Hg [Co (SCN)$_4$] as the calibrant.
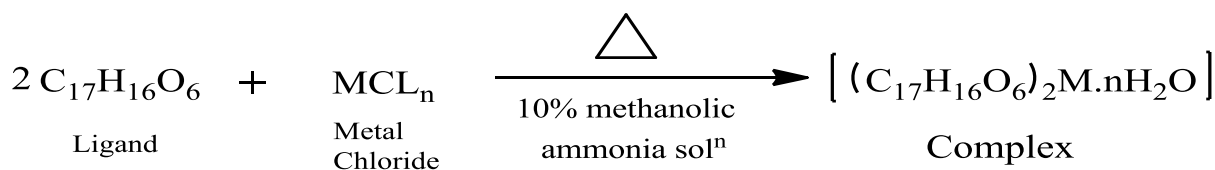
Synthesis of the ligand (HL) :-

A solution of 0.01mol of dehydroacetic acid, 10 drops of piperidine& 0.01 mol of 3-ethoxy-4-hydroxy benzaldehyde in 25 ml chloroform were refluxed for 8-10 hrs, 10 ml of the chloroform-water azeotrope mixture was separated by distillation. Crystal of product separated on slow evaporation of the remaining chloroform. The resulting precipitate was filtered, washed several times with ethanol & recrystallized from chloroform[22-23].

Dehydroacetic Acid   3-ethoxy-4-hydroxy benzaldehyde   Chalcone

Reflux in CHCL$_3$ for 6-7 hrs
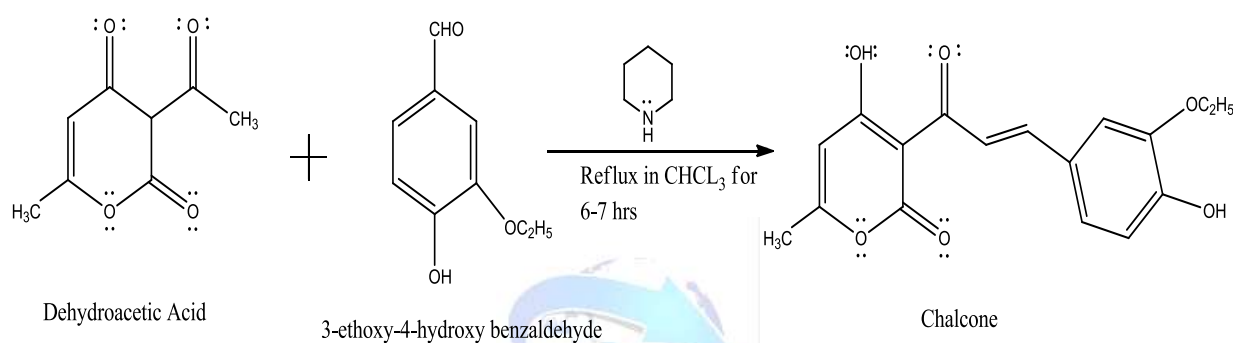
Scheme : Synthesis of Ligand

Preparation of metal complexes :-

To a chloroform solution (30ml) of the ligand (2mmol), methanolic solution (20ml) of metal chlorides was added with constant stirring. The PH of the reaction mixture was maintained around 7-7.5 by adding 10% methanolic solution of ammonia. It was then refluxed for 2hr. the resulting metal complex was filtered in hot condition & washed with ethyl acetate methanol, pet-ether & dried over calcium chloride in vaccumdesicator.

$$2\,C_{17}H_{16}O_6 \; + \; MCL_n \xrightarrow[\text{ammonia sol}^n]{\text{10\% methanolic}} \left[(C_{17}H_{16}O_6)_2 M.nH_2O\right]$$

Ligand   Metal Chloride   Complex

Scheme :Preparation of Metal Complex

Results and Discussion:

Physical characteristics, micro analytical data of ligand and its metal complexes are given inTable 1.The analytical data of complexes reveal 1:2 molar ratio (metal: ligand) and correspond well with the general formula[ML$_2$X$_2$] (where M=Fe(III), Mn (II), Co(II), Ni(II), Cu (II), L=C$_{17}$H$_{16}$O$_6$). The magnetic susceptibilitiesof M=Fe(III), Mn(II), Co(II), Ni(II), Cu(II)complexes at room temperature are consistent with octahedral &distortedoctahedral structure with two water molecules coordinated to metal ion. The presence oftwo coordinated water molecules was also confirmed byTGA–DTA analysis.

Table I : Physical and Analytical data of ligand and its metal complexes.

Ligand/ complexes	F.W.	M.P./decomp. Temp.(^{0}C)	Yield %	Colour	Found (Calcd.), %			
					M	C	H	O
Ligand HL $C_{17}H_{16}O_6$	316	159	70	Red Orange	-	64.52 (64.55)	5.09 (5.10)	30.31 (30.35)
$C_{34}H_{30}FeO_{12}$	686	300<	20	Brown	8.09 (8.14)	59.38 (59.49)	4.40 (4.41)	27.84 (27.97)
$C_{34}H_{30}CuO_{12}$	694	272	55	Apricot	9.06 (9.15)	58.69 (58.83)	4.34 (4.36)	27.60 (27.66)
$C_{34}H_{30}CoO_{12}$	689	300<	40	Amber	8.51 (8.55)	59.20 (59.22)	4.35 (4.39)	27.70 (27.84)
$C_{34}H_{30}MnO_{12}$	685	300<	45	Bronze	7.98 (8.01)	59.57 (59.67)	4.40 (4.41)	27.96 (28.01)
$C_{34}H_{30}NiO_{12}$	689	236	80	Lemon	6.55 (6.47)	57.33 (57.70)	4.40 (4.57)	29.19 (29.89)

^{1}H-NMR Spectra of ligand :-

The ^{1}H NMR spectra of ligand in CDCL$_3$ at room temperature shows the following signals. δ 1.50 (t, 3H, -CH$_3$), 2.30 (s, 3H, -CH$_3$), 4.22 (q, 2H,–OCH$_2$ gr),5.97 (s,1H, phenolic –OH), 6.10 (s,1H, C$_5$-hydrogen of DHA moiety),6.98(dd,1H, Ar-H), 7.22(dd, 1H, Ar-H),7.24(s, 1H, Ar-H),7.92(d,1H, olefinic proton) and 8.16(d,1H, olefinic proton).The existence of strong hydrogen bonding between the phenolic hydrogen and acetyl carbonyl of dehydroacetic acid moiety, is confirmed by 15.56 (s,1H, enolic OH of DHA moiety).

Mass Spectra of ligand :-

Mass spectroscopy regard as clear and strong evidence to prove the formation of molecules via the observation of the mother ion at molecular weight equivalent value and this observed in the mass fragmentation spectra of ligand , that the mother ion appear clear band at (317 m/e) , this was a good agreement for the formation of the new ligand.

IR Spectra of ligand :-

The FTIR spectrum of free ligand shows characteristic bands at 3502, 3232,1747, 1697, 1242cm^{-1} assignable to ν (OH) of the phenyl group side chain, ν (OH) of the intramolecular phenolic group of the dehydroacetic acid moiety,ν (C=O) (lactone carbonyl), ν(C=O) (acetyl carbonyl) & ν (C-O) (phenolic) stretching mode, respectively[22]. In the IR spectra of all the metal chelates, no band was observed in the region of 3200-3000cm^{-1}. Instead, in its place, a broad band characteristic of ν (OH) of coordination water was observed in the region 3570-3200cm^{-1}. The absence of ν (OH) (Phenolic) at 3100cm^{-1} suggests subsequent deprotonation of the phenolic group and coordination of phenolic oxygen to the metal ion. This was supported by an upward shift in ν (C-O) (phenolic)[23] by 10-45cm^{-1}. The ν (C=O) (acetyl carbonyl) was shifted to lower energy with respect to the free ligand, suggesting the participation of the acetyl carbonyl in the coordination[22-24]. The IR spectra of all the compounds showed a prominent band at ≈1377 & ≈ 970cm^{-1}, typical of ν (C-O-C) and trans –CH=CH- absorption. The presence of new bonds in the region 600-450cm^{-1} can be assigned to ν (M-O) vibration[25]. Important spectral bands for the ligand and its metal complexes are presented in Table II.

TABLE II. Characteristic IR frequencies (cm-1) of the ligand and its metal complexes

Compound	ν (OH) (side chain phenyl moiety)	ν (OH) (dehydroacetic acid moiety)	ν (C=O) (lactone)	ν (C=O) (acetyl carbonyl)	ν (C-O) (phenolic)	ν (C=C) (trans)	ν (M-O)
Ligand HL $C_{17}H_{16}O_6$	3505	3232(m)	1747(w)	1697(s)	1242(s)	979(s)	-
$C_{34}H_{30}FeO_{12}$	3296	-	1681(s)	1647(s)	1223(m)	972(m)	532(m) 498(m)
$C_{34}H_{30}CuO_{12}$	3370	-	1672(s)	1647(s)	1282(s)	979(s)	548(w) 465(m)
$C_{34}H_{30}CoO_{12}$	3407	-	1672(m)	1643(s)	1258(m)	980(s)	522(w) 480(m)
$C_{34}H_{30}MnO_{12}$	3300	-	1675(s)	1645(s)	1268(s)	974(s)	545(w) 472(m)
$C_{34}H_{30}NiO_{12}$	3307	-	1681(m)	1647(w)	1248(w)	972(w)	564(w) 544(m)

Magnetic measurement and electronic absorption spectra :-

The electronic spectra of all the complexes were recorded in DMF solution. The magnetic and electronic spectral data are given in table III.Three electronic transitions were observed in the electronic spectrum of the Fe(III) complex, at 14771 cm^{-1}(ε= 22 dm^{3}mol^{-1}cm^{-1}), 21978 cm^{-1}(ε= 26 dm^{3}mol^{-1}cm^{-1}) and 24213 cm^{-1}(ε= 32 dm^{3}mol^{-1}cm^{-1}), which are assigned to $^6A_{1g} \rightarrow ^4T_{1g}(G)$, $^6A_{1g} \rightarrow ^4T_{2g}(G)$ and $^6A_{1g} \rightarrow ^4E_g(G)$, respectively, suggesting an octahedral complex of Fe(III),which was confirmed by the value of magnetic moment (5.91$_{\mu B}$)[26].

The spectrum of the Cu(II) complex consisted of a broad band at 14409 cm^{-1}(ε= 94 dm^{3}mol^{-1}cm^{-1}), assigned to the $^2E_g \rightarrow ^2T_{2g}$transition of a distorted octahedral geometry[27]. In addition to this band, the band observed at 25510 cm–1 (ε= 1143 dm^{3}mol^{-1}cm^{-1}) arises from intra ligand charge transfer.

TABLE III.Magnetic And electronic absorption spectral data (in DMSO) of the compounds.

Compound	μ_{eff}/μ_B	ν /cm^{-1}	Band assignment	Geometry
Ligand HL $C_{17}H_{16}O_6$	-	32442 40545	INCT[a] INCT	-
$C_{34}H_{30}FeO_{12}$	5.91	14771 21978 24213	$^6A_{1g} \rightarrow ^4T_{1g}(G)$ $^6A_{1g} \rightarrow ^4T_{2g}(G)$ $^6A_{1g} \rightarrow ^4E_g(G)$	Octahedral
$C_{34}H_{30}CuO_{12}$	2.07	14409 25510	$^2E_g \rightarrow ^2T_{2g}$ INCT	Distorted Octahedral
$C_{34}H_{30}CoO_{12}$	4.61	9852 18348 24509	$^4T_{1g}(F) \rightarrow ^4T_{2g}(F)$ $^4T_{1g}(F) \rightarrow ^4A_{2g}(F)$ $^4T_{1g}(F) \rightarrow ^4T_{1g}(P)$	Octahedral
$C_{34}H_{30}MnO_{12}$	5.89	19120 19881 31546	$^6A_{1g} \rightarrow ^4T_{1g}(G)$ $^6A_{1g} \rightarrow ^4T_{2g}(G)$ $^6A_{1g} \rightarrow ^4A_{1g}$	Octahedral
$C_{34}H_{30}NiO_{12}$	2.97	9460 14641 23148	$^3A_{2g} \rightarrow ^3T_{2g}(F)$ $^3A_{2g} \rightarrow ^3T_{1g}(F)$ $^3A_{2g} \rightarrow ^3T_{1g}(P)$	Octahedral

The electronic spectrum of the Co(II) complex exhibited three bands at 9852 cm^{-1}(ε= 17 dm^{3}mol^{-1}cm^{-1}), 18348 cm^{-1}(ε= 59 dm^{3}mol^{-1}cm^{-1}) and 24509 cm^{-1}(ε= 98 dm^{3}mol^{-1}cm^{-1}), which are assigned to $^4T_{1g}(F) \rightarrow ^4T_{2g}(F)$, $^4T_{1g}(F) \rightarrow ^4A_{2g}(F)$ and $^4T_{1g}(F) \rightarrow ^4T_{1g}(P)$, respectively, indicating octahedral configuration around the Co(II) ion. The magnetic moment of the Co(II) complex was 4.61$_{\mu B}$.

The electronic spectrum of the Mn(II) complex exhibited three bands at 19120 cm^{-1}(ε= 26 dm^{3}mol^{-1}cm^{-1}), 19881 cm^{-1}(ε= 16 dm^{3}mol^{-1}cm^{-1}) and 31546 cm^{-1}(ε= 28 dm^{3}mol^{-1}cm^{-1}), which are assigned to $^6A_{1g} \rightarrow ^4T_{1g}(G)$, $^6A_{1g} \rightarrow ^4T_{2g}(G)$ and $^6A_{1g} \rightarrow ^4A_{1g}$, $^4E_{1g}(4G)$ transitions, respectively, indicating an octahedral configuration[26,27]around the Mn(II) ion. The octahedral geometry of Mn(II) was further confirmed by the value of the magnetic moment (5.89$_{\mu B}$).

The electronic spectrum of the Ni(II) complex exhibited three bands at 9460 cm^{-1}(ε= 34 dm^{3}mol^{-1}cm^{-1}), 14641 cm^{-1}(ε= 67 dm^{3}mol^{-1}cm^{-1}) and 23148 cm^{-1}(ε= 188 dm^{3}mol^{-1}cm^{-1}), which are assigned to $^3A_{2g} \rightarrow ^3T_{2g}(F)$, $^3A_{2g} \rightarrow ^3T_{1g}(F)$ and $^3A_{2g} \rightarrow ^3T_{1g}(P)$, respectively. These values, as well as the magnetic moment value (2.97$_{\mu B}$), support an octahedral geometry of the Ni(II) complex[26].

Powder X-ray diffraction analysis :-

The X-ray diffractograms of the Co(II), Mn(II) and Fe(III) complexes were scanned in the range 5–100° at a wavelength of 1.543 Å. The diffractograms and associated data depict the 2θvalue for each peak, the relative intensity and inter-planar spacing (d-values). The X-ray diffraction pattern of these complexes with respect to major peaks of relative intensity greater than 10 % were indexed using a computer programme[28].This indexing method also yields the Miller indices (h, k, l), the unit cell parameters and the unit cell volume. The unit cell of Co(II) complex yielded values of lattice constants: a= 8.8904 Å, b= 8.4161 Å and c= 4.7854 Å, and a unit cell volume V= 378.2311 Å3. The unit cell of the Mn(II) complex yielded values of lattice constants: a= 25.0082 Å, b= 4.4756 Å, c= 5.7666 Å, and a unit cell volume V= 622.2078Å3. The unit cell of the Fe(III) complex yielded values of lattice constants: a= 7.0706 Å, b= 14.9154 Å, c= 5.3601 Å, and a unit cell volume V= 829.4479 Å3. In concurrence with these cell parameters, conditions such as a ≠ b ≠ cand α= γ= 90° ≠ βrequired for a monoclinic sample were tested and found to be satisfactory. Hence, it can be concluded that the Co(II), Mn(II) and Fe(III) complexes were monoclinic crystal systems. The experimental density values ofthe complexes were determined using the specific gravity method[29]and found to be 2.2008, 2.4982, and 2.0622 g cm^{-3} for the Co(II), Mn(II) and Fe(III) complexes, respectively. Using the experimental density values, ρ, the molecular weight of the complexes, M, Avogadro's number, N, and the volume of the unit cell, V, the number of molecules per unit cell, n, were calculated using the equation ρ= nM/NVand they were found to be one for Co(II) and two for the Mn(II) and Fe(III) complexes. With these values, the theoretical densities were computed and found to be 2.1904, 2.4589 and 2.0701 g cm^{-3}for the respective complexes. Comparison of experimental and theoretical density value shows good agreement within the limits of experimental error[30].

Thermal Studies Of The Ligand (L3) And Their Some Metal Complexes

The TG-DTA study of the metal chelates such as cobalt(II), manganese(II) and iron(III) derived from 3-[3-(3-ethoxy-4-hydroxyphenyl)acryloyl]-4-hydroxy-6-methyl-2H-pyran-2-oneligandwas scans from normal temperature to 900^{0}C in a nitrogen air through α-Al$_2$O$_3$ as the reference[33-34].

The thermogravimetric and Differential thermal analysis summary of cobalt (II) complex

of 3-[3-(3-ethoxy-4-hydroxyphenyl)acryloyl]-4-hydroxy-6-methyl-2H-pyran-2-oneligand (shows no molecular mass loss equal to 149°C. The initial stepmolecular mass loss of 6.29% (calcd. 6.56%) is seen in the temperature range 162-265°Cit agree to the elimination of two water molecules . After the initial step decay is in the temperature range 270 - 410°C by 26.2% molecular mass loss (calcd.26.35%) this is second step of decomposition, it predicted to the deduction of non-chelated portion of the 3-[3-(3-ethoxy-4-hydroxyphenyl)acryloyl]-4-hydroxy-6-methyl-2H-pyran-2-oneligand. The third step molecular mass loss continues and follows sluggish decay of remaining fragment of the ligand48.6%(calcd.,48.94). The molecular mass of the final residue resembles to CoO, 14.3%(calcd.14.8%).
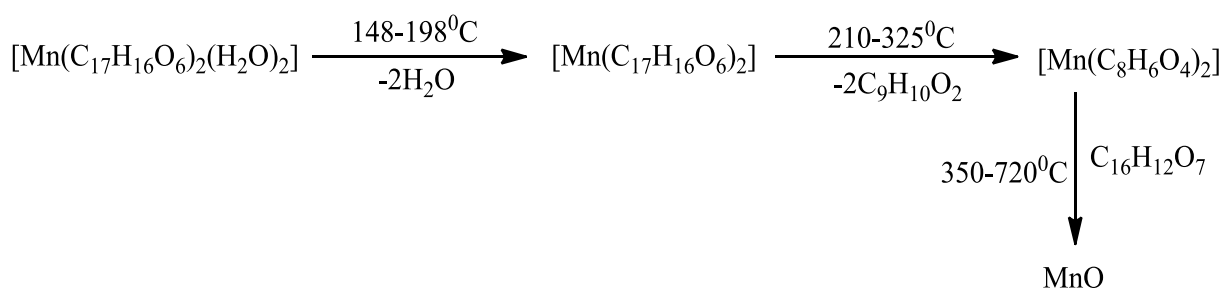
The all above thermogravimetric and DTA data it again confirmed that the cobalt(II) complex are more stable octahedral structure.The temperature range and fragmentation pattern of cobalt complex are as fallows.

$$[Co(C_{17}H_{16}O_6)_2(H_2O)_2] \xrightarrow[-2H_2O]{162\text{-}265^0C} [Co(C_{17}H_{16}O_6)_2] \xrightarrow[-2C_9H_{10}O_2]{270\text{-}410^0C} [Co(C_8H_6O_4)_2]$$

$$\xrightarrow[\;]{420\text{-}870^0C \;\; C_{16}H_{12}O_7} CoO$$
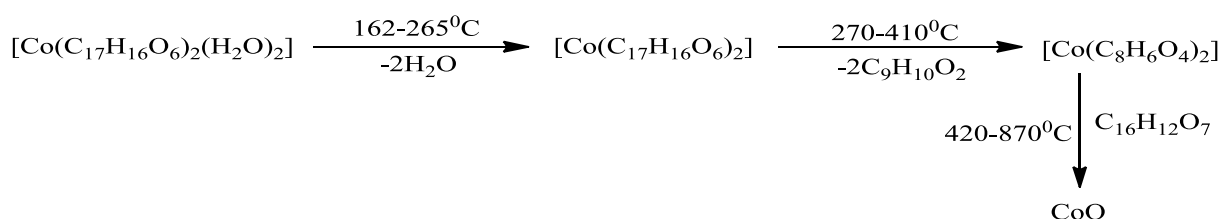
Geetha Parameshwaran[35]in there thermogravimetric and differential thermalanalysis of Co(II) chelates of Cinnamaldehyde andanthranilic acid discribed that, the chelates does not possess water of hydration. On the other hand a molecular weight loss in the temperature range 110 - 180°C is for the reason that of chelated water molecules. The TG-DTA curve of Co(II) complexes presented very sharp specific step decay way. They reported that this performance may be for the reason that of the rapid decay of the chelate.

In the thermal studies of cobalt(II) chelate of 2-hydroxy-3-bromo-4-methoxy-5-methyl chalconeoxime, Bhave and Kharat[36] listed that the deduction of water molecules below 200°C on the basis of endothermic curve in differential thermal analysis.

On the TG-DTA studies ofMn(II) complexprepared from3-[3-(3-ethoxy-4-hydroxyphenyl)acryloyl]-4-hydroxy-6-methyl-2H-pyran-2-one ligand, the preliminary step shows a clear slope in the temperature range 148-198°C by a molecular weight beating of 6.7% (calcd.,6.9%), indications the deduction of chelated two water molecules,it look like to dehydration point. The dehydratedcompound in afterward step decays in a tiny temperature range 210-325°C by a 27.1 % mass loss (calcd,27.30 %). In this phase may be abstraction of non-chelated fragment of the ligand. Now the residual compound in third step agrees to decay of chelated part of the ligand then in the temperature range of 350-720°C by a compound weight loss 56.4 %(calcd.,56.9%). The weight of the final residue equivalent to the stable MnO, 12.4% (calcd.,12.55%). The above all decomposition pattern decided that the Mn(II) complex has most stable octahedral confirmation.The decomposition pattern of Mn(II) complex are as fallows.

$$[Mn(C_{17}H_{16}O_6)_2(H_2O)_2] \xrightarrow[-2H_2O]{148\text{-}198^0C} [Mn(C_{17}H_{16}O_6)_2] \xrightarrow[-2C_9H_{10}O_2]{210\text{-}325^0C} [Mn(C_8H_6O_4)_2]$$

$$\xrightarrow[\;]{350\text{-}720^0C \;\; C_{16}H_{12}O_7} MnO$$

The decompositionanalysis of Mn(II) chelate of N,N-triethylenediaminebis(3-carboxypropanamide) defined[37] by Viswanathan et al.shows three phases. These are 378–533 K (40 % loss), 533 – 613 K (10 % loss) then 613–693K (25.6 % loss) and a residue (24.4%) is finally obtained.

Related to our investigation, the Mn(II) chelate of bis(5-methyl dithiocarbazate) diacetophenone defined by Makode et al.[38]reported minor weight loss equal to 210ºC, signifying non-appearance of some water molecule. The decay of the transition metal chelate elaborate two stages, out of which the major step is due to the circumstance that, the non-chelated fragment of the ligand decays prominent (250-350ºC), whereas the really chelated portion decays second (350-690ºC) foremost to decision by means of formation of metal oxide.

The thermal characterization of Fe(III) complex of 3-[3-(3-ethoxy-4-hydroxyphenyl)acryloyl]-4-hydroxy-6-methyl-2H-pyran-2-one ligand(L3)(Fig. B3.21)show nomolecular mass beating upto 150ºC then an clear slope in the range160º-195ºC in it indicates compound weight loss 6.05% (calcd.,6.31%) by the elimination of two water molecules. The dehydratedresidue in next step decays in a tiny temperature range 215-340ºC by a 26.3 % mass loss (calcd, 26.39 %). In this period may be removal of non-chelated fragment of the ligand. The rate controlling route of decay is originated to be random nucleation by one nucleus on each component. In the third step be similar to decompositionin the temperature range 400-845⁰C remaining part of the ligand through a compound weight loss 48.4%(calcd, 49.1 %). The weight of the final residue 15.3% does not be similar to any stoichiometric end product. The decomposition of Fe(III) complex with respect to the temperature range and the tentative weight losses of the decay reaction are shown below.

$$[Fe(C_{17}H_{16}O_6)_2.(H_2O)_2] \xrightarrow[-2H_2O]{160\text{-}195^0C} [Fe(C_{17}H_{16}O_6)_2] \xrightarrow[-2C_9H_{10}O_2]{215\text{-}340^0C}$$

$$[Fe(C_8H_6O_4)_2] \xrightarrow[C_{16}H_{12}O_8]{400\text{-}845^0C} Residue$$
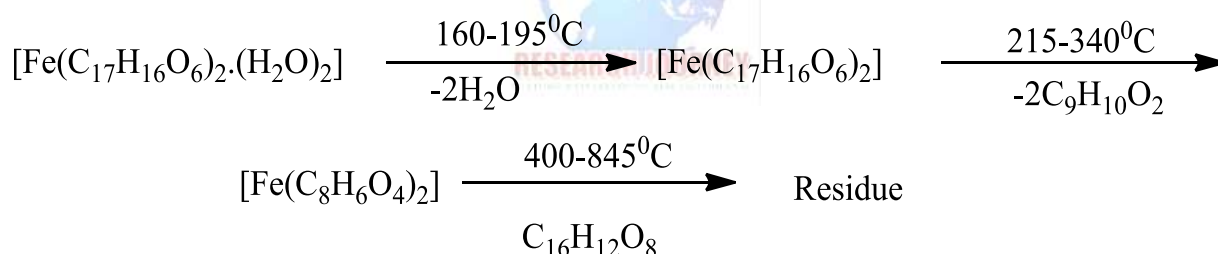
Thermal study of Iorn(III) complexes of related Schiff bases synthesized from DHAwith substituted anilines, the molecular mass loss numerous between the temperature range 67-87ºC reinforced by a comprehensive endotherm at the similar point in DTA curve relates to one molecule of water, crystallization has been defined by Mane et al.[39]. The peak at 247ºC reported to decay of organic substance and 328ºC expressions decay of the metal chelate.

Subsequently the TG curve Gour et al.[40]reported to the two stage of decay of mixed organic compoundof Fe(III) chelate of 2,3-dihydroxy pyridine as well as nitrogen donor organic ligands. The primary step decay at 173-303ºC correspond to the beating of two molecules of nitrogen.

Conclusion :-

Based on the physicochemical and spectral data discussed above, a distorted octahedral geometry for the Cu(II) complex and an octahedral geometry for the Mn(II), Fe(III), Co(II) and Ni(II) complexes are proposed. The ligand behaves as bidentate, coordinating through the phenolic oxygen and the acetyl carbonyl group of the dehydroacetic acid moiety.High

decomposition points of the complexes it indicate excellent thermal stability at normal temperature. In TG/DTA studies also supportive for the presence of coordinated two water molecule and Lattice water molecules in corresponding complexes. The X-ray diffractograms results shows that Co(II), Mn(II), Cu(II) and Ni(II) complexes are monoclinic system with lattice type-P.

References :-

1. K.Krishanankutty, V.D.John, *Synth.React.Inorg.Metal-Org.Chem,* 33 (2003) 343.
2. V.D.John, G.Kuttan and K.Krishanakutty, *J.Exp.Clin.Caner.Res*, 21 (2002) 219.
3. K.Krishanakutty and P.Vanugopalan, *Synth.React.Inorg.Metal.Org.Chem,* 28 (1998) 1313.
4. H.J.J.Pabon, *Reac.Trans.Chim,* 83 (1964) 237.
5. V.S.Govindrajan, *CRC Critical review in food science and nutrition,* 12 (1980) 199.
6. R.J.Anto, K.N.DineshBabu, K.N.Rajasekharan and R.Kutton, *Cancer.Lett,* 94 (1995) 74.
7. M.T.Haung, Z.Y.Wang, C.A.Geogiadis, J.D.Lasken and A.H.Canney,*Carcinogensis,* 13 (1992) 2183.
8. S.M.Khopde, K.IndiraPriyadarsini, P.Venteketesan and M.N.A.Rao, *Biophys.Chem,* 80 (1999) 85.
9. R.Kuttan, P.C.Sudheeran and C.D.Joseph, *Tumori* 73 (1987) 29.
10. M.Nagabushan and S.V.Bhide, *J.Am.Coll.Nutr,* 11 (1992) 192.
11. T.S.Roa, N.Basu and H.H.Siddique, *Indian.J.Med.Res,* 75 (1982) 574.
12. O.P.Sharma, BioChem,*Pharmacol,* 25 (1976) 1811.
13. K.K.Soudamini and R.Kuttan, *Ethnopharmacol,* 27 (1989) 227.
14. R.C.Srimal and B.N.Dhawan, *J.Pharm.Pharmacol,* 25 (1973) 447.
15. Surya raoD.,sadasivareddyC., JohnV.T., GonorkarM.C..*Curr. Sco.*(1980) 49, 511.
16. Surya raoD., SubharaoB.L.,JohnV.T., GonorkarM.C.,*Nat. Acad. Sci.let.* (1978) 1, 402.
17. SchleiffenbaumB.,SpertiniO., TedderThomasF., *J. cell.Biol.* (1992) 119, 229.
18. Stanley, V.G., WoldesenbetS.,CassandraG., *Poult. Sci.* (1996) 75, 42.
19. LevaiA.,JekeJ., Monatsh. *Chem.* (2006) 137, 339.
20. ThornberryH.H.,*Phytopathology* (1950) 40, 419.
21. BauerA.W.,KirbyW.M.M., ShesiesJ.C., TurckM., *Am. J. Clin. Pathol.* (1966)44, 93.
22. RamaraoN.,RaoV.P., TyagaRajuV.J., GanorkarM.C., *Indian J.Chem.* A (1985) 24, 877.
23. RaoP.V.,NarasaiahA.V., *Indian J. chem. A* (2003) 42, 1896.
24. CarugoO.,CastellaniC.B., RizziM., *Polyhedron* (1990) 9, 2061.
25. NakamotoK.,*Infrared spectra of inorganic & coordination compounds, Wiley, New York,* (1970), pp. 159,167,214.
26. AfkarK. A. H., *Indian J. Chem., A*(1994)33, 879.
27. LeverA. B. P., *Inorganic electronic spectroscopy, Elsevier, Amsterdam,*(1968)55, 789.
28. CarvajalJ. R., RoisnelT.,Winplotr, *A Graphic Tool for Powder Diffraction, Laboratoire Leon Brillouin (ceal/cnrs) 91191 Gif sur Yvette Cedex, France,*(2004)27, 339.
29. ShoemakerD. P., GarlandC. W., *Experiments in Physical Chemistry, 5thed., McGraw-Hill International Edition, New York,*(1989)48, 536.
30. DeshmukhM. B., Dhongade-DesaiS., ChavanS. S., *Indian J. Chem.*(2005)44, 1659.
31. Barry BL. "Procedure and theoretical consideration for testing antimicrobial agents in agar media", 5thEdn, William Wilkins Baltimore (1991).

32. Harsfall JG. Bot Rev. (1945)11,357.

33. Patange V.N., Ph.D. Thesis, Dr.BabasahebAmbedkarMarathwada University, July 2009.

34. Balaji H. Jawale and shridhar D. salunke, Research Journal of Pharmaceutical, Biological and Chemical Sciences,2017,8(2),1260.

35. Geethaparameswaran and B. Sleema, Asian journal of chemistry,15(2) (April,2003),803-807.

36. Bhave N.S. and Kharat, J. Ind. Chem. Soc. 74(1997)75-78.

37. B.Viswanathan, J Gopalakrishan, V Srinivasan and MVC Sastri, Journal of thermal analysis, 3(4) (1971)429-431.

38. Makode J.J. and Aswar A.S. Indian.J.Chem, 43A (2004) 2120.

39. P.S.Mane, S.D.Salunke, S.G.Shirodkar and T.K.Chondhekar, J. Indian Chem.Soc., 79 (7), (2002) 611-613.

40. Willium F. Goure and Thomas J Barton, Journal of Organometallic Chemistry,199(1)(1980)33-41.

Synthesis of Co3o4 Nanomaterial and Study There Appliccation in Antmicrobial Activity and Photocatalytical Degridtion Studis

Suresh G. Muthe

Department of Chemistry, Agasti Arts, Commerce and Dadasaheb Rupwate Science College, Akole. Maharashtra 422601, India.

Ashok R.Bambale

Department of Chemistry, S. N. Arts, D. J. Malpani Commerce and B. N. Sarda Science College, Sangamner, Maharashtra 422605, India.

Sulochana B. Dhindale

Adv. M. N. Deshmukh Arts, Science and Commerce College, Rajur. Maharashtra 422604, India.

Abstract:

In the present work we prove that Photocatalytical Degradation of Rossaaniline Hydrochloride dye by using Co_3O_4 as catalyst. The Co_3O_4 nanoparticles were synthesized by chemical Co- precipitation. Co_3O_4 nanoparticle photocatalytically degradation studies were carried out the Rossaaniline Hydrochloride dye by using Co_3O_4 nanoparticle in aqueous solution .different parameter like catalyst properties , effect of ppm concentration aqueous solutions and antimicrobial activities have been studied to optimize reaction condition. In present work the use of semiconductor metal oxide a photo- catalyst for degradation of pollutant has attracted attention of researcher.

The material used for synthesis of nanoparticles is 0.01 M Cobalt Nitrate, 0.02M Cobalt Sulphate, 1:1 Ammonium solution and Distilled water. The Co-precipitation is one of famous method for synthesis of Co_3O_4 nanoparticles. A colorless crystal organic base ,$C_{20}H_{21}N_3O$ or more of these base's yellow-brown or green crystalline Hydrochloride salt which from red solution in water derived from aniline & use in the manufacture of fuchsine & other dyes & in Schiff's reagent. The degradation of Rossaaniline Hydrochloride dye is studied into two sets; first one is before degradation and after degradation. Change in color and absorbance after and before degradation of Rossaaniline Hydrochloride dye by using Co3O4nanoparticle photo catalytically at 460nm wavelength. Bioassay is important and crucial in evaluation of bioactivity of compound and helpful .In the present work all derivative have been for their anti-microbial activities against different bacteria like as Pseudomonas , S.Aurious & E –coli .The are many applications are mentioned in this present work.

Introduction:

The preparation of nano particle of Co_3O_4 nanoparticle. In present era the use of semiconductor metal oxide a photo- catalyst for degradation of pollutant has attracted attention of researcher. Semiconductor metal oxide nano particle have been studied to their novel optical electromagnetic thermal and Anti-microbial activity properties and potential application in catalyst dye are not removed by traditional method such as chemical method.

Now a day the advance oxidation process is use for the detoxification of contaminated dye solution. Now a days advantages as complete minimization of the pollutants are selective process can be use contaminated and can be combine with other method .advance oxidation process are based on generation reactive species though illumination of solar light of same active material. These process use to oxidise organic and inorganic alternative in future for with low

photo catalytically activity. Degradation of organic pollutant and toxic dyes has been important aspect to study the photo catalytically efficiency of magnetic composite

Rosa aniline Hydrochloride dye use Co_3O_4 nanocomposite as catalyst photo catalytically degradation is carried out and also study the degradation kinetics of Rosa aniline Hydrochloride on Co_3O_4 nano composite

Synthesis of nanoparticle: Co_3O_4 material

1)0.01M Cobalt Nitrate = 2.910gm Co(NO3)3.9H2O 2)0.02M Cobalt sulphate = 5.622 CoSO4.H2O

3)   Distilled water =80

4)   1:1 Ammonium solution PROCEDURE

Co3O4 magnetic particles were prepared by Co-precipitation method .A complete Co-precipitation of Co3O4was achieved under basic condition by maintaining molar ratio of Co(NO3)3.9H2O :CoSO4.H2O as 1:2 in this experiment Co(NO3)3.9H2O and CoSO4.H2O were dissolve in 80ml distilled water with vigorous magnetic stirring after stirring after stirring this solution heated up to 80o C then slowly added 1:1 ammonia solution up to pH 11 .At this condition complete growth of Co3O4 crystal was observed . The resulting nanoparticles were filtered and repeatedly.

Synthesis of nanoparticle: Co_3O_4 material

Degradation:

Photocatalytical degradation of Rossaaniline Hydrochloride dye by using Co_3O_4 as catalyst Information about Rossaaniline Hydrochloride dye A colorless crystal organic base, $C_{20}H_{21}N_3O$ or more of these base's yellow-brown or green crystalline Hydrochloride salt which from red solution in water derived from aniline & use in the manufacture of fuchsine & other dyes & in Schiff's reagent.

Experimental WorkPart- 1

Prepare different type of ppm solution of dye with Co_3O_4 nanoparticles using as a catalyst dissolve both 100ml distilled water and check the absorbance of the solution using Spectrophotometer .then keep all the solution in direct sun light about 2 hrs. At time of atmosphere is more after 2hrs check the absorbance of all solution of dye and observe the changes.

PART-2

After doing above process the solution which is having absorbance is chosen for the preparation of solution keep the quantity of dye as it is and changes the quantity of Co_3O_4 nanoparticle dissolves in 100ml water and dye solution. Now kept it again indirect sunlight for 2 hrs and check the absorbance .I have done the photo- catalytically degradation of Rossaaniline Hydrochloride dye using Co_3O_4.

Preparation of different ppm solution of Rossaaniline Hydrochloride dye

1) 10 ppm solution - 1ml Rossaaniline Hydrochloride dye+0.1gm Co_3O_4+99ml distilled water
2) 20 ppm solution -2ml Rossaaniline Hydrochloride dye+0.1gm Co_3O_4+98ml distilled water
3) 30ppm solution -3ml Rossaaniline Hydrochloride dye+0.1gm Co_3O_4+97ml distilled water
4) 40 ppm solution- 4ml Rossaaniline Hydrochloride dye+0.1gm Co_3O_4+96ml distilled water
5) 50ppm solution -5ml Rossaaniline Hydrochloride dye+0.1gm Co_3O_4+95ml distilled water
6) 60 ppm solution- 6ml Rossaaniline Hydrochloride dye+0.1gm Co_3O_4+94ml distilled water
7) 70ppm solution -7ml Rossaaniline Hydrochloride dye+0.1gm Co_3O_4+93ml distilled water
8) 80 ppm solution- 8ml Rossaaniline Hydrochloride dye+0.1gm Co_3O_4+92ml distilled water
9) 90 ppm solution -9ml Rossaaniline Hydrochloride dye+0.1gm Co_3O_4+91ml distilled water
10) 100ppm solution- 10ml Rossaaniline Hydrochloride dye+0.1gm Co_3O_4+90ml distilled water

Part -1: OBSERVATION TABLEWAVELENTH -460

DIFFERENT TYPE OF PPM SOLUTION DYE + CATAYST	ABSOURBANCE (INITIAL ABSOURBANCE)	ABSOURBANCE (FINAL ABSOURBANCE)
10 PPM	0.983	0.190
20PPM	1.055	0.330
30 PPM	1.129	0.540
40PPM	1.184	0.710
50 PPM	1.240	0.970
60 PPM	1.256	1.029
70 PPM	1.263	1.057
80PPM	1.289	1.069
90 PPM	1.296	1.082
100 PPM	1.303	1.092

Photocatalytical Degradation

Before Degradation (Co_3O_4)

After degradation (Co_3O_4)

Part -2

After completion the above processes choose that solution which is having high absorbance i.e. 100ppm solution which is having high absorbance make the 100ppm solution of dye with variable quantity of catalyst for further process

Solution Preparation

1) 100 PPM SOLUTION -10ml Rossaaniline Hydrochloride dye +0.1 gm Co_3O_4 nanoparticles+ 90 mlDistilled water

2) 100 PPM SOLUTION -10ml Rossaaniline Hydrochloride dye +0.2gm Co_3O_4 nanoparticles + 90 mlDistilled water

3) 100 PPM SOLUTION -10ml Rossaaniline Hydrochloride dye +0.3 gm Co_3O_4 nanoparticles+ 90 mlDistilled water

4) 1100 PPM SOLUTION -0ml Rossaaniline Hydrochloride dye +0.4 gm Co_3O_4 nanoparticles+ 90 mlDistilled water

5) 100 PPM SOLUTION -10ml Rossaaniline Hydrochloride dye +0.5 gm Co_3O_4 nanoparticles+ 90 mlDistilled water

6) 100 PPM SOLUTION -10ml Rossaaniline Hydrochloride dye +0.6 gm Co_3O_4 nanoparticles+ 90 mlDistilled water

PART -2 OBSERVATION TABLE

CONSTANT PPM SOLUTION WITH DIFFERENT QUNTITY OF CATALYST	ABSOURBANCE (INITIAL ABSOURBANCE	ABSOURBANCE (FINAL ABSOURBANCE)
100 PPM+0.1gm Co_3O_4	1.902	1.784
100PPM+0.2gm Co_3O_4	1.890	1.785
100 PPM +0.3gm Co_3O_4	1.859	1.797
100 PPM+ 0.4gm Co_3O_4	1.712	1.655
100 PPM +0.5gm Co_3O_4	1.605	1.570
100PPM +0.6gm Co_3O_4	1.583	1.563

'RESEARCH JOURNEY' *International E- Research Journal*
Special Issue – 333 : Innovative & Sustainable Chemistry
Impact Factor 6.625 (SJIF)   Peer Reviewed Journal

E-ISSN :
2348-7143
December - 2023

Photocatalytical degradation

Before degradation – Co_3O_4

After degradation – Co_3O_4

Graph of removal of dye

% Removal of dye is carried out by using following

%Removal =Ai-Af/Ai

Where

Ai=Initial absorbance

Af= final absorbance

Graph of Conc. of Dye mg/lit Vs % of degradation of Dye is shown as follow

SET-1

Rossaaniline Hydrochloride & Co_3O_4 (Wavelength- 460 nm)

PPM	% REMVOAL
10	0.399
20	0.689
30	0.521
40	0.400
50	0.210
60	0.180
70	0.163
80	0.170
90	0.165
100	0.161
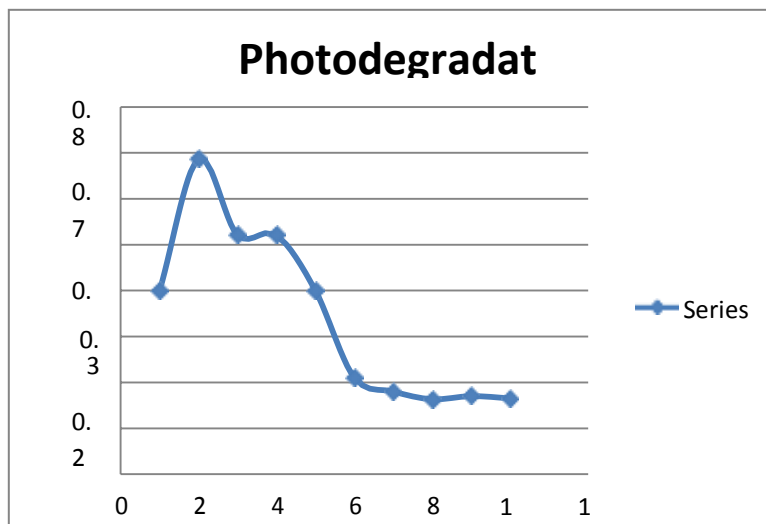
SET-2

Rossaaniline Hydrochloride dye & Co_3O_4 (WAVELENTH -460 nm)

AMOUNT OF Co3O4 WITH 100PPM	% REMOVAL
0.1	0.062
0.2	0.055
0.3	0.033
0.4	0.032
0.5	0.021
0.6	0.012

Resutl Of Photocatalytycal Degridation
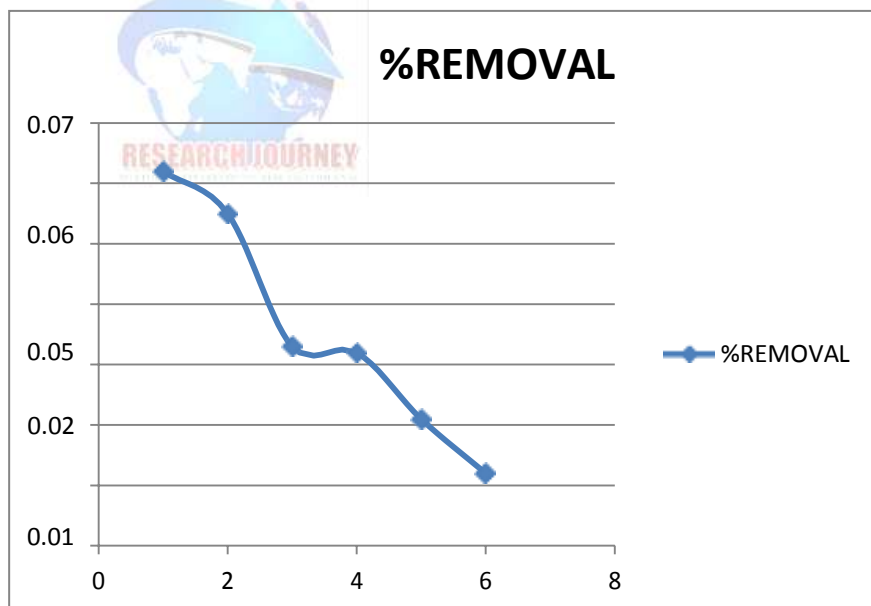
SR.No	DEGRIDATION	% of Removal
1	SET -1	20%=0.689
2	SET-2	0.1=0.62

Density

In general, nanoparticle of Co_3O_4 is denser than water. The magnitude of ϱ, in the case of nanoparticle depends upon the constituent of cat ion and anion. For the instance, the ϱ value of nanoparticle varies with % concentration the density of comparable ionic liquid increases with increase in concentration.

Further, the density of nanoparticle also depends upon the mass. Normally ϱ of nanoparticles inthe range of 1.22 to 1.33 at room temperature.

Gravity bottle

Observation
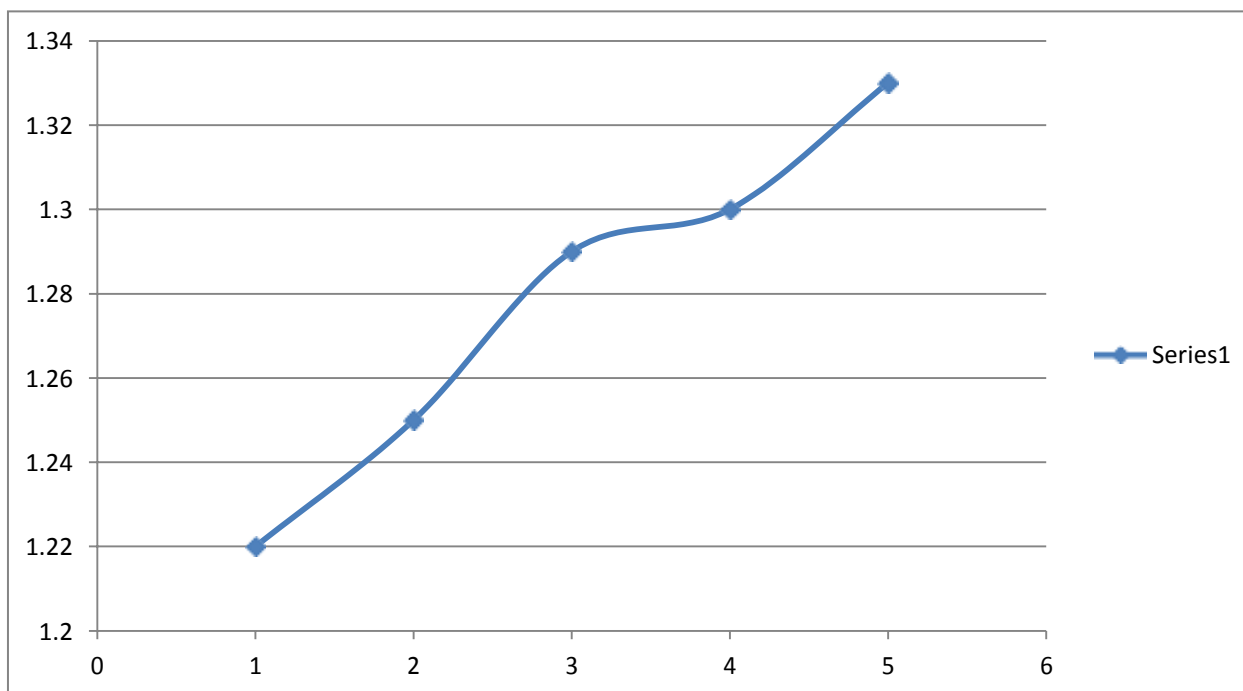
The empty weight of gravity bottle

(W2) =17.18 gmGRAVITY BOTTLE

Observation Table:

Sr No	Percentage of solution	Weight of gravity bottle of solution	W_2-W_1	Density =mass/volume
1	1%	29.380	12.2	1.22
2	2%	29.710	12.5	1.25
3	3%	30.130	12.9	1.29
4	4%	30.270	13.09	1.30
5	5%	30.540	13.3	1.33

'RESEARCH JOURNEY' *International E- Research Journal*
Special Issue – 333 : Innovative & Sustainable Chemistry
Impact Factor 6.625 (SJIF)   Peer Reviewed Journal

E-ISSN : 2348-7143
December - 2023

GRAPH OF DENSITY

Study of Antimicrobial Activity Of Nano Partical
Peaparation Of The Nutient Growth Cluture

The nutrient agar is prepared which solidified after cooling is poured in petriplate with the condition along with these microorganism are poured on the nutrient agar solution then separation are made

By making the small portion of filter paper with the help of machine the small portion of filter are dipped in perception solution which was then placed inside the petriplates in which the agar solution was already poured

After this plate were incubated for 24 hr and result as summarized

Sr no	Nano particle	Zone of inhibition in mm
1	Co_3O_4	**8 mm**

Bioassys

- Bioassay is important and crucial in evaluation of bioactivty of compound and helpful .In the presnt work all all derivative have been for their anti microbial activities aganst different bacteria like as Pseudomonas , S.aurious & E –coile
- >Microbial activity of the nano composites solution
- Microorganism use is
- 1)Pseudomonas
- 2) S.aurious
- 3)E-coile
- labelling of the sample

Result and Discussion of the Test Microbial Test :

As microbe use example of E-coile which is found in our body intestine which is pathogen organism cause urinary tract infection

B)All result are positive .that zone of inhibition was absent ,suggestion that above nano composite can inhibited growth of microorganism

The microbial testing was done by making two or four quadrant in petriplate which as show in the following figure

Antimicrobial activities

S.Aurious   Pseudomonas

E-coile

Result & Conclusion:

1. Colour of the Rossaaniline Hydrochloride dye solution changes after degradation it become intense in colure
2. Absorbance of the solution with increases with catalyst (Co3O4) concentrated .
3. The antimicrobial activity of (Co3O4) nanopartical is all result is positive.

Applications:

1. The synthesis of magnetic nanoparticles has been intensively developed not only for its fundamental scientific interest but also for many technological.

2. A catalyst in the manufacture off all allyl alcohol ceramics colored glass in biosensors, coating plastics nanowire nanofiber and textiles

3. As a magnetic nanoparticle for magnetic data storage and magnetic resonance imaging .

4. The Co3O4 is magnetic nanoparticle uses in micro- batteries and specific alloy and catalyst application.

5. Also microelectronics, superconductor, electronics –ceramics ,electro chromic devices .

References:

1. Orfao j, Silva A ,Perira J, Barata S, Fonseca I,Faria P.J, col.inter sci 2006,480-9

2. Yazdanbakhsh ,Khosarvi M, Goharshadi I , Youssefi E.K.,J hazard Mater ,2010 ,184,684-689.

3. Irie shibanuma H ,Kamiya T, Miura k, Yokoyama S, Hashimoto T App.catal,2010 B 96 142-147.

4. fuko, Hashimoto k,Kominami k, H.chem commun., 2010,46,5118,5120

5. Valenzuela bosch M.A ,Jimenez –Becerrill P Quiroz A.I,Paez A.I , j.phtochem photobial .,2002A 148,177-182.

6. selvan, Gedanken R.K. Anilkumar A Manikandan P , karunakaran G , J .Cluster Sci 2009,20,291-305 .

7. waldmann, Paz N.S.Y, J .Phys chem 2010,C 114,18946-18952.

8. Imashi, M Hashimoto , K.kominami ,appl.Catal 2010B 97,213-219.

9. Zhang Zhang W W Chen J .Y. Catal commun 2009,10 1781-1785.

10. Zhang, Zhang W W , Lan J.Y Chen X Wang Z.Y, Catal Commun.2010,11,1140-1180.

11. Tang, Zou J .W , Ye Z.G Chem .mater 2004,16,1644-1649.

12. Tang J.W Zou Z. G , Yin J .H ,Chem .phys lett., 2003 ,382,175-179.

13. Fan Gu G.L Yang Z. J, Li L , chem eng J 2009,155,534-541.

14. Cao, zhu S.W , Cheng.Y.J Huaug .G.F, J Hazard mater 2009,171,431-435.

15. Amekura H, Umeda N,takeda N Tadaka Y , Lu J and kishmoto N, appl phy lett ., 2004 85,6

16. Grutter C and teller J , J magnMagn .,1999,194,8-15.

17. Guo L, Huang J , Li X Y and Yang S.H.Phys chem .,2001,3 1661-1665

18. Estepa L and Daudon M, Biospectroscopy ,1997,3 347-369.

Synthesis of CoO, NiO Nanoparticles, CoO@pani and NiO@pani Nanocomposites CoNiO₂, CoNiO₂ Doped PANI and Investigation of its Photocatalyst Activity

Ramdas S. Suralkar[1], Deepak M. Nagrik[2], Umesh S. Shelke[3] Ravi S. Balaskar[4]

[1] Pratap College Amalner (M.S.) India.

[2] G. S. College Khamgaon (M.S.) India

[3] Rajarshi Chhatrapati Shahu College Kolhapur (M.S.) India

[4] Pratap College Amalner (M.S.) India

Abstract:

The use of ZnO, TiO₂ as photocatalyst for dye degradation has been reported with varying conc, pH, temperature conditions. The catalyst can be prepared by various method includes hydro thermal, Co-precipitation, gel filtration techniques. In this work Synthesis of CoO, NiO Nanoparticles, CoO@Pani and NiO@Pani nanocomposites CoNiO₂, CoNiO₂ doped PANI as photocatalyst for dye degradation are synthesize by Co-precipitation method.

Keywords: Dye degradation. Photocatalyst, nanoparticles, nanocomposites

1. Introduction:

Large quantities of toxic organic dyes are produced in the industry, which can cause many environmental problems and result in varying types of cancer throughout humans. Therefore, the development of cheap and environmentally friendly methods to remove these hazardous materials from the environment and underground water has become a critical challenge. In recent decades, the progressed photocatalysts have attracted a lot of attention, as well as the interest of many that consider the usage of photocatalyst technology as a new approach in discovering a solution for cleaning environmental pollutants. Healthy water is defined as the water that has lost its toxic chemicals and pathogens, and its existence is essential for continuing life. Besides, water stands as a vital raw material in many major industries including electronics, medicine, and food technologies. Nowadays, the transit of science and technology, along with the rapid progress of varying fields of technologies, have been able to provide new resolutions and achievements in various areas of science, especially throughout the treatment of industrial wastewater and sewage. Nanoscience has an exceptional stance on the subject of recognizing and eliminating various organic pollutants. Recently, the advent of novel technologies in the treatment of water and industrial waste has provided and introduced new resolutions, which involve the utilization of nanotechnology.

2. Experimental:

2.1 Material:

Aniline monomer, Ni $(NO_3)_2.6H_2O$, Co $(NO_3)_2.6H_2O$, ammonium persulfate (APS), acetone, methanol and hydrochloric acid all of GR grade, are purchased from a Merck (India) company, and they were used as received without further purification process. Double distilled water was used throughout this work.

2.2 Synthesis of CoO nanoparticles:

100 ml of 0.5 N NaOH is added drop by drop to the solution of 100 ml of 0.1N Co $(NO_3)_2.6H_2O$ with constant stirring for 1 hr. after complete addition the mixture is stirred for 2 hrs. then the precipitate is filtered and washed 2 to 3 times with distilled water and kept in an

oven at 40 ^{0}C for 48 hrs for complete drying. Then the ppt is calcinated in a muffle furnace for 3 hrs at 500 ^{0}C to get CoO nanoparticles.

2.3 Synthesis of CoO nanoparticles

100 ml of 0.5 N NaOH is added drop by drop to the solution of 100 ml of 0.1N Co $(NO_3)_2.6H_2O$ with constant stirring for 1 hr. after complete addition the mixture is stirred for 2 hrs. then the precipitate is filtered and washed 2 to 3 times with distilled water and kept in an oven at 40 ^{0}C for 48 hrs for complete drying. Then the ppt is calcinated in a muffle furnace for 3 hrs at 500 ^{0}C to get CoO nanoparticles.

2.4 Synthesis of CoO@Pani nanocomposites

Take 10 ml of 1 M HCl solution in a 250 ml RB flask and add 0.1 gm of CoO nanoparticles in it. The mixture is sonicated in an ultrasound bath for 30 minutes. 1 ml aniline is added in 100 ml 1 M HCl solution in a beaker. This solution is added in RB flask and sonicated for 30 minutes.2.84 gm of ammonium peroxy sulphate (APS) equal molar with aniline is added in 100ml 1M HCl solution in a beaker. This solution is filled in a burette and added dropwise to the mixture in an RB flask kept on magnetic stirrer. This RB flask is kept in glass bowl filled with ice to maintain temperature below 4 ^{0}C to achieve polymerization of aniline to polyaniline (Pani). green colour is developed to the mixture which indicate start of polymerisation reaction. After complete addition of APS solution, the mixture kept on constant stirring for 1 hr. the solution is filtered and washed several times with distilled water and kept in an oven at 45 ^{0}C for complete drying. The dried powder is obtained as 10% CoO doped Pani as nanocomposite.

2.5 Synthesis of NiO@Pani nanocomposites

Take 10 ml of 1 M HCl solution in a 250 ml RB flask and add 0.1 gm of NiO nanoparticles in it. The mixture is sonicated in an ultrasound bath for 30 minutes. 1 ml aniline is added in 100 ml 1 M HCl solution in a beaker. This solution is added in RB flask and sonicated for 30 minutes.2.84 gm of ammonium peroxy sulphate (APS) equal molar with aniline is added in 100ml 1M HCl solution in a beaker. This solution is filled in a burette and added dropwise to the mixture in an RB flask kept on magnetic stirrer. This RB flask is kept in glass bowl filled with ice to maintain temperature below 4 ^{0}C to achieve polymerization of aniline to polyaniline (Pani). green colour is developed to the mixture which indicate start of polymerisation reaction. After complete addition of APS solution, the mixture kept on constant stirring for 1 hr. the solution is filtered and washed several times with distilled water and kept in an oven at 45 ^{0}C for complete drying. The dried powder is obtained as 10% NiO doped Pani as nanocomposite.

3. Result and Discussion:

3.1 Measurement of Photocatalyst Activities:

The photocatalytic degradation of Methyl orange (MO), Congo red (CR) and Crystal violet (CV) dyes was performed under the irradiation of natural sunlight in the presence of the NiO, CoO nanoparticles or the NiO@Pani and CoO@Pani nanocomposite as catalyst. In the photocatalytic treatment of the dyes, a known concentration (50 ppm) of the dye solution was taken in a beaker. 1mg/ml of catalysts was added to the dye solution. Before irradiation of the dye solution, the suspension was stirred for 10 min to realize adsorption−desorption equilibrium in the presence of the catalyst. This procedure was applied to all dye solutions. After that, the suspensions were irradiated without stirring. In order to determine the photocatalytic activity of the catalyst under natural sunlight irradiation, all experiments were done under open atmosphere

and clear sky between 1:00 p.m. and 5:00 p.m. when the solar intensity fluctuations were minimal, in the months of March and April 2023. The photocatalytic degradation of organic dyes was investigated at room temperature in the presence of different catalysts, under sunlight irradiation. The concentrations of MO, CV and CR organic dyes were analysed using visible colorimeter. The degradation efficiency of dye is calculated by the following equation:

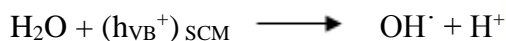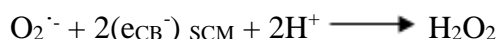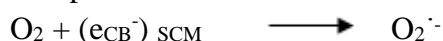$$\text{degradation (\%)} = \frac{C_o - C_t}{C_o} \cdot 100$$

where C_0 is the initial concentration of dye before irradiation and C_t is the concentration of dye after a certain irradiation time.

3.2 Possible Mechanism of dye degradation

The general understanding of the photocatalysis mechanism is that the photo absorption of a semiconducting material causes the electrons to excite from the valence band (VB) to the conduction band (CB), leaving positive holes in the VB resulting in the electron−hole pair e_{CB}^- / h_{VB}^+ generation. It is known that PANI homopolymer is a conducting polymer. Photons are absorbed by the PANI homopolymer or the PANI/metal oxide catalyst when the energy (hν) is equal to or greater than the semiconductor band gap, and electron−hole pairs are generated in these semiconducting materials (SCM)

$$\text{SCM (NiO, CoO, PANI/NiO, PANI/CoO)} + h\nu \longrightarrow (e_{CB}^-)_{SCM} + (h_{VB}^+)_{SCM}$$
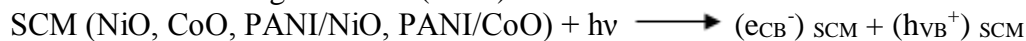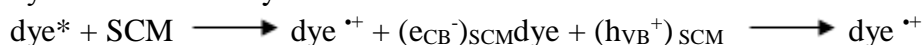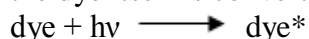
Then, the photogenerated electron−hole pairs migrate to the surface of the catalyst and react with the species adsorbed on the surface.

$$O_2 + (e_{CB}^-)_{SCM} \longrightarrow O_2^{\cdot -}$$
$$O_2^{\cdot -} + 2(e_{CB}^-)_{SCM} + 2H^+ \longrightarrow H_2O_2$$
$$(e_{CB}^-)_{SCM} + O_2^{\cdot -} + 2H^+ \longrightarrow OH^{\cdot} + OH^-$$
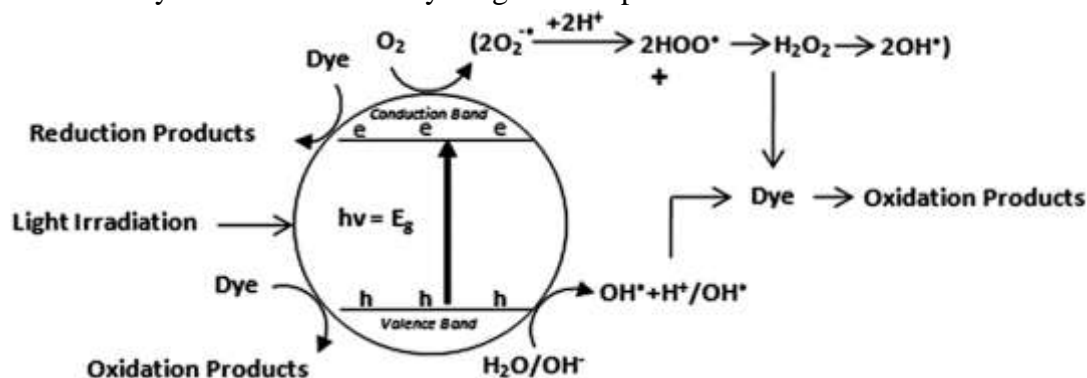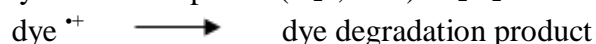$$H_2O + (h_{VB}^+)_{SCM} \longrightarrow OH^{\cdot} + H^+$$

These reactions prevent the electron−hole pairs from recombining which reduces the efficiency of photocatalytic activity.

A sensitized photocatalytic process may be able to be operated in the presence of a coloured organic compound; in this case the adsorbed dye molecules are excited by visible light and thus act as photosensitizers. The excited dye molecule subsequently transfers electrons into the conduction band of the PANI homopolymer or the PANI/NiO, PANI/CoO nanocomposite, while the dye itself is converted to its cationic radical.

$$dye + h\nu \longrightarrow dye^*$$
$$dye^* + SCM \longrightarrow dye^{\cdot +} + (e_{CB}^-)_{SCM} \quad dye + (h_{VB}^+)_{SCM} \longrightarrow dye^{\cdot +}$$

These reactive species produced in the above manner can then react with the dye to form the degradation products and thus are responsible for the discoloration of MO, CV and CR dyes.

$$dye + \text{radical species } (O_2^{\cdot -}, OH^{\cdot})/ H_2O_2 \longrightarrow \text{degradation product}$$
$$dye^{\cdot +} \longrightarrow \text{dye degradation product}$$

3.3 CoO,NiO, CoO@Pani and NiO@Pani nanocomposites as Photocatalyst for dye degradation
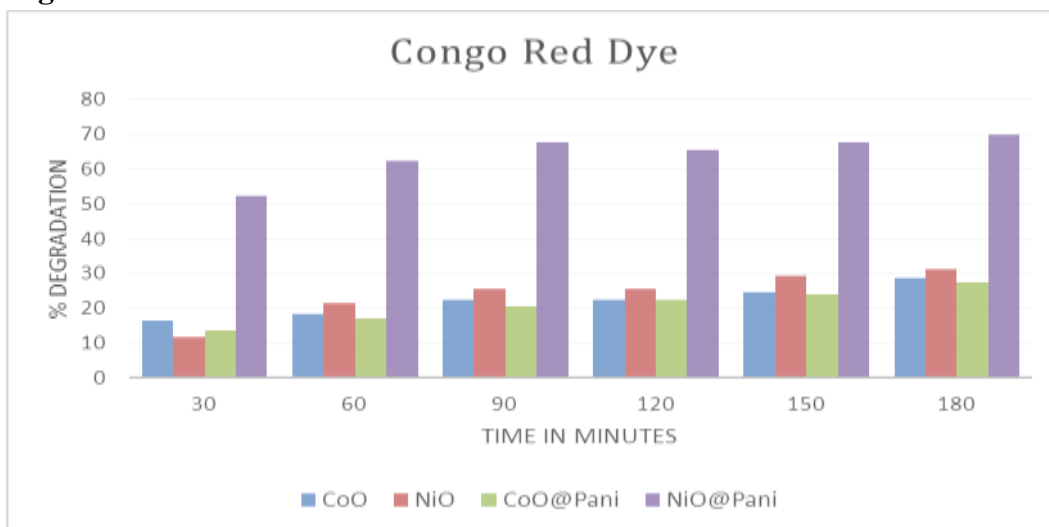

Figure 1: Use CoO,NiO, CoO@Pani and NiO@Pani nanocomposites as Photocatalyst For CR dye at pH 4 without H_2O_2
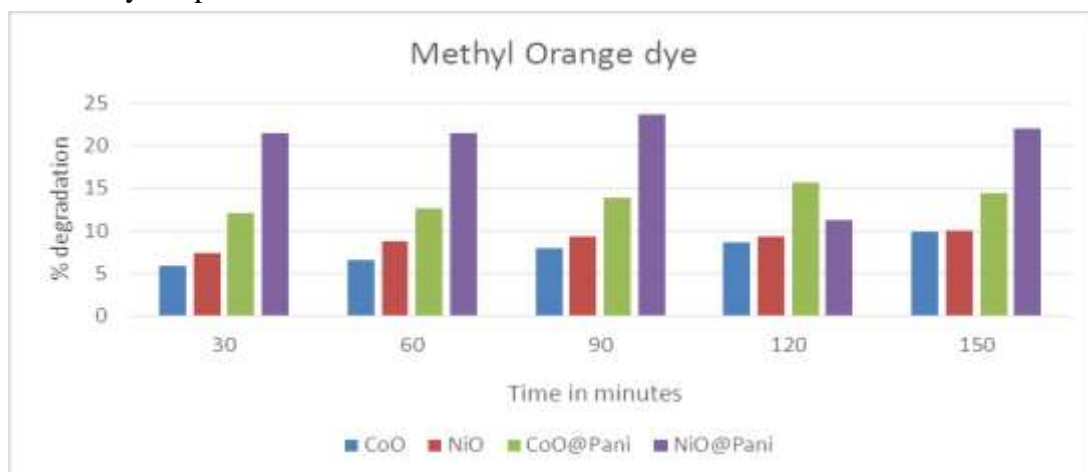

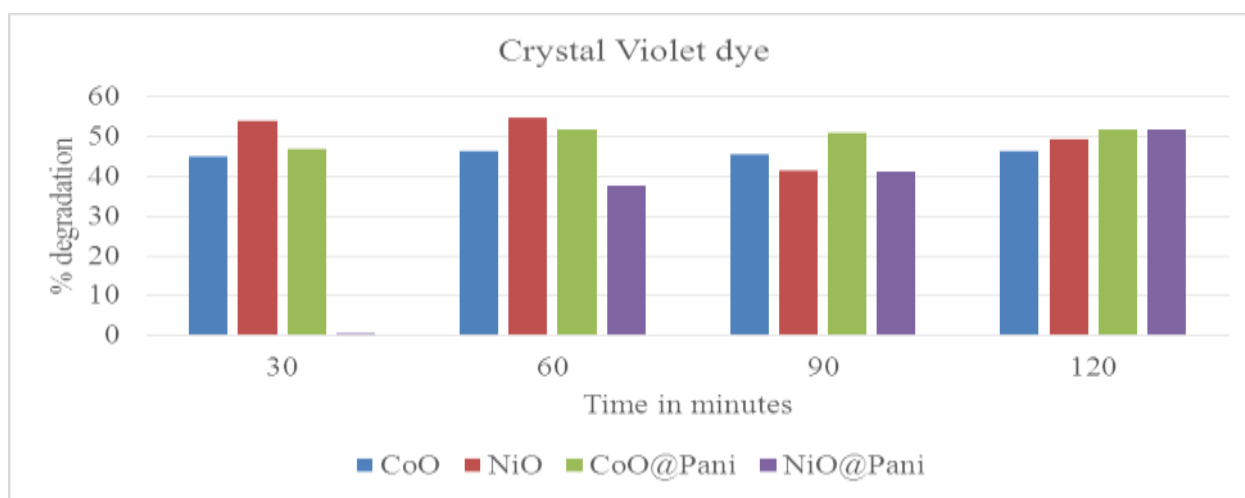**Figure 2:** Use CoO,NiO, CoO@Pani and NiO@Pani nanocomposites as Photocatalyst For MO dye at pH 4, H_2O_2 8mM

Figure 3: Use CoO,NiO, CoO@Pani and NiO@Pani nanocomposites as Photocatalyst For CR dye at pH 9, H_2O_2 8mM
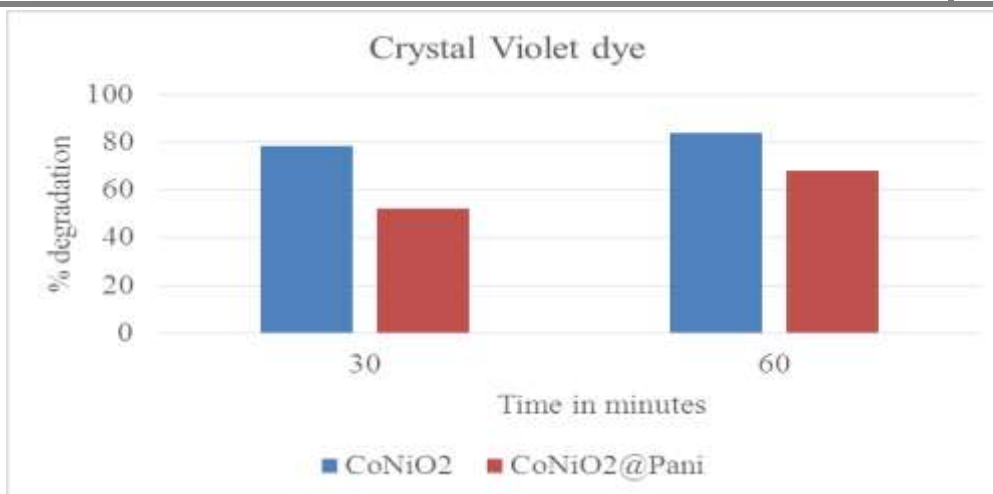
Figure 4: Use of $Co_x Ni_{(1-x)} O_2$ nanoparticles and $Co_x Ni_{(1-x)} O_2$ @ Pani nanocomposites as Photocatalyst for CV dye at pH 9 without H_2O_2.
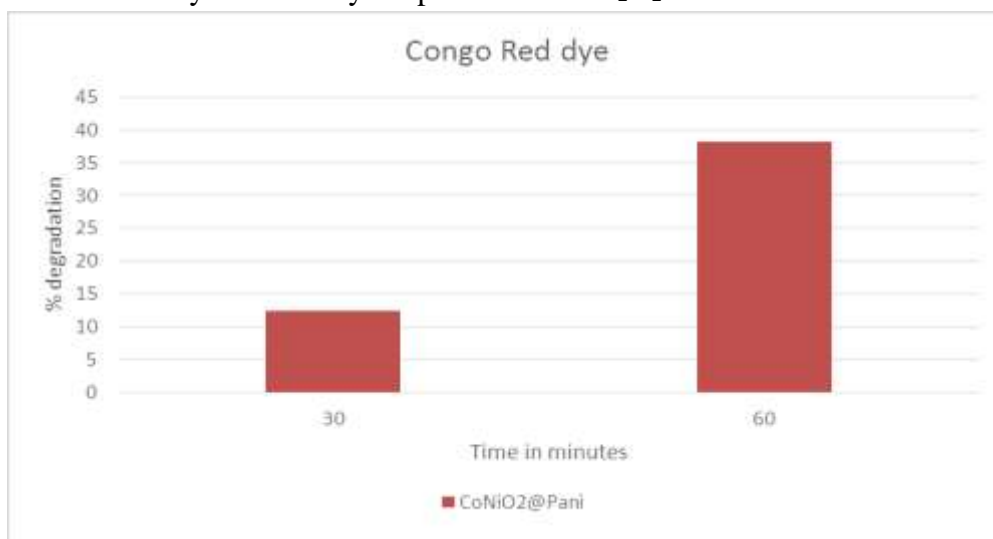
Figure 5: Use of $Co_x Ni_{(1-x)} O_2$ @ Pani nanocomposites as Photocatalyst for CR dye at pH 9 without H_2O_2

4. Conclusion

- ❖ NiO@Pani nanocomposite material is best catalyst for CR dye at pH 4 gives 70 % degradation in 3 hrs without using H_2O_2.
- ❖ NiO@Pani nanocomposites material is best catalyst for MO dye at pH 4, using H_2O_2 8mM.
- ❖ CoO@Pani and NiO@Pani nanocomposites are more efficient Photocatalyst for CV dye at pH 9, H_2O_2 8mM.
- ❖ $Co_x Ni_{(1-x)} O_2$ nanoparticles as binary metal oxide is more efficient Photocatalyst for CV dye at pH 9 without H_2O_2.
- ❖ Use of $Co_x Ni_{(1-x)} O_2$ @ Pani nanocomposites is better Photocatalyst for CR dye at pH 9 without H_2O_2.

5. References:

1. Vosoughifar, Photodegradation of dye in waste water using CaWO4/NiO nanocomposites; Co-precipitation preparation and characterization, J. Mater. Sci.- Mater. Electron. 29 (2018) 3194–3200.

2. N. Duraisamy, K. Kandiah, R. Rajendran, S. Prabhu, R. Ramesh, G. Dhanaraj, Electrochemical and photocatalytic investigation of nickel oxide for energy storage and wastewater treatment, Res. Chem. Intermed. 44 (2018) 5653–5667.

3. M. Qamar, M.A. Gondal, Z.H. Yamani, Synthesis of nanostructured NiO and its application in laser-induced photocatalytic reduction of Cr (VI) from water, J. Mol. Catal. A – Chem. 341 (2011) 83–88.

4. S.R. Dave Sushma, Use of Nanoparticles in Water Treatment: A review International Research Journal of Environment Science, 4 (2015) 103–106.

5. X. Cai, Y. Liu, H. Zeng, Y. Cai, H. Li, F. Zhang, Y. Wang, Synthesis and characterisation of alkali metal (Mn, Fe) oxide–ZnO nanorod composites and their photocatalytic decolourization of rhodamine B under visible light, Mater. Technol. 27 (2012) 380–387.

6. P.P. Hung, T.T. Dat, D.D. Dung, N.N. Trung, M.H. Hanh, D.N. Toan, L.H. Bac, Effect of annealing temperature on structural, optical and visible-light photocatalytic properties of NiTiO3 nanopowders, J. Electron. Mater. 47 (2018) 7301–7308.

7. B. Elahi, M. Mirzaee, M. Darroudi, R.K. Oskuee, K. Sadri, M.S. Amiri, Preparation of cerium oxide nanoparticles in Salvia Macrosiphon Boiss seeds extract and investigation of their photo-catalytic activities, Ceram. Int. (2018).

8. M.R. Esfahani, S.A. Aktij, Z. Dabaghian, M.D. Firouzjaei, A. Rahimpour, J. Eke, I.C. Escobar, M. Abolhassani, L.F. Greenlee, A.R. Esfahani, Nanocomposite membranes for water separation and purification: fabrication, modification, and applications, Sep. Purif. Technol. (2018).

9. X. Ren, P. Gao, X. Kong, R. Jiang, P. Yang, Y. Chen, Q. Chi, B. Li, $NiO/Ni/TiO_2$ nanocables with Schottky/pn heterojunctions and the improved photocatalytic activities.

10. Y.C. Sharma, V.S., V.K.S., S.N.K., C.H. Weng, Nano-adsorbents for the removal of metallic pollutants from water and wastewater, Environ. Technol. 330 (2009) 583–609.

11. The application of nanoparticles for wastewater remediation, Fut. Sci. (2013).

12. A.I. Uzaira Rafique, Abida K. Khan, Synthesis, characterization and application of nanomaterials for the removal of emerging pollutants from industrial waste water, kinetics and equilibrium model, J. Water Sustain. 2 (2012) 233–244.

13. M. Chakhoum, A. Boukhachem, M. Ghamnia, N. Benameur, N. Mahdhi, K. Raouadi, M. Amlouk, An attempt to study (111) oriented NiO-like TCO thin films in terms of structural, optical properties and photocatalysis.

Review on Environmental Monitoring Sensors and Their Applications

Shaikh Asif Karim[1], Sayyed Mujeeb Hadi[2]
Dept. Of Physics, Sir Sayyed College, Aurangabad

Abstract:

Today, environmental monitoring is becoming important for people to ensure a safe and prosperous life. Monitoring requirements vary widely depending on the environment, leading to the specific use it needs adaptability. Environmental monitoring sensors help protect the public and the environment from toxic contaminants and pathogens. Different types of environmental sensors and their applications are discussed in this article. Environmental sensors are used to measure, monitor and record environmental parameters such as humidity, temperature and heat loss. Environmental sensors are widely used in air pollution monitoring, smart homes, consumer electronics and other devices.

Introduction:

Monitoring of environmental pollution is necessary and considered a crucial element in the assessment of air quality in cities and rural areas. Detection and monitoring of odorous and chemical pollutants in the environment have become a major challenge for the modern developed and developing countries. Annually billions of tons of organic and inorganic chemical pollutants are released into air, water, and soil, which affect the health risks to plants, animals, and humans. Environmental pollution monitoring essential pollutants include sulfur dioxide, carbon monoxide, nitrogen dioxide, and volatile organic compounds Air pollutants include sulfur dioxide, carbon monoxide, nitrogen dioxide, and volatile organic compounds that come from sources such as vehicle emissions, power plants, refineries and industrial and laboratory processes. Soil and water contaminants can be classified as microbiological, radioactive, inorganic, synthetic organic and volatile organic compounds. Pesticides and herbicides are applied directly to plants and soil and accidental releases of other contaminants can come from spills, leaking pipes, underground storage tanks, landfills, and waste storage facilities. Some of these contaminants can persist for many years and migrate over large areas of land until they reach water sources, where they may pose an ecological threat or a threat to human health.

Environmental Monitoring System:

1.   Smart Water Pollution Monitoring System

Various kinds of literature have been studied on intelligent water pollution monitoring (SWPM) methods and systems using machine learning, IoT and wireless sensors

Remote sensing images were analyzed and machine learning was used to predict pollution levels in the water, useful for agriculture. This work used conventional neural network-based machine learning and the prediction results were not very satisfactory. Water contamination classification was studied and water was classified as clean or polluted water using machine learning methods and IoT devices.The table below shows some significant contributions in the field of smart water pollution monitoring systems.

Methods used	Purpose
Machine learning for classification: drinkable or non-potable water	Drinking Water Analysis
Neural network for classification: drinkable or non-drinkable water	Water Contamination analysis
IoT for surface water quality assessment	Water quality monitoring
SVM for classification as polluted or clean water	Water contamination surveillance

2. Air Quality Monitoring:

Air quality assessment has been implemented usingfixed and mobile sensor capable of monitoring air quality in both stationary and mobile ways.compatible sensors have been deployed as mobile nodes that can perform satisfactorily in a moving environment. The data captured through smart sensor nodes was processed and analyzed using machine learning techniques. Another air quality management process was studied using IoT and machine learning techniquesfocusing on air pollution assessment. The deployment of gas sensors to help capture air particles and analysis of pollutants mixed in the air. Air quality monitoring sensor networks have been constructed in moving vehicles using machine-learning mobile sensor nodes and WSNs have been deployed. Infrared sensors have been deployed to assess air quality, particularly analyzing volatile organic compounds (VOCs) using machine learning methods.

Methods Used	Purpose
Heterogenous sensors	Air Quality
Gas Sensors, IoT, and Machine Learning	Air Quality
Infrared Sensors	Organic Compound Detection
Temperature, Humidity, Dust and Carbon Dioxide Sensor, LoRaWAN	Air Quality

Conclusion:

This article presents an extensive and critical review of research studies on various environmental monitoring systems used for various purposes. The analysis and discussion of the review suggested the main recommendations. There is need for extensive research on deep learning, and big data processing. We focused primarily on water quality and air quality monitoring as intelligent agricultural systems that can address environmental challenges.

References:

1. Sayed E., Ahmed A., Yousef M.E. Internet of things in Smart Environment: Concept, Applications, Challenges, and Future Directions. World Sci. News. 2019.
2. Jamil M.S., Jamil M.A., Mazhar A., Ikram A., Ahmed A., Munawar U. Smart Environment Monitoring System by Employing Wireless Sensor Networks on Vehicles for Pollution Free Smart Cities. Procedia Eng. 2015.
3. Bhoomika K.N., Deepa C., Rashmi R.K.S. Internet of Things for Environmental Monitoring. Int. J. Adv. Netw. Appl. 2016.
4. Kulkarni P.H., Kute P.D. Internet of Things Based System for Remote Monitoring of Weather Parameters and Applications. Int. J. Adv. Electron. Comput. Sci. 2016
5. Pavithra G. Journal of Agricultural Science and Intelligent Monitoring Device for Agricultural Greenhouse Using IOT. J. Agric. Sci. Food Res. 2018.
6. Li Y., Wang X., Zhao Z., Han S., Liu Z. Lagoon water quality monitoring based on digital image analysis and machine learning estimators. Water Res. 2020.
7. Ragi N.M., Holla R., Manju G. Predicting Water Quality Parameters Using Machine Learning; Proceedings of the 4th IEEE International Conference on Recent Trends on Electronics, Information & Communication Technology (RTEICT-2019); Bengaluru, India.
8. Gardner J. Smart Sensors in Mobile Phones for Environmental Monitoring; Proceedings of the Core-Group Meeting at Eurosensors—2014.
9. Jalal D., Ezzedine T. Toward a smart real time monitoring system for drinking water based on machine learning; Proceedings of the The 27 th International Conference on Software, Telecommunications and Computer Networks 2019.

Molecular interaction studies of binary systems of 2- (Dimethylamino) Ethanol with Cresols at298.15K and various compositions

S. J. Bhadane*[1], A.P.Manake[2] P. M. Raotole[3] and S.R. Patil [4].

1-Department of Chemistry, Uttamrao Patil Arts and Science College, Dahiwel (M.S.) India.
2-Department of Chemistry Pratap College Amalner (M.S.) India
3-   &4 Department of Chemistry, Arts and Science College, Chopda (M.S.), India.
srpatil_001@rediffmail.com

Abstract:

Viscosity (η), density (ρ), and ultrasonic velocity (U) studies of binary systems of 2-(Dimethylamino) ethanol with O-Cresol, P- Cresol and m-Cresol at various compositions and 298.15K were studied. The viscosity, density and ultrasonic velocity data are used for the determination of excess molar volume (V^E), the viscosity deviation (Δη) and isentropic compressibility (ΔKs). The viscosity value was observed to decrease with an increase in concentration of 2-(Dimethylamino) ethanol. A significant decrease in ultrasonic velocity was observed with a decrease in concentration in of 2- (Dimethylamino) ethanol. The positive value of isentropic compressibility (ΔKS) and negative excess molar values have been reported for 2-(Dimethylamino) ethanol   with cresols binary system is due to stronger dipole- dipole interactions.

1. Introduction:

Molecular interactions play an important role in liquid mixtures. They affect the arrangement, orientation, and conformation of molecules in solutions. The ultrasonic velocity is very useful in agriculture, medicine, engineering, and industry. [1-2]. The Viscosity (η), Density (ρ), and Ultrasonic velocities (U) measurements find wide applications in characterizing the physicochemical behavior of liquid mixtures [3-5]. 2-(Dimethylamino) ethanol is a tertiary amine and has been claimed to show good chemical stability and moderate regeneration energy requirements. [6] Physical and chemical data of this amine are required before it can potentially be applied as an absorbent for chemical processes. [7, 8] 2-(Dimethylamino) ethanol is a bifunctional compound containing both tertiary amine and primary alcohol functional groups. Amino-alcohols are bi-functional organic compounds having two kinds of polar groups, hydroxyl, and amino groups, leading to complicated intermolecular interactions with the molecules having polar groups. They are used as chemical intermediates for the pharmaceutical industry[2, 9]. It is important to study how the individual functional groups in multifunctional molecules interact with other molecules with suitable hydrogen bonding. In multifunctional molecules, the exact hydrogen bonding with suitable molecules will result in micro and complicated competition between various possibilities. So the binarysystem of 2-(Dimethylamino) ethanol with O-Cresol, P-Cresol, and m-Cresol is of considerable interest for finding the intra and intermolecular behavior of a present solvent system.

In this study, the measurement of viscosity, density, and ultrasonic velocity of a binary mixture of 2- (Dimethylamino) ethanol with O-Cresol, P-Cresol and m-Cresol at different compositions and at temperature

298.15K was carried out.

2. Material and method:

2-(Dimethylamino)ethanol, O-Cresol, P-Cresol, and m-Cresol used are 99% pure from E-Merck, Germany, and Sd Fine chemicals, India, without purification.

The purities of the above chemicals were checked by density determination at 298.15K the uncertainty is less than $\pm$ 1x10^{-4} g cm^{-3}. The binary liquid mixtures of different known compositions were prepared in stopper measuring flasks. The density, viscosity, and ultrasonic velocity were measured as a function of the composition of the binary liquid mixture of 2-(Dimethylamino) ethanol, O-Cresol, P-Cresol, and m-Cresol respectively at

298.15 K. The density was determined using a Bi-capillary pycnometer. The weight of the sample was measured using an electronic digital balance with an accuracy of $\pm$ 0.1 mg (Model: Shimadzu AX-200). An Ubbelohde viscometer (20ml) was used for the viscosity measurement and efflux time was determined using a digital clock to within $\pm$0.01s. An ultrasonic interferometer having a frequency of 2 MHz (Mittal Enterprises, New Delhi, Model: F-81) with an overall accuracy of $\pm$ 0.1% has been used for velocity measurement. An electronically digitally operated constant temperature bath has been used to circulate water through the double-walled measuring cell made up of steel containing the experimental solution at the desired temperature with an accuracy of $\pm$ 0.01 K.

Excess volumes are determined by:

$$V^E = (M_1 X_1 + M_2 X_2) / \rho_{12} - (M_1 X_1) / \rho_1 - (M_2 X_2) / \rho_2 \qquad (1)$$

The viscosity of Binary Mixtures is determined by:

$$\ln \eta_m = X_1 \ln \eta_1 + X_2 \ln \eta_2 \qquad (2)$$

Deviation in Viscosity of Binary Mixtures is determined by:

$$\Delta \eta_m = \eta_{12} - X_1 \eta_1 - X_2 \eta_2 \qquad (3)$$

Deviation in isentropic compressibility have been evaluated by using the equation

$$\Delta K_S = K_S - (\Phi_1 K_{S1} + \Phi_2 K_{S2}) \qquad (4)$$

Where k_{S1}, k_{S2}, and K_S are the isentropic compressibility of liquid mixtures and Φ is the volume fraction of pure Components.

3. Result and discussion:

The experimental values of ultrasonic velocity, density, and viscosity in case of all the mixtures over the entire range of composition and at temperatures 298.15 K are given in table 1 to 3. A plot of respective deviation/excess parameters V^E, $\Delta \eta$, and ΔK_S against mole fraction of 2-(Dimethylamino) ethanol for all the mixtures is given in figures 1 to 3. The excess or deviation values reflect the interactions between the mixing species, which mainly depend upon the composition, the molecular sizes and shapes of the components, and temperature. The important effects, which influence the values of an excess thermodynamic function, are divided into physical, chemical, and structural contributions: 1.The physical contributions are comprised of nonspecific physical interactions, e.g. dispersion forces or weak dipole–dipole interaction leading to a positive contribution towards $\Delta \eta$ and negative contribution towards V^E and ΔK_S. 2. The chemical effect includes charge transfer forces, formation of H-bonds and other complex-forming interactions making a negative contribution towards V^E and ΔK_S. and a positive contribution towards $\Delta \eta$. The positive values of $\Delta \eta$ suggest that the mixtures are less compressible than the corresponding ideal mixture.

The values of $\Delta \eta$ can be explained on the basis of the complex formation between 2-(Dimethylamino) ethanol with cresol (o-cresol, m-cresol, and p-cresol) molecules through hydrogen bonding between the oxygen atom of 2-(Dimethylamino) ethanol and hydrogen atom of

the hydroxyl group in cresols.[10], which suggests thatliquids of different molecular sizes usually mix with a decrease in volume yielding positive Δη values. The observed Δη values indicate that the molecular interactions are stronger in all the mixtures. The excess molar volume, V^E, versus mole fraction, X_1, is plotted and presented in Figure 2 over the entire composition range andat 298.15 K. The V^E values are found to be negative for all the systems at X_1= 0.1 to 0.7 for all systems. It can be understood from Figure 1 that the negative value of V^E is in the following order, (2 -(Dimethylamino) ethanol +p-cresol) > (2-(Dimethylamino) ethanol + m-cresol) > (2-(Dimethylamino) ethanol + o-cresol). The negative values of V^E indicate the strong molecular interactions due to H-bonding [11]. The excess molar volume V^E becomes negative when the intermolecular interaction between unlike molecules is stronger than that in like molecules [12, 13]

The ΔK_S values are negative at X_1= 0.1 to 0.6 for all systems showing the strong molecular interactions through charge transfer dipole induced dipole and dipole-dipole interactions [12]. This is also due to strong interactions between unlike molecules than like molecules shown in Figure 3.

4. Conclusions:

The excess molar volumes V^E were negative for all mixtures and temperature dependent. This indicates efficient molecular packing and the existence of strong intermolecular interactions such as H-bonds among unlike molecules in the mixtures. In case of para cresol the excess volume is found to be most negative where as viscosity deviation is most positive indicating very strong molecular interactions between 2-(Dimethylamino) ethanol and para cresol. This is due to its planer structure(14). The viscosity deviation obtained from experimental values of density, ultrasonic velocity and viscosity is positive for all the binary systems at higher concentrations of cresols considered in the present study. It clearly suggests the presence of strong interactions between the molecules of all the binary mixtures. Fig:- 1,2 and 3 follows the same trend for molecular interaction order hence justifies each other. Due to Planer structure of p- cresol is has strong solute solvent interactions as compared to other cresols. The ortho and meta cresols shows dominant intra molecular forces(15).

Table:1 Values of density (ρ) viscosity (η), ultrasonic velocity, excess molar volume (V^E) , viscosity deviations (Δη) and isentropic compressibility (ΔK_S) for the binary system of 2-(Dimethylamino) ethanol (1) with o-cresol(2).

X1	P (gm/cm^3)	η x10^3 (Nsm^{-2})	U (m/s)	V^E x10^6 (m^{3}mole^{-1})	Δη x 10^3 (Kg m^{-1} s^{-1})	ΔKS
.0000	1.024818	7.701145	1504.2	0.0000	0.000	0.0000
0.1189	1.018504	15.877473	1503.3	-1.0192	869.336	-17.52
0.2328	1.008119	26.141526	1503.8	-1.5730	1945.345	-32.30
0.3421	0.992628	25.919848	1502.2	-1.5587	1970.777	-43.39
0.4472	0.975656	21.472809	1439.5	-1.3425	1571.843	-13.53
0.5482	0.957562	16.314641	1438.4	-0.9538	1100.011	-21.18
0.6454	0.939387	11.494679	1535.6	-0.4997	660.345	-26.67
0.7390	0.921294	8.0922866	1371.7	0.0036	360.869	16.95
0.8292	0.905083	5.7925599	1370.9	0.3529	170.178	11.67
0.9161	0.886353	4.2217435	1366.6	1.0454	50.941	12.06
1.0000	0.88310	3.346187	1365.4	0.0000	0.000	0.0000

Table: 2 Values of density (ρ) viscosity (η), ultrasonic velocity, excess volume (V^E), and viscosity deviations (Δη)and isentropic compressibility (ΔK$_S$) for the binary system of 2-(Dimethylamino) ethanol (1) with p-cresol (2).

X1	P (gm/cm^3)	η x10^3(Nsm^{-2})	U(m/s)	V^E x10^6 (m^{3}mole^{-1})	Δη x 10^3 (Kg m^{-1} s^{-1})	ΔKS
0.0000	1.006558	14.372194	1502.2	0.0000	0.000	0.00
0.1189	1.021586	57.074057	1505.8	-3.0185	4401.032	-27.40
0.2328	1.011527	48.034669	1504.4	-3.3885	3622.789	-40.58
0.3421	0.99242	43.906457	1502.2	-2.7968	3330.482	-48.63
0.4472	0.973206	25.8339	1438.8	-2.1438	1639.110	-16.12
0.5482	0.955013	15.425026	1436.8	-1.5464	709.585	-22.12
0.6454	0.946025	10.511672	1434.0	-1.8949	325.423	-31.73
0.7390	0.920694	7.4961086	1432.8	-0.4298	127.070	-32.71
0.8292	0.903654	5.5932421	1430.8	0.1872	36.238	-36.82
0.9161	0.886465	4.2878804	1466.3	0.8732	1.4070	11.47
1.0000	0.88310	3.346187	1465.7	0.0000	0.000	0.00

Table:3 Values of density (ρ) viscosity (η), ultrasonic velocity, Excess volume (V^E), and viscosity deviations (Δη) and Isentropic compressibility (ΔK$_S$) for the binary system of 2-(Dimethylamino) ethanol (1) with m-cresol (2).

X1	ρ(gm/cm^3)	η x10^3 (Ns m^{-2})	U	V^E x10^6 (m^{3}mole^{-1})	Δη x 10^3 (Kg m^{-1} s^{-1})	ΔKS
0.0000	1.01411	13.639915	1501.4	0.0000	0.000	0.00
0.1189	1.02274	53.348961	1505.8	-2.4327	4093.264	-25.54
0.2328	1.002569	48.034669	1504.4	-1.8582	3678.977	-34.71
0.3421	0.995704	43.906457	1502.2	-2.6080	3378.666	-48.50
0.4472	0.974578	25.8339	1438.8	-1.8454	1679.598	-15.54
0.5482	0.95499	15.425026	1436.8	-1.1823	742.677	-21.11
0.6454	0.937173	10.511672	1434.0	-0.6537	351.397	-26.12
0.7390	0.919784	7.4961086	1432.8	-0.1198	146.190	-31.66
0.8292	0.903173	5.5932421	1430.8	0.3783	48.752	-36.21
0.9161	0.889472	4.2878804	1366.6	0.5928	7.669	9.56
1.0000	0.88310	3.346187	1365.4	0.0000	0.000	0.00

Fig. 1: V^E Vs X$_1$ for the binary system of 2-(Dimethylamino) ethanol (1) with Cresols (2) at 298.15K.

'RESEARCH JOURNEY' *International E- Research Journal*
Special Issue – 333 : Innovative & Sustainable Chemistry
Impact Factor 6.625 (SJIF)   Peer Reviewed Journal

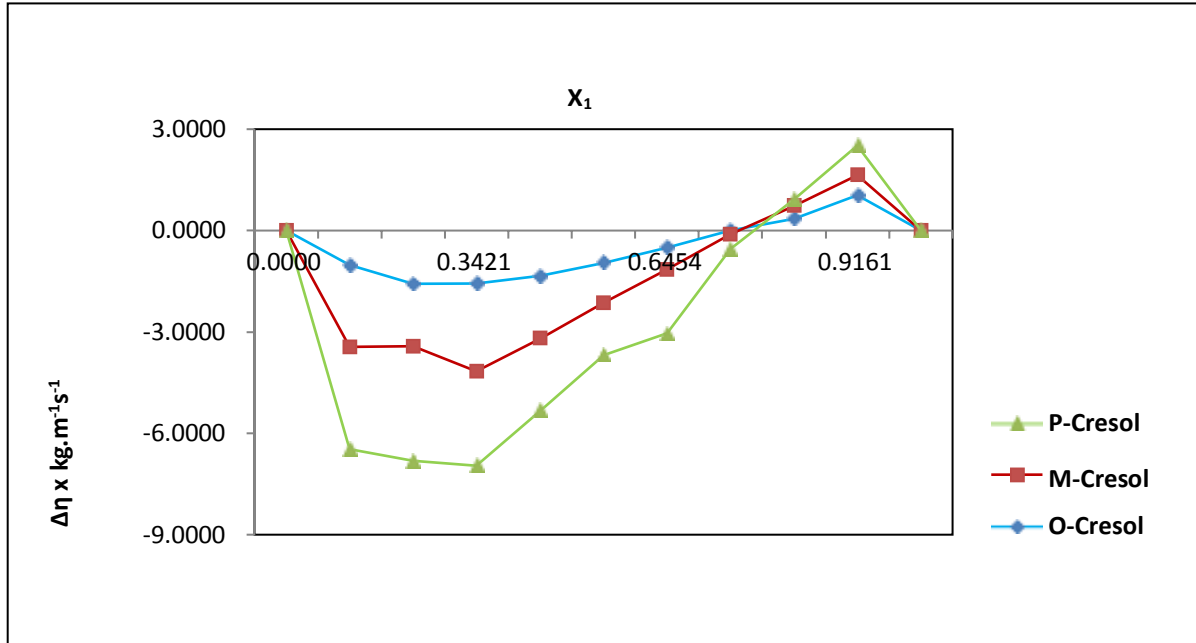E-ISSN :
2348-7143
December - 2023

Fig-2: Δη Vs X₁ for the binary system of 2-(Dimethylamino) ethanol (1) with Cresols (2) at 298.15K.
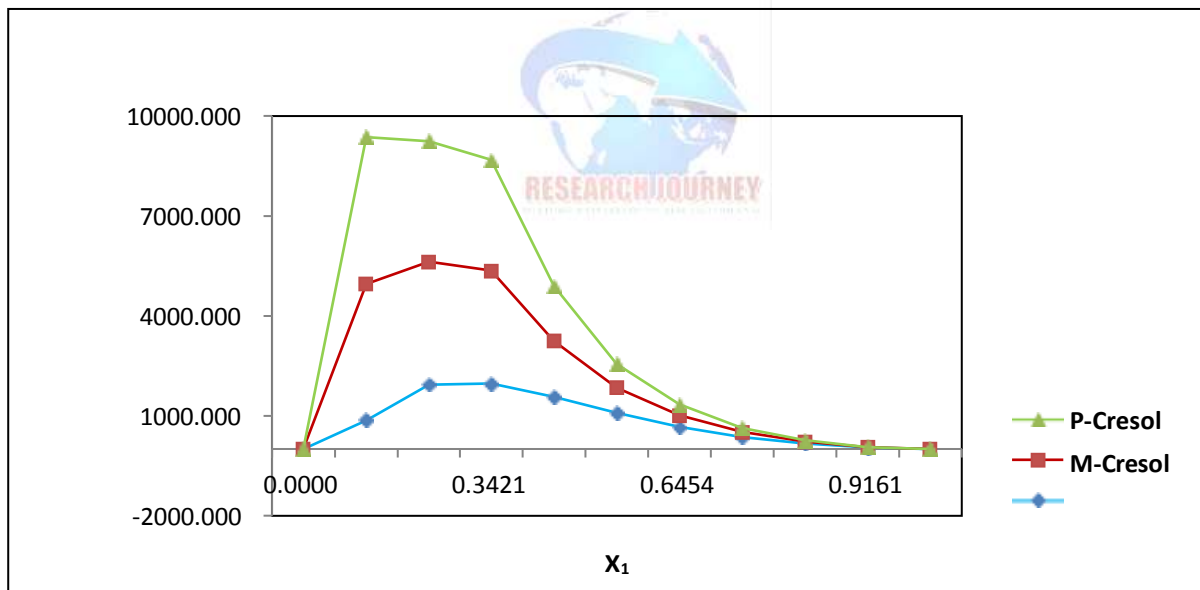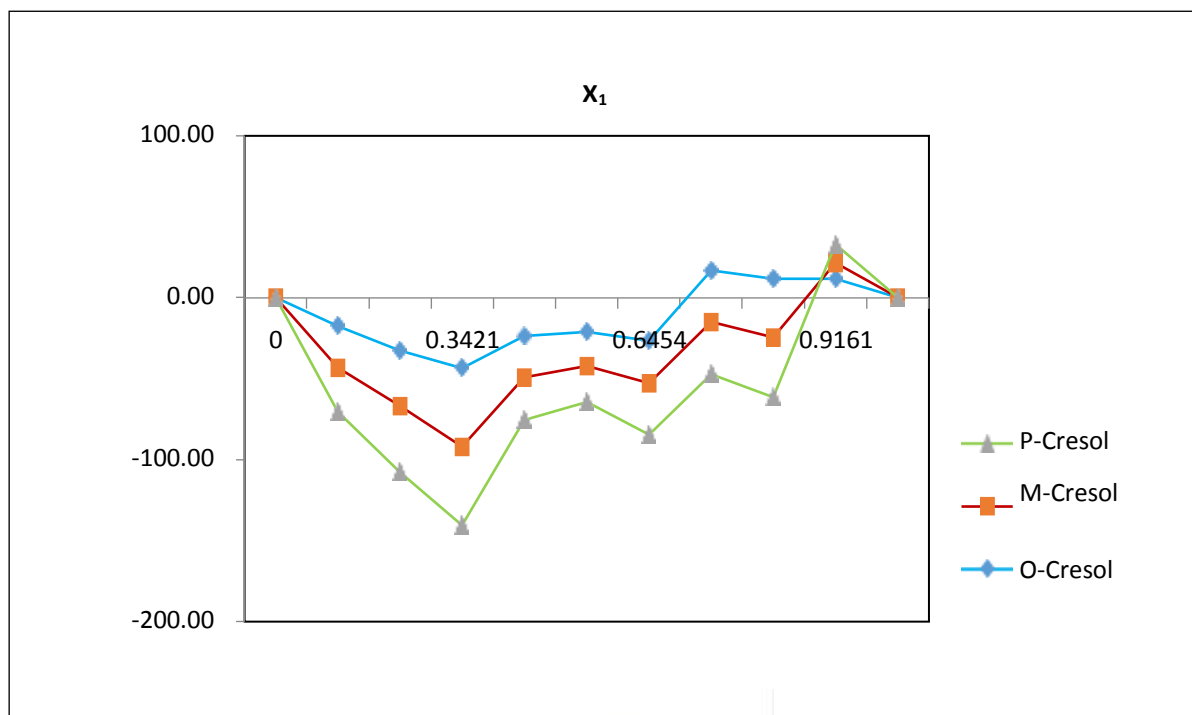
Fig- 3: ΔK_S Vs X_1 for the binary system of 2-(Dimethylamino) ethanol (1) with Cresols (2) at

298.15 K.

5. References:

1. UB Kadam; AP Hiray; AB Sawant; M Hassan. J. Chem. Eng. Data, 51, (2006), 60.
2. SC Bhatia; RBhatia; GP Dubey. J. Chem. Thermodyn., 42, (2010), 114.
3. K Narendra; P Narayanamurthy; Ch Srinivasu. E-J. Chem., 7(3), (2010), 927.
4. K Narendra; Ch Srinivasu; Sk Fakruddin; P Narayanamurthy. J.Chem. Thermodyn., 43, (2005), 1604.
5. R Palani; S Saravanan; R Kumar. Rasayan J. Chem., 2(3), (2009), 622.
6. Fernandes, D.; Conway, W.; Wang, X.; Burns, R.; Lawrance, G.; Maeder, M.; Puxty, G. Protonation Constants and Thermodynamic D D Perrin, WLF Armarego. Purification of Lab. Chem., 3rd ed., Pergamon Press, Oxford, 1980.
7. Zhang, J.; Fennell, P. S.; Trusler, J. P. M. Density and Viscosity of Partially Carbonated Aqueous Tertiary Alkanolamine Solutions at Temperatures between (298.15 and 353.15) K. J. Chem. Eng. Data 60, (2015), 2392−2399.
8. H Iloukhani; N Zoorasna; R Soleimani. J. Phys. Chem. Liquids, 43, (2005), 391.
9. R.J. Fort, W.R. Moore, Trans. Faraday Soc. 61 (1965) 2102–2110
10. S.C. Bhatia et al.;J.Chem Thermodynamics 43(2011),479-486; http://dx.doi.org/10.1016/j.jct.2010.10.025
11. Ma, D.; Liu, Q.; Zhu, C.; Feng, H.; Ma, Y.;J. Chem. Thermodyn. 134, (2019), 5–19.
12. Begum, S.K; et al. J. Mol. Liq. 177, (2013), 11–18.
13. Rai R.D.et.al. J.Chem Thermodynamics 21(1989)125.
14. P. P. Patil, R. S. Patil, S. R. Patil & A. U. Borse, Rasayan Journal of Chemistry, 11(3),(2018) 1103-1112.
15. P. P. Patil, R. S. Patil, S. R. Patil & A. U. Borse, Rasayan Journal of Chemistry, 3 (2011), 599-604

COSMOS IMPACT FACTOR

Search Journal   Search

Category

INDEXED JOURNAL

SUGGEST JOURNAL

JOURNAL IF

REQUEST FOR IF

DOWNLOAD LOGO

CONTACT US

SAMPLE CERTIFICATE

SAMPLE EVALUATION SHEET

Journal Detail

Journal Name	RESEARCH JOURNEY
ISSN/EISSN	2348-7143
Country	IN
Frequency	Quarterly
Journal Discipline	General Science
Year of First Publication	2014
Web Site	www.researchjourney.net
Editor	Prof. Dhanraj Dhangar & Prof. Gajanan Wankhede
Indexed	Yes
Email	researchjourney2014@gmail.com
Phone No.	+91 7709752380
Cosmos Impact Factor	2015 : 3.452

GIF GLOBAL IMPACT FACTOR

News Updates   Due to large number of application please allow us time to update your journal

Research Journey

SJIF 2019:

6.625

Area: Multidisciplinary

Evaluated version: online

Previous evaluation SJIF	
2018:	6.428
2017:	6.261
2016:	6.087
2015:	3.986

The journal is indexed in:

SJIFactor.com

Basic information

Main title	Research Journey
Other title [English]	Research Journey
Abbreviated title	
ISSN	2348-7143 (E)
URL	http://WWW.RESEARCHJOURNEY.NET
Country	India
Journal's character	Scientific
Frequency	Quarterly
License	Free for educational use
Texts availability	Free

Contact Details

Editor-in-chief	Prof. Dhanraj Dhangar
	M.G.V.'S ARTS & COMMERCE COLLEGE, YEOLA, DIST NASHIK
	India
Publisher	MRS. SWATI SONAWANE

Get Involved

Home

Evaluation Method

Journal List

Apply for Evaluation/Free Service

Journal Search

Recently Added Journals

Research Journey

ISSN	2348-7143
Country	India
Frequency	Querterly
Year publication	2014-2015
Website	researchjourney.net
Global Impact and Quality Factor	
2014	0.565
2015	0.676

Swatidhan Publications

Price : Rs. 1000/-

For Details Visit To : www.researchjourney.net